Drug Response Profiling to Identify New Targets in Refractory Leukemia

Dissertation
zur
Erlangung der naturwissenschaftlichen Doktorwürde
(Dr. sc. nat.)

vorgelegt der
Mathematisch-naturwissenschaftlichen Fakultät
der
Universität Zürich
von

Viktoras Frismantas

aus
Litauen

Promotionskomitee
PD Dr. Bourquin Jean-Pierre (Vorsitz und Leitung der Dissertation)
Dr. Beat Bornhauser
Prof. Dr. Alex Hajnal
Prof. Dr. Freddy Radtke

Zürich, 2016

STATEMENT OF AUTHORSHIP

I declare that I have used no other sources and aids other than those indicated. All passages quoted from publications or paraphrased from these sources are indicated as such, i.e. cited and/or attributed. This thesis was not submitted in any form for another or diploma at any university or other institution of tertiary education.

Zürich, July 2016

Viktoras Frismantas

Summary

Acute lymphoblastic leukemia (ALL) accounts for one third of all diagnosed cancers in children. The event-free survival rate for ALL has steadily increased and exceeds 85%. Despite this significant progress, disease recurrence and late side effects of intensive chemotherapy for survivors constitute a real challenge. Recent genomic and proteomic studies unveiled pathways to a resistant disease that could be exploited with the precision medicine. However, clinical translation of molecularly targeted agents remains very limited, given the difficulty to establish predictive markers for convincing drug activity in the clinical setting. Therefore in my thesis I describe a functional assay to determine phenotypic response of resistant primary ALL to a novel therapeutics and provide compelling preclinical evidence using humanized mouse models and first clinical correlations to support the value of this approach.

Genomic characterisation of ALL revealed that the mutational landscape in ALL is complex and heterogenous, which implies that individual differences may play a bigger role than ever anticipated. Furthermore clonal complexity and selection to relapse adds to the heterogeneity of the disease. The complexity of the underlying molecular circuitry would suggest that it will be difficult to predict drug response solely based on genomic information. To detect druggable leukemia dependencies we have developed a standardized large scale drug response profiling platform for the primary ALL co-cultured on a bone marrow stromal cells. For this platform we have compiled custom compound library of more than 100 agents that are in the clinical use or in the late clinical development. Informative patterns of drug sensitivity were detected for a more than 90 patients from defined subgroups, including refractory relapse cases, the unfavourable *MLL-AF4* and *TCF3-HLF* positive ALL genetic subtypes, and a subsets of resistant T-ALL. Most importantly, unexpected activity of several agents allowed us to identify patient populations that may benefit from such agents.

In cases with refractory disease, we found drug profiles with marked patterns of drug resistance but exceptional responses to new agents that could be immediately translated into the clinic. One subgroup is defined by its dependence on the anti-apoptotic regulator BCL2. The BCL2-inhibitor venetoclax was active below 10 nM in BCP-ALL subsets including *MLL-AF4* and *TCF3-HLF* ALL, and in some T-ALLs, predicting *in vivo* activity in the mouse xenograft model. Interestingly, this activity could not be necessarily inferred using biomarkers that have been proposed previously. Another new subgroup was identified in T-ALL based on very high sensitivity to the ABL1 and SRC inhibitor dasatinib, with IC50 values below 20 nM. Dasatinib activity correlated with similar cytotoxic activity other drugs that target SRC, including the SRC Inhibitor KX2-391. Drug response correlated with higher levels of SRC phosphorylation in T-ALL and inhibition of SRC phosphorylation. A patient with refractory T-ALL was treated with dasatinib based on drug profiling information and achieved a five-month remission. Given the complete lack of alternatives for patients with relapsed T-ALL, this discovery provides a new option of patients based on individual drug profiling.

Succesful anticancer therapy requires combination therapy in most cases. Our plaftform provides thae basis for synthetic lethal screens and combination testing. We could show that the BCL2-inhibitor venetoclax acts synergistically with the standard of care drugs dexamethasone and vincristine, as well

as the BRD4 inhibitors JQ1 and OTX-015 that target epigenetic mechanisms. Impressive responses were obtained *in vivo* with venetoclax in combination with dexamethasone and vincristine in *TCF3-HLF* and *MLL-AF4* xenografts that were predicted to be sensitive on drug profiling platform. For the first time we could achieve cure in a mouse xenograft model of TCF3-HLF positive ALL using a combination of venetoclax, dexamethasone and vincristine. Thus our approach detects actionable targets and altered molecular circuities in pediatric ALL that otherwise would be difficult to predict. Furthermore our results clearly indicate that drug profiling may provide important information to guide patient selection for targeted therapy more precisely. This will become highly relevant in disease where small subgroups of patients share distinct features that could be targeted. Our approach will therefore now be tested in the setting of an international clinical trial for the treatment of relapsed ALL.

Zusammenfassung

Die akute lymphatische Leukämie (ALL) ist die häufigste Krebserkrankung bei Kindern und präsentiert sich in einem Drittel aller diagnostizierter Krebserkrankungen. Die ereignisfreie Überlebensrate für pädiatrische ALL hat in den vergangenen Jahren deutlich zugenommen und übersteigt heute 85%. Trotz erheblicher Fortschritte erfahren aber immer noch etwa 15% der Kinder mit ALL einen Rückfall welcher mit einer sehr schlechten Prognose einhergeht. Die aktuellen Studien der Genomik und Proteomik haben Resistenzmechanismen in der ALL identifiziert, welche für neue Behandlungsmethoden genutzt werden könnten. Jedoch bleibt die Überführung der molekular spezifischen Wirkstoffe in klinische Studien eine Herausforderung, da die Wirkstoffaktivität im Patienten schwer vorauszusagen ist. Das Ziel dieser Arbeit war die Etablierung einer Methode zur Bestimmung der Aktivität von neuen Wirkstoffen auf primäre Zellen von resistenten ALL-Patienten. Zusammen mit einem Mausmodel zur Generierung von vorklinischen Daten sowie präliminären klinischen Korrelationen wurde die Funktionalität der Methode demonstriert.

Die genomische Charakterisierung der ALL Proben zeigte, dass jeder Patient ein komplexes und heterogenes Mutations-Muster aufweist, was einen Hinweis darauf liefert, dass individuelle Unterschiede einen grösseren Einfluss haben können, als bisher angenommen wurde. Außerdem wird die Heterogenität der Krankheit im Falle eines Rezidivs noch durch klonale Komplexität und Selektion erweitert. Basierend auf diesem komplexen Netzwerk von zugrunde liegenden Signalwegen und Mechanismen erscheint es schwer aufgrund von genetischen Informationen die Reaktion eines Patienten auf einen Wirkstoff vorherzusagen. Zur Identifikation von möglichen therapeutischen Zielen haben wir eine standardisierte Hochdurchsatzplattform entwickelt, in der primäre ALL Proben in einem Ko-Kultursystem mit mesenchymalen Stromazellen des Knochenmarks analysiert werden können. Für diese Plattform haben wir eine Wirkstoffkollektion mit über 100 Substanzen zusammengestellt, welche bereits im klinischen Einsatz oder in der späten klinischen Entwicklung sind. Mehr als 90 Patienten aus definierten ALL-Subklassen, darunter refraktäre Rezidive, resistente MLL-AF4 und TCF3-HLF positive B-ALL, sowie resistente T-ALL Patienten, wurden mit der Plattform untersucht und Reaktivitätsprofile erstellt.

Die refraktären Fälle zeigten eindeutige Muster von Wirkstoffresistenzen aber auch ausserordentliche Reaktivitäten auf neue Substanzen welche direkt in klinischen Studien eingesetzt werden könnten. Eine Subgruppe konnte durch die Abhängigkeit des antiapoptotischen Regulators BCL2 definiert werden. Der BCL2-Inhibitor Venetoclax zeigte eine Reaktivität bei einer Konzentration unter 10 nM in B-ALL, einschliesslich der MLL-AF4 und der TCF3-HLF positiven Fälle, und mehreren T-ALL Fälle, was eine Reaktivität in unserem Xenotransplantationsmodel in vivo erwarten lässt. Interessanterweise konnte die Wirksamkeit des BCL2-Inhibitors nicht anhand von bekannten Biomarkern vorhergesagt werden. Innerhalb der T-ALL Kohorte konnte eine zweite Subgruppe identifiziert werden, welche sich durch die Sensitivität auf den ABL1 und SRC Inhibitor Dasatinib mit einem IC50 von unter 20 nM charakterisiert. Die Wirkung von Dasatinib korreliert mit ähnlichen Medikamenten, die die Kinase SRC inhibieren, wie zum Beispiel KX2-391, aber auch der Höhe SRC-Phosphorylierung in primären T-ALL Proben. Ein Patient mit refraktärer T-ALL, welcher eine gute Reaktivität auf SRC-Inhibitoren in unserer Plattform

zeigte, wurde daraufhin mit Dasatinib behandelt und erlangte eine fünfmonatige Remission. Beachtet man den bisherigen Mangel an Behandlungsalternativen für Patienten mit rezidivierter T-ALL, stellt unsere Plattform zur individuellen Wirkstofftestung eine wichtige Option zur Validierung wirksamer Medikamente dar.

In den meisten Fällen reicht eine Monotherapie nicht aus um die Krebserkrankung dauerhaft zu behandeln, so dass fast alle Patienten mit einer Kombinationstherapie behandelt werden. Unsere Plattform bietet auch die Möglichkeit Kombinationstherapien zu testen und deren Effektivität in vivo vorherzusagen. Die systematische Analyse von Wirkstoffkombinationen zeigte, dass der BCL2-Inhibitor Venetoclax synergistisch mit den etablierten Chemotherapeutika Dexamethason und Vincristin, sowie mit den epigenetisch wirksamen BRD4 Inhibitoren JQ1 und OTX-015, reagiert. Besonders deutlich war die Wirksamkeit der Kombination von Venetoclax mit Dexamethason und Vincristin in vivo zu sehen. Patientenproben der TCF3-HLF und MLL-AF4 positiven B-ALL zeigten eine hohe Sensitivität in vitro in der Plattform, welche im Xenotransplantat in vivo bestätigt werden konnte. Die Behandlung des xenotransplantierten Mausmodels zeigte eine komplette Remission der Krankheit und eine vollständige Heilung durch die Kombination von Venetoclax, Dexamethason und Vicristin. Dies zeigt, dass unsere Methode wirksame Medikamente für pädiatrische ALL-Patienten identifizieren kann, welche anhand von bekannten Biomarkern nicht definiert werden konnten. Des Weiteren zeigen unsere Ergebnisse, dass diese methodische Suche nach wirksamen Substanzen wichtige Informationen zu den Patienten liefern kann, welche eine bessere Stratifizierung und zielgerichtete Therapie ermöglichen. Dies wird besonders relevant für Patienten, deren Subgruppen nur in kleinen Fallzahlen bekannt sind und zu denen bisher noch keine passende Therapie definiert wurde. Unsere Methode wird daher bereits im Rahmen einer internationalen klinischen Studie für die Behandlung von ALL-Rezidiven getestet.

Table of content

1. Introduction

1.1. Pediatric Acute Lymphoblastic Leukemia

Acute lymphoblastic leukemia (ALL) is the most common childhood malignancy. ALL originates either from the T-cell (15%) or B-cell (85%) lineage (immunophenotype) blocked in different maturation stages (1). ALL occurs at an annual rate of 30 cases per 1 million people younger than 20 years, with the peak of incidence between 3 to 5 years of age (2). ALL is diagnosed more frequently in males than in females (56.1% vs. 43.9% (3)) and are more frequent in some ethnicities, with a higher incidence (>2x) in Caucasians than in African-descent individuals (4,5). Over the past 30 years, childhood ALL incidence gradually increased by an average of 1.4% per year (6). Presenting symptoms of ALL include bruising or bleeding due to thrombocytopenia, pallor and fatigue from anemia, and infection caused by neutropenia. Leukemic cells accumulate in primary and secondary hematopoietic sites like the liver, spleen, lymph nodes, thymus and mediastinum, at diagnosis (4). Extramedullary leukemia in the central nervous system (CNS) or testicles may also be presented at diagnosis and require specific modifications in therapy. The progressive improvement of multiagent chemotherapy regimen efficacy and better patient stratification by clinical and molecular features led to a steady improvement in overall survival (Figure 1) (4).

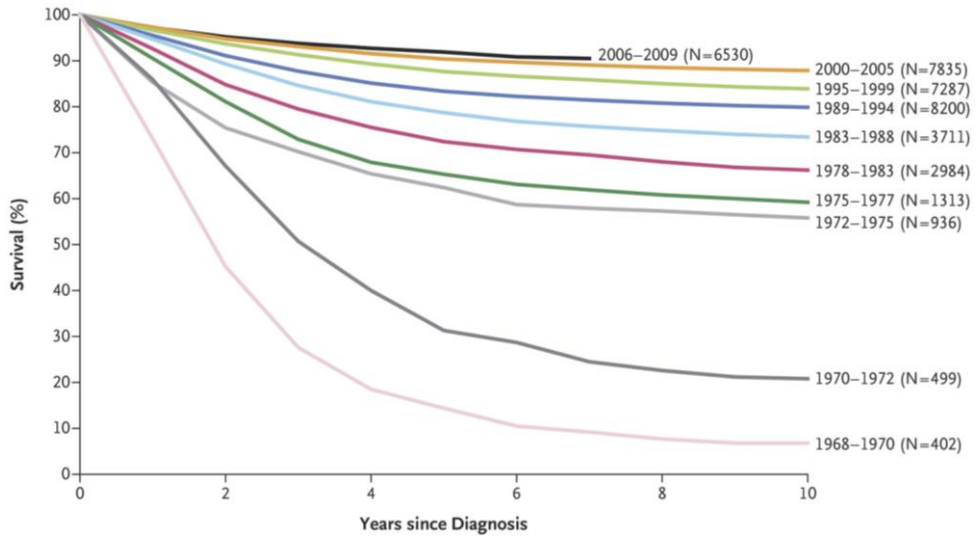

Figure 1. Overall survival among children with ALL enrolled in Children's Cancer Group and Children's Oncology Group Clinical Trials, 1968–2009. Reproduced from (4).

Developing better treatment options have increased patient survival to more than 90% today. Newly-introduced treatment protocols decreased instances of death by 20% from 1999 until 2014. Leukemia is currently no longer the most frequent death cause in children, and has been surpassed by brain cancer (7). Despite significant progress, a considerable number of patients still experience relapse that require better therapeutic options. Moreover, many ALL survivors have a high rate of illness owing to chronic health conditions resulting from harsh chemotherapy regimens (8). Osteonecrosis is the most severe long-term complication associated with current ALL therapy, and occurs in 5-10% of patients (9). Additional treatment-related effects include secondary malignancies (10), obesity (11), cardiovascular impairment (12), and CNS and peripheral nervous system toxic effects (12).Thus, an

important long-term goal is to tailor drug exposure according to the predicted risk of relapse, and by doing so, to reduce toxic side effects. In addition, much effort is put into understanding the molecular basis of ALL, which could be used in designing precision therapies. Treatment decisions might be guided by genomic, proteomic and functional response information.

1.1.1. ALL diagnostic

The prognosis and therapy for ALL and acute myeloid leukemia (AML) differ greatly, and it is therefore crucial to differentiate these two neoplastic processes. A morphological bone marrow assessment represents the first step in the primary diagnosis of ALL and its differentiation from AML (13). The presence of myeloperoxidase (MPO), Auer rods (needle-like bodies), or monocyte-associated esterases in leukemic blasts readily identifies most cases of AML. In contrast, the leukemic blasts of ALL do not present with unique morphologic or cytochemical features. Immunologic tests, or immuphenotyping, is an essential component of the diagnostic routine, and helps classify the lineage of ALL, its stage of differentiation, and define acute leukemia of ambiguous lineage (14). The cluster of differentiation (CD) is a system used for the identification and investigation of primarily hematopoietic and lymphoid cells. The CD molecules may be ligands, receptors, adhesion and migration molecules, or cytokines. As of 2016, 371 CD markers have been described (15). ALL cell CD marker expression profiles are mostly similar to those in normal B- and T-lineage cells and are used as a basis for the immunological classification of ALL. However, the intensity of frequently aberrant antigen expression differentiate blasts of acute leukemia from their normal lymphoid cells. Current B- and T-cell lineage ALL classification markers are summarized in Table 1.

BCP cell lineage	Pro-B	Common-B	Pre-B	Mature-B
All are positive for CD19 and/or CD79a and/or CD22; most cases, except mature-B, are TdT positive	$CD10^{neg}$, anti-$c\mu^{neg}$, anti-$SmIg^{neg}$	$CD10^{pos}$, anti-$c\mu^{neg}$, anti-$SmIg^{neg}$	$CD10^{pos}$, anti-$c\mu^{pos}$	Anti-c or Sm κ or λ Now classified and treated as non-Hodgkin's lymphoma
T cell lineage	**Pro-T**	**Pre-T**	**Cortical-T**	**Mature-T**
All positive for c or Sm CD3; Some cases are CD10 positive	$CD7^{pos}$, $CD2^{neg}$, $CD5^{neg}$, $CD8^{neg}$, $CD1a^{neg}$	$CD2^{pos}$ and/or $CD5^{pos}$ and/or $CD8^{pos}$, $CD1a^{neg}$	$CD1a^{pos}$, Sm $CD3^{pos}$ or ^{neg}	Sm $CD3^{pos}$, $CD1a^{neg}$, Anti-$TCR\alpha\beta^{pos}$ or Anti-$TCR\gamma\delta^{pos}$

c – cytoplasmic, CD – cluster of differentiation, Ig – immunoglobulin, Sm – surface membrane, TdT – terminal deoxynucleotidyl transferase, TCR – T-cell receptor

Table 1. European Group for the Immunological Characterization of Leukemia (EGIL) classification of BCP- and T-ALL (1).

Immunophenotyping is important for the differentiation between ALL and non-Hodgkin's lymphoma, since the latter need very specific treatment. Currently, B-lineage ALL that express mature B cell markers (Table 1) are classified and treated as non-Hodgkin's lymphoma. Other B-cell precursor (BCP-) ALL comprise more than 93% of B cell lineage leukemia. The most frequent ALL immunophenotypes, according to the EGIL classification (1), are precursor B-cell common BCP-ALL (>60%) and among T-cell derived ALL, cortical T-ALL (~50%) (3,16) (Table 1).

1.2. ALL prognostic factors

Treatment advances have been achieved with the identification of prognostic factors that permit risk-adapted treatment strategies. Major prognostic factors that are predictive of the cure rate include range of clinical, biological and genetic features.

1.2.1. Clinical features

Risk assessment is mainly performed through clinical factors such as initial white blood cell count (WBC), liver and spleen enlargement, CNS involvement, mediastinal tumor, patient age and early response to the treatment (Table 2).

Variable	Favourable factor	Adverse factor
Age (years)	1 to <10	<1 or ≥10
Initial white-cell count (WBC)	Lower (<50,000/mm^3)	Higher (≥50,000/mm^3)
Immunophenotype	B-cell lineage	T-cell lineage
Cytogenetic features	*ETV6-RUNX1*, hyperdiploidy, favourable chromosome trisomies	*BCR-ABL1*, *MLL* rearrangements, hypodiploidy
Genomic features	*ERG* deletions	*IKZF1* deletions or mutations; Philadelphia chromosome–like ALL with kinase gene alterations
Response to glucocorticoid therapy	Good response to prednisone (<1000 blasts/mm^3)	Poor response to prednisone (≥1000 blasts/mm^3)
MRD quantitation during or at end of induction	Reaching low (<0.01%) or undetectable MRD by specific time points	Persistence of MRD ≥0.01% at specific time points; the higher it is, the worse the prognosis

Table 2. Pediatric ALL risk stratification factors. Adapted from (4).

Historically patients with T-ALL immunephenotypes were associated with inferior survival rates compared to BCP-ALL, but recently the gap has been substantially narrowed (17). After adjusting for sex, race, radiation therapy, primary tumor location, and immunophenotype, patient age at diagnosis is the most crucial prognostic variable before the treatment. ALL patients diagnosed between 1 and 9 years of age have the highest chance of survival (18). The lowest survival is observed among patients diagnosed during infancy, followed by children diagnosed between 15 and 19 years of age (19). Based on clinical data, initial high white-cell count (≥50,000 per cubic millimetre) at diagnosis has been associated with poor treatment outcome (20). Early response to therapy, determined by the level of minimal residual disease (MRD) at the end of induction, is currently the most important prognostic factor of treatment outcome in patients with ALL (21).

1.2.1.1. Minimal residual disease (MRD)

The presence of MRD following therapy for ALL patients is an important prognostic marker of relapse (21). MRD testing is part of most pediatric ALL treatment protocols, though there is a considerable variability in the time points selected for the MRD analysis and in the levels of MRD used to define the risk of relapse. MRD is detected either by flow cytometry or by polymerase chain reaction (PCR) amplification of immunoglobulin or T-cell receptor gene rearrangements (22). These methods can detect one ALL cell per 10^3-10^4 normal cells in clinical samples. Patients that reach MRD levels below

0.01% during therapy have a greater chance of survival, while patients with higher MDR levels have a higher (three to five times) risk of relapse (23,24). Depending on the study group, MRD can be measured at day 15, 33 and 78 or day 8 and 29 (22). For instance, according to the Children's Oncology Group (COG) treatment protocol, MRD is measured at the end of induction therapy (day 29) and risk assignment cut-off levels are set above 0.01% (Figure 2) (21).

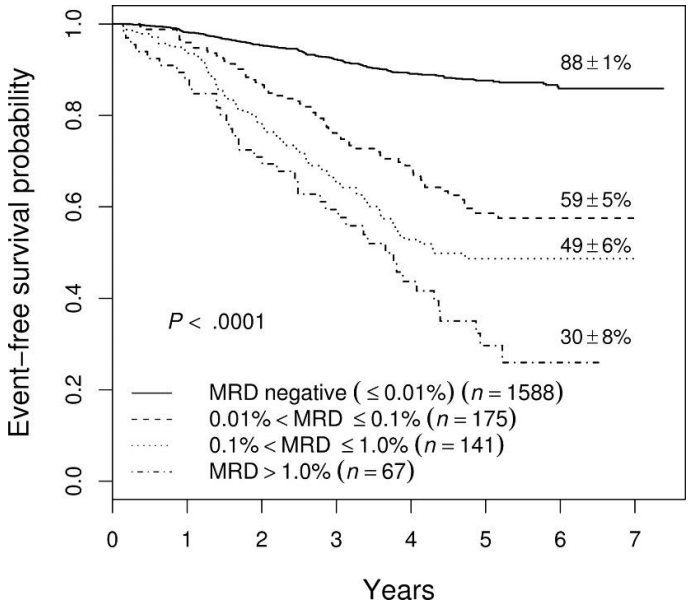

Figure 2. Event-free survival of all patients enrolled in COG studies (year 2000-2005) with MRD measurement at the end of induction therapy (day 29). Reproduced from (21)

MRD alone outweighs the prognostic value of other clinical and biological parameters. As demonstrated by AIEOP-BFM ALL 2000 study, risk classification algorithm based on MRD measurements on treatment days 33 and 78 were more predictive than other stratification criteria (25).

1.2.2. Genomic and biological factors contributing to ALL

ALL is likely to arise from interactions between exogenous or endogenous exposure, inherited susceptibility, and pure chance (26). The identification of relevant exposures and inherited genetic variants, and how and when they contribute to ALL initiation (usually *in utero*), remains a major challenge (27). Epidemiological studies have identified more than twenty candidate exposures that may contribute to the development of pediatric ALL (28). Some are more relevant that others, like smoking or treatment with certain medication during pregnancy (28). Overall, infection remains the strongest candidate exposure behind childhood ALL (29). Two specific hypotheses have been proposed, supported by epidemiological data, that ALL results from an abnormal response to a viral or bacterial infection in susceptible individuals (28). So far there is no evidence that ALL could be caused by a single transforming virus (28). It is believed that the pre-leukemic clone is generated *in utero* and later leukemia is developed after acquiring additional supporting lesions (28). There is very little evidence of inherited predisposition to ALL (30). To date, common allelic variants in *IKZF1*, *ARID5B*, *CEBPE*, *GATA3* and *CDKN2A* genes have been associated with childhood ALL by increasing odds ratios by 1.3 to 1.7 fold (31-34). In addition, rare germline mutations in *PAX5* and *ETV6* are linked to familial ALL

(35,36). Individuals with Down syndrome also have substantially elevated risk of developing ALL (~40-fold at age 0–4 years) (37). The molecular basis behind this association has not been completely elucidated (37). Nonetheless, there is a significant difference in the frequency of common mutations compared with other ALL patients. For instance, children with Down syndrome that develop ALL had significantly lower frequencies of *ETV6-RUNX1* translocation (2.5% vs. 24%) and hyperdiploidy (7.7% vs. 24%) compared to other ALL patients. These ALL subtypes are associated with favorable treatment outcomes (38). Down syndrome is one of the most important leukemia-predisposing syndromes, and has been linked to significant differences in treatment response and toxicity profiles compared to other patients.

1.3. Genetic basis of ALL

Most ALL genomes harbor sequence and structural DNA alterations in coding and noncoding elements (39). Approximately 80% of BCP-ALLs have gross genetic abnormalities, including aneuploidy or structural chromosomal rearrangements, which result in expression of a chimeric fusion proteins (39). In addition, childhood ALL genomes usually contain 10 to 20 nonsynonymous coding mutations at the time of diagnosis and about twice as many at the time of relapse (39).

1.3.1. Aneuploidy in ALL

High hyperdiploidy (51–67 chromosomes) is one of most common cytogenetic abnormalities, occurring in 25–30% of BCP-ALL cases, and is associated with good prognosis (40). This BCP-ALL genetic subtype is characterised by a non-random gain of chromosomes (41). Hyperdiploidy is most frequent among 3–5 year old patients with low WBC count at diagnosis (41). In contrast, hypodiploidy (<44 chromosomes) is less common among leukemia patients (2–3%of cases) and correlates with poor survival (42,43). Hypodiploidy, based on the chromosome number, is subclassified into near-haploid (24–31), low-hypodiploid (32–39) and high-hypodiploid (40–43) (44). All subclasses have distinguishable mutational landscapes (44). Near-haploid ALL harbor alterations in receptor tyrosine kinases (RTK), RAS signaling pathway components and *IKAROS* family genes (44). In contrast, low-hypodiploid cases have frequently mutated *TP53*, *RB1*, and *IKZF2* genes (44).The three-year event-free survival for newly diagnosed near-haploid and low-hypodiploid BCP-ALL is only 30% (43). In contrast, near-diploid cases with 44–45 chromosomes have good survival prognosis (44).

1.3.2. ALL initiating translocations

Major chromosomal translocations are the hallmark of ALL (45). Chromosomal rearrangements are early, possibly initiating events, of leukemogenesis (39,46). Chimeric fusion genes caused by translocation involve hematopoietic transcription factors, epigenetic modifiers, cytokine receptors, and tyrosine kinases (45). Most common B-lineage and T-lineage ALL rearrangements are summarised in Table 3, together with its prevalence across lineages, and associated prognoses:

Translocation	Fusion gene	Prevalence (%)	Prognosis
BCP-ALL:			
t(12;21)(p13;q22)	ETV6-RUNX1	15-25	Excellent prognosis
t(1;19)(q23;p13)	TCF3-PBX1	2-6	Excellent prognosis
t(9;22)(q34;q11.2)	BCR-ABL1	2-4	Poor prognosis
t(4;11)(q21;q23)	MLL-AF4	1-2	Poor prognosis
t(8;14)(q24;q32), t(2;8)(q12;q24), t(2;8)(q12;q24)	MYC rearrangements	2	Favourable prognosis
Xp22.3/Yp11.3	CRLF2 rearrangements (IGH-CRLF2; P2RY8-CRLF2)	5-7	Poor prognosis
PAX5 rearrangement	Multiple partners	2	
Complex structural alterations of chromosome 21	iAMP21	2	Poor prognosis
T-ALL:			
t(1;7)(p32;q35), t(1;14)(p32;q11), interstitial 1p32 deletion	TAL1 dysregulation	15-18	Favourable prognosis
t(11;14)(p15;q11) and 5' LMO2 deletion	LMO2 dysregulation	10	Favourable prognosis
t(10;14)(q24;q11), t(7;10)(q35;q24)	TLX1 [HOX11] dysregulation	7	Good prognosis
t(5;14)(q35;q32)	TLX3 dysregulation	20	poor prognosis
t(10;11)(p13;q14)	PICALM-MLLT10 [CALM-AF10]	10	May have poor outcome
t(11;19)(q23;p13.3)	MLL-MLLT1 [MLL-ENL]	2-3	
9q34 amplification	NUP214-ABL1	6	
t(7;9)(q34;q34)	Rearrangement of NOTCH1	<1	

Table 3. Key translocations found in BCP-ALL and T-ALL. Adapted from (4), data from (47).

It is interesting that the distribution of major genetic translocations in ALL differs across age groups (Figure 3) (45). Moreover, as these translocations are linked to different patient outcomes, the overall survival for separate age groups are likewise different (45). For instance, *MLL* (mixed-lineage-leukemia) rearrangements occur most frequently in infants (48). In contrast, *BCR-ABL1* translocation is significantly more frequently detected in adult ALL patients (49). Both aberrations are associated with poor prognosis (49). Only *TCF3-PBX1* translocation is detected at approximately the same rate in all age groups (45).

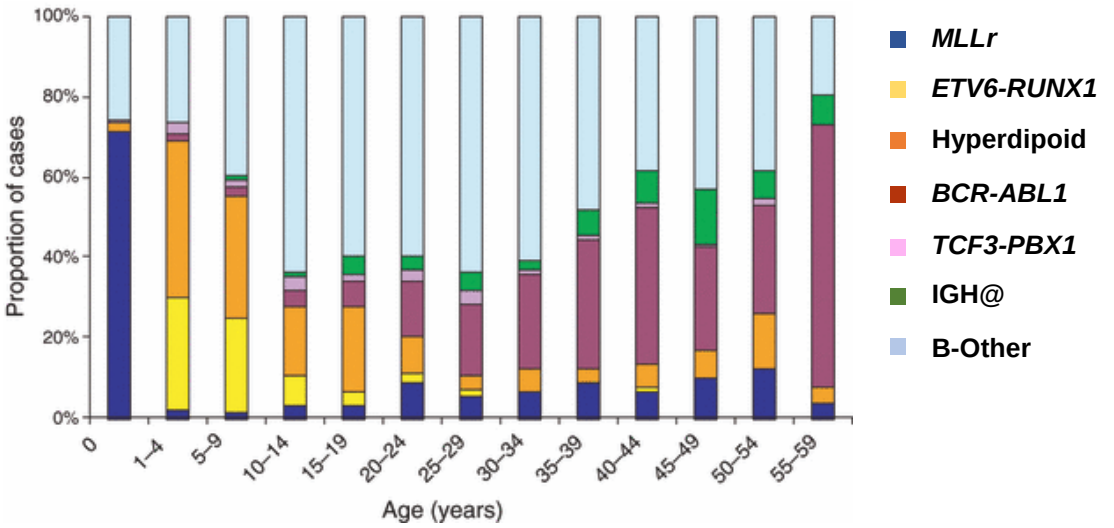

Figure 3. Distribution of the major cytogenetic subgroups in ALL broken down according to age. Reproduced from (45).

1.3.3. Ph-like ALL

Ph-like ALL is a newly-described common subtype ALL that has been associated with poor survival (~60%) (50,51). The prevalence of Ph-like ALL increases with age, from 10–15% of childhood B-ALL to over 25% of ALL in young adults (52). Patients with Ph-like ALL have a gene expression profile similar to that of *BCR-ABL1*–positive ALL, but lack the *BCR-ABL1* fusion gene (50). This ALL group is characterised by the presence of various kinase-activating translocations and mutations, which could be exploited by targeted therapies (52). Rearrangements of *ABL1*, *ABL2*, *CRLF2*, *CSF1R*, *EPOR*, *JAK2*, *NTRK3*, *PDGFRB*, *PTK2B*, *TSLP*, or *TYK2* and sequence mutations of *FLT3*, *IL7R*, or *SH2B3* were detected in >90% of Ph-like ALL (50). Deletions or mutations of the lymphoid transcription factor gene *IKZF1* are found in ~70% of *BCR-ABL1*–positive ALL and ~40% of Ph-like ALL (52,53). In contrast, only 10-15% of other BCP-ALL cases have the *IKZF1* mutations associated with an unfavourable treatment outcome (54).

1.3.4. Frequently mutated pathways in BCP-ALL

The nature and frequency of genetic lesions vary among BCP-ALL subtypes. For instance *MLL*-rearranged leukemias harbor very few additional alterations, while ALL with *ETV6-RUNX1* or *BCR-ABL1* translocations harbor between 6-8 additional alterations (51). Genetic lesions within B-lymphocyte development and differentiation regulators are present in ~40% of BCP-ALL (55). *PAX5*, which encodes a transcription factor necessary for normal hematopoietic development, has the most frequent somatic mutations, being altered in ~30% of cases (55). In addition, high-risk BCP-ALL analysis revealed a higher frequency of recurrent somatic alterations in the B-cell development- and differentiation-regulating genes (68% of cases), the TP53/RB1 tumor suppressor pathway (54% of cases), RAS signaling (50% of cases), and JAK/STAT signaling (11% of cases) (56). At least 10% of high-risk BCP-ALLs have mutations in *NRAS*, *KRAS*, *PAX5*, and *JAK2* (56). In addition, *CRLF2* (cytokine receptor-like factor 2) gene alterations occur in 6-16% BCP-ALL patients, with a higher

incidence rate among ALL patients with Down syndrome (>50%) (57), and has been linked with poor survival (53). FLT3 (fms-tyrosine kinase 3) is found mutated in ~25% of *MLL*-rearranged and high hyperdiploid BCP-ALL (58).

Recurrent epigenetic alterations were identified across all BCP-ALL subtypes studied, suggesting that certain epigenetic events are required for leukemic transformation (59). Approximately 7.5% of childhood BCP-ALL have mutated *WHSC1* gene, which codes for a histone-lysine N-methyltransferase; its incidence is higher in BCP-ALL patients with *ETV6-RUNX1* (20%) and *TCF3-PBX1* (15%) translocations (60). Almost 20% of relapsed BCP-ALL (especially hyperdiploid ALL) have aberrations in *CREBBP*, which is a transcriptional coactivator and acetyltransferase for the CREB binding protein (61). Other mutations in epigenetic regulators, such as *SETD2, MSH6, KDM6A* and *MLL2*, occur in 25% of BCP-ALL patients (62). Furthermore, analysis revealed that mutations in *SETD2*, coding H3K36me3 histone-lysine N-methyltransferase, were enriched in *MLL*-rearranged (22%) and *ETV6-RUNX1* (13%) positive BCP-ALL (62). Mutations in the *NT5C2* gene have been described in ~20% of relapsed BCP-ALL and T-ALL (63). NT5C2 is a 5'-nucleotidase responsible for the inactivation of nucleosidase-analog drugs (6-mercaptopurine or 6-thioguanine) (63). Finally, mutations and deletions in the transcription factor *ETV6* had been detected in 12% of high-risk leukemia cases (56).

1.3.5. Frequently mutated pathways in T-ALL

T-ALL is primarily caused by aberrant activation of the NOTCH1 signaling pathway, detected in nearly 60% of T-ALL cases (64). NOTCH signaling plays a critical role in cell lineage commitment decisions during development. In addition, about 15% of T-ALL cases bear *FBXW7* mutation, which impairs proteasomal degradation in the context of activated NOTCH1 signaling (65). Nonetheless, the most frequent abnormality detected in T-ALL (>70%) is the deletion of *CDKN2A* (66).

Another unique T-ALL feature is chromosomal translocation-driven aberrant expression of oncogenic transcription factors, which include *TAL1*, *LMO1*, *LMO2*, *TLX1*, *TLX3*, *MYC*, *MYB TAN1* and others (67). Notably, aberrant expression of *TAL1*, *LMO2* and *TLX3* occurs in ~60%, ~45% and ~25% of T-ALL cases (67). Additional genomic lesions disrupting the function of key transcriptional regulators such as *WT1*, *LEF1*, *BCL11B*, *GATA3*, *RUNX1*, and *ETV6* were found in 10%, 15%, 10%, 5%, 20%, and 13% of T-ALL cases, respectively (67). The T-ALL mutation landscape also includes genetic alterations disrupting the function of epigenetic factors as *EP300*, *PHF6*, *SETD2*, *EZH2*, *EED* and *SUZ12* (66).

Additional aberrations have been detected in the pathways regulating growth, proliferation and lineage commitment (67), such as *CCND2* and *NUP214-ABL1* translocations and mutations in *IL7R*, *FLT3*, *PTEN* and *NRAS* (68). ~10% of T-ALLs bear gain-of-function mutations in the *IL7R* gene that are activating JAK/STAT signaling (69). *RAS*-activating mutations have been found in 5-10% of T-ALL cases and are significantly higher in early T cell precursor ALL (70).

1.4. Standard-of-care pediatric ALL therapy

The basic pediatric ALL treatment protocol includes three phases: induction, consolidation and maintenance. Induction therapy lasts 4 to 6 weeks and consist of glucocorticoid (prednisone or dexamethasone), vincristine and L-asparaginase. Additionally, an anthracycline (doxorubicin or

daunorubicin) or intrathecal chemotherapy might be included. This therapy block is aimed to induce complete remission and approximately 95% of all patients achieve this goal (71). Following consolidation phase of intensive chemotherapy lasts for 6 to 8 months and is designed to maintain remission and prevent CNS relapse. This treatment block includes agents not used in the induction phase (6-mercaptopurine, 6-thioguanine, methotrexate, cyclophosphamide, etoposide and cytarabine). Finally, the maintenance phase is the longest treatment stage and is used to lower the risk of relapse once remission has been established. Patients receive low-intensity antimetabolite-based treatment regimens for 18 to 30 months. This therapy consists of 6-mercaptopurine or 6-thioguanine and methotrexate. All treatment plans include intrathecal administration of chemotherapeutics (dexamethasone, high-dose methotrexate, cytarabine and L-asparaginase) or cranial radiation during remission induction phase. Cranial radiation, however, is associated with an increased risk of secondary CNS tumors, delayed growth, endocrinopathies, and neurocognitive effects (72). Therefore, now less than 20% of newly diagnosed children receive CNS radiation.

Patients who fail to achieve remission after induction chemotherapy are termed ‘induction failures’ and patients who experience a leukemia recurrence after complete remission are said to have a relapse. For those with induction failure, an allogeneic hematopoietic stem cell transplant (HSCT) is usually pursued (73). The optimal donor has historically been a matched sibling, although advances with alternative donor sources are yielding promising results (74).

1.4.1. Relapse risk in childhood ALL

Despite significant advances in the treatment, approximately 15% to 20% of patients with ALL will relapse and only 30%-50% of all children with relapsed ALL can be cured (75). Prognostic factors at relapse include the time to relapse (a shorter time is associated with a worse prognosis), immunophenotype (T-cell immunophenotype is associated with a worse prognosis), and the site of relapse (bone marrow disease is associated with a worse prognosis than extramedullary disease) (75). Patients with the T-cell phenotype, *BCR-ABL1*–positive and Ph-like ALL, and patients with *MLL* rearrangements are associated with higher rates of relapse and poor survival.

1.4.1.1. T-cell lineage ALL

Treatment outcomes for T-ALL have improved in recent decades and is now resulting in up to 80% long-term event-free survival rates (76). In spite of this, 20-25% of children with T-ALL experience relapse, most of whom cannot be salvaged using standard therapies (75). Only a few of the numerous genetic alterations identified in T-ALL might have clinical significance. For instance, overexpression of transcription factors LYL1, TAL1, TLX3 in T-ALLs are associated with poor (30-40%) survival (77).

Early T-cell precursor (ETP) ALL is a recently-described subtype of high-risk ALL defined by reduced expression of T-cell markers (CD1a, CD8, and CD5) and aberrant expression of myeloid or stem cell markers (78). In children, ETP-ALL accounts for 15% of all T-ALL and has distinctive features. This subtype has fewer *CDKN2A/B* deletions and activating mutations in *NOTCH1*; it also shows a higher prevalence of mutations typically found in AML (70). A number of studies reported poor ETP-ALL

response to therapy and dismal prognosis (78). Other studies indicate, however, that it is not always associated with poor prognosis, and may thus exhibit some heterogeneity (79).

1.4.1.2. MLL gene rearrangements

Translocations involving the *MLL* gene are present in ~80% of infant leukemia and ~2-5% of all childhood ALL (80). Most common rearrangements, accounting for 93% of cases, include four partner genes: *AF4* (49%), *ENL* (22%), *AF9* (17%), and *AF10* (5%) (81). The *MLL* gene codes a protein with histone methyltransferase activity, and that is essential for the regulation of *HOXA* and *MEIS1* gene expression. *MLL* rearrangements are associated with adverse outcomes, with a four-year event-free survival of 35% (48). Thus, new therapeutic approaches are also needed to improve cure rates for these patients. *MLL*-rearranged ALL is characterised by a distinct gene expression profile (82), with striking *FLT3* overexpression (83). *FLT3* overexpression has been shown to confer especially poor prognosis in *MLL*-rearranged infant ALL (0% OS) (84). FLT3 inhibition results in a selective killing of *MLL*-rearranged samples and synergizes with chemotherapy (85). An ongoing clinical trial AALL0631 is the first to incorporate a novel FLT3 inhibitor, lestaurtinib, into the frontline treatment of infant ALL (86).

1.4.1.3. BCR-ABL1–positive and Ph-like BCP-ALL

BCP-ALL harboring the t(9;22)(q34;q11) translocation express the fusion oncogene, BCR-ABL1. This translocation is present in nearly all cases of chronic myeloid leukemia (CML), in 25% of adult ALL, and only 3-5% pediatric ALL cases. (80). In pediatric oncology, this translocation is associated with older patients, higher leukocyte count, and more frequent CNS involvement at the time of diagnosis (87). The use of ABL1 tyrosine kinase inhibitors (TKIs) such as imatinib, has been revolutionary in the treatment of *BCR-ABL1*–positive BCP-ALL. Once associated with dismal outcomes, use of TKIs combined with intensive chemotherapy has significantly improved the 5-year event-free survival in children and adolescents with no appreciable increase in toxicity (88).

Among patients with Ph-like ALL, depending on the age at diagnosis, the 5-year event-free survival varies between 24.1% and 58% (50). It is believed that these patients will respond to TKIs targeting specific lesions, but is yet to be confirmed with prospective clinical trials.

1.4.1.4. TCF3-HLF–positive BCP-ALL

The translocation t(17;19)(q22;p13), resulting in the fusion gene *TCF3-HLF*, defines a rare subtype of BCP-ALL (<1% of pediatric ALL). *TCF3-HLF* positive cases are typically associated with relapse and death within two years after the diagnosis (89). Possible transcription targets of TCF3-HLF include the transcription factor *LMO2*, which is implicated in the initiation of T-cell ALL (90), and the transcriptional repressor *SNAI1* (*SLUG*), which regulates embryonic development and apoptosis (91). Deletions of *PAX5* and *VPREB1* genes have been associated with *TCF3-HLF* ALL. Both genes are involved in early B-cell development regulation. In addition, mutations in *NRAS*, *KRAS* and *PTPN11* are more frequently detected in TCF3-HLF–positive ALL than other subtypes (92). Overall, *TCF3-HLF* fusion results in severe transcriptional reprogramming, dedifferentiation, and the presentation of stem-like features (92).

1.5. Individualised treatment: personalised or precision medicine?

Current treatment regimens are mostly non-targeted and accompanied by significant toxicities, a consideration specifically important for pediatric patients. Additional, non-specific intensification of therapy is unlikely to raise cure rates of relapsed leukemias further. Consequently, new initiatives transition from 'one-size-fits-all' approaches towards individualised treatment approaches.

Two terms – 'personalized medicine' and 'precision medicine' – are used to describe similar fields and are often confused. Personalised medicine simply means the selection of treatment tailored according to the individual patient's specific characteristics (93). Precision medicine, in contrast, is a much newer term and describes how molecular diagnostics could allow physicians to unambiguously diagnose the cause of a disease (93). Precision medicine and personalised medicine overlap significantly and in practice there is little difference between the two. Nonetheless, in my work I am using a top-to-bottom approach and rely on larger patient cohorts to identify subtypes that could respond to certain treatment. For this, I will use precision medicine term.

1.5.1. Precision medicine redefines clinical trials

Classical trial design is limited by leukemia heterogeneity, and a more personalised approach that takes inter-individual variability into account could be more appropriate. For instance, N-of-1 trials focus on a single individual using objective, data-driven criteria to tailor the treatment (94). N-of-1 studies are a promising way to advance precision medicine among a wide variety of patients. Alternatively, Basket trials comprise a new and evolving form of clinical trial design. Such trials are based on the hypothesis that the presence of a molecular marker predicts response to a targeted therapy, regardless of tumor histology. In 2015, NCI launched a phase II clinical trial called NCI-MATCH (clinical trial number: NCT02465060). It plans to recruit 3000 patients who will be allocated to one of 24 treatment arms with targeted compounds independent of tumor histology (95). Unlike basket studies, umbrella trials are designed to test the impact of different drugs on different mutations in a single cancer type. This design allows the validation of a treatment strategy based on a mixture of biomarkers and drugs.

1.6. Towards precision medicine in childhood leukemia

Recent genomic sequencing efforts have provided new insights into the classification and genetic basis of ALL (51,56). A number of chromosomal rearrangements, DNA copy number alterations and sequence mutations that perturb a key cellular pathways in ALL have been described (56). These mutations can affect lymphoid development, RAS and JAK/STAT kinase signaling, TP53/RB1 tumor suppressor, drug metabolism and epigenetic regulation genes (56); these findings have several implications for the precision medicine in ALL.

In 2000, Hanahan and Weinberg proposed the concept of hallmarks of cancer (96). They suggested that most cancers have acquired the same set of functional capabilities during their development, albeit through various mechanistic strategies (Figure 4) (96). With further refinement (97), four additional cancer hallmarks have been added (avoiding immune destruction, tumor-promoting inflammation, genome instability and deregulation of cellular energetics).

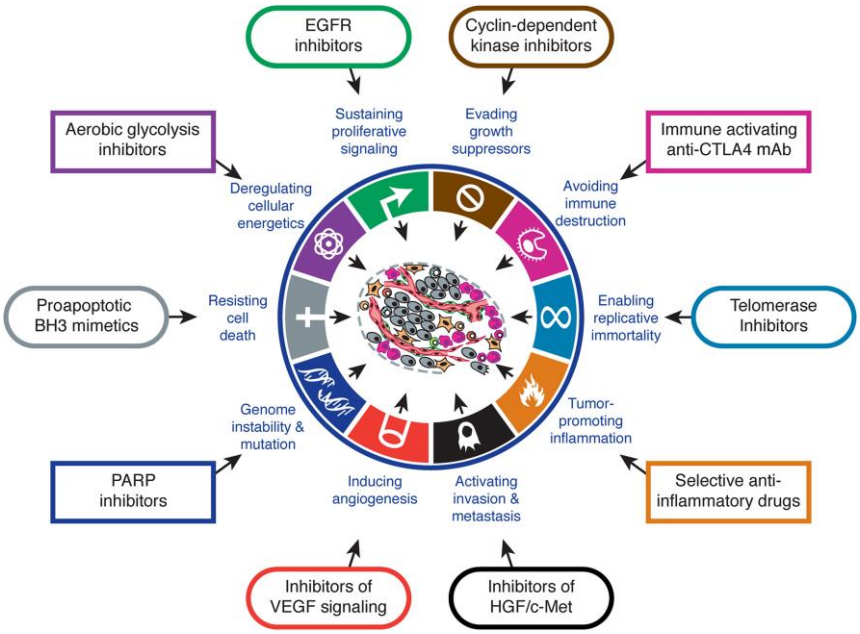

Figure 4. Therapeutic targeting of the Hallmarks of Cancer. Reproduced from (97).

Approaches to target various hallmarks proposed over time were also reviewed, with targeted therapeutics categorised according to their respective effects on one or more cancer hallmarks (Figure 4). Currently, a number of drugs interfering with acquired capabilities necessary for tumor survival are in clinical trials, or in some cases, approved for clinical use to treat certain forms of malignancies (97). In response to therapy, however, cancer cells may reduce their dependence on a particular hallmark by mutation, epigenetic reprogramming, or remodelling of the stromal microenvironment (97). This generally results in resistance and almost inevitable relapse. Consequently, novel treatment approaches should be exploited both as single compounds as well in combinations to overcome adaptive cancer cell properties and to target new cancer cell dependencies/hallmarks.

1.6.1. B- and T-cell differentiation pathways

Leukemia is characterized by arrest during normal differentiation. Consequently, several therapies have been designed to reverse aberrant differentiation arrest. For instance, effects of *PAX5*, *IKZF1*, and *EBF1* mutations in BCP-ALL patients (98) can be indirectly inhibited by targeting downstream activated pathways, ABL1 and/or JAK-STAT (99). In addition, kinase fusions and sequence mutations found in ALL induces cytokine-independent proliferation and can be targeted by TKIs. For instance, imatinib and dasatinib could be used to target ABL-class fusions, and JAK2 inhibitors to target JAK-STAT activating alterations (50,100).

The TAL1 protein, overexpressed in 60% of T-ALL cases, can be downregulated using histone deacetylase inhibitors (HDACi) (101). Phase I studies using class I selective HDACi MS-275 showed promising results in patients with refractory leukemia and metastatic melanoma (102).

1.6.1.1. Targeting NOTCH1 pathway in T-ALL

The NOTCH signaling pathway is involved in the regulation of cell proliferation, differentiation, development and homeostasis. NOTCH signaling is activated when the receptor is bound by one of five

ligands (delta-like ligand 1 (DLL1), delta-like ligand 3 (DLL3), delta-like ligand 4 (DLL4), Jagged-1 (JAG1) and Jagged-2 (JAG2)) (Figure 5) (103). Upon activation, a two-step proteolytic cleavage of the receptor follows. The first cleavage (S2) is mediated by metalloproteinase ADAM10 or ADAM17 and the second cleavage (S3) by γ-secretase, which releases the NOTCH1 intracellular domain (NICD); NICD then translocates into the nucleus and forms a complex with CSL (CBF-1/suppressor of hairless/Lag1) (103). Upon binding, NICD displaces corepressors and recruits the Mastermind-like protein 1 (MAML1) coactivator, forming an active transcription complex (103) (Figure 5). This complex regulates several genes important for the T-cell lineage progenitors, such as the *HES* family, *MYC*, *CCND3* (coding Cyclin D3) and others (104). *NOTCH1* mutations found in almost 60% of T-ALL are located at two hotspots in the HD (heterodimerization domain) and PEST domains. HD mutations result in ligand-independent activation or ligand hypersensitivity, while PEST domain aberrations lead to extended NICD stability (103).

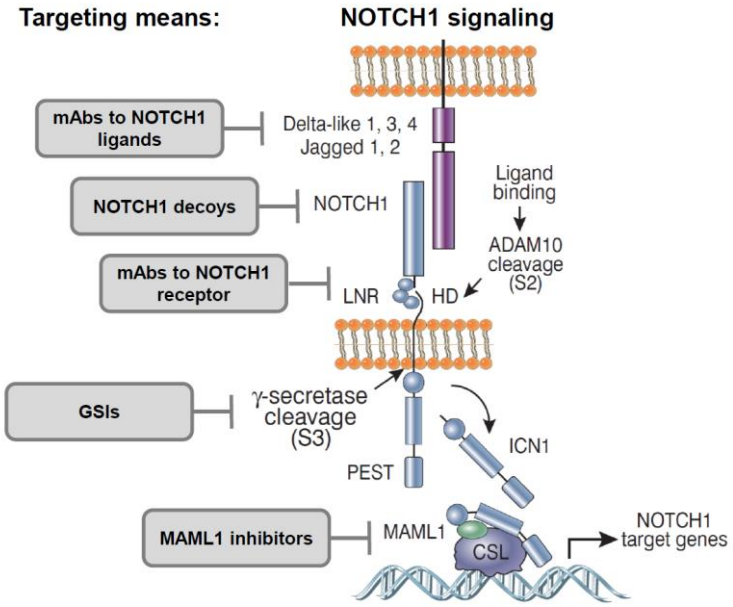

Figure 5. NOTCH1 signaling pathway and therapeutic means exploited to target aberrant activation. Adapted from (105) and (104).

Several approaches to target the NOTCH1 pathway have been proposed (104) (Figure 5). NOTCH1 activation can be prevented by blocking S3 cleavage using gamma secretase inhibitors (GSIs) (105). Initial GSI clinical trials, however, were halted because of life-threatening diarrhea caused by aberrant induction of intestinal Goblet cell differentiation (106). Alternatively, monoclonal antibodies (mAbs) have been developed to target NOTCH1 ligands or receptors. For instance, antibodies targeting DLL4 were found to promote human umbilical vein endothelial cell growth and disorganised angiogenesis (104). A recent study showed direct DLL4 effects on NOTCH1 signaling in T-ALL with wild-type NOTCH1 or NOTCH1 with mutations in the PEST domain (107).

Interesting alternative approaches to interfere with NOTCH1 signal activation have been proposed. Different EGF-like repeats of the NOTCH1 extracellular domain fused to human IgG Fc have been used to create a soluble NOTCH1 inhibitor called the 'NOTCH1 decoy' (108). This decoy recognises ligands

and prevents binding to the receptor. Though not widely considered as a druggable target, the NICD transcription complex could still be an attractive therapeutic option. For example, downregulation of MAML1 can be achieved by GSK3β (glycogen synthase kinase-3β) inhibition (109).

1.6.2. Overcoming death resistance in ALL

Evasion of apoptosis is a hallmark of human cancers. In leukemia, this may be mediated by oncogene activation following chromosomal translocation (110). Defects in apoptosis pathways are frequently associated with resistance to anti-cancer therapies. Apoptosis in ALL cells can be restored by inhibiting pro-survival proteins of the BCL and IAP (inhibitor of apoptosis protein) families. The BCL family consists of anti-apoptotic proteins (BCL-2, BCL-XL and MCL1), pro-apoptotic molecules (BAX, BAK) and BH3 domain-only molecules (BID, BIM, BIK, NOXA, PUMA) (111). Overexpression of BCL2, BCL-XL, and MCL1 have been associated with tumor initiation, progression, and chemoresistance (112). Several compounds have been recently developed and tested in the clinical trials targeting this axis, namely the BCL2 and BCL-XL inhibitor, navitoclax and the BCL2 inhibitor venetoclax. Although navitoclax has shown activity in hematological malignancies, the efficacy of this agent was limited by the BCL-XL inhibition-associated thrombocytopenia (113). In contrast, venetoclax is not associated with this dose-limiting toxicity and received FDA approval after successful clinical trials (114,115). Not all patients will benefit from venetoclax treatment, however, highlighting the need for patient preselection. As BCL2 family proteins regulate cellular fate, several biomarkers have been developed to predict tumor cell response to BCL2 and BCL-XL inhibition, such as BH3 profiling (116) and BCL2 family protein ratios (117). BH3 profiling is a functional assay that identifies the tumor cells' addiction to BCL2, BCL-XL and MCL1 using synthetic peptides.

A growing number of studies demonstrate that there are other programmed cell death pathways that could be exploited in cancer cells (118). For instance, necroptosis is a form of regulated necrosis that can be activated by death receptors under apoptosis-deficient conditions (119). IAP proteins have important roles in both apoptotic and necroptotic death pathways (120). Birinapant is a novel SMAC mimetic that can efficiently antagonise IAPs; it is currently being tested in clinical trials as a single agent and in combination with standard-of-care chemotherapy in solid tumors (121). Pre-clinical studies suggest that birinapant is a promising drug for leukemia patients (122).

1.6.3. Targeting cell cycle regulation

Cell proliferation controlling Rb-E2F and MDM2-p53 pathways are defective in most, if not all, human tumors, underscoring the central role of uncontrolled cell division in tumorigenesis (123). ALL represents a pathological manifestation of uncontrolled cell division; most of the tremendous success of ALL therapy have been achieved mostly with chemotherapy targeting DNA replication and cell division. Additionally, new therapeutics targeting cyclin-dependent kinases (CDKs) have been proposed as promising treatment alternatives (124). It has been demonstrated that many tumorigenic events drive proliferation by impinging CDK4 or CDK6 complexes in the G1 cell cycle phase (124). During cell cycle progression, CDKs 4/6 inactivate Rb, permitting E2F-mediated S-phase gene transcription (124). In leukemias, *CDKN2A/B* loss is a common event that leads to enhanced E2F activity. These and other

findings provide the rationale to test CDK inhibitors in ALL. The first generation of CDK inhibitors was relatively nonspecific and most clinical trials results have been disappointing (124). Second generation CDK inhibitors seemed to be particularly promising in pre-clinical studies, but only a few progressed past phase I clinical trials, such as dinaciclib (CDK1/2/5/9 inhibitor) (124), with clinical trials in MM (125) and CML (126) demonstrating significant dinaciclib clinical activity. It is difficult, however, to predict the anti-leukemic activity of such drugs.

Additionally, other means to inhibit cell proliferation are explored in clinical trials. Given the activity of the antitubulin agent vincristine, it is also possible that new anti-mitotic drugs such as namely Aurora kinase inhibitors may prove active in the therapy of ALL (127).

1.6.4. Approaches to target epigenetic changes in ALL

Mutations in epigenetic modifiers such as *CREBBP* and *SETD2* are enriched at relapse (39,128), and are in T-ALLs, particularly ETP-ALL (70). The histone methyltransferase DOT1L plays an important role in the *MLL* translocation-driven leukemic transformation and is an attractive therapeutic target (129). The small molecule EPZ-5676 has been developed to inhibit DOT1L enzymatic activity (130) and is currently being investigated in a Phase I clinical trial (NCT01684150).

Histone acetylation leads to chromatin remodelling, which alters gene expression (131): acetylation is usually associated with the transcription activation, while deacetylation leads to gene repression (131). Given the compelling evidence of HDAC involvement in tumor development and progression, HDAC inhibitors have emerged as attractive therapeutic options in hematologic malignancies (132). Vorinostat, an HDAC inhibitor, was identified as a promising candidate in relapse ALL samples (132). Currently, phase I-II clinical trials are evaluating the efficacy of several HDAC inhibitors as monotherapy and in combination with other chemotherapeutic agents for the treatment of pediatric ALL (133,134).

The bromodomain and extra-terminal (BET) family controls gene expression, mitosis and recently have emerged as a potential therapeutic targets in cancer (135). BRD4 has been found to be a critical in the leukemia maintenance and its inhibition ablated the expression and function of MYC (136). JQ1 is a novel compound designed to bind acetyl lysine pocket of the conserved BET domains (136). Gene expression analysis after JQ1 treatment revealed that *IL7R*, *MYC* and *BCL2* are among the most down-regulated genes (137,138). Currently, OTX015, a synthetic small molecule against BRD proteins is under evaluation in a phase I trial in relapsed leukemias (trial number: NCT01713582).

1.6.5. Immunotherapy

Monoclonal antibodies (mAbs) represent a new tool in the treatment of hematological malignancies. ALLs are particularly suitable for mAbs therapy because in most instances (with the possible exception of *MLL*, *BCR-ABL1* and biphenotypic leukemias) these express targetable lymphoid surface markers. The most investigated ALL targets include CD19, CD20, CD22, and CD52 (139). The surface antigen CD20 is found on 30% to 50% of BCP-ALL while CD19 is found almost on all BCP-ALL (140,141). The anti-CD20 antibody rituximab and bispecific anti-CD19 antibody blinatumomab have demonstrated significant clinical response (142-144). Other monoclonal antibodies targeting CD19 and CD22 are under evaluation in clinical trials of refractory-relapsed BCP-ALL with various success (139).

Additionally, immune checkpoints are involved in the downregulation of anti-tumor immunity. This function could be restored using mAbs against PD-1 (programmed cell death protein 1) and its principal ligand (PD-L1). PD-1 is expressed in activated T cells, B cells, and myeloid cells (145) while PD-L1 is highly expressed in leukemia cells (146). A phase I clinical trial with patients suffering from different hematopoietic malignancies demonstrated anti-PD-1 mAb efficacy (147).

Alternatively, T cells can be engineered to express a chimeric antigen receptor (CAR) and used for targeted immunotherapy against B-cell malignancies (141). Clinical trials have demonstrated striking clinical responses in patients with ALL that were otherwise considered incurable (148). The most common severe toxicity associated with CAR-T therapy is cytokine release syndrome (CRS), but it could be successfully resolved using interleukin-6 receptor (IL6R) inhibitor tocilizumab (148).

However, clinical trials indicate that many patients will develop resistance to immunotherapy and mechanisms underlying resistance acquisition has yet to be determined (149). In addition, immunotherapy in ALL is limited to BCP-ALL patients; T-ALL patients still need alternative treatment approaches.

1.6.6. Promising tyrosine kinase inhibitors for ALL

Currently, more than 25 tyrosine kinase inhibitors (TKIs) have been approved, and additional therapeutics are in various stages of clinical evaluation (150). These small molecules are designed to compete with adenosine triphosphate (ATP) binding and inhibit kinase activity. Kinase signaling pathways drive proliferation, survival, motility, metabolism, angiogenesis, and evasion of anti-tumor immune responses (97). The human genome codes >500 kinases (151), but many of these enzymes have unknown biology. Abnormal kinase activation results from multiple types of genetic and epigenetic changes (152) which result in increased kinase activity, overexpression, or loss of negative regulation (Table 4). The most frequent aberrations are somatic mutations in kinase conservative domain hotspots (153), constitutively activated chimeric forms (kinase translocations) or gene amplifications (150). Approximately 20% of BCP-ALL cases harbor kinase-activating lesions that may be targeted by TKIs.

Activation mechanism	Kinases
Point mutations	ACVR1B, ACVR2B, AKT1, ALK, ALPK2, ATM, BRAF, CDK12, CDK4, EGFR, EPHA2, ERBB2, ERBB3, FGFR1, FGFR2, FGFR3, FGFR4, FLT3, JAK1, JAK2, KIT, MAP2K1, MAP3K1, MAP4K3, MET, MTOR, PIK3CA, SGK1, STK19, TGFBR2
Gene amplification	CDK4, CDK6, CRKL, EGFR, ERBB2, FGFR1, FGFR2, FGFR3, FLT3, IGF1R, KIT, MET, PAK1, PDGFRA, PIK3CA, PRKCI
Gene amplification or fusion of a kinase ligand	FGF19 (FGFR4), HGF (MET), NRG1 (ERBB3), VEGFA (VEGFR)
Gene fusions	ALK, ABL1, BRAF, CRLF2, EGFR, FGFR1, FGFR2, FGFR3, FGR, JAK2, MET, NTRK1, NTRK2, NTRK3, PDGFRA, PDGFRB, PIK3CA, PRKACA, PRKCA, PRKCB, RAF1, RET, ROS1, SYK

Table 4. Examples of known mechanisms of kinase activation in cancer. Adapted from (150).

There are several FDA approved TKIs that target specific aberrations such as imatinib for the *BCR-ABL1*–positive leukemias; crizotinib and other ALK kinase inhibitors for the cancers driven by *ALK* fusions; lapatinib for *ERBB2*-amplified tumors; gefitinib and erlotinib for *EGFR* mutated tumors;

vemurafenib for *BRAF* mutant tumors and others (150). Each compound demonstrated clinical benefit, but most patients who initially responded later relapsed. In most cases, additional point mutations led to resistance mechanisms (150).

In 2001, imatinib became the first kinase inhibitor approved for targeted therapy against *BCR-ABL1*–positive leukemia (154). Unfortunately, 33% of patients develop resistance (155); consequently, new TKIs had to be developed. Dasatinib, a second generation BCR-ABL1 TKI, is a dual ABL1 and SRC inhibitor. Unlike imatinib, dasatinib crosses the blood–brain barrier and is active in CNS-infiltrating disease (156).

In addition, future therapies are likely to rely on combinations of inhibitors to prevent the emergence of resistance. For example, targeting the MAPK pathway (NRAS, MEK1/2) improved event-free survival in a melanoma resistant to the BRAF inhibitors (157).

1.7. Drug discovering approaches

Pre-clinical compound screening and validation is essential to ensure that the most promising drugs enter clinical trials. Drug discovery and development involve the utilisation of *in vitro* and *in vivo* experimental models. The selection and application of the correct model, as well as appropriate data analyses and interpretation, are critical to successfully advance candidate drugs. Previously it was widely believed that one drug might work for all patients, but this 'blockbuster' model completely failed in oncology. Nonetheless, drugs continue to be designed in a reductionist approach: one molecule – one target. Unfortunately, many patients do not respond to targeted therapies predicted by single biomarkers. Additional information has to be gleaned on tumor-associated pathway addictions. As our knowledge of drug response determinants improves, it seems that single-biomarker diagnostics will quickly become obsolete. While interest in one-size-fits-all drug discovery approaches is declining, the new approach – 'the right drug for the right patient' is emerging.

1.7.1. *In vitro* drug discovery models

Drug candidate and toxicity screenings rely on results from early-stage *in vitro* cell-based assays expected to represent essential aspects of *in vivo* pharmacology and toxicology. Several *in vitro* designs are optimised for the high-throughput screening applications where entire libraries of potential pharmacologically-relevant molecules can be screened.

1.7.1.1. Cell line based drug discovery

The National Cancer Institute's NCI-60 cell line panel, the most extensively-characterised set of cell lines in existence, is frequently used as a screening tool in drug discovery (158). This panel incorporated 60 different human tumor cell lines (brain, breast, colon, leukemia, lung, melanoma, ovarian, prostate and renal) (158). Since its inception, the NCI-60 panel has helped to unveil mechanisms of drug action and select drugs for clinical trials (159). Perhaps the most notable contribution of the NCI-60 to current cancer chemotherapy was the development of bortezomib, which was approved by the FDA in 2003 (158). As NCI-60 incorporates a relatively small number of cell lines, an extended panel of 1200 cell lines, known as CMT1000 platform, have been compiled in 2006 (160). Though this panel is much

larger, it poses certain technical challenges and is now rather used to investigate the genetic basis of sensitivity and resistance. For instance, the use of the CMT1000 platform enabled the response to ALK inhibitors to be correlated with ALK-activating chromosomal translocations, found in only 3–7% tumors, in non-small-cell lung carcinoma (NSCLC) (161). Similarly, NSCLC sensitivity to a PDGFR kinase inhibitor was associated with co-amplification of genes encoding PDGFR receptor and one of its ligands (161).

This approach has several limitations. For instance, cultured cell lines grow much faster than primary tumors. Moreover, genomic studies revealed that cell lines have upregulated growth-controlling genes (e.g. cell cycle and primary metabolic processes) (162). *In vitro* culture conditions affect characteristics and select for subpopulations of cells that differ from primary tumor (163), although it appears that driver mutations are nonetheless preserved (164). Nonetheless, the transcriptomic level differs so much that cancer cell lines bear more resemblance to each other rather than to the primary tumor they should represent (164). In addition, other *in vivo* factors modulate chemoresistance (e.g. tumor microenvironment) that are not represented in this model. Cell lines, however, are still widely used for initial compound selection as this model is technically simple and provides valuable indicative data of drug mechanistic activity and target interaction.

1.7.1.2. Primary tumor cell based drug discovery

More effort should be directed towards the development of new *ex vivo* models to test primary tumor samples. This approach requires to closely mimic the cancer microenvironment and to preserve primary tumor features. Such models offer several advantages. For instance, novel therapeutics can be evaluated considering primary tumor heterogeneity, which is not possible using cell lines. Additionally, *in vitro* drug responses of assays in primary cells correlate well with the clinical outcome (165). In the past, primary cell cultures successfully assisted the development of new anti-cancer drugs (166).

Several groups have developed methods for *in vitro* culture of patient ALL samples, including culture in suspension, on stromal feeders and under reduced oxygen conditions (167-169). The leukemia microenvironment plays an important role in modulating drug resistance (170,171), yet most drug discovery programmes involving high-throughput screening use monoculture ALL suspensions. Two distinct bone marrow microenvironment niches were identified, referred to as the osteoblastic (172) and the vascular (173) niches. The vascular niche, which is localised on the sinusoidal wall, is composed of reticular cells, endothelial cells, perivascular stromal cells and mesenchymal stromal cells (MSCs) (173). The osteoblastic niche, on the other hand, is comprised of osteoblasts, osteoclasts and MSCs. *In vitro* osteoblastic and vascular niche models could support primary leukemia cells and modulate drug response, thus proving superiority over monocultures.

1.7.1.3. 3D organoids

More complex 3D models, namely organoids, were developed to mimic multicellular architecture resembling human organs and solid tumors, derived from primary tissues or stem cells (174). Multicellular tumor spheroid models have been shown to recapitulate *in vivo*-like growth and have been used for high-throughput drug discovery (175). 3D cell cultures usually rely on hydrogels that promote

cell polarisation and interaction with other cells (176). In some instances, these anatomically correct spheroid models can model complex human conditions (177). Nonetheless, these still have serious limitations: for example, cells are usually not exposed to normal mechanical cues, including fluid shear stress, tension and compression, which influence organ development and function in health and disease (178).

1.1.1.1. Microfluidic Organ-on-a-chip

Recently, a new technology called organs-on-chips has been developed to overcome current primary cell model limitations. Organs-on-chips are microfluidic devices for culturing living cells in continuously perfused, micrometer-sized chambers mimicking physiological functions of tissues and organs. Organs-on-chips have great potential for the investigation of basic mechanisms of organ physiology and disease. Researchers have fabricated chips for multiple organs, including the spleen (179), bone marrow (180) and blood-brain barrier (181). Organs-on-chips can be used to model disease. For example, the lung-on-a-chip was used to model pulmonary edema induced by the cancer drug interleukin-2 (182). This approach might be used to investigate precision medicine further, especially in the context of microenvironment biological and physiological cues.

1.7.2. *In* vitro drug response analysis

Several curve fitting models are used to analyse *in vitro* drug response. Most drug response parameters are well captured by a classical 4-parameter logistic fit. Nevertheless, there are instances where the dose response curve presents more than one inflection point, or several outliers preclude an accurate data fit; there are also cases where a 3-parameter function might be more appropriate compared to a 4-parameter fit (183). In general, however, there are several parameters to evaluate tested sample sensitivity after exposing to multiple drug concentrations (Figure 6). A common parameter to estimate drug efficacy is IC_{50} (the concentration of a compound to achieve 50% cell reduction). Other parameters used to describe pharmacological drug *in vitro* effects include EC_{50} (concentration giving 50% of maximum response), AUC (area under the curve) and E_{max} (effect at the maximal concentration) (Figure 6). The IC_{50} is sometimes confused with the EC_{50}, which is the analogous quantity of interest when the response is increasing with dose. Several studies suggested that widely used IC_{50} parameter is not as accurate as AUC (184). AUC captures both E_{max} and IC_{50}. Nonetheless, the IC_{50} is still more appreciated as it indicates drug concentration rather than a parameter that does not translate directly to dosing information.

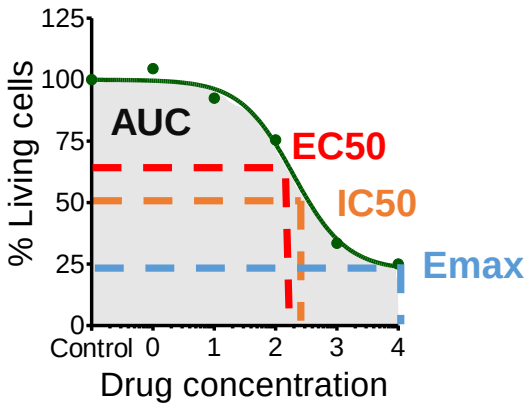

Figure 6. Key dose-response parameters (IC_{50}, EC_{50}, AUC and E_{max}) calculated following curve fitting to the cell survival data.

Alternative ways to represent quantitative drug sensitivity have been introduced, such as the Drug Sensitivity Score (DSS) (185). The curve fitting parameters are used to calculate the AUC relative to

the total area between 10% threshold and 100% inhibition. It is a new parameter and so far not widely accepted.

1.7.3. *In vitro* drug combination analysis

Drug combination therapy is commonly used in clinical practice in order to achieve synergistic therapeutic effects, which result in reduced drug doses and toxicity, and to minimise or delay the induction of drug resistance. To understand combined drug behaviour, scientists often perform *in vitro* combination studies, which typically entails tests using various concentration combinations of two drugs (combination matrix) followed by cell viability assessment. The aim of these tests is to determine whether the observed combination effect departs from the expected effect of treatment with either of the single drugs. There are various definitions of synergy, including Loewe additivity and Bliss independence. The degree of synergy is typically quantified using the Chou-Talalay method (186). The Combination Index (CI) are defined for additive (CI=1), synergistic (CI<1), and antagonistic (CI>1) effects. This method is based on the median-effect equation, in turn, derived from mass action kinetics (186). There are, however, several limitations to the CI. For instance, CI calculation methods are mainly for hyperbolic, and not sigmoidal, dose-effect relationships; furthermore, the CI takes only the degree of potency, but totally ignores the shape of the dose-effect curves (187). So far results are inconclusive if *in vitro* synergistic effects predict *in vivo* responses as some authors could find correlations (188) while others concluded the opposite based on the meta-analysis of clinical and pre-clinical data (189).

1.7.4. *In vivo* drug discovery and validation models

Historically, the murine system has played an important role in modeling human leukemia. Mouse models have been used to investigate leukomogenesis and to examine responses to therapies. Leukemia murine models can be subdivided into three categories: transplantable tumors, genetically engineered syngeneic models and humanised mouse models.

1.7.4.1. Transplantable tumors

Transplantable tumors have been used to investigate immunology and immunotherapy. Studies using these systems have uncovered many important mechanistic features: tumour-specific antigens, the intrinsic immunogenicity of dying tumour cells and anti-tumor immune responses by the host (190). The commonly used cell lines in this model either originated spontaneously or were induced by carcinogens in inbred mouse strains. Among the most thoroughly characterised models are the B16 melanoma, CT26 colon carcinoma, 4T1 breast carcinoma, EL4 T lymphoma, Lewis lung carcinoma (190).

1.7.4.2. Syngeneic murine ALL models

A greater knowledge of leukemia-initiating mutations has helped in engineering syngeneic mouse models (191). These models are used to study the leukemia microenvironment, given that some signaling factors (e.g. cytokines, growth factors) do not function across species, and would not be possible to study in the xenograft model. For example, the human CRLF2 receptor found on BCP-ALL does not interact with mouse ligands (192). To engineer transgenic BCP-ALL mice models, genomic aberrations have been introduced into the lymphoid compartment. Several syngeneic BCP-ALL mouse

models have been successfully developed (193) such as the *BCR-ABL1* (194), *TCF3-PBX1* (195) and *MLL* (193) translocation-driven murine leukemia models. Nonetheless, all attempts failed to generate *TCF3-HLF* (196) or *ETV6-RUNX1* (197) positive ALL murine models. It seems that there are secondary, and so far, unknown events that are necessary to initiate these BCP-ALL.

Development of syngeneic T-ALL models have been less successful. Nonetheless, there are few syngeneic mouse T-ALL models available. For instance, transgenic mice expressing NICD or bearing activating *NOTCH1* mutations could initiate T-ALL (198). Finally, overexpression of *TAL1* and *LYL1* have led to T-ALL formation in mice (199).

1.7.4.3. Patient derived xenograft (PDX) model

Engineering of the severe combined immunodeficiency (SCID) mouse was a major breakthrough that allowed engraftment of human hematopoietic cells (200). These mice have a deletion in *Prkdc* (involved in VDJ recombination), and do not have functional immune cells. However, these mice have functional NK cells. To improve the mode, a SCID-beige mouse was developed by adding a mutation in the lysosome trafficking regulator (Lyst), which helped reduce NK function. This model has been used to engraft primary leukemia samples (201). Similarly, NOD-SCID mice were generated by crossing the SCID mouse with the non-obese diabetic (NOD) mouse to further reduce NK cell function (200). Crossing the interleukin 2 receptor gamma knockout mice with the NOD-SCID mouse, an immunodeficient NOD-SCID IL2rγnull (NSG) mouse strain that completely lacks NK cells was bred. Successful leukemia engraftment has been achieved in NSG mice (202,203). Scientists have since used NSG mice to establish patient derived xenograft (PDX) models and expand primary cell repositories for biobanking. Recent studies demonstrated that PDXs preserve primary tumor clonal composition, mutation landscapes and gene expression patterns over serial transplantations (it is recommended not to exceed ten passages) (164,204).

1.8. Drug efficacy testing in mice models and transition into clinical trials

The traditional path of drug development passes from *in vitro* screening to the assessment of selected drugs in the mouse model. Testing new compounds *in vivo* typically include an analysis of drug pharmacology, pharmacodynamics and toxicology. Characterizing the relationship between the pharmacokinetics (concentration vs. time) and pharmacodynamics (effect vs. time) is used to select drug dosing schedules and effective concentration (205). In theory, if an *in vitro* system completely mimics the *in vivo* environment with respect to target interaction, then concentrations needed to reach *in vitro* effects (e.g. IC_{50}) should manifest into *in vivo* response. However, the extrapolation of *in vitro* to *in vivo* results a biomedical problem that remains to be solved. Nonetheless, single agent and combinations validation in PDX models correlated with clinical patient trial outcomes (164).

When a drug of interest has been evaluated in animal models and found to be safe, it is advanced into a phase I clinical trial. Transition into the clinical trials has to be managed very carefully, given that compound safety profiles in animals might not predict all toxicities in humans (206). Unfortunately, clinical trials in oncology have the highest failure rate (>93%, from entering phase I until FDA approval) compared with other therapeutic areas (average of 86%, (207)). While there are many aspects that

could cause these trials to fail, it is certain that drug and patient selection for follow-up procedures have to be optimized.

1.8.1. Are mouse models predictive for humans?

Mouse models are the most frequently-used animals in pre-clinical drug evaluation. Differences in pharmacokinetics in an animal model and humans may lead to results with limited relevance in clinical practice. Furthermore, humans may form a major metabolite that is not produced in the animals (and vice versa), resulting in a reduction of drug efficacy or having unpredicted side effects. For instance, fialuridine, a nucleoside analog, induced hepatic toxicity that led to five fatalities in a clinical trial (208). This severe toxicity had not been predicted from mouse studies (208). Finally, drug bioavailability (the fraction of a drug that reaches the systemic circulation) in animals is frequently different compared to humans (209). So far researchers are struggling to accurately predict how therapeutics will behave in humans based on animal studies.

2. Subject of the investigation and my contribution

Rapid incorporation of new agents into clinical protocols has been hampered by the lack of predictive biomarkers to select patients that would benefit from treatment. Identification of genetic ALL signatures is often insufficient to determine druggable targets or to convey prognostic information. To address this, we propose systematic drug response profiling of primary samples that can provide functional data which might be eventually associated with biological ALL features. The major aims of my PhD thesis were:

1. To establish an *in vitro* drug response profiling platform for primary ALL cells and perform screening of leukemia samples with the most dismal prognoses.
2. To identify new agents with distinct activity in selected ALL subtypes with unmet therapeutic needs
3. To perform synthetic lethality screenings for selected agents.
4. To evaluate candidate drug activity in a xenograft model in single agent or in combination with standard-of-care chemotherapy.

My project resulted in four publications to which I significantly contributed:

- Manuscript 1: *Ex vivo* drug response profiling detects extraordinary drug activity in resistant ALL (equal first author)
  Major contributions to all Figures.

- Manuscript 2: Targeting BET family proteins improves the therapeutic efficacy of BCL-2 inhibition in T-cell acute lymphoblastic leukemia (equal first author)
  Major contributions to Figures 1, 2, 5; Supplemental Figures 1-4

- Manuscript 3: Cell and molecular determinants of in vivo efficacy of the BH3 mimetic ABT-263 against pediatric acute lymphoblastic leukemia xenografts. (fourth author)
  Major contributions to Figure 4; Supplemental Figure 4, 7

- Manuscript 4: Genomics and drug profiling of fatal *TCF3-HLF*–positive acute lymphoblastic leukemia identifies recurrent mutation patterns and therapeutic options
  Major contributions to Figure 5, 6

3. Results

Manuscript 1

Ex vivo drug response profiling detects extraordinary drug activity in resistant ALL

Viktoras Frismantas[1,2,*], Maria Pamela Dobay[3*], Anna Rinaldi[1,2,*], Joelle Tchinda[1,2], Samuel H. Dunn[4], Joachim Kunz[5], Paulina Richter-Pechanska[5], Blerim Marovca[1,2], Orrin Pail[1,2], Silvia Jenni[1,2], Ernesto Diaz-Flores[6], Bill H. Chang[7], Timothy J. Brown[8], Robert H. Collins[8], Salome Higi[1,2], Sabrina Eugster[1,2], Pamela Voegeli[9], Mauro Delorenzi[3,10], Gunnar Cario[11], Mignon L. Loh[12], Martin Schrappe[11], Martin Stanulla[13], Andreas E. Kulozik[5], Martina U. Muckenthaler[5], Vaskar Saha[14,15], Julie A. Irving[16], Roland Meisel[17], Thomas Radimerski[18], Arend Von Stackelberg[19,20,21], Cornelia Eckert[19,20,21], Jeffrey W. Tyner[22], Peter Horvath[23,24], Beat C. Bornhauser[1,2,*] and Jean-Pierre Bourquin[1,2,*]
*equal contribution to this work

Abstract

Drug sensitivity and resistance testing on diagnostic leukemia samples should provide important functional information to guide actionable target and biomarker discovery. We provide proof of concept data by profiling 60 drugs on 68 acute lymphoblastic leukemia (ALL) samples mostly from resistant disease in co-cultures on bone marrow stromal cells. Patient-derived xenografts retained the original pattern of mutations found in the matched patient material. Stromal co-culture did not prevent leukemia cell cycle activity, while a specific sensitivity profile to cell cycle related drugs identified samples with higher cell proliferation both *in vitro* and *in vivo* as leukemia xenografts. In cases with refractory relapses, individual patterns of marked drug resistance, but also exceptional responses to new agents of immediate clinical relevance were detected. The BCL2-inhibitor venetoclax was highly active below 10 nM in BCP-ALL subsets including *MLL-AF4* and *TCF3-HLF* ALL, and in some T-ALLs, predicting *in vivo* activity as a single agent and in combination with dexamethasone and vincristine. Unexpected sensitivity to dasatinib with IC50 values below 20 nM was detected in two independent T-ALL cohorts, which correlated with similar cytotoxic activity of the SRC Inhibitor KX2-391 and inhibition of SRC phosphorylation. A patient with refractory T-ALL was treated with dasatinib based on drug profiling information and achieved a five-month remission. Thus, drug profiling captures disease-relevant features and extraordinary sensitivity to relevant drugs, which warrants further exploration of this functional assay in the context of clinical trials in order to personalize drug repurposing strategies for patients with urgent medical needs.

For detailed information see attached Manuscript 1.

Manuscript 2

Targeting BET proteins improves the therapeutic efficacy of BCL-2 inhibition in T-cell acute lymphoblastic leukemia

Sofie Peirs[1,2,*], Viktoras Frismantas[3,*], Filip Matthijssens[1,2], Wouter Van Loocke[1,2], Tim Pieters[1,2,4,5], Niels Vandamme[2,4,5], Béatrice Lintermans[1,2], Maria Pamela Dobay[6], Geert Berx[2,4,5], Bruce Poppe[1,2], Beat C Bornhauser[3], Jean-Pierre Bourquin[3,**] and Pieter Van Vlierberghe[1,2,**]
*equal contribution to this work

Abstract

Inhibition of anti-apoptotic BCL-2 has recently emerged as a promising new therapeutic strategy for the treatment of a variety of human cancers, including leukemia. Here, we used T-cell acute lymphoblastic leukemia as a model system to identify novel synergistic drug combinations with the BH3 mimetic venetoclax (ABT-199). *In vitro* drug screening in primary leukemia specimens that were derived from patients with high risk of relapse or relapse and cell lines revealed synergistic activity between venetoclax and the BET bromodomain inhibitor JQ1. Notably, this drug synergism was confirmed *in vivo* using a T-ALL cell line xenograft model. Moreover, the therapeutic benefit of this drug combination might, at least in part, be mediated by an acute induction of the pro-apoptotic factor *BCL2L11* and concomitant loss of BCL-2 upon BET bromodomain inhibition, ultimately resulting in an enhanced binding of BIM (encoded by *BCL2L11*) to BCL-2. Altogether, our work provides a rationale to develop a new type of targeted combination therapy for selected subgroups of high-risk leukemia patients.

For detailed information see attached Manuscript 2.

Manuscript 3

Cell and molecular determinants of *in vivo* efficacy of the BH3 mimetic ABT-263 against pediatric acute lymphoblastic leukemia xenografts.

Santi Suryani[1,‡], Hernan Carol[1,‡], Triona Ni Chonghaile[2], Viktoras Frismantas[3], Chintanu Sarmah[1], Laura High[1], Beat Bornhauser[3], Mark J Cowley[4], Barbara Szymanska[1], Kathryn Evans[1], Ingrid Boehm[1], Elise Tonna[1], Luke Jones[1], Donya Moradi Manesh[1], Raushan T. Kurmasheva[5], Catherine Billups[6], Warren Kaplan[4], Anthony Letai[2], Jean-Pierre Bourquin[3], Peter J Houghton[5], Malcolm A Smith[7], and Richard B Lock[1]

‡equal contribution to this work

Abstract

PURPOSE: Predictive biomarkers are required to identify patients who may benefit from the use of BH3 mimetics such as ABT-263. This study investigated the efficacy of ABT-263 against a panel of patient-derived pediatric acute lymphoblastic leukemia (ALL) xenografts and utilized cell and molecular approaches to identify biomarkers that predict *in vivo* ABT-263 sensitivity.

EXPERIMENTAL DESIGN: The in vivo efficacy of ABT-263 was tested against a panel of 31 patient-derived ALL xenografts composed of MLL-, BCP-, and T-ALL subtypes. Basal gene expression profiles of ALL xenografts were analyzed and confirmed by quantitative RT-PCR, protein expression and BH3 profiling. An *in vitro* coculture assay with immortalized human mesenchymal cells was utilized to build a predictive model of *in vivo* ABT-263 sensitivity.

RESULTS: ABT-263 demonstrated impressive activity against pediatric ALL xenografts, with 19 of 31 achieving objective responses. Among BCL2 family members, *in vivo* ABT-263 sensitivity correlated best with low MCL1 mRNA expression levels. BH3 profiling revealed that resistance to ABT-263 correlated with mitochondrial priming by NOXA peptide, suggesting a functional role for MCL1 protein. Using an *in vitro* coculture assay, a predictive model *of in vivo* ABT-263 sensitivity was built. Testing this model against 11 xenografts predicted *in vivo* ABT-263 responses with high sensitivity (50%) and specificity (100%).

CONCLUSION: These results highlight the in vivo efficacy of ABT-263 against a broad range of pediatric ALL subtypes and shows that a combination of *in vitro* functional assays can be used to predict its *in vivo* efficacy.

For detailed information see attached Manuscript 3.

Manuscript 4

Genomics and drug profiling of fatal *TCF3-HLF*–positive acute lymphoblastic leukemia identifies recurrent mutation patterns and therapeutic options

Ute Fischer[#1], Michael Forster[#2], Anna Rinaldi[#3], Thomas Risch[#4], Stéphanie Sungalee[#5], Hans-Jörg Warnatz[#4], Beat Bornhauser[3], Michael Gombert[1], Christina Kratsch[6], Adrian M. Stütz[5], Marc Sultan[4], Joelle Tchinda[3], Catherine L. Worth[4], Vyacheslav Amstislavskiy[4], Nandini Badarinarayan[2], André Baruchel[7], Thies Bartram[8], Giuseppe Basso[9], Cengiz Canpolat[10], Gunnar Cario[8], Hélène Cavé[11], Dardane Dakaj[3], Mauro Delorenzi[12,13], Maria Pamela Dobay[13], Cornelia Eckert[14], Eva Ellinghaus[2], Sabrina Eugster[3], Viktoras Frismantas[3], Sebastian Ginzel[1,15], Oskar A. Haas[16], Olaf Heidenreich[17], Georg Hemmrich-Stanisak[2], Kebria Hezaveh[1], Jessica I. Höll[1], Sabine Hornhardt[18], Peter Husemann[1], Priyadarshini Kachroo[2], Christian P. Kratz[19], Geertruy te Kronnie[9], Blerim Marovca[3], Felix Niggli[3], Alice C. McHardy[6], Anthony V. Moorman[17], Renate Panzer-Grümayer[16], Britt S. Petersen[2], Benjamin Raeder[5], Meryem Ralser[4], Philip Rosenstiel[2], Daniel Schäfer[1], Martin Schrappe[8], Stefan Schreiber[2], Moritz Schütte[20], Björn Stade[2], Ralf Thiele[15], Nicolas von der Weid[21], Ajay Vora[22], Marketa Zaliova[19,23], Langhui Zhang[1,24], Thomas Zichner[5], Martin Zimmermann[19], Hans Lehrach[4,20,25], Arndt Borkhardt[1,27], Jean-Pierre Bourquin[3,27], Andre Franke[2,27], Jan O. Korbel[5,27], Martin Stanulla[19,27], Marie-Laure Yaspo[4,27]

[#]equal contribution to this work

Abstract

TCF3-HLF–fusion positive acute lymphoblastic leukemia (ALL) is currently incurable. Employing an integrated approach, we uncovered distinct mutation, gene expression, and drug response profiles in *TCF3-HLF*–positive and treatment-responsive *TCF3-PBX1*–positive ALL. Recurrent intragenic deletions of *PAX5* or *VPREB1* were identified in constellation with *TCF3-HLF*. Moreover somatic mutations in the non-translocated allele of *TCF3* and a reduction of *PAX5* gene dosage in *TCF3-HLF* ALL suggest cooperation within a restricted genetic context. The enrichment for stem cell and myeloid features in the *TCF3-HLF* signature may reflect reprogramming by *TCF3-HLF* of a lymphoid-committed cell of origin towards a hybrid, drug-resistant hematopoietic state. Drug response profiling of matched patient-derived xenografts revealed a distinct profile for *TCF3-HLF* ALL with resistance to conventional chemotherapeutics, but sensitivity towards glucocorticoids, anthracyclines and agents in clinical development. Striking on-target sensitivity was achieved with the BCL2-specific inhibitor venetoclax (ABT-199). This integrated approach thus provides alternative treatment options for this deadly disease.

For detailed information see attached Manuscript 4.

4. Discussion

In this dissertation I describe a top-to-bottom drug discovery approach where we use our established primary ALL high-throughput drug profiling platform to identify remarkable patient sensitivity patterns that would not have been predicted from genomic information. Moreover, functional ALL response could be linked to biomarkers, and response patterns could be replicated in the xenograft model. Finally, we are evaluating screening platform in the co-clinical setting.

4.1. The biobank of patient derived xenografts (PDX)

Pediatric ALL patients that fail induction therapy or suffer from the relapse have poor survival (4). The treatment outcome of the more favourable relapse subgroups has been improved due to better patient selection for the HSCT (210). Nonetheless, high-risk patients, who represent more than one-third of the relapsed ALL cases, have event-free survival probabilities below 30% (211). About 10% of patients, so-called relapse refractory cases, will not respond at all to salvage chemotherapy. In addition, only a subset (7-23%) of the relapsed T-ALL patients survive beyond five years treated with current salvage chemotherapy (212). As a part of European BFM consortium, we had access to the biobank of diagnostic and relapse samples of the AEIOP-BFM-ALL (*de novo* resistant cases) and IntReALL (heavily pre-treated cases) studies. We selected high-risk patients based on cytogenetic features (Table 3) and MRD status to establish the PDX biobank. Currently the PDX biobank contains more than 250 ALL cases from groups that need treatment improvement. In collaboration with the Berlin–Frankfurt–Münster (BFM) study group partners, we aimed to expand our collection with the T-ALL samples.

Primary samples were transplanted using intra-femural (IF) injections into NSG mice as established in our laboratory (213). This method demonstrated superiority over intra-venous (IV) transplantation in limited dilution experiments (214). Overall we transplanted 52 matched diagnostic and relapsed T-ALL samples, of which 37 (71%) have engrafted. Notably, relapse cases initiated leukemia more frequently than diagnostic samples (~85% vs. ~60%). In the final PDX sample cohort, we had 14 matched T-ALL PDX pairs (same patient diagnosis and relapse cases). All PDX identity were confirmed by sample fingerprinting. Engraftment success was similar as for BCP-ALL. So far, we have not explored why relapse cases have superior engraftment rates in NSG mice, but it might be that relapse ALL are less dependent on microenvironment signals. In addition, we and others (215) observed that some cases engraft in both female and male mice, while others preferentially engraft in one gender, which is not related to the ALL patients' gender. The reason for these differences are currently unknown, but it is possible that the different sex hormones influence the niche where the ALL cells engraft.

4.1.1. PDX preserve genetic features of the primary ALL samples

We have used several approaches to investigate PDX and primary ALL sample mutational landscapes. T-ALL samples have been analysed using MLPA (Multiplex Ligation-dependent Probe Amplification) to detect copy number alterations (CNS) together with targeted sequence of the selected genes. Additionally, a panel of 52 genes – selected by the members of IntReALL and AEIOP-BFM-ALL study groups – have been sequenced in BCP-ALL primary and PDX samples. BCP-ALL cases without established abnormalities (B-others) or targetable kinase-activating lesions were analysed with

fluorescence in-situ hybridization (FISH) to detect rare translocations. Results are reported in Manuscript 1. In contrast to previous publications (216), primary T-ALL patients' driver oncogenic mutations (e.g. *NOTCH1*, *WT1*, *PTEN*, *IL7R* etc.) were preserved in PDX samples. BCP-ALL PDX samples were enriched for some of the frequently mutated genes including, RAS pathway mutations (*KRAS* and *NRAS*), *TP53* and *NT5C2* genes. Overall, 75% of the mutations were preserved by the xeno-amplification of the BCP-ALL samples. Similar findings have been reported in Manuscript 4, where we performed exome and transcriptome sequence of primary and PDX samples derived from the BCP-ALL with *TCF3-PBX1* or *TCF3-HLF* translocations.

Given that targeted sequencing provides limited information, we therefore performed more detailed analyses of selected samples. In collaboration with the Kulozik group (University Hospital of Heidelberg), we performed whole exome sequence (WES) for eleven paired T-ALL primary and PDX cases (Figure 7). In agreement with our previous observations, T-ALL mutational landscapes have been largely preserved in PDX. Mutations in the *NOTCH1*, *WT1* etc. driver genes were present in almost all analysed T-ALL primary and matching PDX cases. Moreover, the fraction of clones bearing mutations in the PDX samples remained similar to those in matching primary samples (Figure 7).

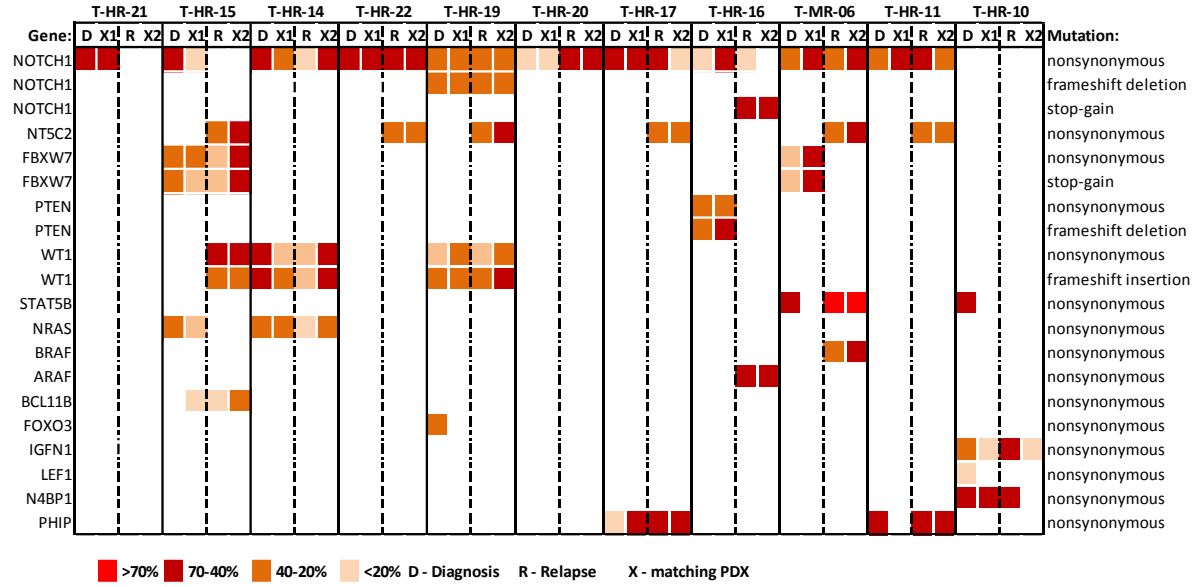

Figure 7. Whole exome sequence of the eleven paired T-ALL primary and PDX samples. Most recurrent mutations had been selected. The allelic frequency of the mutation is indicated as a heatmap.

As previously reported, some of the relapsed T-ALL have gained mutations in the *NT5C2* gene. Two cases lost *NOTCH1* gene mutations (Figure 7). Apart from these two genes, there are very few other recurrent mutations across the samples. Few mutations have been either lost or gained after PDX amplification (Figure 7). Note that mutation gains and losses in both the PDX or primary sample occur at a low frequency. To confirm the presence of such low-frequency mutations, we will need to perform ultra-deep sequence. These results allow us to conclude that there are rarely (if at all) introduced *de novo* mutations during amplification in the mouse.

In my thesis, I have collected compelling evidence that leukemia expansion in NSG mice preserved tumor heterogeneity that is support by other published data (202,217).

4.2. Establishing high-throughput drug profiling platform for the primary ALL

Oncology has become the largest therapeutic area in the pharmaceutical industry (218). The majority of new drugs originated from target-based discovery, with only about 32% of all FDA approved molecules discovered using phenotype-based approaches (219). Moreover, the majority of the first-in-class molecules were discovered without previously validated molecular mechanisms of action (219). For the past 50 years, drug discovery has relied on cancer-derived cell lines (220). However, cell line models are poor surrogates of the actual disease (221). Therefore new *in vitro* models are needed to improve drug pre-clinical selection.

Previously, drug response profiling platforms have been established using primary leukemia monocultures (e.g. AML (185) and ALL (222)).This approach offers several advantages. For instance, the primary tumor sample provides a representative clonal composition of the disease, and can therefore capture any relevant differences in response. In addition, primary samples demonstrate marked differences compared with cell lines drug response (223). It is important to mention that it is difficult to culture primary cells *ex vivo* and external cues for survival have to be added (e.g. feeder cells, cytokines). The tumor microenvironment contributes to the cancer cell survival, metastasis and drug resistance, therefore there is a very strong rationale to incorporate these into screenings.

4.2.1. Mesenchymal stromal cells (MSC) provide long-term support for the primary ALL

The lack of suitable *in vitro* culture conditions for primary ALL cells prevents their use in *in vitro* drug testing. Several methodological approaches to maintain primary ALL cells *ex vivo* were developed using cytokine-enriched media (224) or in co-culture with feeder cells from bone marrow (171). Short-term *in vitro* ALL monoculture assays have been previously used for testing drugs (167-169). However, their use has not been widely adopted as ALL cell viability rapidly declines even without exposure to any anti-leukemic compounds. We and others have demonstrated that immortalised normal human mesenchymal stem cells (MSCs) provide long-term support for the patient-derived ALL samples ((224), Manuscript 1). We have demonstrated that some of the primary ALLs depend on cell-to-cell contact with MSCs, while some only require soluble factors. Only a small fraction (~10%) was not supported (225). We have tested several mesenchymal stromal cell lines that have previously been used for the co-culture: human MSC (225), murine OP9 stromal cells (226), human HS-5 (227) or murine 3T3 (228). They all have provided adequate support for the primary ALL *in vitro*. Among these, we chose MSCs for further assays as this cell line grows slowly, does not spontaneously differentiate, and could be in co-culture for a long time without the requirement for frequent medium change or culture splitting.

4.2.2. Primary ALL *in vitro* survival and proliferation in co-culture with MSCs

We have characterised our ALL co-culture model in terms of cell proliferation and apoptosis over the course of time. Most of the currently available ALL chemotherapy target proteins or structures involved in the cell proliferation (microtubule, aurora kinase, or topoisomerase inhibitors, or antimetabolites). Therefore these compounds have to be tested on proliferating cells. Furthermore, some compounds

target anti-apoptotic proteins. If primary ALL cells *in vitro* are undergoing rapid apoptosis independently of the treatment, it could interfere with the response to compounds targeting cell death pathways.

We have analysed primary ALL behaviour (proliferation and apoptosis rates) in our established drug screening platform. We determined the proportion of ALL cells in S-phase and apoptosis rates at different time points (day 1, 4 and 7, reported in Manuscript 1). All tested samples had a variable proportion of cells in S-phase (from 10 to 70%). Interestingly, a greater number of tested T-ALLs have more than 40% of cells in S-phase compared to BCP-ALLs. These results correlate with observed rapid T-ALL cell increase *in vitro* as opposed to BCP-ALL. The proportions of cells in different proliferation stages were maintained at measured time points. Finally, we measured the proportion of apoptotic ALL cells for each sample by 7-AAD staining. Changes in live ALL cell counts at day 4 in co-culture was dependent on the ratio of cells in S-phase and fraction of apoptotic cells. If the ratio (S-phase/apoptotic cells in %) was greater than 1, then the counted cell number at day 4 were greater than what was seeded.

4.2.3. Compound library

We have selected compounds for our screening platform mostly based on their clinical relevance. Most of the included therapeutics are in the late clinical or pre-clinical investigation. To set up our drug response profiling platform, we used 384-well plate-handling robots. Eppendorf EpMotion 5070 and Tecan D300 robots were used for dispensing drugs. We initially selected 102 compounds that target hallmarks of cancer (discussed in the 1.6. section). Our compiled library included standard of care ALL drugs, compounds targeting epigenetic regulators, cell death-regulating proteins, various kinase inhibitors and other relevant compounds (Table 5). We handled our small molecule compound library according to published recommendations (229). Briefly, we diluted all compounds in DMSO (to reach 10mM concentration) and stored these in -80C. Thawing was not performed more than four times.

For the pilot study, we have analysed compounds in five concentrations (duplicates). Screening revealed that not all compounds were effective as predicted by others (discussed in other chapters). We have revised our library and included new experimental drugs and excluded those that were ineffective across all the samples tested in a pilot batch. Eventually, we reduced the list to 85 compounds that we are currently using. In the final screening setup, we have used eight drug concentrations (in duplicates) covering an adjusted dose range per compound. This dose range is based on the full response ranges observed in pilot screens. Screening results had been reported in Manuscript 1.

	Drug classes			Drug Name	Synonyms	Initial	Final
1	Antimetabolites			Clofarabine			
2				Cytarabine			
3				Gemcitabine			
4				6-mercaptopurine			
5				Methotrexate			
6				6-thioguanine			
7				5-azacitidine			
8	Antimitotics		Microtubule	Docetaxel			
9			Microtubule	Paclitaxel			
10			Microtubule	Vincristine			
11	Glucocorticoids			Dexamethasone			
12				Prednisolone			
13	Topoisomerase inhibitors		Topoisomerase II	Doxorubicine			
14				Etoposide			
15				Idarubicine			
16				Mitaxantrone			
17			Topoisomerase I	Toptecan			
18	Epigenetic regulators	HSP inhibitors	HSP70	Elesclomol			
19			HSP90		AT13387		
20					KW-2478		
21				Luminespib	NVP-AUY922		
22				NVP-HSP990	NVP-HSP990		
23					PU-H71		
24		HDAC inhibitors	HDAC1/3	Entinostat	MS-275		
25			HDAC	Givinostat	ITF2357		
26			pan-HDAC	Panobinostat	NVP-LBH589		
27			pan-HDAC	Vorinostat			
28			HDAC6	Nexturstat A			
29			HDAC1/3		RG2833		
30		BET bromdomains inhibitors	BRD3/4		iBET		
31			BRD4		JQ-1		
32			BRD2/3/4		OTX015		
33			BD2		RVX-208		
34	Cell death		BCL2	Venetoclax	ABT-199		
35			BCL2, BCL-XL	Navitoclax	ABT-263		
36			BCL family	Obatoclax	GX15-070		
37			Survivin promoter		YM155		
38			SMAC mimetic	Birinapant			
39			SMAC mimetic		NVP-LCL161		
40			RIP1		Necrostatin-1		
41			PARP	Olaparib	AZD-2281		
42			PARP	Veliparib	ABT-888		
43			Telomerase		BIBR-1532		
44	Proteosome inhibitors			Bortezomib	Velcade		
45				Carfilzomib			
46	Transcription		NOTCH1		Compound A		
47					CB103		
48			GSI		DAPT		
49					MK0752		
50			WNT/B-CATENIN		XAV-939		

	Drug classes			Drug Name	Synonyms	Initial	Final
51	Kinase inhibitors	AURK/PLK/CDK	AURORA A/B, JAK2/3		AT9283	■	■
52			AURORA A/B/C		ZM-447439	■	■
53			AURORA B	Barasertib	AZD1152-HQPA	■	■
54			CDK1		RO-3306	■	
55			CDK1/2/5/7/9		CGP-60474	■	■
56			CDK1/2/5/9	Dinaciclib	SCH727965		■
57			CDK4/6	Palbociclib	PD-0332991	■	
58			CDKs	Seliciclib		■	
59			CHK		AZD-7762		■
60			PDK1, TBK1, IKK, AURKB		BX795	■	■
61			PLK1/2/3		BI-2536	■	■
62			PLK1/3		GW843682X	■	
63			RHO		6H05		■
64			RSK1/2/3/4, PLK1, AURKB		BI-D1870	■	
65		PI3K/AKT/mTOR	AKT1/2/3	Ipatasertib	GDC-0068		■
66			AKT1/2		AKT1/2 inhibitor	■	
67			AKT1/2/3		MK-2206	■	■
68			mTOR		AZD8055	■	■
69				Everolimus	RAD001	■	
70					PP242	■	■
71				Temsirolimus		■	■
72					TORIN-1	■	■
73			pan-PI3K	Buparlisib	NVP-BKM120	■	■
74			PI3K		NVP-BYL719	■	
75			PI3K/mTOR	Dactolisib	NVP-BEZ235	■	■
76		RTK/SRC/SYK/ITK/JAK	ABL1, SRC	Dasatinib		■	■
77			BCR-ABL1, PDGFR, c-KIT	Imatinib	NVP-STI571	■	■
78			BCR-ABL1, PDGFR, c-KIT	Nilotinib	NVP-AMN107	■	■
79			BTK		BTK inhibitor I	■	
80			BTK, BLK, BMX, CSK	Ibrutinib	PCI-32765		■
81			c-MET		PHA-665752	■	
82			EGFR	Gefitinib		■	
83			EPHB4, RAF, SRC, ABL		NVP-BHG712		■
84			FAK		PF-00562271	■	
85			Pan-FGFR		NVP-BGJ398	■	■
86			FLT3	Quizartinib	AC220		■
87			FLT3, c-KIT, VEGFR2, PDGFR, PKC	Midostaurin	NVP-PKC412	■	■
88			FLT3, JAK2, TRKA	Lestaurtinib	CEP-701	■	■
89			IGF1R		NVP-AEW541	■	■
90			IGF1R, AURORA A, SRC		XL228	■	■
91			ITK		BMS-509744	■	■
92			JAK1/2	Ruxolitinib			■
93			JAK1/2/3	Momelotinib	CYT387		■
94			JAK2		NVP-BVB808	■	■
95			JAK2, FLT3, RET	Fedratinib	SAR302503		■
96			JAK2, TYK2, JAK3, JAK1		NVP-BSK805	■	■
97			PDGFRA, PDGFRB	Crenolanib	CP-868596		■
98			PDGFRA, PDGFRB, VEGFR, KIT, FLT3	Sunitinib		■	■
99				Sorafenib		■	
100			SRC		KX2-391		■
101			SRC family, ABL1	Saracatinib	AZD-0530	■	
102			SYK		BAY 61-3606	■	■
103			VEGFR	Axitinib		■	
104				Vatalanib	NVP-PTK787	■	
105			VEGFR, ERBB1, HER2		NVP-AEE788	■	
106			VEGFR,FGFR, PDGFR	Dovitinib	NVP-TKI258	■	■
107		RAF/MEK/JNK	JNK		AEG 3482	■	
108			MEK, ERK		PD-0325901	■	■
109			MEK1/2	Trametinib	GSK1120212		■
110			MEK1, ERK1/2	Selumetinib	AZD6244	■	■
111			RAF, VEGFR2		NVP-RAF265	■	■
112			RAF, VEGFR2, DDR2, LYN		AZ628	■	
113		Other	AMPK		COMPOUND C	■	
114			GSK-3		GSK-3 inhibitor IV	■	
115			SGK1		GSK-650394	■	
116	Other inhibitors		NFKB1	Parthenolide		■	
117			P53		PRIMA-1	■	
118			P53 MDM2 antagonist		NUTLIN-3	■	■
119			CRM1	Selinexor	KPT-330		■
120			SMO antagonist	Erismodegib	NVP-LDE225	■	
121			Metalloproteinase	Tosedostat	CHR2797	■	
122			Phosphodiesterase	Rolipram		■	

Table 5. Compound library. Grey blocks under the “Initial” and “Final” columns indicate which compounds were used in the pilot and final screens.

4.2.4. Adapting automated live cell imaging

Biochemical assays are commonly used to assess cell viability. These methods are based on the tetrazolium or resazurin reduction, protease markers, and ATP detection (230), and provide fast, indirect readouts of cell viability. However, their use is also associated with a few disadvantages. For instance, some of the compounds could be autofluorescent and distort the results. In addition, these methods offer no direct information about cell-to-cell heterogeneity or subcellular localisation. Given that our setup is an ALL co-culture with MSCs, indirect cell viability readouts assessing metabolic activity would be insufficient to discriminate live ALLs from the dead cells and MSCs. In particular, MSCs are more resistant to tested compounds, and would inflate viability, while contributing to variability, in the indirect readout.

Flow cytometry and high content imaging help overcome these limitations. With these methods, several cell types can be analysed simultaneously. Flow cytometry, however, is time-consuming, so we have restricted its use to validation of results for selected active drugs detected in the screening. The latest advances in fluorescence imaging technologies can be applied to the complex *in vitro* model systems to distinguish several cell types in a rapid manner. We thus used the automated high-throughput fluorescent microscopy approach to asses ALL cell viability.

4.2.4.1. Live cell staining

We needed a live cell staining protocol that discriminates between dead ALL background, live ALLs and MSCs. There are multiple established viable cell stains (231), including calcein acetoxymethyl ester (calcein AM) and ethidium homodimer-1 (EHD). Calcein AM detects esterase activity in live cells, while EHD stains dead cells that had lost membrane integrity. We selected the cell viability dye CyQuant (Life technology), which provided the highest contrast between live ALLs, MSCs and dead ALL background (Figure 8). This dye has two components: one intercalates with the DNA in all cells, while the second component penetrates only dead cell nuclei, where it suppresses the signal of the first component. MSC nuclei are larger than ALL nuclei, and DNA in ALL cells are more condensed. DNA condensation makes the signal intensity in ALL cells much higher. While we have used cell viability staining to indicate cell death in this project, other readout parameters should be considered in the future. For instance, some of the drugs modulate cell behaviour without initiating cell death signaling. Drug-induced effects can be manifested as changes in cell shape and size, migration patterns, or interactions with MSCs. Such modifications can be vital for the ALL cells in the context of some drugs, and such additional information might improve drug selection for further analysis. There is also a great interest to discriminate between cell death pathways. Recently, there have been a number of staining methods developed to identify events linked to autophagy, apoptosis or necroptosis; these methods could be integrated in the drug screening platform in the future (232).

A microscopy-based approach has its own pitfalls. For instance, standard microscopes can be focused on the plate's bottom, and cannot be used to visualize cells in the supernatant. Other research groups reported that ALL can migrate beneath the MSC layer (pseudoemperipolesis) (233), and cannot be detected with the microscope. In order to check this, we validated our screening results using flow cytometry. As we reported in Manuscript 1, the correlation between microscopy and flow cytometry is

very high (Spearman ρ>0.8). Clearly, these issues could be addressed using advanced fluorescent microscopy methods that have been specifically developed for drug discovery applications (234). PDX samples which have been used to establish the platform, have >95% ALL blasts, but primary samples in some instances can contain as little as 20-30% blasts. In order to discriminate ALL cells from normal lymphocytes, we might need to integrate CD markers.

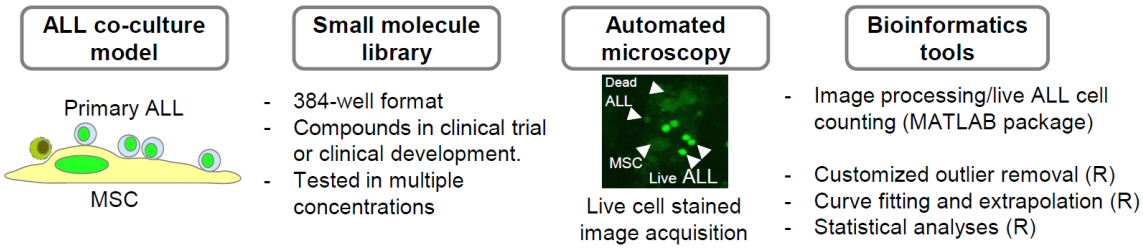

Figure 8. Primary ALL drug response profiling workflow.

4.2.5. High-content analysis of live stained ALL cells

In collaboration with the group of Dr Peter Horvath (Eidgenössische Technische Hochschule Zürich (ETH)), we have used the MATLAB (http://www.mathworks.com/) image analysis toolkit and employed modified Advanced Cell Classifier packages (http://acc.ethz.ch/, http://cellprofiler.org/) to analyse collected images. Several features have been used in a machine learning algorithm that are useful for recognising live ALL cells and discriminating it from dead ALL cells and MSCs. These features include the fluorescence intensity, size and shape of the nucleus, granularity and the surrounding background. Using machine learning, we could precisely calculate live ALL cell number per well. Downstream drug response analyses have been performed using in-house data extraction and bioinformatics tools.

4.2.5.1. Establishing drug response analysis tools

In 2012, two large pharmacogenomics studies – the Cancer Genome Project (CGP) published by Garett et al. (235) and the Cancer Cell line Encyclopedia (CCLE) published by Barretina et al. (236) – reported drug response in a large panel of cell lines. The CGP tested 138 anti-cancer drugs against 727 cell lines while the CCLE tested the response of 24 drugs against 1,036 cell lines. For our compound library, we used both pilot test results and pharmacological data for hematological cell lines (available in the supplemental material) to select compounds (total 62). In late 2013, a study by Heibe-Kains et al. (237) reported inconsistencies between CGP and CCLE results that can be primarily traced back to reported drug response profiles. This analysis highlighted the fundamental problem represented by the lack of standardisation in drug assays and data analysis methods. Therefore researchers should be cautious interpreting CCLE and CGP drug response data (http://portals.broadinstitute.org/ccle/home and http://cancer.sanger.ac.uk/cosmic).

To prevent similar issues from arising in our high-throughput drug screening analysis, we collaborated with Dr Maria Pamela Dobay from the Swiss Institute of Bioinformatics (SIB) to develop an in-house analysis tool that directly uses the output from the image analysis platform. This tool is also used to fit the drug response curves according to a four-parameter log-logistic function and calculate response parameters including IC_{50}, AUC, and E_{max}. Using the open-source program R and the drc package, a drug response profiling analysis pipeline has been established and published in Manuscript 1. The code

is available via GitHub (https://github.com/pampernickel/drTools). The script is able to recognise and deal with the outliers and positive slopes (i.e. cases where cells proliferate in the presence of the drug). This pipeline has been used to reanalyse CGP and CCLE cell line drug profiling data; after comparing published drug response parameters with the newly generated results (Figure 9), we could detect several discrepancies. For instance, some compounds reported as active in fact were inactive and *vice versa*.

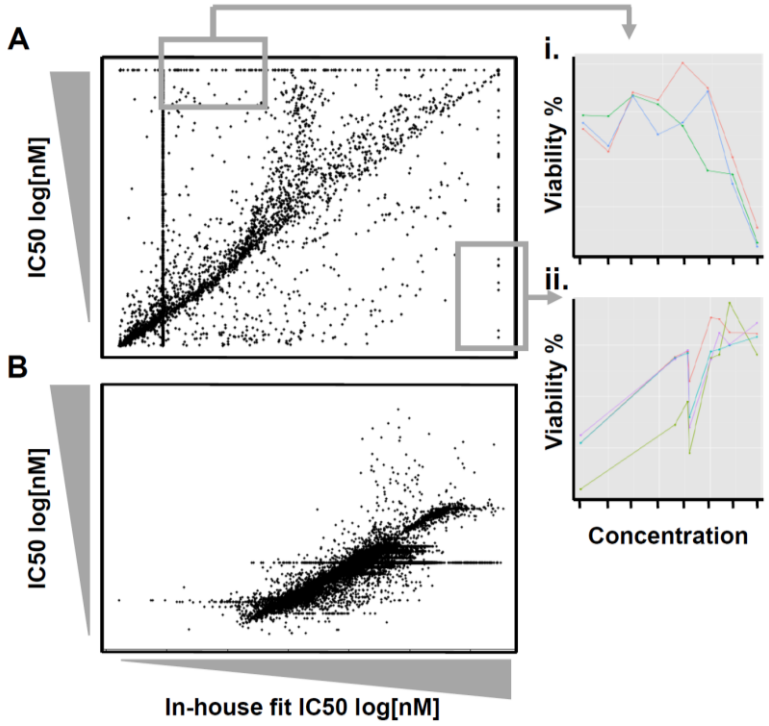

Figure 9. Comparison of reported cell line drug response IC_{50} to values generated using our in-house tools for the (**A**) CCLE and (**B**) CGP dataset. Several curve examples with inconsistent IC_{50} demonstrated in **A i.** and **ii.** .

4.3. Detecting druggable perturbations in primary ALL

Compound development has shifted from one-size-fits-all approach that emphasised generally cytotoxic chemotherapy to precision medicine strategies that exploit particular cancer cell weakness. To achieve this, it is essential to distinguish between passenger mutations and less frequent driver mutations to which the tumor is addicted (238). We believe that functional drug response profiling may refine our understanding of how cells are wired and detect actionable dependencies.

4.3.1. Relapse associated drug resistance

As reported in section 4.1.1, we have performed WES for eleven paired T-ALL samples (Figure 7). We could compare drug responses at diagnosis and relapse, and perform correlative analysis with its mutational landscape. Not surprisingly, very few additional mutations have been detected at relapse (Figure 7). Each patient also bore a unique set of mutations, adding complexity to the integrative analysis. As reported by Meyer et al. (63), a high number of relapse T-ALLs gained mutations in the *NT5C2* gene. This *de novo* aberration has been associated with the resistance to purine analogs, which are standard-of-care drugs (6-mercaptopurine, 6-thioguanine). Interestingly, this *de novo* mutation at

relapse is more frequent in T-ALL than in BCP-ALL (19% vs. 3%) (63). We could detect similar correlations with the *in vitro* response to 6-thioguanine for paired T-ALL samples (Figure 10). Leukemia cells responded to 6-thioguanine at high concentrations, but E_{max} values have changed significantly in relapse cases with the *de novo NT5C2* mutation. One diagnosis case was initially resistant, and remained resistant at relapse; another case was sensitive at diagnosis but became resistant at relapse without gaining *NT5C2* mutation. This indicates that there are other acquired resistance mechanisms not related to *NT5C2* mutation, and that could be already present at diagnosis. Additionally, we have noticed that samples that became resistant to 6-thioguanine *in vitro* engrafted much slower in NSG mice (Figure 10). This was true for diagnosis samples that gained *NT5C2* mutation at relapse as well.

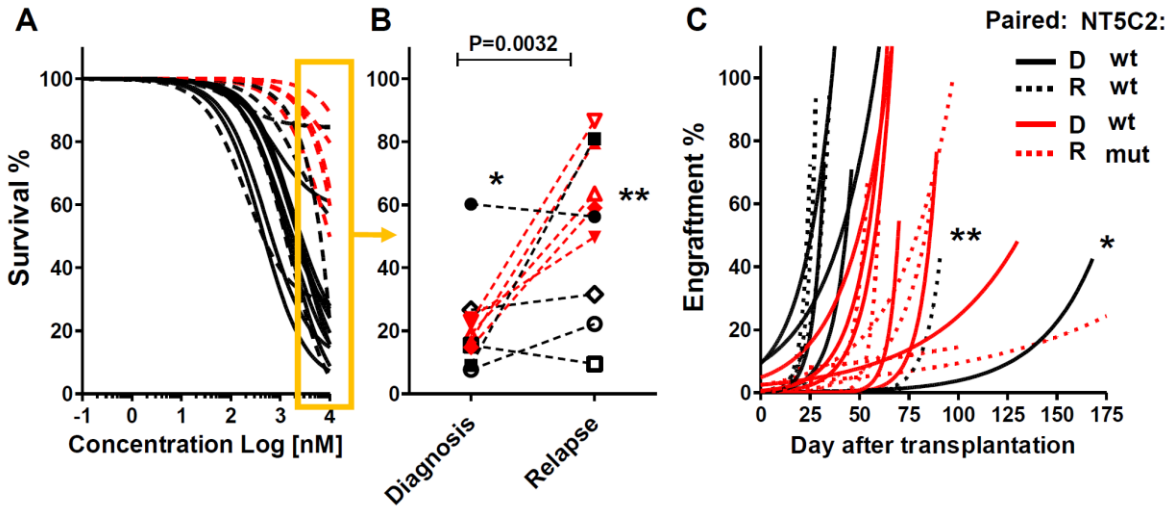

Figure 10. Paired T-ALL sample response to 6-thioguanine. Samples in red have gained *NT5C2* mutations at relapse (data from Figure 7). **A.** Response curves of eleven matched T-ALL samples **B.** E_{max} values of matched samples (diagnosis and relapse). **C.** Paired T-ALL engraftment kinetics (two animals per sample, blasts measured by FACS in the peripheral blood (mCD45 vs. hCD45)), D – diagnosis, R – relapse, wt – wild type, mut - mutation.

4.3.2. Anti-apoptosis BCL family members targeting drugs

The balance between the BCL family pro- and anti-apoptotic members is affected by genetic or epigenetic changes, signalling pathway alterations and post-translational modifications. Upregulation of BCL2, BCL-XL and MCL1 have been reported in human hematological malignancies (239). These changes provide a selective advantage to leukemia cells by allowing them to survive under various stressful conditions. Based on this assumption, BCL family proteins represent a molecular vulnerability that could be exploited to eliminate cancer cells. We have included several compounds targeting anti-apoptotic BCL2 and BCL-XL proteins (Table 7), such as navitoclax and venetoclax.

In collaboration with Dr R. Lock (Children's Cancer Institute, Australia), we have evaluated navitoclax in resistant ALL subsets *in vitro* and *in vivo* (Manuscript 3). Here, a panel of 31 PDX ALL samples comprised of MLL-, BCP- and T-ALL cases were tested. Three samples (10%) were not supported in our co-culture setup and could not be evaluated. In the majority of the remaining samples, *in vivo* responses were correctly predicted from results generated with our drug response profiling platform (Manuscript 3). This was the first report of a functional assay able to accurately predict *in vivo* single-agent navitoclax responses.

One of the most promising compounds identified on our screening platform was a related pro-apoptotic compound, venetoclax (reported in Manuscript 1 and Manuscript 4). Very resistant ALL with *TCF3-HLF* and *MLL-AF4* translocations, as well as a subset of T-ALL demonstrated IC_{50} values below 10nM. Interestingly, a higher number of BCP-ALLs than T-ALLs were identified as venetoclax sensitive. Similar response patterns were replicated *in vivo* as we tested seven cases selected based on *in vitro* screening results (Manuscript 1). Not all patients are expected to benefit from BH3 mimetics, and for this reason, several predictive biomarkers have been proposed. For instance, a functional assay, BH3 profiling, measures the degree of mitochondrial outer membrane permeabilization by an array of functionally-distinct BH3 peptides (116). We have reported that our established *in vitro* drug response profiling could predict *in vivo* response more accurately compared to BH3 profiling (Manuscript 3). In a second assay, leukemia cell sensitivity to navitoclax or venetoclax has been associated with the ratio of anti-apoptotic BCL2 and BCL-XL proteins (240). We have determined the expression of BCL family proteins by western blot and flow cytometry and checked the degree of correlation between BCL family expression or expression ratios with the sensitivity to navitoclax and venetoclax (Manuscript 1 and 3). We could only detect a very weak correlation (Spearman ρ=-0.43) of BCL2:BCL-XL protein ratios with the response to venetoclax. Moreover, different ratios were associated with distinct leukemia subtypes, highlighting the complexity behind apoptosis resistance. Moreover, we could not detect any significant correlation of ALL response to venetoclax or navitoclax and mutations detected by targeted sequence and WES (Manuscript 1).

4.3.3. Cell cycle targeting drugs

Cycle regulating kinases (checkpoint kinases (CHKs), cyclin-dependent kinases (CDKs), Polo-like kinases (PLKs) and Aurora kinases) are often overexpressed in tumor cells (241), therefore these proteins are believed to be important therapeutic targets. We have included several CHKs, CDKs, PLKs and Aurora kinases in our screenings (Table 5).

We have identified potent cell cycle targeting drugs that demonstrated selective activity at low nM range (IC_{50}<100nM, Manuscript 1). In particular, anti-leukemic activity was detected for Aurora kinase inhibitors barasertib, AT9283, XL228; CDK inhibitor CGP-60474 and PLK inhibitor BI-2536 (Manuscript 1). These findings are consistent with clinical trial results in hematological malignancies for barasertib (242), AT9283 (243) and BI-2536 (244). Similarly, XL228 and AT9283 are under investigation in leukemia patients (clinical trial numbers: NCT00464113 and NCT01431664).

We have determined primary cell behaviour in co-culture with MSCs (discussed in section 4.2.2.) and correlated drug response profiles with the ALL cell fraction in S-phase. Not surprisingly, there was a correlation between these two variables for the cell cycle-targeting drugs: antimetabolites (e.g. cytarabine, 6-thioguanine), aurora and microtubule inhibitors (e.g. XL228, docetaxel) and topoisomerase inhibitors (topotecan, etoposide) (Manuscript 1). Interestingly, samples with high *in vitro* S-phase cell counts engrafted in NSG mice much faster (median 35 days) compared to samples with low proliferative capabilities *in vitro* (median 81 days) (Manuscript 1). We investigated if this S-phase/drug response correlation was an artefact of our screening platform or if it can be recapitulated in the xenograft model as well. We selected eight samples (four sensitive with high *in vitro* proliferation;

four resistant with low proliferation *in vitro*) and tested the *in vivo* response to cytarabine and docetaxel. We took advantage of an experimental layout of one animal per tested condition (164), which allowed us to test more patients with fewer animals. We could confirm that *in vivo* drug response patterns can be predicted from the drug response profiles even for cell cycle targeting compounds (Manuscript 1).

4.3.4. Unexpected activity of kinase inhibitors

Using our established screening platform, we could also detect unexpected leukemia response to kinase inhibitors. For instance, we could detect extraordinary dasatinib sensitivity in a considerable fraction (~30%) of T-ALL (Manuscript 1). In addition, dasatinib responders had a tenfold increase in sensitivity compared to the most sensitive BCP-ALL. We could not detect ABL1-associated translocations in sensitive cases (e.g. NUP214-ABL1). In contrast to imatinib, dasatinib additionally inhibits SRC family (SRC, LCK, YES, FYN), c-KIT, EPHA2, and PDGFRβ (245). We have investigated these targeted pathways in T-ALL and found that SRC activation (measured by phosphorylation of TYR416) correlated with the response to dasatinib (Manuscript 1). Sensitive T-ALL cases have much higher levels of pSRC compared to resistant cases and upon short (2h) *in vitro* treatment, could be completely downregulated. We also found that dasatinib response positively correlated with the response to the selective SRC inhibitor, KX2-391 (Manuscript 1). After comparing drug response profiles, we have found a positive correlation between dasatinib response with RTK inhibitors (e.g. XL228 and crizotinib). It has been reported that SRC is an important link in modulating RTK signaling (246). So far, there is limited information on T-ALL SRC dependency; our data suggest that it might be a relevant target in the selected patient group.

Furthermore, we have validated dasatinib response in the xenograft model in four resistant and six sensitive cases that we selected. We have again used a single mouse per condition for each patient to test responses to dasatinib (Manuscript 1). After five days of treatment (50mg/kg), T-ALL engraftment was checked in different mouse organs (bone marrow, peripheral blood, spleen and liver) and compared to the control mouse. We could see a clear tendency towards blast reduction in the bone marrow of mice transplanted with sensitive T-ALLs. Nonetheless, it is the significant reduction of blasts in other organs (peripheral blood and spleen) that had a significant correlation with the *in vitro* sensitivity.

Similar observations could be detected in independent pediatric and adult T-ALL cohorts, where a high number of tested samples responded to dasatinib (247). Based on these drug profiles, one completely refractory T-ALL patient was selected for treatment with dasatinib (reported in Manuscript 1); the patient had an initial complete response, but relapsed after five months.

4.3.5. Novel Notch1 inhibitor

As NOTCH1-activating mutations are the most frequent abnormality in T-ALL, much effort has been dedicated to identify oncogenic pathways that it controls. Several studies demonstrated that NOTCH1 directly regulates ribosome biosynthesis, protein translation and amino acid metabolism, which promote T-ALL cell growth (248). As discussed in the chapter 1.6.1.1, there are several therapeutic approaches to intervene with NOTCH1 signaling.

For our screenings, we have included several NOTCH1 inhibitors (Table 5). We have tested several GSI inhibitors (DAPT and MK0752), but found little effect on T-ALL survival. Similar results have been observed in the clinical trial of the GSI inhibitor MK0752 (249). Only one patient had a partial response, which lasted for 28 days. Alternatively, NOTCH1 signaling can be disrupted by preventing the formation of the transcriptional complex, NICD-CSL-MAML1 (250). We have evaluated the novel NOTCH1 inhibitor CB-103, specifically targeting NICD-CSL-MAML1, on our screening platform. This small orally active molecule has been developed in the laboratory of Dr Freddy Radtke (Ecole Polytechnique Federale de Lausanne (EPFL)). We have tested the response of 20 primary T-ALL samples to CB-103, and most samples with the NOTCH1 mutation have responded in the 50-4000 nM range (Figure 11A). In addition, we have determined NICD expression using western blot after 72h incubation with DMSO or CB-103 (Figure 11B).

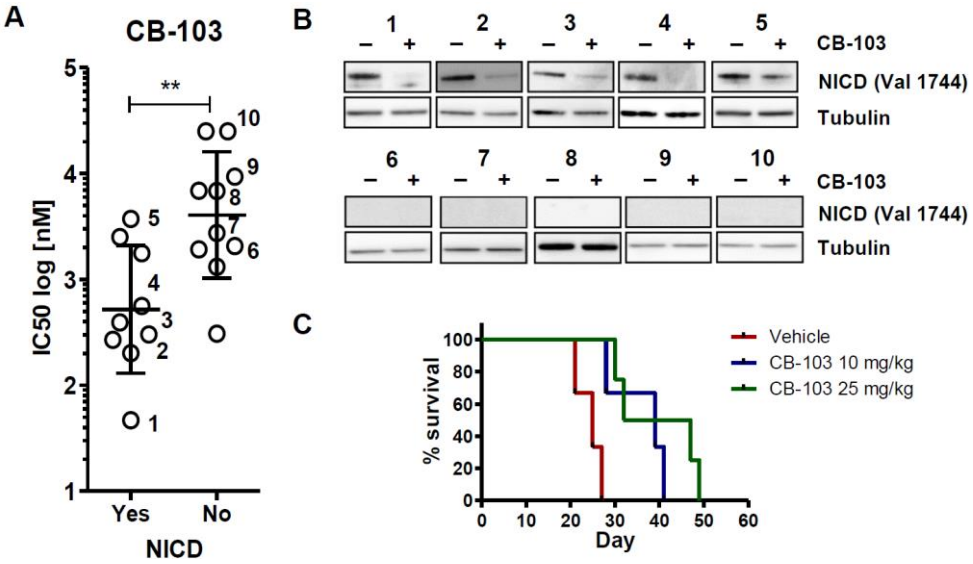

Figure 11. CB103 impedes the growth of NOTCH1–positive primary human T-ALL. **A.** Response to CB103 of T-ALL cells (N=20) *in vitro* divided by NICD expression. ***, p-value<0.005* **B.** NICD levels decrease upon treatment with CB-103. NICD detection on Western blots after 72h exposure to DMSO or CB103 are shown. **C.** Event-free survival analysis after treatment of leukemia xenograft of one selected case. 3-4 animals were used per treatment arm. Treatment was inititated when 10% of ALL blasts were detected in the peripheral blood. Events were defined as the occurrence of 30% ALL blasts in the peripheral blood.

Based on screening results, we have selected one case to test in the xenograft model. We could prolong mouse survival with CB-103 treatment (Figure 11C), and its general *in vivo* effect is comparable to GSIs (138), but without cytotoxic side effects. To exploit the full potential of NOTCH1 inhibition, a combination approach with standard chemotherapy should be considered.

4.3.6. Targeting non-oncogene addictions in ALL

Cancer cells may display an increased dependence on the normal cellular functions of certain genes that are not oncogenes, a phenomenon coined as ‘non-oncogene addiction’ (251). During our screening, we have identified potential ALL dependencies on non-oncogenic pathways that are not associated with the ALL mutational landscapes (Manuscript 1). For instance, we have identified HSP90 inhibitors (e.g. luminespib, NVP-HSP990) as promising compounds. HSPs (Heat-shock proteins) are

molecular chaperones present in almost every cellular compartment (252). These proteins protect cells from stress-induced damage by increasing protein stability (252). Overexpression of HSPs in hematological malignancies, in particular HSP90, is associated with the oncogenic protein stabilisation as well regulation of apoptotic proteins (253). In the first-in-human HSP90 phase I solid tumor clinical trial of the NVP-HSP990 inhibitor, severe neurological toxicity that not been predicted from animal studies was revealed (254). Despite this drawback, further phase II and III clinical trials are ongoing for other HSP90 inhibitors (254).

Another non-oncogenic addiction is underlined by ALL sensitivity to the proteasome inhibitor bortezomib. Interestingly, bortezomib combined with dexamethasone, doxorubicin, vincristine and L-asparaginase results in complete response in 80% of tested BCP-ALL patients (255). However, the mechanism of by which bortezomib exerts anti-cancer activity is still elusive, given that proteasome inhibition can stabilise different proteins. As not all patients will benefit from proteasome inhibition, selective criteria should be established *a priori*. *In vitro* proteasome inhibitors are extremely potent (IC_{50} 0.1-10nM, Manuscript 1), and it is therefore challenging to establish a predictive model, given the lack of a clear separation between potentially resistant and sensitive samples tested *in vitro* (Figure 12A). Nonetheless, we can apply a similar approach as we did for navitoclax, which has a similar activity profile (Manuscript 3). Using E_{max} instead of IC_{50} as a response endpoint, we have identified that samples had the greatest variation in response at 1-1.5nM drug concentration range (Figure 12A). We have additionally analysed an independent sample cohort with known bortezomib responses in NSG mice (256) (Figure 12A and B), as well as two completely refractory patients that have been selected for the bortezomib treatment (Patient 1 and 4, Manuscript 1). Our results suggest that we can correctly predict patients exhibiting resistance (Figure 12C).

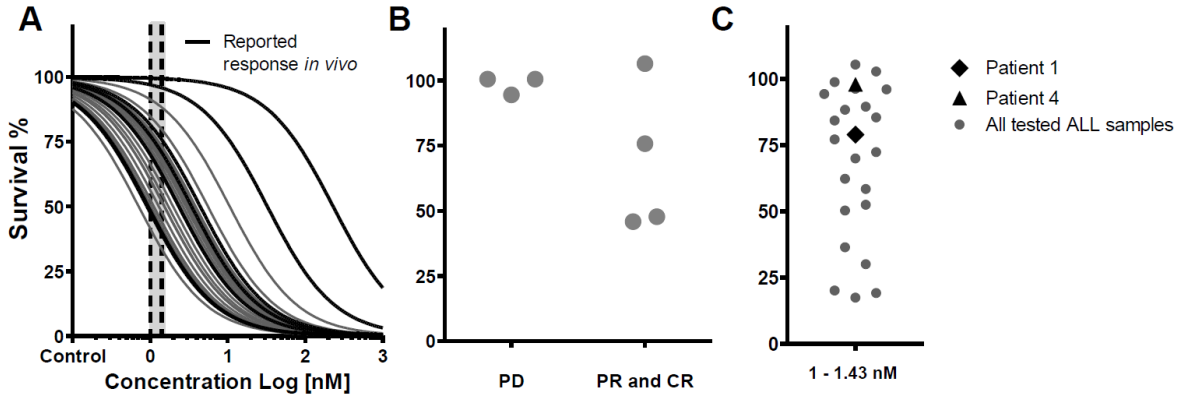

Figure 12. *In vitro* response to bortezomib. **A.** *In vitro* response curves as determined by drug profiling. Black lines indicate samples evaluated *in vivo* (256). **B.** *In vitro* E_{max} at 1nM for ALL samples tested *in vivo*. Samples are grouped according to the *in vivo* response: PD – partial delay, PR – partial response, CR – complete response. **C**. Two patients sample E_{max} that had been treated with bortezomib.

4.3.7. Intrinsic drug response differences between primary ALL and cell lines

After initial screening based on 24 primary ALL samples, we revised our list of selected compounds after some drugs which were reported active in the cell lines (235) showed no effect on primary ALL cells. For example, MEK/RAF pathway inhibitors, selected as promising compounds for hematological

malignancies based on the cancer cell line investigations (257), had little or no effect on ALL samples. For this reason, three (PD0325901, AZ628, Compound C) out of five MEK inhibitors were not considered for further evaluation.

As could be expected, most established hematological cell lines were more sensitive to tested drugs compared to the primary ALL samples with a few important exceptions (Figure 13). Not surprisingly, cell lines were very sensitive to cell cycle targeting drugs as antimetabolite (methotrexate) or microtubule inhibitors (vincristine and docetaxel). Cytarabine (antimetabolite) forms an exception to which cell lines and primary ALL responded similarly. In contrast, majority of primary ALL samples were very sensitive to the BCL2/BCL-XL inhibitor navitoclax while cell lines demonstrated persistent resistance. Therefore, BCL2 targeting compounds would not have been selected for further clinical evaluation if the selection was based exclusively on results from cell lines. Similar to the observation of BCL2 inhibition, very few cell lines were sensitive to ABL1/SRC inhibitor dasatinib (Figure 13). In contrast, primary ALL demonstrated an extraordinary response to dasatinib. Notably, the response was exclusively observed in patients with T-cell immunephenotypes. As in the case of navitoclax/venetoclax sensitivity, this finding (reported in Manuscript 1) would be undetected if cell line screenings were used. In contrast, established cell lines were selectively sensitive towards mTOR (temsirolimus) and PI3K/mTOR (dovitinib) inhibition, while very few primary ALL cells responded in the same range (Figure 13). Notably, PI3K and mTOR inhibitor clinical trials enrolling ALL patients delivered fairly disappointing results (258).

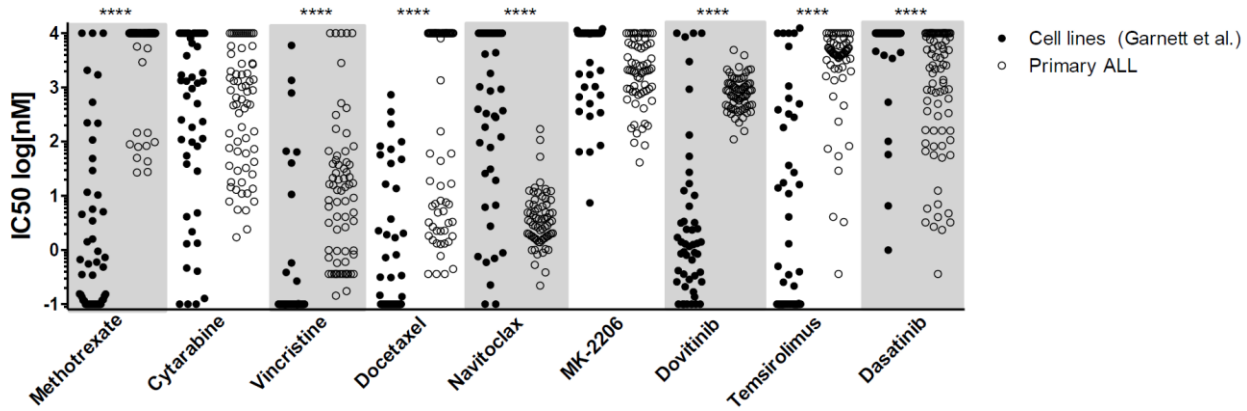

Figure 13. Comparing hematological cell line (Garett et al. (235)) and primary ALL (Manuscript 1) response (IC_{50}) to selected agents. *****, p-value<0.0001*

Similar differences for mentioned drugs (with a few exceptions) have been observed by other researchers comparing AML primary cell and cell line *in vitro* responses (223). Intriguingly, AML cell lines and primary AML had been similarly sensitive to MEK inhibitor trametinib and mTOR inhibitor temsirolimus (223), which is the opposite of what has been observed in primary ALL screenings. The origin of these discrepancies should be further evaluated. It might arise from the MSC co-culture setup, given that AMLs were screened in the monoculture, or from intrinsic molecular differences between AML and ALL.

4.3.8. Exploring drug combinations

Tumorigenesis is driven by interaction (enhancement or suppression) of different genes rather than a single gene independent action. This is bad news for therapy, especially targeted, as one or more pathways in a cancer cell can compensate for the inactivation of another arm. However, it is still possible for combined losses of interacting genes to be lethal for the cancer cell in an effect known as synthetic lethality (259). Functional screenings demonstrated that one nonessential gene might have 10-30 synthetic lethal partners (249). The activity of drug combinations is said to be synergistic when the effect of the combined drugs on the target cells is greater than the sum of effects caused by individual compounds (186). We have explored the potential of our screening platform to detect synthetic lethality and validated our findings in the xenograft model.

4.3.8.1. Detecting synthetic lethality in primary ALL

We have used our platform to screen selected compounds from our complete drug library that would be of interest to test in combination with venetoclax. This approach is described in Manuscript 2, where we identified venetoclax synthetic lethality partners. Initially, we tested sublethal dose of venetoclax in six T-ALL patients combined with a selected clinically-relevant compounds. T-ALL demonstrated heterogeneous synergistic or additive effect landscapes, and only a few compounds exhibited notable effects in all samples. We have calculated combination effects using the Chou-Talalay method described in chapter 1.7.3. True synthetic lethality could be achieved when venetoclax was combined with the BRD4 inhibitor JQ1. Initial screening results have been validated in a co-titration experiments testing venetoclax and JQ1 in a wide range of concentrations. Similar synergistic effects have been detected in the T-ALL cell lines (Manuscript 2), and have been recapitulated *in vivo* in the xenograft model using primary T-ALL and cell lines. In both models, JQ1 and venetoclax monotherapies had a small impact on disease progression, but could significantly delay leukemia progression when combined (Manuscript 2).

Additional promising venetoclax combinations were observed with standard-of-care drugs (dexamethasone and vincristine). Intriguingly, positive effects could be observed in almost all tested samples and could be extended to BCP-ALL as well. Therefore we took advantage of our resistant *MLL-AF4* and *TCF3-HLF* BCP-ALL xenograft models and tested the efficacy of a combination of all three compounds (reported in Manuscript 1). Monotherapy of venetoclax, dexamethasone and vincristine could delay progression, but only the three compound combination could completely eradicate leukemia. One year after treatment completion, mice were still leukemia-free. It is worth to mention that selected patients material used in *in vivo* experiment were linked to initially sensitive to all three compounds, and *in vitro* detection of the synergistic effect was difficult. Calculated CIs indicated average performance or additivity. Data nonetheless suggest that patients might benefit from the combination of compounds with low IC_{50} regardless of whether the effect is highly synergistic or only additive *in vitro*.

4.4. Selecting patients for the targeted therapy

Drug development success in oncology depends on the ability to identify subsets of patients that will benefit from prescribed treatment. New targeted therapies are costly and in some cases, only a fraction of patients will respond to the medication. For example, sorafenib (RAS family kinase inhibitor) could cost up to $140,000 a year for a renal cell cancer patient (260). However, only patients with upregulated VEGFR stand to benefit from therapy (261). Therefore, predictive biomarkers have to be established and used to exploit the full potential of the precision medicine approach. However, it has been challenging to identify such biomarkers, and in some cases they do not work as expected. For example, just two-thirds of melanoma patients with *BRAF* mutated gene responded to the RAF inhibitor dabrafenib (262). Clinical results highlight the fact that even if the target is present, it does not necessary mean that cancer cell is still dependent on it.

4.4.1. Biomarkers used to guide targeted therapy

Signaling pathway activation in cancer cells often result from genomic alterations (mutations, translocations and copy number gains or losses), which are the prime biomarker candidates for targeted therapies. Identifying cancer cell driver mutations is a major challenge that will not be solved through the analysis of sequence data alone. There are currently only several FDA approved genomic markers used to guide treatment selection (263).

4.4.2. Strategies to integrate predictive biomarkers

There are several strategies to design and advance biomarker into clinical trials. But in most cases biomarker selection is driven by pre-clinical studies. For instance, one recent publication demonstrated AML PDX model driven biomarker selection and validation (264). Authors evaluated JAK2 inhibitors, fedratinib and ruxolitib, in 64 patient samples *in vivo* in the xenograft model. 59% of AML samples responded to fedratinib, but just a few samples responded to ruxolitinib. They could associate fedratinib sensitivity to an activated STAT5 pathway, which is downregulated by this compound (264). In addition, authors observed that pSTAT5 levels correlated with the activated SRC pathway. They hypothesised that combining dasatinib and fedretinib could synergise. And indeed they had observed the synergistic effect *in vivo* (264). As shown in this study, off-target effects could not be predicted by genomic lesions alone. This clearly indicates that combining different biomarkers could help in patient selection.

Similarly, we reported in Manuscript 1 how we could select drugs based on the functional response and then associate sensitivity with the predictive molecular biomarker. We have identified remarkable T-ALL response to dasatinib that could be associated with the activated SRC levels. In contrast, we have not associated isolated genomic lesions with dasatinib sensitivity.

4.5. Access to new agents in the clinical setting

Many of the new compounds that are advancing in clinical trials might be out of reach for patients with life-threatening conditions. FDA developed a system of expanded access to permit such patients to receive investigational drugs before formal drug approval. There are several practical, legal, and ethical issues associated with prescribing investigational drugs even if the patient has positive biomarkers

(265). Companies might be discouraged from participating in this program given that only a limited amount of data, which may not be useful for the company or the FDA, is collected from the drug's exceptional use. In contrast, all adverse events that occur in the patient during its preapproval period must be reported to the FDA.

Based on our findings published in Manuscript 1, venetoclax has been considered for several relapse patients. Unfortunately, the company (Abbvie) refused to release this compound to patients. In order to improve situation, broader international efforts must take place. Working parties joined by physicians and scientists have been organised to help move new therapies into the clinics and to design new treatment protocols.

4.5.1. Pediatric oncology groups to advance novel therapeutics

European consortium 'Innovative Therapies for Children with Cancer' (ITCC) was established with the aim to evaluate novel agents in pre-clinical cancer models and conduct early clinical trials (266). ITCC combines 49 institutions across eleven European countries (including Israel). Between 2003 and 2015, consortium initiated 35 phase I and II trials exploring 37 new anti-cancer drugs and treating 1109 children. For instance, phase I dasatinib evaluation in the pediatric leukemia setting have had similar positive results as in adult trials (267). Currently, ITCC is testing several compounds in refractory leukemia patients: nilotinib (trial number: ITCC-011), a BRAF inhibitor dabrafenib (trial number: ITCC-03) and a sequential combination of cytarabine (trial number: ITCC-044). Apart from ITCC, several other important EU pediatric clinical research groups initiate clinical trials, including The Cancer Drug Development Forum (CDDF), the European Society for Pediatric Oncology (SIOPE), the European Network for Cancer Research in Children and Adolescents (ENCCA). The International BFM Study Group (I-BFM-SG) have conducted clinical trials for leukemia and lymphoma for over 25 years and operate under the SIOPE umbrella. I-BFM-SG is one of the most successful and among the world's largest leukemic study groups involving multiple research centres from more than 30 countries.

As in Europe, several very successful clinical trials for childhood malignancies have been initiated in the United States. The Children's Oncology Group (COG), a National Cancer Institute (NCI)-supported clinical trial group, is the world's largest organisation devoted to pediatric cancer research. COG has been conducting research for over 60 years and has contributed substantially to the rise of survival from 10% in the mid-50s to almost 90% today. Current and future COG ALL trials will focus on using existing and newly-discovered biomarkers to stratify patients into different risk groups and testing novel agents and treatment strategies for patients predicted to have a poor outcome (268). Just to name several COG ALL trials: dasatinib for a *BCR-ABL1*–positive leukemia (clinical trial number: NCT01460160), phase II bortezomib trial in newly diagnosed T-ALL (clinical trial number: NCT02112916).

4.5.1.1. ITCC precision medicine programs

ITCC initiated clinical trials that will allocate targeted therapy based on molecular biomarker (WES, transcriptome, immunophenotype). For instance, the German dkfz (Deutsches Krebsforschungszentrum) centre initiated the INFORM (INdividualized Therapy FOr Relapsed Malignancies in Childhood) registry (https://www.dkfz.de/en/inform/). The aim of this registry is to

biologically characterize tumor samples for all pediatric patients with relapsed or refractory high-risk tumors for which no further standard-of-care therapy is available. No therapy recommendation will be given within this registry study, but the molecular data will be made available to the treating physician. This registry might help associate treatment outcomes to molecular markers.

One of the recent ITCC-initiated program is called e-SMART (European Proof-of-Concept Therapeutic Stratification Trial of Molecular Anomalies in Relapsed or Refractory Tumors, clinical trial number: NCT02813135). The e-SMART trial will explore the effectiveness of 10 investigational oncology drugs (single agents or in combination) from at least three different pharmaceutical companies. This is the first molecular profiling protocol in Europe to determine multiple actionable alterations in pediatric cancers. The ITCC goal is that by 2020, more than one out of two patients with incurable, relapsed disease would have access to at least one innovative therapy.

4.5.2. Drug response profiling in the co-clinical trials

Most pediatric ALL cases could be cured with current multiagent regiments, but a subset of patients will have significantly worse outcome and eventually succumb to the disease (269). Such patients will undergo salvage therapy that might include immunotherapy (e.g. blinatumumab) or HSCT. Despite all treatment strategies, some patients will fail to reach complete remission (so-called refractory relapse cases). These cases then are eligible for individually-tailored experimental treatments.

The University Children's Hospital Zurich is a part of the ITCC consortium and together with other centres, participate in the clinical trials as well as in the INFORM registry. Together with ten German institutions (e.g. Charité Hospital, OHC, Berlin; Hannover Medical School, Hannover; Heidelberg University Hospital, Heidelberg and others), we aim to generate a leukemia molecular portrait for each relapse refractory patient. In the INFORM framework, we have incorporated our established drug response profiling platform where we examine the functional response to the drugs, while other centres perform WES and RNA sequencing. This information eventually will be available on established, well-annotated European clinico-biological database. We hope that the accumulation of primary data will help in designing and guiding clinical trials in the future.

During my project, we have screened more than 90 PDX samples from distinct subtypes. From these studies, we have determined drug activity ranges, and characteristic sample distributions per drug. These data can be used as a background against which we can compare new primary sample screening results. To date, we have performed drug response profiling for six relapse refractory patients for the INFORM registry (Figure 14), which are reported in Manuscript 1. As expected, these patients were resistant to standard of care drugs (Figure 14). Nonetheless, we have detected distinct sensitivity patterns to several new experimental compounds, for instance venetoclax and birinapant. In addition, several samples demonstrated sensitivity towards proteasome inhibitors (bortezomib and carfilzomib), as well vincristine or mitoxantrone. This is of great interest as these drugs are evaluated or will be evaluated in the relapse ALL trials. For instance, some relapse BCP-ALL patients have responded to bortezomib (270). Similarly, mitoxantrone has been associated with the great improvement in a relapse ALL survival (271). Venetoclax has recently received FDA approval for CLL and other clinical trials in

hematological malignancies will follow. In addition, a recent report (122) demonstrated that birinapant has a great potential *in vitro* and *in vivo*, but so far there are no clinical trials in children. These findings reinforce the need for patient selection from *in vitro* screening results, as clinical trials tend to show that only a fraction of patients will eventually benefit from these drugs.

Incorporating screening platform results into co-clinical trials nonetheless has its challenges. First of all, only a limited amount of primary cells are available for profiling. Consequently we had to prioritise compounds that might have the greatest impact. Until now, we were able to test 20-30 drugs for each patient.

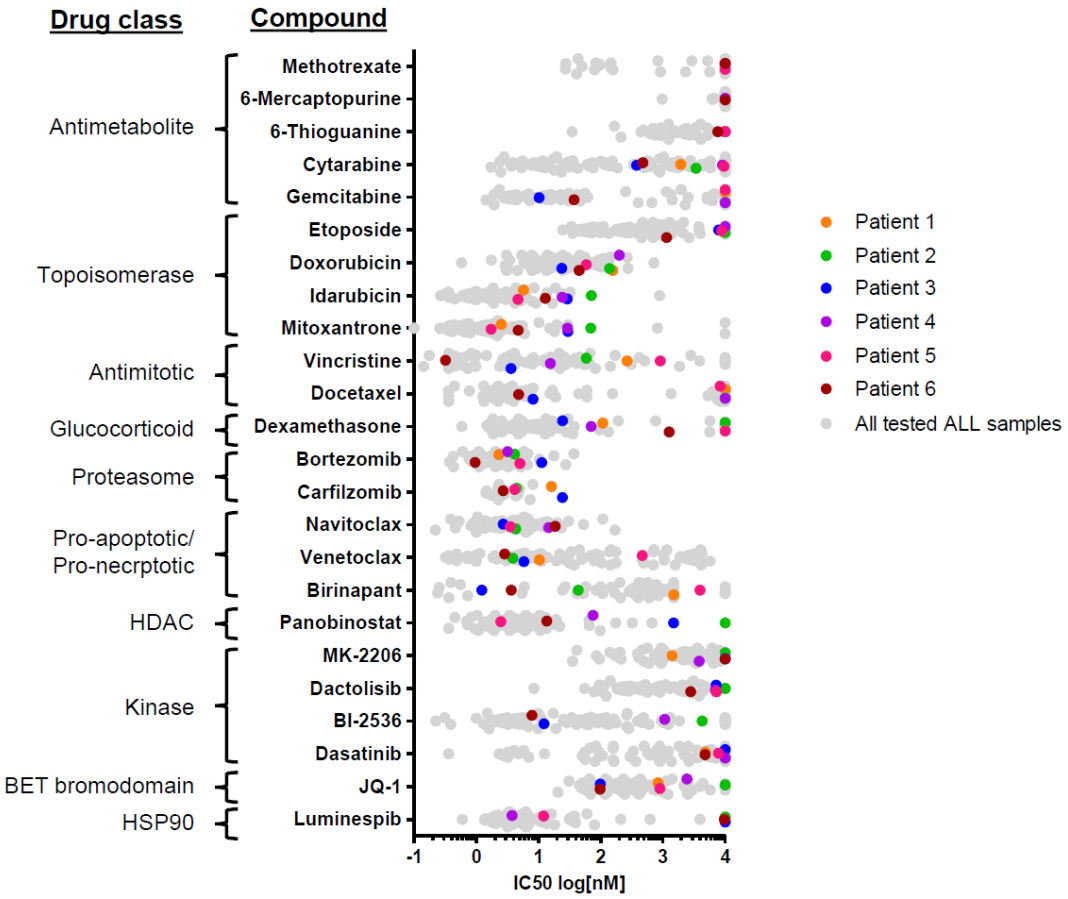

Figure 14. Drug response profiles of six refractory relapse primary ALL samples compared to all other tested ALLs.

As screening results accumulate, we will establish *in vitro* predictive parameters for *in vivo* response. Most likely we will have to integrate multiple biomarkers in order to increase confidence in sensitivity prediction. Several issues that have to be addressed include the choice of *in vitro* parameter with the best predictive power (E_{max}, IC_{50}, AUC), the interaction of the drug with other chemotherapy, and the identification of other parameters that correlate with response (genomic mutations, kinase activation, target expression etc.).

4.6. Future challenges and prospects for drug profiling in the clinical setup

We have used good laboratory practice guidelines in establishing our drug response profiling platform. We developed standardised tools that could be easily used in other facilities. The experimental layout has been directed towards optimising time required to perform ALL analysis and results would be

available within five days. Nonetheless, there are aspects that need be addressed in order to exploit the full potential of this new tool, and for it to become an integral part of the diagnostic routine.

4.6.1. Cross-platform standardisation

Though in principle our approach is simple, robust and reproducible, certain crucial aspects have to be monitored closely. To date, we were analysing primary patient and PDX samples in co-culture with MSC cells. Other research units (e.g. Dr J. Tyner at OHSU (Oregon Health & Science University) or Dr K. Porkka at FINN (Institute for Molecular Medicine Finland)) have established screening platforms using leukemia cell monocultures enriched with growth factors. In collaboration with these two groups, we have initiated a cross-platform validation program. We will analyse the same samples to identify differences seen using different experimental setups.

Additionally, there are no standard practices accepted in the primary sample drug response profiling. We have used an image-based readout, but biochemical readouts are more widely-used. Theoretically, this should not affect recorded responses. Not only are experimental readouts different, but the experimental setup could vary significantly: number of concentrations tested, incubation length, tested concentration range etc. These small details can make the difference in cross-platform comparisons. One of the biggest sources of differences, however, could result from data analyses pipelines. So far, tools available for academic use for customized, high-throughput, drug response platforms are limited. As seen from the cell line studies, lax settings in fitting software could result in problematic results, which in the clinical setup, are unacceptable. Therefore, together with the SIB, we have developed an in-house analysis tool that deals directly with the raw data, and that specifically handles the most common mistakes linked to fitting. The pipeline is easily adapted for different platforms and layouts.

4.6.2. Screening automation

From our experience, manual handling introduces a considerable level of variation and require a significant amount of time. We have established our platform on a 384-well plate format, which is manageable with simple robotics and compact enough for multiple drug testing. As the number of novel targeted therapy molecules in clinical trials increase, we might need to scale down to a 1536-well plate format in order to test more drugs with the same amount of available primary cells. This will require to use more precision robotics as well automate compound library handling and storage.

4.6.3. Costs of genomic and drug profiling for precision medicine

Targeted therapy alone is worthless unless it is guided by the equally precise means to identify responders, which might include next generation sequencing solutions, or other functional and molecular assays. Today the whole exome and genome sequence price has dropped below 1000 and 1500 CHF respectively, and is still falling (https://www.genome.gov/sequencingcosts/). Nonetheless, the cost and complexity of NGS analysis remain substantial barriers to adapt this approach in routine clinical care. It is estimated that analysis alone costs about 1000 CHF, not including archiving NGS data. Several initiatives try to optimise analyses workflows using ‘cloud’ computation and storage (272). In addition, a genome repository has to be established and available for medical professionals, such as the INFORM registry, to facilitate data meta-analysis and interpretation.

Similarly, drug response profiling is not a standard diagnostic procedure in the clinical setting yet. To setup a screening platform, precision robotics and automated microscopes are needed. Once a routine workflow is established, however, the running costs are relatively low. For instance, to perform drug screening for one patient in our current setup costs about 400 CHF. As it is a high-throughput system, it can serve multiple patients simultaneously and in principle one centre could provide this service for several regions (e.g. Germany and Switzerland). Finally, we have to make drug profiling data easily accessible to other medical centres, for which we will have to create a database.

4.7. Summary

In my thesis, I provide compelling evidence that informative differences can be detected in ALL patient groups from a functional drug discovery approach: with our primary cell screening platform, we could detect extraordinary activity of different classes of agents that would not have otherwise been predicted based on genomic information.

We have established drug profiling platform using PDX samples from clinically-relevant ALL subgroups and tested response in a serum-free conditions co-cultured on h-TERT immortalized human bone marrow MSCs. Drug testing was performed using automated microscopy and a customized image analysis program. We have demonstrated that PDX samples largely preserved genomic landscapes and responded similarly to compounds as primary ALL samples. Drug response profiles revealed clusters of activity in high-risk and relapse leukemia for a number of novel, clinically-relevant agents, identifying actionable targets not exploited in conventional treatment. For instance, our results indicate that a relatively large proportion of BCP-ALL cases may respond to venetoclax, including *TCF3-HLF* and *MLL-AF4*–positive ALL. We also reported unexpected activity of dasatinib in a T-ALL subset that would not have been identified based on genomic information. Moreover, we have demonstrated that the same *in vitro* response patterns could be replicated in our xenograft model for a navitoclax, venetoclax, docetaxel, cytarabine and dasatinib. Additionally, we exploited the screening platform to identify synthetic lethality for a selected compound. We have demonstrated the synergistic activity of venetoclax with standard-of-care drugs (dexamethasone and vincristine), as well as JQ1. All combinations have proved to be very effective in the xenograft model. Finally, we show a complete response to dasatinib in a patient with previously refractory T-ALL whose treatment was designed based on drug profiling data.

Our results provide a strong rationale to include *in vitro* drug profiling into clinical trials to improve the identification of patients that may benefit from novel compounds. Our preliminary co-clinical drug screening data suggest that a primary patient profiling could reveal vulnerabilities in resistant leukemia. We are establishing the workflow for the systematic use of this drug profiling platform in the two clinical trials, IntReALL HR, for the treatment of high risk ALL relapse patients, and INFORM, a registry for the genomic characterization of refractory ALL.

5. References

1. Bene MC, Castoldi G, Knapp W, Ludwig WD, Matutes E, Orfao A, et al. Proposals for the immunological classification of acute leukemias. European Group for the Immunological Characterization of Leukemias (EGIL). Leukemia 1995;9(10):1783-6.
2. Ward E, DeSantis C, Robbins A, Kohler B, Jemal A. Childhood and adolescent cancer statistics, 2014. CA: a cancer journal for clinicians 2014;64(2):83-103.
3. Ratei R, Schabath R, Karawajew L, Zimmermann M, Moricke A, Schrappe M, et al. Lineage classification of childhood acute lymphoblastic leukemia according to the EGIL recommendations: results of the ALL-BFM 2000 trial. Klinische Padiatrie 2013;225 Suppl 1:S34-9.
4. Hunger SP, Mullighan CG. Acute Lymphoblastic Leukemia in Children. The New England journal of medicine 2015;373(16):1541-52.
5. Lim JY, Bhatia S, Robison LL, Yang JJ. Genomics of racial and ethnic disparities in childhood acute lymphoblastic leukemia. Cancer 2014;120(7):955-62.
6. Shah A, Coleman MP. Increasing incidence of childhood leukaemia: a controversy re-examined. British journal of cancer 2007;97(7):1009-12.
7. Siegel RL, Miller KD, Jemal A. Cancer statistics, 2016. CA: a cancer journal for clinicians 2016;66(1):7-30.
8. Oeffinger KC, Mertens AC, Sklar CA, Kawashima T, Hudson MM, Meadows AT, et al. Chronic health conditions in adult survivors of childhood cancer. The New England journal of medicine 2006;355(15):1572-82.
9. Te Winkel ML, Pieters R, Wind EJ, Bessems JH, van den Heuvel-Eibrink MM. Management and treatment of osteonecrosis in children and adolescents with acute lymphoblastic leukemia. Haematologica 2014;99(3):430-6.
10. Ng AK, Kenney LB, Gilbert ES, Travis LB. Secondary malignancies across the age spectrum. Seminars in radiation oncology 2010;20(1):67-78.
11. Zhang FF, Kelly MJ, Saltzman E, Must A, Roberts SB, Parsons SK. Obesity in pediatric ALL survivors: a meta-analysis. Pediatrics 2014;133(3):e704-15.
12. Ness KK, Armenian SH, Kadan-Lottick N, Gurney JG. Adverse effects of treatment in childhood acute lymphoblastic leukemia: general overview and implications for long-term cardiac health. Expert review of hematology 2011;4(2):185-97.
13. Lai R, Hirsch-Ginsberg CF, Bueso-Ramos C. Pathologic diagnosis of acute lymphocytic leukemia. Hematology/oncology clinics of North America 2000;14(6):1209-35.
14. van den Ancker W, Terwijn M, Westers TM, Merle PA, van Beckhoven E, Drager AM, et al. Acute leukemias of ambiguous lineage: diagnostic consequences of the WHO2008 classification. Leukemia 2010;24(7):1392-6.
15. Clark G, Stockinger H, Balderas R, van Zelm MC, Zola H, Hart D, et al. Nomenclature of CD molecules from the Tenth Human Leucocyte Differentiation Antigen Workshop. Clinical & translational immunology 2016;5(1):e57.
16. Ferrando AA, Neuberg DS, Staunton J, Loh ML, Huard C, Raimondi SC, et al. Gene expression signatures define novel oncogenic pathways in T cell acute lymphoblastic leukemia. Cancer cell 2002;1(1):75-87.
17. Hunger SP, Lu X, Devidas M, Camitta BM, Gaynon PS, Winick NJ, et al. Improved survival for children and adolescents with acute lymphoblastic leukemia between 1990 and 2005: a report from the children's oncology group. Journal of clinical oncology : official journal of the American Society of Clinical Oncology 2012;30(14):1663-9.
18. Hossain MJ, Xie L, McCahan SM. Characterization of pediatric acute lymphoblastic leukemia survival patterns by age at diagnosis. Journal of cancer epidemiology 2014;2014:865979.
19. Howlader N, Noone AM, Krapcho M, Garshell J, Miller D, Altekruse SF, et al. SEER Cancer Statistics Review, 1975-2012, National Cancer Institute. Bethesda, MD, http://seer.cancer.gov/csr/1975_2012/, based on November 2014 SEER data submission, posted to the SEER web site, April 2015.
20. Smith M, Arthur D, Camitta B, Carroll AJ, Crist W, Gaynon P, et al. Uniform approach to risk classification and treatment assignment for children with acute lymphoblastic leukemia. Journal of clinical oncology : official journal of the American Society of Clinical Oncology 1996;14(1):18-24.
21. Borowitz MJ, Devidas M, Hunger SP, Bowman WP, Carroll AJ, Carroll WL, et al. Clinical significance of minimal residual disease in childhood acute lymphoblastic leukemia and its relationship to other prognostic factors: a Children's Oncology Group study. Blood 2008;111(12):5477-85.

22. Campana D. Minimal residual disease in acute lymphoblastic leukemia. Hematology / the Education Program of the American Society of Hematology American Society of Hematology Education Program 2010;2010:7-12.
23. Campana D. Minimal residual disease monitoring in childhood acute lymphoblastic leukemia. Current opinion in hematology 2012;19(4):313-8.
24. Pui CH, Pei D, Coustan-Smith E, Jeha S, Cheng C, Bowman WP, et al. Clinical utility of sequential minimal residual disease measurements in the context of risk-based therapy in childhood acute lymphoblastic leukaemia: a prospective study. The Lancet Oncology 2015;16(4):465-74.
25. Conter V, Bartram CR, Valsecchi MG, Schrauder A, Panzer-Grumayer R, Moricke A, et al. Molecular response to treatment redefines all prognostic factors in children and adolescents with B-cell precursor acute lymphoblastic leukemia: results in 3184 patients of the AIEOP-BFM ALL 2000 study. Blood 2010;115(16):3206-14.
26. Inaba H, Greaves M, Mullighan CG. Acute lymphoblastic leukaemia. Lancet 2013;381(9881):1943-55.
27. Greaves MF, Wiemels J. Origins of chromosome translocations in childhood leukaemia. Nature reviews Cancer 2003;3(9):639-49.
28. Greaves M. Infection, immune responses and the aetiology of childhood leukaemia. Nature reviews Cancer 2006;6(3):193-203.
29. Roman E, Simpson J, Ansell P, Kinsey S, Mitchell CD, McKinney PA, et al. Childhood acute lymphoblastic leukemia and infections in the first year of life: a report from the United Kingdom Childhood Cancer Study. American journal of epidemiology 2007;165(5):496-504.
30. Moriyama T, Relling MV, Yang JJ. Inherited genetic variation in childhood acute lymphoblastic leukemia. Blood 2015;125(26):3988-95.
31. Papaemmanuil E, Hosking FJ, Vijayakrishnan J, Price A, Olver B, Sheridan E, et al. Loci on 7p12.2, 10q21.2 and 14q11.2 are associated with risk of childhood acute lymphoblastic leukemia. Nature genetics 2009;41(9):1006-10.
32. Trevino LR, Yang W, French D, Hunger SP, Carroll WL, Devidas M, et al. Germline genomic variants associated with childhood acute lymphoblastic leukemia. Nature genetics 2009;41(9):1001-5.
33. Sherborne AL, Hosking FJ, Prasad RB, Kumar R, Koehler R, Vijayakrishnan J, et al. Variation in CDKN2A at 9p21.3 influences childhood acute lymphoblastic leukemia risk. Nature genetics 2010;42(6):492-4.
34. Perez-Andreu V, Roberts KG, Harvey RC, Yang W, Cheng C, Pei D, et al. Inherited GATA3 variants are associated with Ph-like childhood acute lymphoblastic leukemia and risk of relapse. Nature genetics 2013;45(12):1494-8.
35. Shah S, Schrader KA, Waanders E, Timms AE, Vijai J, Miething C, et al. A recurrent germline PAX5 mutation confers susceptibility to pre-B cell acute lymphoblastic leukemia. Nature genetics 2013;45(10):1226-31.
36. Zhang MY, Churpek JE, Keel SB, Walsh T, Lee MK, Loeb KR, et al. Germline ETV6 mutations in familial thrombocytopenia and hematologic malignancy. Nature genetics 2015;47(2):180-5.
37. Hasle H, Clemmensen IH, Mikkelsen M. Risks of leukaemia and solid tumours in individuals with Down's syndrome. Lancet 2000;355(9199):165-9.
38. Maloney KW, Carroll WL, Carroll AJ, Devidas M, Borowitz MJ, Martin PL, et al. Down syndrome childhood acute lymphoblastic leukemia has a unique spectrum of sentinel cytogenetic lesions that influences treatment outcome: a report from the Children's Oncology Group. Blood 2010;116(7):1045-50.
39. Ma X, Edmonson M, Yergeau D, Muzny DM, Hampton OA, Rusch M, et al. Rise and fall of subclones from diagnosis to relapse in pediatric B-acute lymphoblastic leukaemia. Nature communications 2015;6:6604.
40. Paulsson K, Johansson B. High hyperdiploid childhood acute lymphoblastic leukemia. Genes, chromosomes & cancer 2009;48(8):637-60.
41. Paulsson K, Forestier E, Lilljebjorn H, Heldrup J, Behrendtz M, Young BD, et al. Genetic landscape of high hyperdiploid childhood acute lymphoblastic leukemia. Proceedings of the National Academy of Sciences of the United States of America 2010;107(50):21719-24.
42. Harrison CJ, Moorman AV, Broadfield ZJ, Cheung KL, Harris RL, Reza Jalali G, et al. Three distinct subgroups of hypodiploidy in acute lymphoblastic leukaemia. British journal of haematology 2004;125(5):552-9.

43. Nachman JB, Heerema NA, Sather H, Camitta B, Forestier E, Harrison CJ, et al. Outcome of treatment in children with hypodiploid acute lymphoblastic leukemia. Blood 2007;110(4):1112-5.
44. Holmfeldt L, Wei L, Diaz-Flores E, Walsh M, Zhang J, Ding L, et al. The genomic landscape of hypodiploid acute lymphoblastic leukemia. Nature genetics 2013;45(3):242-52.
45. Harrison CJ. Cytogenetics of paediatric and adolescent acute lymphoblastic leukaemia. British journal of haematology 2009;144(2):147-56.
46. Mullighan CG, Phillips LA, Su X, Ma J, Miller CB, Shurtleff SA, et al. Genomic analysis of the clonal origins of relapsed acute lymphoblastic leukemia. Science 2008;322(5906):1377-80.
47. Pui CH, Carroll WL, Meshinchi S, Arceci RJ. Biology, risk stratification, and therapy of pediatric acute leukemias: an update. Journal of clinical oncology : official journal of the American Society of Clinical Oncology 2011;29(5):551-65.
48. Pieters R, Schrappe M, De Lorenzo P, Hann I, De Rossi G, Felice M, et al. A treatment protocol for infants younger than 1 year with acute lymphoblastic leukaemia (Interfant-99): an observational study and a multicentre randomised trial. Lancet 2007;370(9583):240-50.
49. Mrozek K, Harper DP, Aplan PD. Cytogenetics and molecular genetics of acute lymphoblastic leukemia. Hematology/oncology clinics of North America 2009;23(5):991-1010, v.
50. Roberts KG, Li Y, Payne-Turner D, Harvey RC, Yang YL, Pei D, et al. Targetable kinase-activating lesions in Ph-like acute lymphoblastic leukemia. The New England journal of medicine 2014;371(11):1005-15.
51. Mullighan CG. The molecular genetic makeup of acute lymphoblastic leukemia. Hematology / the Education Program of the American Society of Hematology American Society of Hematology Education Program 2012;2012:389-96.
52. Roberts KG, Mullighan CG. Genomics in acute lymphoblastic leukaemia: insights and treatment implications. Nature reviews Clinical oncology 2015;12(6):344-57.
53. van der Veer A, Waanders E, Pieters R, Willemse ME, Van Reijmersdal SV, Russell LJ, et al. Independent prognostic value of BCR-ABL1-like signature and IKZF1 deletion, but not high CRLF2 expression, in children with B-cell precursor ALL. Blood 2013;122(15):2622-9.
54. Waanders E, van der Velden VH, van der Schoot CE, van Leeuwen FN, van Reijmersdal SV, de Haas V, et al. Integrated use of minimal residual disease classification and IKZF1 alteration status accurately predicts 79% of relapses in pediatric acute lymphoblastic leukemia. Leukemia 2011;25(2):254-8.
55. Mullighan CG, Goorha S, Radtke I, Miller CB, Coustan-Smith E, Dalton JD, et al. Genome-wide analysis of genetic alterations in acute lymphoblastic leukaemia. Nature 2007;446(7137):758-64.
56. Zhang J, Mullighan CG, Harvey RC, Wu G, Chen X, Edmonson M, et al. Key pathways are frequently mutated in high-risk childhood acute lymphoblastic leukemia: a report from the Children's Oncology Group. Blood 2011;118(11):3080-7.
57. Mullighan CG. Molecular genetics of B-precursor acute lymphoblastic leukemia. The Journal of clinical investigation 2012;122(10):3407-15.
58. Wellmann S, Moderegger E, Zelmer A, Bettkober M, von Stackelberg A, Henze G, et al. FLT3 mutations in childhood acute lymphoblastic leukemia at first relapse. Leukemia 2005;19(3):467-8.
59. Figueroa ME, Chen SC, Andersson AK, Phillips LA, Li Y, Sotzen J, et al. Integrated genetic and epigenetic analysis of childhood acute lymphoblastic leukemia. The Journal of clinical investigation 2013;123(7):3099-111.
60. Jaffe JD, Wang Y, Chan HM, Zhang J, Huether R, Kryukov GV, et al. Global chromatin profiling reveals NSD2 mutations in pediatric acute lymphoblastic leukemia. Nature genetics 2013;45(11):1386-91.
61. Inthal A, Zeitlhofer P, Zeginigg M, Morak M, Grausenburger R, Fronkova E, et al. CREBBP HAT domain mutations prevail in relapse cases of high hyperdiploid childhood acute lymphoblastic leukemia. Leukemia 2012;26(8):1797-803.
62. Mar BG, Bullinger LB, McLean KM, Grauman PV, Harris MH, Stevenson K, et al. Mutations in epigenetic regulators including SETD2 are gained during relapse in paediatric acute lymphoblastic leukaemia. Nature communications 2014;5:3469.
63. Meyer JA, Wang J, Hogan LE, Yang JJ, Dandekar S, Patel JP, et al. Relapse-specific mutations in NT5C2 in childhood acute lymphoblastic leukemia. Nature genetics 2013;45(3):290-4.
64. Aster JC, Pear WS, Blacklow SC. Notch signaling in leukemia. Annual review of pathology 2008;3:587-613.

65. O'Neil J, Grim J, Strack P, Rao S, Tibbitts D, Winter C, et al. FBW7 mutations in leukemic cells mediate NOTCH pathway activation and resistance to gamma-secretase inhibitors. The Journal of experimental medicine 2007;204(8):1813-24.
66. Van Vlierberghe P, Ambesi-Impiombato A, De Keersmaecker K, Hadler M, Paietta E, Tallman MS, et al. Prognostic relevance of integrated genetic profiling in adult T-cell acute lymphoblastic leukemia. Blood 2013;122(1):74-82.
67. Van Vlierberghe P, Ferrando A. The molecular basis of T cell acute lymphoblastic leukemia. The Journal of clinical investigation 2012;122(10):3398-406.
68. Graux C, Cools J, Melotte C, Quentmeier H, Ferrando A, Levine R, et al. Fusion of NUP214 to ABL1 on amplified episomes in T-cell acute lymphoblastic leukemia. Nature genetics 2004;36(10):1084-9.
69. Shochat C, Tal N, Bandapalli OR, Palmi C, Ganmore I, te Kronnie G, et al. Gain-of-function mutations in interleukin-7 receptor-alpha (IL7R) in childhood acute lymphoblastic leukemias. The Journal of experimental medicine 2011;208(5):901-8.
70. Zhang J, Ding L, Holmfeldt L, Wu G, Heatley SL, Payne-Turner D, et al. The genetic basis of early T-cell precursor acute lymphoblastic leukaemia. Nature 2012;481(7380):157-63.
71. Cooper SL, Brown PA. Treatment of pediatric acute lymphoblastic leukemia. Pediatric clinics of North America 2015;62(1):61-73.
72. Krull KR, Brinkman TM, Li C, Armstrong GT, Ness KK, Srivastava DK, et al. Neurocognitive outcomes decades after treatment for childhood acute lymphoblastic leukemia: a report from the St Jude lifetime cohort study. Journal of clinical oncology : official journal of the American Society of Clinical Oncology 2013;31(35):4407-15.
73. Schrappe M, Hunger SP, Pui CH, Saha V, Gaynon PS, Baruchel A, et al. Outcomes after induction failure in childhood acute lymphoblastic leukemia. The New England journal of medicine 2012;366(15):1371-81.
74. Hochberg J, Khaled S, Forman SJ, Cairo MS. Criteria for and outcomes of allogeneic haematopoietic stem cell transplant in children, adolescents and young adults with acute lymphoblastic leukaemia in first complete remission. British journal of haematology 2013;161(1):27-42.
75. Locatelli F, Schrappe M, Bernardo ME, Rutella S. How I treat relapsed childhood acute lymphoblastic leukemia. Blood 2012;120(14):2807-16.
76. Asselin BL, Devidas M, Wang C, Pullen J, Borowitz MJ, Hutchison R, et al. Effectiveness of high-dose methotrexate in T-cell lymphoblastic leukemia and advanced-stage lymphoblastic lymphoma: a randomized study by the Children's Oncology Group (POG 9404). Blood 2011;118(4):874-83.
77. Kraszewska MD, Dawidowska M, Szczepanski T, Witt M. T-cell acute lymphoblastic leukaemia: recent molecular biology findings. British journal of haematology 2012;156(3):303-15.
78. Coustan-Smith E, Mullighan CG, Onciu M, Behm FG, Raimondi SC, Pei D, et al. Early T-cell precursor leukaemia: a subtype of very high-risk acute lymphoblastic leukaemia. The Lancet Oncology 2009;10(2):147-56.
79. Schrappe M, Valsecchi MG, Bartram CR, Schrauder A, Panzer-Grumayer R, Moricke A, et al. Late MRD response determines relapse risk overall and in subsets of childhood T-cell ALL: results of the AIEOP-BFM-ALL 2000 study. Blood 2011;118(8):2077-84.
80. Teachey DT, Hunger SP. Predicting relapse risk in childhood acute lymphoblastic leukaemia. British journal of haematology 2013;162(5):606-20.
81. de Boer J, Walf-Vorderwulbecke V, Williams O. In focus: MLL-rearranged leukemia. Leukemia 2013;27(6):1224-8.
82. Kang H, Wilson CS, Harvey RC, Chen IM, Murphy MH, Atlas SR, et al. Gene expression profiles predictive of outcome and age in infant acute lymphoblastic leukemia: a Children's Oncology Group study. Blood 2012;119(8):1872-81.
83. Armstrong SA, Staunton JE, Silverman LB, Pieters R, den Boer ML, Minden MD, et al. MLL translocations specify a distinct gene expression profile that distinguishes a unique leukemia. Nature genetics 2002;30(1):41-7.
84. Chillon MC, Gomez-Casares MT, Lopez-Jorge CE, Rodriguez-Medina C, Molines A, Sarasquete ME, et al. Prognostic significance of FLT3 mutational status and expression levels in MLL-AF4+ and MLL-germline acute lymphoblastic leukemia. Leukemia 2012;26(11):2360-6.

85. Stam RW, den Boer ML, Schneider P, Nollau P, Horstmann M, Beverloo HB, et al. Targeting FLT3 in primary MLL-gene-rearranged infant acute lymphoblastic leukemia. Blood 2005;106(7):2484-90.
86. Salzer WL, Jones TL, Devidas M, Dreyer ZE, Gore L, Winick NJ, et al. Decreased induction morbidity and mortality following modification to induction therapy in infants with acute lymphoblastic leukemia enrolled on AALL0631: a report from the Children's Oncology Group. Pediatric blood & cancer 2015;62(3):414-8.
87. Crist W, Carroll A, Shuster J, Jackson J, Head D, Borowitz M, et al. Philadelphia chromosome positive childhood acute lymphoblastic leukemia: clinical and cytogenetic characteristics and treatment outcome. A Pediatric Oncology Group study. Blood 1990;76(3):489-94.
88. Schultz KR, Bowman WP, Aledo A, Slayton WB, Sather H, Devidas M, et al. Improved early event-free survival with imatinib in Philadelphia chromosome-positive acute lymphoblastic leukemia: a children's oncology group study. Journal of clinical oncology : official journal of the American Society of Clinical Oncology 2009;27(31):5175-81.
89. Inukai T, Hirose K, Inaba T, Kurosawa H, Hama A, Inada H, et al. Hypercalcemia in childhood acute lymphoblastic leukemia: frequent implication of parathyroid hormone-related peptide and E2A-HLF from translocation 17;19. Leukemia 2007;21(2):288-96.
90. Hirose K, Inukai T, Kikuchi J, Furukawa Y, Ikawa T, Kawamoto H, et al. Aberrant induction of LMO2 by the E2A-HLF chimeric transcription factor and its implication in leukemogenesis of B-precursor ALL with t(17;19). Blood 2010;116(6):962-70.
91. Inoue A, Seidel MG, Wu W, Kamizono S, Ferrando AA, Bronson RT, et al. Slug, a highly conserved zinc finger transcriptional repressor, protects hematopoietic progenitor cells from radiation-induced apoptosis in vivo. Cancer cell 2002;2(4):279-88.
92. Fischer U, Forster M, Rinaldi A, Risch T, Sungalee S, Warnatz HJ, et al. Genomics and drug profiling of fatal TCF3-HLF-positive acute lymphoblastic leukemia identifies recurrent mutation patterns and therapeutic options. Nature genetics 2015;47(9):1020-9.
93. Katsnelson A. Momentum grows to make 'personalized' medicine more 'precise'. Nature medicine 2013;19(3):249-49.
94. Schork NJ. Personalized medicine: Time for one-person trials. Nature 2015;520(7549):609-11.
95. Do K, O'Sullivan Coyne G, Chen AP. An overview of the NCI precision medicine trials-NCI MATCH and MPACT. Chinese clinical oncology 2015;4(3):31.
96. Hanahan D, Weinberg RA. The hallmarks of cancer. Cell 2000;100(1):57-70.
97. Hanahan D, Weinberg RA. Hallmarks of cancer: the next generation. Cell 2011;144(5):646-74.
98. Hunger SP, Mullighan CG. Redefining ALL classification: toward detecting high-risk ALL and implementing precision medicine. Blood 2015;125(26):3977-87.
99. Roberts KG, Morin RD, Zhang J, Hirst M, Zhao Y, Su X, et al. Genetic alterations activating kinase and cytokine receptor signaling in high-risk acute lymphoblastic leukemia. Cancer cell 2012;22(2):153-66.
100. Schinnerl D, Fortschegger K, Kauer M, Marchante JR, Kofler R, Den Boer ML, et al. The role of the Janus-faced transcription factor PAX5-JAK2 in acute lymphoblastic leukemia. Blood 2015;125(8):1282-91.
101. Cardoso BA, de Almeida SF, Laranjeira AB, Carmo-Fonseca M, Yunes JA, Coffer PJ, et al. TAL1/SCL is downregulated upon histone deacetylase inhibition in T-cell acute lymphoblastic leukemia cells. Leukemia 2011;25(10):1578-86.
102. West AC, Johnstone RW. New and emerging HDAC inhibitors for cancer treatment. The Journal of clinical investigation 2014;124(1):30-9.
103. Nowell C, Radtke F. Cutaneous Notch signaling in health and disease. Cold Spring Harbor perspectives in medicine 2013;3(12):a017772.
104. Takebe N, Miele L, Harris PJ, Jeong W, Bando H, Kahn M, et al. Targeting Notch, Hedgehog, and Wnt pathways in cancer stem cells: clinical update. Nature reviews Clinical oncology 2015;12(8):445-64.
105. Palomero T, Ferrando A. Therapeutic targeting of NOTCH1 signaling in T-cell acute lymphoblastic leukemia. Clinical lymphoma & myeloma 2009;9 Suppl 3:S205-10.
106. van Es JH, van Gijn ME, Riccio O, van den Born M, Vooijs M, Begthel H, et al. Notch/gamma-secretase inhibition turns proliferative cells in intestinal crypts and adenomas into goblet cells. Nature 2005;435(7044):959-63.

107. Minuzzo S, Agnusdei V, Pusceddu I, Pinazza M, Moserle L, Masiero M, et al. DLL4 regulates NOTCH signaling and growth of T acute lymphoblastic leukemia cells in NOD/SCID mice. Carcinogenesis 2015;36(1):115-21.
108. Kangsamaksin T, Murtomaki A, Kofler NM, Cuervo H, Chaudhri RA, Tattersall IW, et al. NOTCH decoys that selectively block DLL/NOTCH or JAG/NOTCH disrupt angiogenesis by unique mechanisms to inhibit tumor growth. Cancer discovery 2015;5(2):182-97.
109. Tosello V, Bordin F, Yu J, Agnusdei V, Indraccolo S, Basso G, et al. Calcineurin and GSK-3 inhibition sensitizes T-cell acute lymphoblastic leukemia cells to apoptosis through X-linked inhibitor of apoptosis protein degradation. Leukemia 2016;30(4):812-22.
110. Rowley JD. Chromosomal translocations: revisited yet again. Blood 2008;112(6):2183-9.
111. Adams JM, Cory S. Bcl-2-regulated apoptosis: mechanism and therapeutic potential. Current opinion in immunology 2007;19(5):488-96.
112. Kirkin V, Joos S, Zornig M. The role of Bcl-2 family members in tumorigenesis. Biochimica et biophysica acta 2004;1644(2-3):229-49.
113. Roberts AW, Seymour JF, Brown JR, Wierda WG, Kipps TJ, Khaw SL, et al. Substantial susceptibility of chronic lymphocytic leukemia to BCL2 inhibition: results of a phase I study of navitoclax in patients with relapsed or refractory disease. Journal of clinical oncology : official journal of the American Society of Clinical Oncology 2012;30(5):488-96.
114. Besbes S, Mirshahi M, Pocard M, Billard C. Strategies targeting apoptosis proteins to improve therapy of chronic lymphocytic leukemia. Blood reviews 2015;29(5):345-50.
115. Roberts AW, Davids MS, Pagel JM, Kahl BS, Puvvada SD, Gerecitano JF, et al. Targeting BCL2 with Venetoclax in Relapsed Chronic Lymphocytic Leukemia. The New England journal of medicine 2016;374(4):311-22.
116. Del Gaizo Moore V, Letai A. BH3 profiling--measuring integrated function of the mitochondrial apoptotic pathway to predict cell fate decisions. Cancer letters 2013;332(2):202-5.
117. Suryani S, Carol H, Chonghaile TN, Frismantas V, Sarmah C, High L, et al. Cell and molecular determinants of in vivo efficacy of the BH3 mimetic ABT-263 against pediatric acute lymphoblastic leukemia xenografts. Clinical cancer research : an official journal of the American Association for Cancer Research 2014;20(17):4520-31.
118. Bonapace L, Bornhauser BC, Schmitz M, Cario G, Ziegler U, Niggli FK, et al. Induction of autophagy-dependent necroptosis is required for childhood acute lymphoblastic leukemia cells to overcome glucocorticoid resistance. The Journal of clinical investigation 2010;120(4):1310-23.
119. Zhou W, Yuan J. Necroptosis in health and diseases. Seminars in cell & developmental biology 2014;35:14-23.
120. Fulda S, Vucic D. Targeting IAP proteins for therapeutic intervention in cancer. Nature reviews Drug discovery 2012;11(2):109-24.
121. Amaravadi RK, Schilder RJ, Martin LP, Levin M, Graham MA, Weng DE, et al. A Phase I Study of the SMAC-Mimetic Birinapant in Adults with Refractory Solid Tumors or Lymphoma. Molecular cancer therapeutics 2015;14(11):2569-75.
122. McComb S, Aguade-Gorgorio J, Harder L, Marovca B, Cario G, Eckert C, et al. Activation of concurrent apoptosis and necroptosis by SMAC mimetics for the treatment of refractory and relapsed ALL. Science translational medicine 2016;8(339):339ra70.
123. Polager S, Ginsberg D. p53 and E2f: partners in life and death. Nature reviews Cancer 2009;9(10):738-48.
124. Asghar U, Witkiewicz AK, Turner NC, Knudsen ES. The history and future of targeting cyclin-dependent kinases in cancer therapy. Nature reviews Drug discovery 2015;14(2):130-46.
125. Kumar SK, LaPlant B, Chng WJ, Zonder J, Callander N, Fonseca R, et al. Dinaciclib, a novel CDK inhibitor, demonstrates encouraging single-agent activity in patients with relapsed multiple myeloma. Blood 2015;125(3):443-8.
126. Flynn J, Jones J, Johnson AJ, Andritsos L, Maddocks K, Jaglowski S, et al. Dinaciclib is a Novel Cyclin Dependent Kinase Inhibitor with Significant Clinical Activity in Relapsed and Refractory Chronic Lymphocytic Leukemia. Leukemia 2015;29(7):1524-29.
127. Gautschi O, Heighway J, Mack PC, Purnell PR, Lara PN, Jr., Gandara DR. Aurora kinases as anticancer drug targets. Clinical cancer research : an official journal of the American Association for Cancer Research 2008;14(6):1639-48.
128. Mullighan CG, Zhang J, Kasper LH, Lerach S, Payne-Turner D, Phillips LA, et al. CREBBP mutations in relapsed acute lymphoblastic leukaemia. Nature 2011;471(7337):235-9.

129. Bernt KM, Armstrong SA. Targeting epigenetic programs in MLL-rearranged leukemias. Hematology / the Education Program of the American Society of Hematology American Society of Hematology Education Program 2011;2011:354-60.
130. Daigle SR, Olhava EJ, Therkelsen CA, Basavapathruni A, Jin L, Boriack-Sjodin PA, et al. Potent inhibition of DOT1L as treatment of MLL-fusion leukemia. Blood 2013;122(6):1017-25.
131. Falkenberg KJ, Johnstone RW. Histone deacetylases and their inhibitors in cancer, neurological diseases and immune disorders. Nature reviews Drug discovery 2014;13(9):673-91.
132. Bhatla T, Wang J, Morrison DJ, Raetz EA, Burke MJ, Brown P, et al. Epigenetic reprogramming reverses the relapse-specific gene expression signature and restores chemosensitivity in childhood B-lymphoblastic leukemia. Blood 2012;119(22):5201-10.
133. Fouladi M, Park JR, Stewart CF, Gilbertson RJ, Schaiquevich P, Sun J, et al. Pediatric phase I trial and pharmacokinetic study of vorinostat: a Children's Oncology Group phase I consortium report. Journal of clinical oncology : official journal of the American Society of Clinical Oncology 2010;28(22):3623-9.
134. Masetti R, Serravalle S, Biagi C, Pession A. The role of HDACs inhibitors in childhood and adolescence acute leukemias. Journal of biomedicine & biotechnology 2011;2011:148046.
135. Muller S, Filippakopoulos P, Knapp S. Bromodomains as therapeutic targets. Expert reviews in molecular medicine 2011;13:e29.
136. Zuber J, Shi J, Wang E, Rappaport AR, Herrmann H, Sison EA, et al. RNAi screen identifies Brd4 as a therapeutic target in acute myeloid leukaemia. Nature 2011;478(7370):524-8.
137. Ott CJ, Kopp N, Bird L, Paranal RM, Qi J, Bowman T, et al. BET bromodomain inhibition targets both c-Myc and IL7R in high-risk acute lymphoblastic leukemia. Blood 2012;120(14):2843-52.
138. Knoechel B, Roderick JE, Williamson KE, Zhu J, Lohr JG, Cotton MJ, et al. An epigenetic mechanism of resistance to targeted therapy in T cell acute lymphoblastic leukemia. Nature genetics 2014;46(4):364-70.
139. Jabbour E, O'Brien S, Ravandi F, Kantarjian H. Monoclonal antibodies in acute lymphoblastic leukemia. Blood 2015;125(26):4010-6.
140. Raponi S, De Propris MS, Intoppa S, Milani ML, Vitale A, Elia L, et al. Flow cytometric study of potential target antigens (CD19, CD20, CD22, CD33) for antibody-based immunotherapy in acute lymphoblastic leukemia: analysis of 552 cases. Leukemia & lymphoma 2011;52(6):1098-107.
141. Scheuermann RH, Racila E. CD19 antigen in leukemia and lymphoma diagnosis and immunotherapy. Leukemia & lymphoma 1995;18(5-6):385-97.
142. Thomas DA, O'Brien S, Faderl S, Garcia-Manero G, Ferrajoli A, Wierda W, et al. Chemoimmunotherapy with a modified hyper-CVAD and rituximab regimen improves outcome in de novo Philadelphia chromosome-negative precursor B-lineage acute lymphoblastic leukemia. Journal of clinical oncology : official journal of the American Society of Clinical Oncology 2010;28(24):3880-9.
143. Nagorsen D, Kufer P, Baeuerle PA, Bargou R. Blinatumomab: a historical perspective. Pharmacology & therapeutics 2012;136(3):334-42.
144. Hoffman LM, Gore L. Blinatumomab, a Bi-Specific Anti-CD19/CD3 BiTE((R)) Antibody for the Treatment of Acute Lymphoblastic Leukemia: Perspectives and Current Pediatric Applications. Frontiers in oncology 2014;4:63.
145. Agata Y, Kawasaki A, Nishimura H, Ishida Y, Tsubata T, Yagita H, et al. Expression of the PD-1 antigen on the surface of stimulated mouse T and B lymphocytes. International immunology 1996;8(5):765-72.
146. Norde WJ, Maas F, Hobo W, Korman A, Quigley M, Kester MG, et al. PD-1/PD-L1 interactions contribute to functional T-cell impairment in patients who relapse with cancer after allogeneic stem cell transplantation. Cancer research 2011;71(15):5111-22.
147. Berger R, Rotem-Yehudar R, Slama G, Landes S, Kneller A, Leiba M, et al. Phase I safety and pharmacokinetic study of CT-011, a humanized antibody interacting with PD-1, in patients with advanced hematologic malignancies. Clinical cancer research : an official journal of the American Association for Cancer Research 2008;14(10):3044-51.
148. Maude SL, Teachey DT, Porter DL, Grupp SA. CD19-targeted chimeric antigen receptor T-cell therapy for acute lymphoblastic leukemia. Blood 2015;125(26):4017-23.
149. Restifo NP, Smyth MJ, Snyder A. Acquired resistance to immunotherapy and future challenges. Nature reviews Cancer 2016;16(2):121-6.

150. Gross S, Rahal R, Stransky N, Lengauer C, Hoeflich KP. Targeting cancer with kinase inhibitors. The Journal of clinical investigation 2015;125(5):1780-9.
151. Manning G, Whyte DB, Martinez R, Hunter T, Sudarsanam S. The protein kinase complement of the human genome. Science 2002;298(5600):1912-34.
152. Vogelstein B, Papadopoulos N, Velculescu VE, Zhou S, Diaz LA, Jr., Kinzler KW. Cancer genome landscapes. Science 2013;339(6127):1546-58.
153. Torkamani A, Verkhivker G, Schork NJ. Cancer driver mutations in protein kinase genes. Cancer letters 2009;281(2):117-27.
154. Druker BJ, Guilhot F, O'Brien SG, Gathmann I, Kantarjian H, Gattermann N, et al. Five-year follow-up of patients receiving imatinib for chronic myeloid leukemia. The New England journal of medicine 2006;355(23):2408-17.
155. Bixby D, Talpaz M. Mechanisms of resistance to tyrosine kinase inhibitors in chronic myeloid leukemia and recent therapeutic strategies to overcome resistance. Hematology / the Education Program of the American Society of Hematology American Society of Hematology Education Program 2009:461-76.
156. Porkka K, Koskenvesa P, Lundan T, Rimpilainen J, Mustjoki S, Smykla R, et al. Dasatinib crosses the blood-brain barrier and is an efficient therapy for central nervous system Philadelphia chromosome-positive leukemia. Blood 2008;112(4):1005-12.
157. Flaherty KT, Infante JR, Daud A, Gonzalez R, Kefford RF, Sosman J, et al. Combined BRAF and MEK inhibition in melanoma with BRAF V600 mutations. The New England journal of medicine 2012;367(18):1694-703.
158. Shoemaker RH. The NCI60 human tumour cell line anticancer drug screen. Nature reviews Cancer 2006;6(10):813-23.
159. Weinstein JN. Spotlight on molecular profiling: "Integromic" analysis of the NCI-60 cancer cell lines. Molecular cancer therapeutics 2006;5(11):2601-5.
160. McDermott U, Sharma SV, Settleman J. High-throughput lung cancer cell line screening for genotype-correlated sensitivity to an EGFR kinase inhibitor. Methods in enzymology 2008;438:331-41.
161. Sharma SV, Haber DA, Settleman J. Cell line-based platforms to evaluate the therapeutic efficacy of candidate anticancer agents. Nature reviews Cancer 2010;10(4):241-53.
162. Gillet JP, Calcagno AM, Varma S, Marino M, Green LJ, Vora MI, et al. Redefining the relevance of established cancer cell lines to the study of mechanisms of clinical anti-cancer drug resistance. Proceedings of the National Academy of Sciences of the United States of America 2011;108(46):18708-13.
163. Holmberg J, Perlmann T. Maintaining differentiated cellular identity. Nature reviews Genetics 2012;13(6):429-39.
164. Gao H, Korn JM, Ferretti S, Monahan JE, Wang Y, Singh M, et al. High-throughput screening using patient-derived tumor xenografts to predict clinical trial drug response. Nature medicine 2015;21(11):1318-25.
165. Yamada S, Hongo T, Okada S, Watanabe C, Fujii Y, Ohzeki T. Clinical relevance of in vitro chemoresistance in childhood acute myeloid leukemia. Leukemia 2001;15(12):1892-7.
166. Cree IA, Kurbacher CM. ATP-based tumor chemosensitivity testing: assisting new agent development. Anti-cancer drugs 1999;10(5):431-5.
167. Armstrong F, Brunet de la Grange P, Gerby B, Rouyez MC, Calvo J, Fontenay M, et al. NOTCH is a key regulator of human T-cell acute leukemia initiating cell activity. Blood 2009;113(8):1730-40.
168. Chiu PP, Jiang H, Dick JE. Leukemia-initiating cells in human T-lymphoblastic leukemia exhibit glucocorticoid resistance. Blood 2010;116(24):5268-79.
169. Cox CV, Martin HM, Kearns PR, Virgo P, Evely RS, Blair A. Characterization of a progenitor cell population in childhood T-cell acute lymphoblastic leukemia. Blood 2007;109(2):674-82.
170. Chiarini F, Lonetti A, Evangelisti C, Buontempo F, Orsini E, Evangelisti C, et al. Advances in understanding the acute lymphoblastic leukemia bone marrow microenvironment: From biology to therapeutic targeting. Biochimica et biophysica acta 2016;1863(3):449-63.
171. Iwamoto S, Mihara K, Downing JR, Pui CH, Campana D. Mesenchymal cells regulate the response of acute lymphoblastic leukemia cells to asparaginase. The Journal of clinical investigation 2007;117(4):1049-57.
172. Mendelson A, Frenette PS. Hematopoietic stem cell niche maintenance during homeostasis and regeneration. Nature medicine 2014;20(8):833-46.
173. Morrison SJ, Scadden DT. The bone marrow niche for haematopoietic stem cells. Nature 2014;505(7483):327-34.

174. Fatehullah A, Tan SH, Barker N. Organoids as an in vitro model of human development and disease. Nat Cell Biol 2016;18(3):246-54.
175. LaBarbera DV, Reid BG, Yoo BH. The multicellular tumor spheroid model for high-throughput cancer drug discovery. Expert opinion on drug discovery 2012;7(9):819-30.
176. Nyga A, Cheema U, Loizidou M. 3D tumour models: novel in vitro approaches to cancer studies. Journal of cell communication and signaling 2011;5(3):239-48.
177. McCracken KW, Cata EM, Crawford CM, Sinagoga KL, Schumacher M, Rockich BE, et al. Modelling human development and disease in pluripotent stem-cell-derived gastric organoids. Nature 2014;516(7531):400-4.
178. Ingber DE. Mechanobiology and diseases of mechanotransduction. Annals of medicine 2003;35(8):564-77.
179. Rigat-Brugarolas LG, Elizalde-Torrent A, Bernabeu M, De Niz M, Martin-Jaular L, Fernandez-Becerra C, et al. A functional microengineered model of the human splenon-on-a-chip. Lab on a chip 2014;14(10):1715-24.
180. Torisawa YS, Spina CS, Mammoto T, Mammoto A, Weaver JC, Tat T, et al. Bone marrow-on-a-chip replicates hematopoietic niche physiology in vitro. Nature methods 2014;11(6):663-9.
181. Griep LM, Wolbers F, de Wagenaar B, ter Braak PM, Weksler BB, Romero IA, et al. BBB on chip: microfluidic platform to mechanically and biochemically modulate blood-brain barrier function. Biomedical microdevices 2013;15(1):145-50.
182. Huh D, Leslie DC, Matthews BD, Fraser JP, Jurek S, Hamilton GA, et al. A human disease model of drug toxicity-induced pulmonary edema in a lung-on-a-chip microdevice. Science translational medicine 2012;4(159):159ra47.
183. Di Veroli GY, Fornari C, Goldlust I, Mills G, Koh SB, Bramhall JL, et al. An automated fitting procedure and software for dose-response curves with multiphasic features. Scientific reports 2015;5:14701.
184. Huang S, Pang L. Comparing statistical methods for quantifying drug sensitivity based on in vitro dose-response assays. Assay and drug development technologies 2012;10(1):88-96.
185. Pemovska T, Kontro M, Yadav B, Edgren H, Eldfors S, Szwajda A, et al. Individualized systems medicine strategy to tailor treatments for patients with chemorefractory acute myeloid leukemia. Cancer discovery 2013;3(12):1416-29.
186. Chou T-C, Talalay P. Analysis of combined drug effects: a new look at a very old problem. Trends in Pharmacological Sciences 1983;4:450-54.
187. Chou TC. Synergy determination issues. Journal of virology 2002;76(20):10577; author reply 78.
188. Chou T-C, Dong H-J, Timmermans PBMWM. Design, experimentation and computerized automated data analysis of synergistic drug combinations against xenograft tumors by Taxotere and T900607. Cancer research 2005;65(9 Supplement):1167-67.
189. Ocana A, Amir E, Yeung C, Seruga B, Tannock IF. How valid are claims for synergy in published clinical studies? Annals of oncology : official journal of the European Society for Medical Oncology / ESMO 2012;23(8):2161-6.
190. Dranoff G. Experimental mouse tumour models: what can be learnt about human cancer immunology? Nature reviews Immunology 2012;12(1):61-6.
191. Hauer J, Borkhardt A, Sanchez-Garcia I, Cobaleda C. Genetically engineered mouse models of human B-cell precursor leukemias. Cell cycle 2014;13(18):2836-46.
192. Savino AM, Izraeli S. On mice and humans: the role of thymic stromal lymphopoietin in human B-cell development and leukemia. Haematologica 2016;101(4):391-3.
193. Jacoby E, Chien CD, Fry TJ. Murine models of acute leukemia: important tools in current pediatric leukemia research. Frontiers in oncology 2014;4:95.
194. Voncken JW, Kaartinen V, Pattengale PK, Germeraad WT, Groffen J, Heisterkamp N. BCR/ABL P210 and P190 cause distinct leukemia in transgenic mice. Blood 1995;86(12):4603-11.
195. Bijl J, Sauvageau M, Thompson A, Sauvageau G. High incidence of proviral integrations in the Hoxa locus in a new model of E2a-PBX1-induced B-cell leukemia. Genes & development 2005;19(2):224-33.
196. Smith KS, Rhee JW, Naumovski L, Cleary ML. Disrupted differentiation and oncogenic transformation of lymphoid progenitors in E2A-HLF transgenic mice. Molecular and cellular biology 1999;19(6):4443-51.
197. Andreasson P, Schwaller J, Anastasiadou E, Aster J, Gilliland DG. The expression of ETV6/CBFA2 (TEL/AML1) is not sufficient for the transformation of hematopoietic cell lines in

vitro or the induction of hematologic disease in vivo. Cancer genetics and cytogenetics 2001;130(2):93-104.
198. Beverly LJ, Capobianco AJ. Perturbation of Ikaros isoform selection by MLV integration is a cooperative event in Notch(IC)-induced T cell leukemogenesis. Cancer cell 2003;3(6):551-64.
199. Condorelli GL, Facchiano F, Valtieri M, Proietti E, Vitelli L, Lulli V, et al. T-cell-directed TAL-1 expression induces T-cell malignancies in transgenic mice. Cancer research 1996;56(22):5113-9.
200. Shultz LD, Ishikawa F, Greiner DL. Humanized mice in translational biomedical research. Nature reviews Immunology 2007;7(2):118-30.
201. Brentjens RJ, Santos E, Nikhamin Y, Yeh R, Matsushita M, La Perle K, et al. Genetically targeted T cells eradicate systemic acute lymphoblastic leukemia xenografts. Clinical cancer research : an official journal of the American Association for Cancer Research 2007;13(18 Pt 1):5426-35.
202. Schmitz M, Breithaupt P, Scheidegger N, Cario G, Bonapace L, Meissner B, et al. Xenografts of highly resistant leukemia recapitulate the clonal composition of the leukemogenic compartment. Blood 2011;118(7):1854-64.
203. Meyer LH, Debatin KM. Diversity of human leukemia xenograft mouse models: implications for disease biology. Cancer research 2011;71(23):7141-4.
204. Anderson K, Lutz C, van Delft FW, Bateman CM, Guo Y, Colman SM, et al. Genetic variegation of clonal architecture and propagating cells in leukaemia. Nature 2011;469(7330):356-61.
205. Tuntland T, Ethell B, Kosaka T, Blasco F, Zang RX, Jain M, et al. Implementation of pharmacokinetic and pharmacodynamic strategies in early research phases of drug discovery and development at Novartis Institute of Biomedical Research. Frontiers in pharmacology 2014;5:174.
206. Attarwala H. TGN1412: From Discovery to Disaster. Journal of young pharmacists : JYP 2010;2(3):332-6.
207. Hay M, Thomas DW, Craighead JL, Economides C, Rosenthal J. Clinical development success rates for investigational drugs. Nature biotechnology 2014;32(1):40-51.
208. Honkoop P, Scholte HR, de Man RA, Schalm SW. Mitochondrial injury. Lessons from the fialuridine trial. Drug safety 1997;17(1):1-7.
209. Shanks N, Greek R, Greek J. Are animal models predictive for humans? Philosophy, ethics, and humanities in medicine : PEHM 2009;4:2.
210. Fagioli F, Quarello P, Zecca M, Lanino E, Rognoni C, Balduzzi A, et al. Hematopoietic stem cell transplantation for children with high-risk acute lymphoblastic leukemia in first complete remission: a report from the AIEOP registry. Haematologica 2013;98(8):1273-81.
211. Paganin M, Zecca M, Fabbri G, Polato K, Biondi A, Rizzari C, et al. Minimal residual disease is an important predictive factor of outcome in children with relapsed 'high-risk' acute lymphoblastic leukemia. Leukemia 2008;22(12):2193-200.
212. Bhojwani D, Pui CH. Relapsed childhood acute lymphoblastic leukaemia. The Lancet Oncology 2013;14(6):e205-17.
213. Schmitz M, Bourquin JP, Bornhauser BC. Alternative technique for intrafemoral injection and bone marrow sampling in mouse transplant models. Leukemia & lymphoma 2011;52(9):1806-8.
214. Schmitz M, Mirkowska P, Breithaupt P, Meissner B, Cario G, Schrauder A, et al. Leukemia-Initiating Cells Are Frequent in Very High Risk Childhood Acute Lymphoblastic Leukemia and Give Rise to Relatively Stable Phenotypes in Immunodeficient Mice. Blood 2009;114(22):86-86.
215. Holmfeldt L, Mullighan CG. Generation of human acute lymphoblastic leukemia xenografts for use in oncology drug discovery. Current protocols in pharmacology / editorial board, SJ Enna 2015;68:14 32 1-19.
216. Clappier E, Gerby B, Sigaux F, Delord M, Touzri F, Hernandez L, et al. Clonal selection in xenografted human T cell acute lymphoblastic leukemia recapitulates gain of malignancy at relapse. The Journal of experimental medicine 2011;208(4):653-61.
217. Notta F, Mullighan CG, Wang JC, Poeppl A, Doulatov S, Phillips LA, et al. Evolution of human BCR-ABL1 lymphoblastic leukaemia-initiating cells. Nature 2011;469(7330):362-7.
218. Arrowsmith J. A decade of change. Nature reviews Drug discovery 2012;11(1):17-8.
219. Swinney DC, Anthony J. How were new medicines discovered? Nature reviews Drug discovery 2011;10(7):507-19.

220. Moffat JG, Rudolph J, Bailey D. Phenotypic screening in cancer drug discovery - past, present and future. Nature reviews Drug discovery 2014;13(8):588-602.
221. Domcke S, Sinha R, Levine DA, Sander C, Schultz N. Evaluating cell lines as tumour models by comparison of genomic profiles. Nature communications 2013;4.
222. Bachmann PS, Gorman R, Mackenzie KL, Lutze-Mann L, Lock RB. Dexamethasone resistance in B-cell precursor childhood acute lymphoblastic leukemia occurs downstream of ligand-induced nuclear translocation of the glucocorticoid receptor. Blood 2005;105(6):2519-26.
223. Malani D, Murumägi A, Yadav B, Pemovska T, Mpindi JP, Kontro M, et al. AML Specific Targeted Drugs Identified By Drug Sensitivity and Resistance Testing: Comparison of Ex Vivo Patient Cells with in Vitro Cell Lines. Blood 2014;124(21):2163-63.
224. Den Boer ML, Harms DO, Pieters R, Kazemier KM, Gobel U, Korholz D, et al. Patient stratification based on prednisolone-vincristine-asparaginase resistance profiles in children with acute lymphoblastic leukemia. Journal of clinical oncology : official journal of the American Society of Clinical Oncology 2003;21(17):3262-8.
225. Boutter J, Huang Y, Marovca B, Vonderheit A, Grotzer MA, Eckert C, et al. Image-based RNA interference screening reveals an individual dependence of acute lymphoblastic leukemia on stromal cysteine support. Oncotarget 2014;5(22):11501-12.
226. Hauer J, Mullighan C, Morillon E, Wang G, Bruneau J, Brousse N, et al. Loss of p19Arf in a Rag1(-/-) B-cell precursor population initiates acute B-lymphoblastic leukemia. Blood 2011;118(3):544-53.
227. Winter SS, Sweatman J, Shuster JJ, Link MP, Amylon MD, Pullen J, et al. Bone marrow stroma-supported culture of T-lineage acute lymphoblastic leukemic cells predicts treatment outcome in children: a Pediatric Oncology Group study. Leukemia 2002;16(6):1121-6.
228. Pramanik R, Sheng X, Ichihara B, Heisterkamp N, Mittelman SD. Adipose tissue attracts and protects acute lymphoblastic leukemia cells from chemotherapy. Leukemia research 2013;37(5):503-9.
229. Dandapani S, Rosse G, Southall N, Salvino JM, Thomas CJ. Selecting, Acquiring, and Using Small Molecule Libraries for High-Throughput Screening. Current protocols in chemical biology 2012;4:177-91.
230. Riss TL, Moravec RA, Niles AL, Duellman S, Benink HA, Worzella TJ, et al. Cell Viability Assays. In: Sittampalam GS, Coussens NP, Nelson H, Arkin M, Auld D, Austin C, et al., editors. Assay Guidance Manual. Bethesda (MD)2004.
231. Johnson S, Rabinovitch P. Ex-vivo imaging of excised tissue using vital dyes and confocal microscopy. Current Protocols in Cytometry 2012;CHAPTER:Unit9.39-Unit9.39.
232. Kepp O, Galluzzi L, Lipinski M, Yuan J, Kroemer G. Cell death assays for drug discovery. Nature reviews Drug discovery 2011;10(3):221-37.
233. Hartwell KA, Miller PG, Mukherjee S, Kahn AR, Stewart AL, Logan DJ, et al. Niche-based screening identifies small-molecule inhibitors of leukemia stem cells. Nature chemical biology 2013;9(12):840-8.
234. Bullen A. Microscopic imaging techniques for drug discovery. Nature reviews Drug discovery 2008;7(1):54-67.
235. Garnett MJ, Edelman EJ, Heidorn SJ, Greenman CD, Dastur A, Lau KW, et al. Systematic identification of genomic markers of drug sensitivity in cancer cells. Nature 2012;483(7391):570-5.
236. Barretina J, Caponigro G, Stransky N, Venkatesan K, Margolin AA, Kim S, et al. The Cancer Cell Line Encyclopedia enables predictive modelling of anticancer drug sensitivity. Nature 2012;483(7391):603-7.
237. Haibe-Kains B, El-Hachem N, Birkbak NJ, Jin AC, Beck AH, Aerts HJ, et al. Inconsistency in large pharmacogenomic studies. Nature 2013;504(7480):389-93.
238. De Palma M, Hanahan D. The biology of personalized cancer medicine: facing individual complexities underlying hallmark capabilities. Molecular oncology 2012;6(2):111-27.
239. Aqeilan RI, Calin GA, Croce CM. miR-15a and miR-16-1 in cancer: discovery, function and future perspectives. Cell death and differentiation 2010;17(2):215-20.
240. Punnoose EA, Leverson JD, Peale F, Boghaert ER, Belmont LD, Tan N, et al. Expression Profile of BCL-2, BCL-XL, and MCL-1 Predicts Pharmacological Response to the BCL-2 Selective Antagonist Venetoclax in Multiple Myeloma Models. Molecular cancer therapeutics 2016;15(5):1132-44.
241. Hartwell LH, Kastan MB. Cell cycle control and cancer. Science 1994;266(5192):1821-8.

242. Kantarjian HM, Sekeres MA, Ribrag V, Rousselot P, Garcia-Manero G, Jabbour EJ, et al. Phase I study assessing the safety and tolerability of barasertib (AZD1152) with low-dose cytosine arabinoside in elderly patients with AML. Clinical lymphoma, myeloma & leukemia 2013;13(5):559-67.
243. Foran J, Ravandi F, Wierda W, Garcia-Manero G, Verstovsek S, Kadia T, et al. A phase I and pharmacodynamic study of AT9283, a small-molecule inhibitor of aurora kinases in patients with relapsed/refractory leukemia or myelofibrosis. Clinical lymphoma, myeloma & leukemia 2014;14(3):223-30.
244. Muller-Tidow C, Bug G, Lubbert M, Kramer A, Krauter J, Valent P, et al. A randomized, open-label, phase I/II trial to investigate the maximum tolerated dose of the Polo-like kinase inhibitor BI 2536 in elderly patients with refractory/relapsed acute myeloid leukaemia. British journal of haematology 2013;163(2):214-22.
245. Hantschel O, Rix U, Superti-Furga G. Target spectrum of the BCR-ABL inhibitors imatinib, nilotinib and dasatinib. Leukemia & lymphoma 2008;49(4):615-9.
246. Scaltriti M, Baselga J. The epidermal growth factor receptor pathway: a model for targeted therapy. Clinical cancer research : an official journal of the American Association for Cancer Research 2006;12(18):5268-72.
247. Tyner JW, Yang WF, Bankhead A, 3rd, Fan G, Fletcher LB, Bryant J, et al. Kinase pathway dependence in primary human leukemias determined by rapid inhibitor screening. Cancer research 2013;73(1):285-96.
248. Palomero T, Lim WK, Odom DT, Sulis ML, Real PJ, Margolin A, et al. NOTCH1 directly regulates c-MYC and activates a feed-forward-loop transcriptional network promoting leukemic cell growth. Proceedings of the National Academy of Sciences of the United States of America 2006;103(48):18261-6.
249. Deangelo DJ, Stone RM, Silverman LB, Stock W, Attar EC, Fearen I, et al. A phase I clinical trial of the notch inhibitor MK-0752 in patients with T-cell acute lymphoblastic leukemia/lymphoma (T-ALL) and other leukemias. ASCO Meeting Abstracts 2006;24:6585.
250. Andersson ER, Lendahl U. Therapeutic modulation of Notch signalling--are we there yet? Nature reviews Drug discovery 2014;13(5):357-78.
251. Luo J, Solimini NL, Elledge SJ. Principles of cancer therapy: oncogene and non-oncogene addiction. Cell 2009;136(5):823-37.
252. Macario AJ, Conway de Macario E. Sick chaperones, cellular stress, and disease. The New England journal of medicine 2005;353(14):1489-501.
253. Mjahed H, Girodon F, Fontenay M, Garrido C. Heat shock proteins in hematopoietic malignancies. Experimental cell research 2012;318(15):1946-58.
254. Spreafico A, Delord JP, De Mattos-Arruda L, Berge Y, Rodon J, Cottura E, et al. A first-in-human phase I, dose-escalation, multicentre study of HSP990 administered orally in adult patients with advanced solid malignancies. British journal of cancer 2015;112(4):650-9.
255. Ko RH, Ji L, Barnette P, Bostrom B, Hutchinson R, Raetz E, et al. Outcome of patients treated for relapsed or refractory acute lymphoblastic leukemia: a Therapeutic Advances in Childhood Leukemia Consortium study. Journal of clinical oncology : official journal of the American Society of Clinical Oncology 2010;28(4):648-54.
256. Houghton PJ, Morton CL, Kolb EA, Lock R, Carol H, Reynolds CP, et al. Initial testing (stage 1) of the proteasome inhibitor bortezomib by the pediatric preclinical testing program. Pediatric blood & cancer 2008;50(1):37-45.
257. Steelman LS, Franklin RA, Abrams SL, Chappell W, Kempf CR, Basecke J, et al. Roles of the Ras/Raf/MEK/ERK pathway in leukemia therapy. Leukemia 2011;25(7):1080-94.
258. Tasian SK, Teachey DT, Rheingold SR. Targeting the PI3K/mTOR Pathway in Pediatric Hematologic Malignancies. Frontiers in oncology 2014;4:108.
259. Ashworth A, Lord CJ, Reis-Filho JS. Genetic interactions in cancer progression and treatment. Cell 2011;145(1):30-8.
260. Hill A, Gotham D, Fortunak J, Meldrum J, Erbacher I, Martin M, et al. Target prices for mass production of tyrosine kinase inhibitors for global cancer treatment. BMJ open 2016;6(1):e009586.
261. Escudier B, Eisen T, Stadler WM, Szczylik C, Oudard S, Staehler M, et al. Sorafenib for treatment of renal cell carcinoma: Final efficacy and safety results of the phase III treatment approaches in renal cancer global evaluation trial. Journal of clinical oncology : official journal of the American Society of Clinical Oncology 2009;27(20):3312-8.
262. Ascierto PA, Minor D, Ribas A, Lebbe C, O'Hagan A, Arya N, et al. Phase II trial (BREAK-2) of the BRAF inhibitor dabrafenib (GSK2118436) in patients with metastatic melanoma.

Journal of clinical oncology : official journal of the American Society of Clinical Oncology 2013;31(26):3205-11.
263. Ow TJ, Sandulache VC, Skinner HD, Myers JN. Integration of cancer genomics with treatment selection: from the genome to predictive biomarkers. Cancer 2013;119(22):3914-28.
264. Chen WC, Yuan JS, Xing Y, Mitchell A, Mbong N, Popescu AC, et al. An Integrated Analysis of Heterogeneous Drug Responses in Acute Myeloid Leukemia That Enables the Discovery of Predictive Biomarkers. Cancer research 2016;76(5):1214-24.
265. Darrow JJ, Sarpatwari A, Avorn J, Kesselheim AS. Practical, legal, and ethical issues in expanded access to investigational drugs. The New England journal of medicine 2015;372(3):279-86.
266. Zwaan CM, Kearns P, Caron H, Verschuur A, Riccardi R, Boos J, et al. The role of the 'innovative therapies for children with cancer' (ITCC) European consortium. Cancer treatment reviews 2010;36(4):328-34.
267. Zwaan CM, Rizzari C, Mechinaud F, Lancaster DL, Lehrnbecher T, van der Velden VH, et al. Dasatinib in children and adolescents with relapsed or refractory leukemia: results of the CA180-018 phase I dose-escalation study of the Innovative Therapies for Children with Cancer Consortium. Journal of clinical oncology : official journal of the American Society of Clinical Oncology 2013;31(19):2460-8.
268. Hunger SP, Loh ML, Whitlock JA, Winick NJ, Carroll WL, Devidas M, et al. Children's Oncology Group's 2013 blueprint for research: acute lymphoblastic leukemia. Pediatric blood & cancer 2013;60(6):957-63.
269. Bhojwani D, Howard SC, Pui CH. High-risk childhood acute lymphoblastic leukemia. Clinical lymphoma & myeloma 2009;9 Suppl 3:S222-30.
270. Messinger YH, Gaynon PS, Sposto R, van der Giessen J, Eckroth E, Malvar J, et al. Bortezomib with chemotherapy is highly active in advanced B-precursor acute lymphoblastic leukemia: Therapeutic Advances in Childhood Leukemia & Lymphoma (TACL) Study. Blood 2012;120(2):285-90.
271. Parker C, Waters R, Leighton C, Hancock J, Sutton R, Moorman AV, et al. Effect of mitoxantrone on outcome of children with first relapse of acute lymphoblastic leukaemia (ALL R3): an open-label randomised trial. Lancet 2010;376(9757):2009-17.
272. Souilmi Y, Lancaster AK, Jung JY, Rizzo E, Hawkins JB, Powles R, et al. Scalable and cost-effective NGS genotyping in the cloud. BMC medical genomics 2015;8:64.

6. Acknowledgments

First and foremost I want to thank my advisors Jean-Pierre Bourquin and Beat Bornhauser. I am very grateful for the opportunity to work on this project and for the supervision of my research. In particular I am thankful for the stimulating ideas and motivation throughout my PhD studies. They have taught me how excellent research is done and inspired me to further pursue career in science. In addition, they have provided me with the opportunity to visit multiple international conferences and introduced me to the international researchers' community via successful collaborations.

My special thanks go to my thesis committee members Alex Hajnal, Freddy Radtke and Maria Pamela Dobay. I very much appreciated their valuable advice and felt constant support during my project. In particular, I would like to thank Pamela for introducing me to a computational science and for correcting my English.

I would like to express my gratitude to the Cancer Network Zurich and Cancer Biology PhD Program operating under the umbrella of Life Science Zurich Graduate School. PhD program has organized excellent courses that helped me to grow as a scientist. As well it gave me an opportunity to connect to other PhD students, principal investigators and researchers in the industry. This would not be possible without Josef Jiricny, a program founder.

To my colleagues from the Leukemia research laboratory: thank you so much for everything, you are the best! You have made my time in the lab and outside it truly special. My warmest thanks goes to all past and present group members that I have had pleasure to work with. Among many, I would like to name my first colleagues – Anna, Blerim, Jeannette and Paulina – that taught me so much in the first year. My special thanks go to my students Salome and Orrin who did tremendous work.

My sincere gratitude goes to all University Children's Hospital Experimental Infectious Diseases and Cancer Research colleagues. I greatly enjoyed weekly meetings and constructive discussions. But foremost I am thankful for the sincere assistance and creative atmosphere.

My thanks goes to Beat Schäfer, head of the department, and Joëlle Tchinda, head of cytogenetics, that allowed me to use University Children's Hospital's infrastructure. As well for helping me to set experiments and for useful advices throughout my doctoral studies.

I would like to express my gratitude to the Krebsliga Zürich that had financially supported my PhD.

Lastly, I would like to thank my family for their support during my PhD. A special thanks go to Agne, my wife, who has believed in me and supported this endeavor at every turn.

7. Curriculum Vitae

VIKTORAS FRISMANTAS

University Children's Hospital Zurich	Phone (lab):	+41 44 634 88 13
Division of Pediatric Oncology	Fax (lab):	+41 44 634 88 59
August-Forelstrasse 1	Phone (home):	+41 76 521 17 33
CH-8008 Zurich, Switzerland	Email:	viktoras.frismantas@kispi.uzh.ch

EDUCATION

University of Zurich, Switzerland

- **PhD, Cancer Biology PhD program** 2012/03-2016/11

Thesis: "Drug response profiling to identify new targets in refractory leukemia"

Advisor: Jean-Pierre Bourquin

Focus: acute lymphoblastic leukemia, *in vitro* co-culture models, drug discovery, biomarkers

Vilnius University, Lithuania

- **MSc, Genetics** 2008/09-2010/06

Project: "Construction and Complementation of Bacteriophage T4 deletion Mutants Lacking Essential Genes *44* and *62*"

Advisor: Lidija Truncaite

Focus: DNA replication machinery, phage discovery, genome editing

- **BSc, Molecular biology** 2004/09-2008/06

Project: "Structural Organization of the Genomic Region between Genes *30.2* and *31* in Bacteriophage VR16"

Advisor: Rimantas S. Nivinskas

Focus: de novo sequencing, gene transcription analysis

RESEARCH EXPERIENCE

- **Junior R&D project coordinator,** JSC 'Nano solutions' (university spin-off) 2011/01-2011/12

Product commercialization, GMP and GLP project coordination

- **Research assistant,** Vilnius University Institute of Biochemistry 2007/06-2010/10

Laboratory management, field expeditions, training and supervising students

KEY TECHNICAL SKILLS

Microbiological cultures: manipulating and maintaining primary tissue samples and cell lines, manipulating bacterial cultures, producing and modifying viruses (lentivirus and bacteriophages); Immuno-techniques: WB, IP, IF; Flow cytometry: immunophenotyping, phosphoflow; Microscopy: manual and automated, light and fluorescent; Cytogenetic techniques: FISH, karyotyping; Molecular biology: cloning, (q)PCR, CRISPR (basic); Protein analysis: labelling, modification; Robotics: Eppendorf, Tecan; *In vivo* practical skills: FELASA B certificate, extensive practise in substance administration (IP, IV, PO); Programming skills: Python, R, Matlab, ImageJ.

LANGUAGES

- **Lithuanian –** native; **English** – fluent; **Russian** – fluent; **German** – reading knowledge.

SCHOLARSHIPS

- ESH-EHA workshop scholarship 2013/02
- Research council of Lithuania: "Promotion of Students Scientific Activities" 2007/06-2007/10
- Vilnius University scholarship 2007/09-2007/12

TEACHING EXPERIENCE

- Instructor for leukemia diagnostic in the clinical setting (flow cytometry), "Prospects of molecular diagnostics in pediatrics", University of Zurich BIO419 block course, autumn semester 2013 and 2014;
- Mentored University of Zurich MSc student (2013/09-2014/06) and Weill Cornell Medical College MD student (2014/09-2015/03).

MEMBERSHIP

- **American Association for Cancer Research (AACR)** 2015/04-present
- **European Hematology Association (EHA)** 2013/06-present

PUBLICATIONS

Frismantas V, Dobay MP, Rinaldi A, Tchinda J, Dunn SH, Kunz J, Richter-Pechanska P, Marovca B Pail O, Jenni S, Diaz-Flores E, Chang BH, Brown TJ, Collins RH, Higi S, EugsterS, Voegeli P, Delorenzi M, Cario G, Loh ML, Schrappe M, Stanulla M, Kulozik AE, Muckenthaler MU, Saha V, Irving JA, Meisel R, Radimerski T, Von Stackelberg A, Eckert C, Tyner JW, Horvath P, Bornhauser BC and BourquinJ-P. *Ex vivo* drug response profiling detects extraordinary drug activity in resistant ALL. Manuscript submitted to Blood after revision.

Peirs S, **Frismantas V**, Matthijssens F, Van Loocke W, Pieters T, Vandamme N, Lintermans B, Dobay MP, Berx G, Poppe B, Bornhauser BC, Bourquin J-P, and Van Vlierberghe P. Targeting BET proteins improves the therapeutic efficacy of BCL-2 inhibition in T-cell acute lymphoblastic leukemia. Manuscript submitted to Leukemia.

Fischer U, Forster M, Rinaldi A, Risch T, Sungalee S, Warnatz HJ, Bornhauser B, Gombert M, Kratsch C, Stütz AM, Sultan M, Tchinda J, Worth CL, Amstislavskiy V, Badarinarayan N, Baruchel A, Bartram T, Basso G, Canpolat C, Cario G, Cavé H, Dakaj D, Delorenzi M, Dobay MP, Eckert C, Ellinghaus E, Eugster S, **Frismantas V**, Ginzel S, Haas O, Heidenreich O, Hemmrich-Stanisak G, Hezaveh K, Höll JI, Hornhardt S, Husemann P, Kachroo P, Kratz CP, Kronnie G, Marovca B, Niggli F, McHardy AC, Moorman AV, Panzer-Grümayer R, Petersen BS, Raeder B, Ralser M, Rosenstiel P, Schäfer D, Schrappe M, Schreiber S, Schütte M, Stade B, Thiele R, von der Weid N, Vora A, Zaliova M, Zhang L, Zichner T, Zimmermann M, Lehrach H, Borkhardt A, Bourquin J-P, Franke A, Korbel JO, Stanulla M, Yaspo ML. 2015. Genomics and drug profiling of fatal TCF3-HLF-positive acute lymphoblastic leukemia identifies recurrent mutation patterns and therapeutic options. Nat Genet 47(9):1020-9.

Suryani S, Carol H, Chonghaile TN, **Frismantas V**, Sarmah C, High L, Bornhauser B, Cowley MJ, Szymanska B, Evans K, Boehm I, Tonna E, Jones L, Manesh DM, Kurmasheva RT, Billups C, Kaplan W, Letai A, Bourquin JP, Houghton PJ, Smith MA and Lock RB. 2014. Cell and molecular determinants of in vivo efficacy of the BH3 mimetic ABT-263 against pediatric acute lymphoblastic leukemia xenografts. Clin Cancer Res 20(17): 4520-4531.

Bandapalli OR, Schuessele S, Kunz JB, Rausch T, Stutz AM, Tal N, Geron I, Gershman N, Izraeli S, Eilers J, Vaezipour N, Kirschner-Schwabe R, Hof J, von Stackelberg A, Schrappe M, Stanulla M, Zimmermann M, Koehler R, Avigad S, Handgretinger R, **Frismantas V**, Bourquin J-P, Bornhauser B, Korbel JO, Muckenthaler MU and Kulozik AE. 2014. The activating STAT5B N642H mutation is a common abnormality in pediatric T-cell acute lymphoblastic leukemia and confers a higher risk of relapse. Haematologica 99(10): e188-192.

8. Manuscripts

Manuscript 1

Ex vivo drug response profiling detects extraordinary drug activity in resistant ALL

Manuscript 2

Targeting BET proteins improves the therapeutic efficacy of BCL-2 inhibition in T-cell acute lymphoblastic leukemia

Manuscript 3

Cell and molecular determinants of *in vivo* efficacy of the BH3 mimetic ABT-263 against pediatric acute lymphoblastic leukemia xenografts.

Manuscript 4

Genomics and drug profiling of fatal TCF3-HLF-positive acute lymphoblastic leukemia identifies recurrent mutation patterns and therapeutic options

Ex vivo drug response profiling detects extraordinary drug activity in resistant ALL

Viktoras Frismantas[1,2,*], Maria Pamela Dobay[3*], Anna Rinaldi[1,2,*], Joelle Tchinda [1,2], Samuel H. Dunn[4], Joachim Kunz[5], Paulina Richter-Pechanska[5], Blerim Marovca[1,2], Orrin Pail[1,2], Silvia Jenni[1,2], Ernesto Diaz-Flores[6], Bill H. Chang[7], Timothy J. Brown[8], Robert H. Collins[8], Salome Higi[1,2], Sabrina Eugster[1,2], Pamela Voegeli[9], Mauro Delorenzi[3,10], Gunnar Cario[11], Mignon L. Loh[12], Martin Schrappe[11], Martin Stanulla[13], Andreas E. Kulozik[5], Martina U. Muckenthaler[5], Vaskar Saha[14,15], Julie A. Irving[16], Roland Meisel[17], Thomas Radimerski[18], Arend Von Stackelberg[19,20,21], Cornelia Eckert[19,20,21], Jeffrey W. Tyner[22], Peter Horvath[23,24], Beat C. Bornhauser[1,2,*] and Jean-Pierre Bourquin[1,2,*]

[1]Department of Oncology, University Children's Hospital Zurich, Zurich, Switzerland

[2]Children's Research Center, University Children's Hospital Zurich, Zurich, Switzerland

[3]SIB Swiss Institute of Bioinformatics, Lausanne, Switzerland

[4]The University of Texas Southwestern Medical School, Dallas, TX, USA

[5]Department of Pediatric Oncology, Hematology and Immunology, University of Heidelberg, Heidelberg, Germany

[6]Department of Pediatrics and Helen Diller Family Comprehensive Cancer Center, University of California-San Francisco, San Francisco, CA, USA

[7]Division of Hematology and Oncology, Department of Pediatrics, Doernbecher Children's Hospital, Oregon Health & Science University, Portland, Oregon

[8]The University of Texas Southwestern Medical Center, Dallas, TX, USA

[9]Institute of Forensic Medicine, University of Zurich, Zurich, Switzerland

[10]Ludwig Center for Cancer Research, University of Lausanne, Lausanne, Switzerland

[11]Department of Pediatrics, University Medical Centre Schleswig-Holstein, Kiel, Germany

[12]Department of Pediatrics, University of California-San Francisco, San Francisco, CA, USA

[13]Department of Pediatric Hematology and Oncology, Hannover Medical School, Hannover, Germany
[14]Division of Molecular & Clinical Cancer Sciences, School of Medical Sciences, Faculty of Biology, Medicine and Health, University of Manchester, Manchester, United Kingdom
[15]Tata Translational Cancer Research Centre, Tata Medical Centre, Kolkata, India
[16]Northern Institute for Cancer Research, Newcastle University, Newcastle upon Tyne, United Kingdom
[17]Division of Pediatric Stem Cell Therapy, Clinic for Pediatric Oncology, Hematology and Clinical Immunology, Medical Faculty, Heinrich Heine University, Düsseldorf, Germany
[18]Disease Area Oncology, Novartis Institutes for BioMedical Research, Basel, Switzerland
[19]Department of Pediatric Oncology/Hematology, Charité Universitätsmedizin Berlin, Germany
[20]German Cancer Consortium (DKTK), Heidelberg, Germany
[21]German Cancer Research Center (DKFZ), Heidelberg, Germany
[22]Department of Cell, Developmental & Cancer Biology, Oregon Health and Science University, Portland, OR, USA
[23]Synthetic and Systems Biology Unit, Hungarian Academy of Sciences, Biological Research Center (BRC), Szeged, Hungary.
[24]Institute for Molecular Medicine Finland, University of Helsinki, Helsinki, Finland.
* equal contribution

Running title: Actionable information by drug response profiling in ALL

Keywords: drug activity profiling, drug resistant acute lymphoblastic leukemia, automated microscopy, BH3-mimetics, precision medicine, dasatinib

Grant Support: This work was supported by the Cancer League of the Canton of Zurich, the Empiris foundation, the foundation “Kinderkrebsforschung Schweiz”, the Sassella foundation, the “Stiftung für Krebsbekämpfung”, the Swiss National Science Foundation (310030-133108,

310030-156407), the Fondation Panacee, the clinical research focus program “Human Hemato-Lymphatic Diseases” of the University of Zurich, the German Childhood Cancer Foundation and the German Cancer Consortium. P.H. acknowledges support from the Hungarian National Brain Research Program (MTA-SE-NAP B-BIOMAG) and the Finnish TEKES FiDiPro Fellow Grant 40294/13. J.W.T. is supported by The Leukemia & Lymphoma Society, the V Foundation for Cancer Research, the Gabrielle’s Angel Foundation for Cancer Research, and the National Cancer Institute (5R00CA151457-04; 1R01CA183947-01).This research received funding from the European Union’s Seventh Framework Programme for research, technological development, and demonstration (Grant agreement no. 278514 - IntReALL).

Correspondence:

Jean-Pierre Bourquin, jean-pierre.bourquin@kispi.uzh.ch

University Children’s Hospital Zurich

Steinwiesstrasse 75

CH-8032 Zurich, Switzerland

Phone, +41 44 266 7304

Fax, +41 44 266 7171

Disclosure of Potential Conflicts of Interest: T.R. is a full-time employee of Novartis Pharma AG. The remaining authors declare no competing financial interests.

Word count: 3993

Number of figures and tables: 6 figures and 1 table

ABSTRACT

Drug sensitivity and resistance testing on diagnostic leukemia samples should provide important functional information to guide actionable target and biomarker discovery. We provide proof of concept data by profiling 60 drugs on 68 acute lymphoblastic leukemia (ALL) samples mostly from resistant disease in co-cultures on bone marrow stromal cells. Patient-derived xenografts retained the original pattern of mutations found in the matched patient material. Stromal co-culture did not prevent leukemia cell cycle activity, while a specific sensitivity profile to cell cycle related drugs identified samples with higher cell proliferation both *in vitro* and *in vivo* as leukemia xenografts. In cases with refractory relapses, individual patterns of marked drug resistance, but also exceptional responses to new agents of immediate clinical relevance were detected. The BCL2-inhibitor venetoclax was highly active below 10 nM in BCP-ALL subsets including *MLL-AF4* and *TCF3-HLF* ALL, and in some T-ALLs, predicting *in vivo* activity as a single agent and in combination with dexamethasone and vincristine. Unexpected sensitivity to dasatinib with IC50 values below 20 nM was detected in two independent T-ALL cohorts, which correlated with similar cytotoxic activity of the SRC Inhibitor KX2-391 and inhibition of SRC phosphorylation. A patient with refractory T-ALL was treated with dasatinib based on drug profiling information and achieved a five-month remission. Thus, drug profiling captures disease-relevant features and extraordinary sensitivity to relevant drugs, which warrants further exploration of this functional assay in the context of clinical trials in order to personalize drug repurposing strategies for patients with urgent medical needs.

Key points:

- *Ex vivo* drug profiling captures disease-relevant features and extraordinary sensitivity to therapeutic agents in ALL
- A subset of resistant T-ALL without mutations in *ABL1* is highly responsive to dasatinib providing a rationale for drug repurposing

INTRODUCTION

The treatment of relapsed and refractory ALL remains challenging[1]. Progress in ALL genomics[2] provides unprecedented insight into potentially actionable targets, such as activating mutations in tyrosine kinases[3], RAS[4] or IL7R[5]. More precise molecular classification, however, had limited impact on risk stratification and personalized therapy so far[1]. Patients who may benefit from innovative therapies are mainly identified based on their impaired response to chemotherapy, defined by persistence of minimal residual disease (MRD)[1,6,7] or by the failure of remission-induction therapy[8]. Only a few recurrent genetic features such as *MLL-AF4* rearrangements, the t(17;19) translocation generating the *TCF3-HLF* fusion[9], and hypodiploid karyotypes[4] are used for risk stratification.

Integration of genomic and drug sensitivity data on cell line panels illustrate the difficulty of extrapolating drug responses based on recurrent genomic lesions[10,11], even though typical pathways were found to be differentially activated in distinct cancer types. Moreover available cancer cell lines do no capture the genetic heterogeneity of leukemia seen in patients. Genomic alterations in relevant pathways may be over- or underrepresented in cell lines, whereas patient-derived xenografts (PDX) appear to resemble the original tumour samples[12]. To obtain insight into inter-patient drug response heterogeneity we developed an *in vitro* platform using leukemia cells directly from patients. We hypothesized that drug activity profiling of ALL even without *a priori* information on genetic lesions or activated pathways will detect sensitivity that may otherwise be overlooked. Indeed, clinically active tyrosine kinase inhibitors could be identified by drug profiling in a few AML patients[13]. Moreover, inhibitor screens identified leukemias with characteristic tyrosine kinase mutations[14] and a subset of ALL with tonic pre-BCR signalling[15].

Taking advantage of PDX from clinically relevant ALL subgroups[16-20] and based on previous reports[13,14,17-19,21,22], we adapted a serum free ALL co-culture system on h-TERT immortalized human bone marrow derived mesenchymal stromal cells (MSC)[23,24] with an automated microscopic image readout for drug testing. This population-based approach reveals clusters

of activity in leukemia for a number of clinically relevant new agents, identifying actionable targets not exploited in conventional treatment. We show that *in vitro* responses correlates better with *in vivo* activity for the BCL2-inhibitor venetoclax[25] than with other biomarkers for BCL2-dependent leukemia[26,27] and provide compelling evidence for venetoclax activity with standard of care ALL chemotherapy in xenografts. We also report unexpected activity of dasatinib in a T-ALL subset that would not have been predicted based on genomic information. Finally, we provide clinical evidence for dasatinib activity in a patient with refractory leukemia based on drug profiling data. These results provide a strong rationale to evaluate drug profiling in clinical trials to assist patient selection for drug repurposing.

MATERIALS AND METHODS

Human samples. Primary human ALL cells were recovered from cryopreserved bone marrow aspirates of patients enrolled in the ALL-BFM 2000, 2009 and ALL-REZ-BFM 2002 studies. Informed consent was given in accordance with the Declaration of Helsinki and the ethics commission of the Kanton Zurich (approval number 2014-0383). Human subjects consented to protocols as reviewed by the Institutional Review Boards at Oregon Health & Science University and UT-Southwestern. Samples were classified as standard risk (SR), medium risk (MR), high risk (HR), very high risk (VHR) according to the stratification in ALL-BFM 2000[18], as relapse (R) and refractory relapse (RR).

Xenograft model. Patient derived xenografts (PDX) were generated as described[19] by intrafemoral injection of $1x10^5$ to $5x10^6$ viable primary ALL cells in NSG mice. Leukemia progression was monitored in the peripheral blood by flow cytometry using anti-mCD45, anti-hCD45, anti-hCD19 or anti-hCD7 antibodies. The identity of xenografts was verified by DNA fingerprinting using the commercial AmpFlSTR® NGM SElectT kit.

Genomic characterization of leukemia samples.

Primary patient material and matched xenografts were analysed by targeted sequencing and multiplex ligation-dependent probe amplification (MLPA). In 19 BCP-ALL, cases without an

established abnormality (B-other)[28] or targetable kinase-activating lesions[3] fluorescence in-situ hybridization (FISH) was performed. FISH probes were designed by Cytocell (Cambridge, UK). Detailed protocols are provided in the supplementary methods section.

***In vitro* drug profiling platform.** Drug responses were assessed in co-culture of ALL cells on hTERT-immortalized primary bone marrow mesenchymal stromal cells (MSC)[16] as described[18] in 384 well plates (Greiner, REF781090). $2.5x10^3$ MSC cells/well were plated in 30µL AIM-V® medium 24h before adding $2\text{-}3x10^4$ ALL cells in 27.5µL medium recovered from cryopreserved samples. Compounds were reconstituted in DMSO (10mM stock concentrations) and stored at -80°C. Drugs in serial dilutions were prepared using epMotion 5070 and Tecan D300 robots. An independent T-ALL cohort was tested as described in[14].

Drug response quantification and statistical analysis. A fitting routine based on the four-parameter log-logistic function (R package drc, version 2.3-96) was applied to data normalized against DMSO-treated samples. Outliers were detected and removed prior to curve fitting by detecting local changes in the slope with a linear fit. Non-convergent cases were identified based on linear fit parameters. R codes are available under https://github.com/pampernickel/Fit.funcs. Hierarchical clustering was performed to group patients according to their drug response profile (R package gplots). Differential responses of patient groups of interest to drugs were evaluated using the non-parametric, Mann-Whitney U-test.

***In vivo* drug treatment.** Venetoclax and combinations: 5-8 mice were transplanted with $1x10^6$ ALL cells i.v. for each treatment arm. Randomized cohorts were treated with vehicle, 100 mg/kg/day venetoclax (Activebiochem[25]) orally, 10.5 mg/kg dexamethasone (Mepha) i.p. twice a week and 0.5 mg/kg Vincristine (Teva) i.p. once a week. Cytarabine, docetaxel and dasatinib: animals (one per condition) were intravenously transplanted with $7x10^6$ ALL cells. After five days, animals were treated with 50mg/kg cytarabine (Sandoz) i.p. for five days, 5mg/kg

185 docetaxel (Taxotere) i.v. twice or 50mg/kg dasatinib (Selleck, dissolved as described[29]) orally
186 for five days. Leukemic burden was determined post-treatment by flow cytometry.

187 **Cell assays.** Viability: Viability in $2.5x10^4$ ALL cells in suspension or co-culture with $2.5x10^3$
188 MSC cells in AIM-V medium was measured by flow cytometry at 1, 4 and 7 days (7-AAD,
189 reported as day 4 mean±SD). Proliferation and apoptosis:$1x10^5$ ALL cells were seeded with
190 $1x10^4$ MSC. Proliferating and apoptotic cells were labelled using the Click-iT EdU Imaging Kit
191 and Cell Event™ Caspase-3/7 Green, respectively. Proliferating and non-proliferating groups
192 were identified with an Expectation-Maximization (EM)-mixture model (R package mixtools).

193 **Intracellular flow cytometry and Western Blot**. $10x10^6$ ALL cells were fixed in 2%
194 paraformaldehyde and permeabilized with ice-cold methanol. Indirect labelling with FITC-
195 labelled antibodies was used. For Western blots (Bio-Rad Criterion™) whole-cell extracts from
196 $3\text{-}5x10^6$ cells were used. Detailed protocols are provided in supplementary methods and
197 materials.

RESULTS

Drug response profiling reveals distinct clusters of activity in ALL

ALL co-cultures on hTERT-immortalized MSC[24] provide a simplified model of the leukemia microenvironment that facilitates survival of B-cell precursor (BCP-) and T-ALL cells in a majority of cases[17]. The protective effect of MSCs towards some therapeutic agents may even increase the stringency of drug testing in this system[30]. We compiled a library of 60 compounds in preclinical or clinical development (**Table S1**) and used an imaging-based cell viability readout on a customized, high-throughput analysis platform[17] (**Figure 1**). We established leukemia xenografts from patient samples including high risk ALL based on MRD persistence, and relapsed and refractory ALL. We applied the same diagnostic workflow for primary samples and PDX, including fluorescence in situ hybridization to capture most recurrent translocations that activate tyrosine kinase pathways (**Table S2A** and **S2B**) and performed targeted sequencing of 52 frequently mutated genes in ALL. We retrieved the expected pattern of mutations (**Figure S1**, **Table S3**), with frequent events in *KRAS* (13/25) and *TP53* (10/25), consistent with the corresponding clinical studies[31,32]. On average 74% of single nucleotide variants (SNVs) and insertions/deletions (indels) were conserved when comparing the primary diagnostic samples to PDX (**Figure 1B**, **Figure S1**). Oncogenic translocations were always maintained. We also included samples from the poor risk *TCF3-HLF* and favourable risk *TCF3-PBX1* positive ALL subtypes, for which we recently reported a strong conservation of the genomic landscape in PDX[33].

To evaluate the potential of this ex-vivo platform, we tested 60 drugs on 24 T-ALL and 44 BCP-ALL PDX, derived from pre-treatment diagnostic samples (ALL-BFM-2000 study[34], **Figure 2**). For each drug, we used eight doses, optimized from an initial five-point screen (**Table S4**). None of the tested compounds affected MSC viability at concentrations lethal to ALL cells, indicating that we identify selective drug activities (**Figure 2**). Unsupervised clustering of drug responses (shown here as IC50 values) identified various patterns of response. Compounds including anthracyclines, the BH3 mimetic navitoclax (ABT-263) and the proteasome inhibitor

bortezomib were effective at low (IC50<10nM) and narrow IC50 range in most cases (cluster A). A second group of agents including the BCL2-specific BH3 mimetic venetoclax, tyrosine kinase inhibitors and conventional cytotoxic agents such as glucocorticoids, topoisomerase inhibitors and nucleotide analogues (gemcitabine, cytarabine) showed responses distributed over a wider concentration range, with high activity in the nanomolar range in some cases and low activity in others (clusters B, C and E). Venetoclax (Cluster C) in particular was generally more active in BCP-ALL, and showed similar activity in a T-ALL subset. In cluster E, we identified two groups of agents, whose separation was driven by differences in response to antimetabolites (cytarabine, gemcitabine), antimitotic drugs (vincristine, docetaxel), the aurora kinase inhibitors AT9283 and barasertib and the Polo-like kinase inhibitor BI-2536. Finally, extraordinary sensitivity was detected in a few ALL cases for drugs that were otherwise generally not active in ALL on this platform (in cluster G). These included SMAC mimetics (e.g. LCL161), an observation which led us to show that a subset in BCP-ALL was extremely responsive to SMAC mimetics through RIP1 kinase-dependent necroptosis and apoptosis[35]; and that the ABL/SRC inhibitor dasatinib is highly active in a T-ALL subset, which we describe below. High peak plasma concentrations (Cmax) were reported for most clinical compounds in our panel (**Figure S2**), suggesting that effective concentrations may be achieved *in vivo*. Our platform provides reproducible ALL drug activity profiles that identify functional phenotypes which can give new insights for therapeutic targeting. Correlative analyses of drug responses with targeted sequencing data did not yield statistically significant results (**Table S5**).

Drug profiling captures leukemia intrinsic differences in cell proliferation and survival

While most ALL samples tested in co-culture survive on MSC, we noticed relative cell survival heterogeneity, suggesting differences in cell proliferation and spontaneous cell death rates across samples (**Figure 3A**). We did not detect ALL migration beneath stromal cells (pseudoemperipolesis) or cobblestone structure-like formation[22] that could interfere with microscopy readouts. Median cell viability on MSCs was 69% of seeded cells for BCP-ALL and 94% for T-ALL, compared to 1.2% and 45.5% in monoculture after 96 hours. A high rate of survival on this platform (viability of >70% at day 3 compared to day 0) correlated with a higher

ratio (r>1) of cells in S-phase versus apoptotic cells (**Figure 3A**). To determine whether these differences are due to stromal co-culture effects or intrinsic features of ALL cells, we compared leukemia proliferation and drug sensitivity patterns *ex vivo* and *in vivo* in leukemia xenografts. Marked differences in sensitivity were detected in both BCP- and T-ALL for drugs whose mechanisms of action require active cycling (**Figure 2** cluster E, **Figure S3**), including inhibitors of mitotic spindle formation, DNA synthesis, cell cycle and mitosis regulatory kinases. We used a mixture model fit to distinguish high and low proliferating ALL cases. ALL samples with high proliferative activity *in vitro* (>40% of cells in S-phase) engrafted significantly faster (p-value=0.0008) in mice compared to samples with low proliferative activity (<40% of cells in S-phase, **Figure 3B**). As expected, drugs with the highest differential activity in high- and low-proliferating samples inhibit targets involved in cell cycle control (**Figure S4**). Most importantly, samples with rapid engraftment kinetics (**Figure 3B**) were more susceptible to cytarabine and docetaxel *ex vivo* (**Figure 3C**), which correlates with stronger anti-leukemic effects *in vivo* (**Figure 3D**). Thus the *ex vivo* co-culture model captures leukemia-specific characteristics with respect to cell cycle activity, which are preserved *in vivo* in the leukemia xenograft model, and that are not caused by the co-culture conditions.

Drug profiling reveals individual patterns of drug sensitivity and resistance in relapsed and refractory ALL

Drug profiling may convey relevant information to select new agents for salvage therapy in patients with highly resistant disease. To compare the activity of different substances in different patients, it is important to evaluate drug activity in a single case against the full response range obtained on the same platform for other leukemia cases, including clinically relevant subsets. We profiled PDX samples of twelve patients with relapsed ALL refractory to salvage therapy (refractory relapse, RR), who did not achieve a second or third remission required for inclusion in early clinical trials, retrospectively (**Figure 4A**), as well as primary leukemia cells from five patients with refractory disease in real time prospectively (**Figure 4B**, **Table 1**). **Figure 4** shows IC50 values for a selection of therapeutic agents in samples of interest against those obtained for all other samples on our platform (grey). RR ALL samples

were generally more resistant to agents used for induction in ALL such as dexamethasone (10/12 cases), cytarabine (9/12 cases) and doxorubicin (9/12 cases), compared to other diagnostic and relapse ALL cases (**Figure 4A**). In contrast, individual samples were highly sensitive to dexamethasone, idarubicin and mitoxanthrone, which are included in the standard of care for relapsed ALL[36], and to new agents from different classes, such as venetoclax, dasatinib, bortezomib, nutlin, JQ1 and panobinostat. Again, we noticed extraordinary responses in a few cases to venetoclax and dasatinib, which we discuss in the next sections. Additionally, sensitivity patterns could be associated with cytogenetic groups. For example *MLL-AF4* ALL cases were sensitive to PI3K/mTOR/AKT or HSP90 inhibitors, consistent with previous reports[37] (**Figure S5**).

To assess the feasibility of our approach in the clinical setting we tested five cases with highly refractory ALL at the time of relapse (**Figure 4B**). Results could be obtained within five days. These highly resistant cases did not respond to standard of care drugs on the platform (dexamethasone, vincristine, doxorubicine or mitoxanthrone), but individual sensitivities to venetoclax (Patients 1, 2, 3) and panobinostat (Patient 5) were detected. Thus drug profiling may provide important information when exploring options for patients with resistant disease.

The response to venetoclax *ex vivo* correlates with strong *in vivo* anti-leukemic activity as single agent and in combination

Given the strong *in vitro* activity of venetoclax in individual cases across ALL subtypes, including a subset of T-ALLs, BCP-ALLs, *TCF3-HLF* ALL and all *MLL-AF4* ALL cases, we evaluated tested venetoclax in seven cases *in vivo* in the xenograft model (**Figure 5A**). Several T-ALL cases responded to venetoclax *in vitro* with IC50 values in the nanomolar range (**Figure 5A**), consistent with recent reports describing activity in early thymic precursor ALL and T-ALL[38-40]. These results were verified using 7-AAD staining by flow cytometry to quantify cell death (**Figure S6**). As expected, the response to oral administration of venetoclax *in vivo* correlated with *in vitro* activity for three T-ALL patients with strong, intermediate and low sensitivity to venetoclax. Single agent venetoclax treatment delayed leukemia progression

significantly in the case with strong *in vitro* sensitivity (HR=20, IC50 <1nM and low Emax, treated vs. untreated, p<0.005) compared to cases with low IC50 (<100nM) but higher Emax (HR=0.07, treated vs. untreated, p<0.005) or high IC50 (>1μM). Additionally, complete response was detected when treating the T-VHR-03 case in mice with high leukemia burden (75% engraftment, **Figure S7**). We recently reported similar venetoclax efficacy in three *TCF3-HLF* ALL cases *in vivo*[33]. Similar correlations were obtained in two cases with *TCF3-HLF* and with *MLL*-rearranged ALL (**Figure 5A**). For all tested cases, venetoclax-induced delays in *in vivo* leukemia progression correlated with *in vitro* responses (**Figure 5B**, Spearman ρ=-0.86, p-value<0.05).

As with most chemotherapeutic agents, single agent venetoclax therapy is unlikely to be effective. Currently, most investigational agents will be tested in combination with a standard of care anti-leukemic regimen, including two to four drugs such as vincristine, dexamethasone, asparaginase and an anthracyclin that are typically used for reinduction chemotherapy at relapse[36]. We detected synergy *in vitro* using co-titration experiments, but this assay is challenging when assessing a drug with such strong *in vitro* activity as venetoclax[41] (**Figure S8**, **Table S4**). As it is impossible to provide supportive care to mice after myelotoxic chemotherapy *in vivo*, we next tested the combination of venetoclax, dexamethasone and vincristine without anthracyclines (**Figure 5A**). Venetoclax or chemotherapy alone delayed leukemia progression for *TCF3-HLF* and *MLL-AF4* rearranged cases (HR=5-22, p-value<0.005). The three-drug combination prevented leukemia progression for more than 300 days for two *TCF3-HLF* samples and in three out of five *MLL-AF4* ALL samples. Leukemia progression was significantly delayed in remaining samples.

The identification of response-predictive biomarkers, in addition to drug profiling, is important for the clinical development of BH3 mimetics. The BCL2:BCL-XL and BCL2:MCL1 ratios were suggested as biomarkers for venetoclax sensitivity in ALL[42] and in AML, respectively. We determined the level of BCL2-family members by intracellular flow cytometry and by Western blotting (**Figure 5C**, **Figure S9**). *In vitro* response to venetoclax neither correlated with BCL2-

family protein expression levels nor BCL2:MCL1 or BCL2:BCL-XL ratios in 36 BCP-ALL and T-ALL samples tested by flow cytometry (**Figure 5C**, **Figure S10**). It will be important to correlate and complement drug response profiling results with BH3-domain profiling in clinical trials to establish predictive biomarkers.

Drug profiling identifies a subset within T-ALL highly responsive to dasatinib

We detected unexpected responses to the ABL1/SRC inhibitor dasatinib (IC50<100nM) in twelve (30%) T-ALL cases without the typical ABL1 kinase translocation (**Figure 6A**). Importantly, these responses were detected in both diagnostic and relapse samples from high risk patients by MRD. Moreover, the IC50 for dasatinib in these cases was at least a tenfold lower than in any of the best BCP-ALL responders tested. These included five ALL cases with rearranged *TCF3-PBX1*, recently linked to active BCR signalling[15,43], that were sensitive to dasatinib but not imatinib (**Figure 6A**). Given that the dasatinib response did not correlate with the response to other BCR-ABL inhibitors, we hypothesized that dasatinib acts via SRC inhibition. By phospho-flow cytometry, we detected higher levels of activated phosphorylated SRC in dasatinib-sensitive samples (**Figure 6B**); SRC phosphorylation was abrogated after exposure to dasatinib. The SRC inhibitor KX2-391, which inhibits SRC at nanomolar concentrations[44], induced cell death in dasatinib-sensitive T-ALL cases at concentrations below 100nM (**Figure 6C**), supporting the relevance of the SRC pathway in this T-ALL subset. Apart from KX2-391, dasatinib response also correlated with responses to other RTK inhibitors (e.g. midostaurin, crenolinib, adj. p-value<0.005; **Figure S11**), consistent with the essential role of SRC in receptor tyrosine kinase (RTK) signalling[45],. *In vitro* dasatinib activity was also predictive of selective, anti-leukemic *in vivo* activity in T-ALL xenografts (**Figure 6D**).

To validate our observations, we checked the drug sensitivity of 33 adult and pediatric T-ALL patients obtained on a liquid monoculture platform[14]. Remarkably, 4/33 responded to dasatinib with IC50 < 10nM (**Figure 6E**), and 9/33 with 10 nM < IC50 < 100nM. One of these dasatinib-sensitive cases was a 58 year old male patient with refractory T-ALL with lymph node involvement on both sides of the diaphragm. The patient relapsed early after 8 cycles of hyper

CVAD chemotherapy and allogeneic stem cell transplantation. After unsuccessful salvage attempts with nelarabine, followed by mitoxanthrone and cytarabine, drug response profiling results were used to design a combination treatment of dasatinib (140 mg/day) with continued pegylated asparaginase at third relapse. On repeat PET/CT, the patient showed complete response with significant reduction in FDG uptake compared to the previous scan (**Figure 6F**). A five-month remission prior to relapse was maintained with dasatinib monotherapy. These results confirm that a subset of drug resistant and relapsed T-ALL can be identified by drug profiling to be particularly sensitive to dasatinib, and warrants further exploration of underlying molecular mechanisms. Given the experience with established combinations of dasatinib with chemotherapy for the treatment of BCR-ABL positive ALL[46], our data provide a strong rationale for drug repurposing based on drug profiling results for selected patients with resistant T-ALL in pediatric and adult patient populations.

DISCUSSION

Here we provide compelling evidence that informative and reproducible differences in drug response profiles can be detected in patient groups of interest while simultaneously revealing patient-to-patient response variations. In particular, we detected extraordinary activity of different classes of agents in patients with otherwise refractory disease, which may be overlooked based on available diagnostic information. We did not observe correlations between drug response phenotypes and mutation status, which may be partly due to the limited size of our ALL cohort. Multivariate analyses based on whole genome or exome sequencing results on a larger cohort would be of interest in the future to establish correlations definitively. However, our results, which indicate that it will be challenging to infer drug activity solely based on genomic data, are consistent with reports in adult hematologic malignancies[13,14].

As a basis for standardization, we opted for co-culture on human MSC[23,24], which efficiently supports a majority of primary ALL samples in serum-free conditions. The fact that we detect subsets with more proliferative activity both *in vitro* and *in vivo* based on drug profiling however shows that important leukemia-intrinsic features are maintained and captured under the *in vitro*

cell culture conditions. We and others[13,14] have demonstrated the use of drug profiling for the identification of responsive phenotypes to new therapeutic agents. Our studies provide a rationale for three classes of agents: we have identified recurrent ALL cases highly sensitive to triggering RIP1-dependent cell death with SMAC mimetics[35], or to BCL2 inhibition in *TCF3-HLF* ALL[33] and in genetically heterogeneous BCP-ALL and T-ALL subsets. Moreover, we discovered a subgroup in T-ALL that is highly sensitive to dasatinib, which is of clinical importance.

The BCL2-specific inhibitor venetoclax[25], which has recently been approved for CLL treatment, is also a promising agent for ALL, provided reliable strategies for patient selection are in place. Our results indicate that a relatively large proportion of BCP-ALL cases may respond to venetoclax, but only a minority of these BCL2-dependent cases share recurrent genomic lesions, including *TCF3-HLF*[33] and *MLL-AF4* positive ALL. Our findings also support a recent independent study showing venetoclax activity in MLL-rearranged ALL[47]. While the BCL2:BCL-XL expression ratio has been reported to be a predictive biomarker for venetoclax response in T-ALL cell lines[42], our results and other data[47] suggest that this approach is not specific enough to identify most responders with the accuracy required for clinical application. Complementary functional information might be obtained from BH3 profiling using synthetic peptides[42,48,49]. The best evidence for correlations between in vitro-sensitivity to venetoclax, BH3 profiling and clinical responses was reported in a phase II study assessing monotherapy with venetoclax in patients with refractory/relapsed AML, and suggests that the combination of such information will be useful[50]. Finally, our results and previous reports[51] provide a strong rationale to explore venetoclax use in combination with conventional anti-leukemic agents in early clinical trials. Thus early clinical trials in ALL should also include *in vitro* drug profiling among other assays to improve the identification of patients that may benefit from venetoclax and include evaluation in combination with other effective chemotherapeutic agents.

New treatment options are desperately needed for relapsed T-ALL[1]. We discovered a T-ALL subset that is highly sensitive to dasatinib and show a complete response in a patient with

previously refractory T-ALL whose treatment was designed based on drug profiling data. A patient with *NUP1-ABL1* positive T-ALL was also reported to respond to dasatinib-based therapy[52]. Our results indicate that the mode of action in most cases may not involve ABL1, but possibly SRC, as these cases neither responded to imatinib nor to nilotinib, but to the SRC inhibitor KX2-391. Dasatinib treatment also resulted in SRC dephosphorylation. Dasatinib combinations with ALL standard of care chemotherapy[46] and a pediatric dose[53] are established. Our results provide a strong rationale for drug profiling use in dasatinib combination chemotherapy evaluation for selected T-ALL patients with resistant disease. Taken together, we demonstrate that *in vitro* drug profiling captures functional data that provide insights into new biological entities, and that may be translated to the clinic. Given the growing interest of clinicians for this approach, prospective evaluation is warranted to assess its value to guide leukemia treatment for patients with resistant disease.

ACKNOWLEDGMENTS

This work was supported by the Cancer League of the Canton of Zurich, the Empiris foundation, the foundation “Kinderkrebsforschung Schweiz”, the Sassella foundation, the “Stiftung für Krebsbekämpfung”, the Swiss National Science Foundation (310030-133108), the Fondation Panacee, the clinical research focus program “Human Hemato-Lymphatic Diseases” of the University of Zurich, the German Childhood Cancer Foundation and the German Cancer Consortium. P.H. acknowledges support from the Hungarian National Brain Research Program (MTA-SE-NAP B-BIOMAG) and the Finnish TEKES FiDiPro Fellow Grant 40294/13. J.W.T. is supported by The Leukemia & Lymphoma Society, the V Foundation for Cancer Research, the Gabrielle’s Angel Foundation for Cancer Research, and the National Cancer Institute (5R00CA151457-04; 1R01CA183947-01).This research received funding from the European Union’s Seventh Framework Programme for research, technological development, and demonstration (Grant agreement no. 278514 - IntReALL). V.S. is a Wellcome-DBT Margdarshi Fellow. M.P.D. is a SystemsX fellow. M.P.D. wishes to thank Dr. Edoardo Missiaglia for helpful discussions.

AUTHORSHIP CONTRIBUTIONS

J.-P.B., B.C.B., V.F., M.P.D., A.R. jointly designed the project. J.-P.B., B.C.B., J.W.T., V.F., A.R., S.H.D. designed experiments. V.F., A.R., J.T., J.K., P.R.-P., P.V., O.P., S.J., B.M., S.H., J.W.T., S.E., S.H.D. performed experiments. G.C., M.Sc., M.St., M.P.D., T.R., P.V., M.D., A.E.K., M.U.M., A.v.S., C.E., B.H.C., T.J.B., R.H.C., E.D.-F., M.L.L., E.D.-F., J.T., R.M., V.S., J.A.I., T.R., T.B., R.H.C., S.D. provided reagents, analysis tools, samples and clinical data. M.P.D., V.F., A.R., P.R.-R., J.K., J.W.T., O.P. S.J. S.H.D., analysed data and prepared tables and figures. J.-P.B., B.C.B. supervised research. J.-P.B., B.C.B., M.P.D., V.F. wrote the manuscript. All authors critically reviewed the manuscript for its content.

CONFLICT OF INTEREST DISCLOSURES

T.R. is a full-time employee of Novartis Pharma AG. The remaining authors declare no competing financial interests.

The online version of the article contains a data supplement.

References

1. Locatelli F, Schrappe M, Bernardo ME, Rutella S. How I treat relapsed childhood acute lymphoblastic leukemia. *Blood*. 2012;120(14):2807-2816.
2. Inaba H, Greaves M, Mullighan CG. Acute lymphoblastic leukaemia. *Lancet*. 2013.
3. Roberts KG, Li Y, Payne-Turner D, et al. Targetable kinase-activating lesions in Ph-like acute lymphoblastic leukemia. *N Engl J Med*. 2014;371(11):1005-1015.
4. Holmfeldt L, Wei L, Diaz-Flores E, et al. The genomic landscape of hypodiploid acute lymphoblastic leukemia. *Nature genetics*. 2013;45(3):242-252.
5. Shochat C, Tal N, Bandapalli OR, et al. Gain-of-function mutations in interleukin-7 receptor-alpha (IL7R) in childhood acute lymphoblastic leukemias. *J Exp Med*. 2011;208(5):901-908.
6. Eckert C, Hagedorn N, Sramkova L, et al. Monitoring minimal residual disease in children with high-risk relapses of acute lymphoblastic leukemia: prognostic relevance of early and late assessment. *Leukemia*. 2015;29(8):1648-1655.
7. Bader P, Kreyenberg H, von Stackelberg A, et al. Monitoring of Minimal Residual Disease After Allogeneic Stem-Cell Transplantation in Relapsed Childhood Acute Lymphoblastic Leukemia Allows for the Identification of Impending Relapse: Results of the ALL-BFM-SCT 2003 Trial. *J Clin Oncol*. 2015.
8. Schrappe M, Hunger SP, Pui CH, et al. Outcomes after induction failure in childhood acute lymphoblastic leukemia. *N Engl J Med*. 2012;366(15):1371-1381.
9. Hunger SP, Devaraj PE, Foroni L, Secker-Walker LM, Cleary ML. Two types of genomic rearrangements create alternative E2A-HLF fusion proteins in t(17;19)-ALL. *Blood*. 1994;83(10):2970-2977.
10. Garnett MJ, Edelman EJ, Heidorn SJ, et al. Systematic identification of genomic markers of drug sensitivity in cancer cells. *Nature*. 2012;483(7391):570-575.
11. Barretina J, Caponigro G, Stransky N, et al. The Cancer Cell Line Encyclopedia enables predictive modelling of anticancer drug sensitivity. *Nature*. 2012;483(7391):603-607.
12. Gao H, Korn JM, Ferretti S, et al. High-throughput screening using patient-derived tumor xenografts to predict clinical trial drug response. *Nat Med*. 2015;advance online publication.
13. Pemovska T, Kontro M, Yadav B, et al. Individualized systems medicine strategy to tailor treatments for patients with chemorefractory acute myeloid leukemia. *Cancer Discov*. 2013;3(12):1416-1429.
14. Tyner JW, Yang WF, Bankhead A, 3rd, et al. Kinase pathway dependence in primary human leukemias determined by rapid inhibitor screening. *Cancer Res*. 2013;73(1):285-296.
15. Geng H, Hurtz C, Lenz KB, et al. Self-Enforcing Feedback Activation between BCL6 and Pre-B Cell Receptor Signaling Defines a Distinct Subtype of Acute Lymphoblastic Leukemia. *Cancer Cell*. 2015;27(3):409-425.
16. Mihara K, Imai C, Coustan-Smith E, et al. Development and functional characterization of human bone marrow mesenchymal cells immortalized by enforced expression of telomerase. *Br J Haematol*. 2003;120(5):846-849.
17. Boutter J, Huang Y, Marovca B, et al. Image-based RNA interference screening reveals an individual dependence of acute lymphoblastic leukemia on stromal cysteine support. *Oncotarget*. 2014;5(22):11501-11512.
18. Bonapace L, Bornhauser BC, Schmitz M, et al. Induction of autophagy-dependent necroptosis is required for childhood acute lymphoblastic leukemia cells to overcome glucocorticoid resistance. *J Clin Invest*. 2010;120(4):1310-1323.
19. Schmitz M, Breithaupt P, Scheidegger N, et al. Xenografts of highly resistant leukemia recapitulate the clonal composition of the leukemogenic compartment. *Blood*. 2011;118(7):1854-1864.

20. Mirkowska P, Hofmann A, Sedek L, et al. Leukemia surfaceome analysis reveals new disease-associated features. *Blood*. 2013;121(25):e149-159.
21. Den Boer ML, Harms DO, Pieters R, et al. Patient stratification based on prednisolone-vincristine-asparaginase resistance profiles in children with acute lymphoblastic leukemia. *J Clin Oncol*. 2003;21(17):3262-3268.
22. Hartwell KA, Miller PG, Mukherjee S, et al. Niche-based screening identifies small-molecule inhibitors of leukemia stem cells. *Nat Chem Biol*. 2013;9(12):840-848.
23. Manabe A, Coustan-Smith E, Behm FG, Raimondi SC, Campana D. Bone marrow-derived stromal cells prevent apoptotic cell death in B-lineage acute lymphoblastic leukemia. *Blood*. 1992;79(9):2370-2377.
24. Iwamoto S, Mihara K, Downing JR, Pui CH, Campana D. Mesenchymal cells regulate the response of acute lymphoblastic leukemia cells to asparaginase. *J Clin Invest*. 2007;117(4):1049-1057.
25. Souers AJ, Leverson JD, Boghaert ER, et al. ABT-199, a potent and selective BCL-2 inhibitor, achieves antitumor activity while sparing platelets. *Nat Med*. 2013;19(2):202-208.
26. Van Vlierberghe P, Ambesi-Impiombato A, De Keersmaecker K, et al. Prognostic relevance of integrated genetic profiling in adult T-cell acute lymphoblastic leukemia. *Blood*. 2013;122(1):74-82.
27. Hogdal L, DeAngelo DJ, Stone RM, et al. BH3 Profiling Predicts On-Target Cell Death Due To Selective Inhibition Of BCL-2 By ABT-199 In Acute Myelogenous Leukemia. *Blood*. 2013;122(21).
28. Moorman AV. New and emerging prognostic and predictive genetic biomarkers in B-cell precursor acute lymphoblastic leukemia. *Haematologica*. 2016;101(4):407-416.
29. Luo FR, Yang Z, Camuso A, et al. Dasatinib (BMS-354825) pharmacokinetics and pharmacodynamic biomarkers in animal models predict optimal clinical exposure. *Clin Cancer Res*. 2006;12(23):7180-7186.
30. McMillin DW, Negri JM, Mitsiades CS. The role of tumour-stromal interactions in modifying drug response: challenges and opportunities. *Nat Rev Drug Discov*. 2013;12(3):217-228.
31. Irving J, Matheson E, Minto L, et al. Ras pathway mutations are prevalent in relapsed childhood acute lymphoblastic leukemia and confer sensitivity to MEK inhibition. *Blood*. 2014;124(23):3420-3430.
32. Hof J, Krentz S, van Schewick C, et al. Mutations and deletions of the TP53 gene predict nonresponse to treatment and poor outcome in first relapse of childhood acute lymphoblastic leukemia. *J Clin Oncol*. 2011;29(23):3185-3193.
33. Fischer U, Forster M, Rinaldi A, et al. Genomics and drug profiling of fatal TCF3-HLF-positive acute lymphoblastic leukemia identifies recurrent mutation patterns and therapeutic options. *Nat Genet*. 2015;47(9):1020-1029.
34. Conter V, Bartram CR, Valsecchi MG, et al. Molecular response to treatment redefines all prognostic factors in children and adolescents with B-cell precursor acute lymphoblastic leukemia: results in 3184 patients of the AIEOP-BFM ALL 2000 study. *Blood*. 2010;115(16):3206-3214.
35. McComb S, Aguade-Gorgorio J, Harder L, et al. Activation of concurrent apoptosis and necroptosis by SMAC mimetics for the treatment of refractory and relapsed ALL. *Sci Transl Med*. 2016;8(339):339ra370.
36. Parker C, Waters R, Leighton C, et al. Effect of mitoxantrone on outcome of children with first relapse of acute lymphoblastic leukaemia (ALL R3): an open-label randomised trial. *Lancet*. 2010;376(9757):2009-2017.
37. Liedtke M, Cleary ML. Therapeutic targeting of MLL. *Blood*. 2009;113(24):6061-6068.
38. Alford SE, Kothari A, Loeff FC, et al. BH3 inhibitor sensitivity and Bcl-2 dependence in primary acute lymphoblastic leukemia cells. *Cancer Res*. 2015.

559 39. Suryani S, Carol H, Chonghaile TN, et al. Cell and Molecular Determinants of In Vivo
560 Efficacy of the BH3 Mimetic ABT-263 against Pediatric Acute Lymphoblastic Leukemia
561 Xenografts. *Clin Cancer Res*. 2014.
562 40. Peirs S, Matthijssens F, Goossens S, et al. ABT-199 mediated inhibition of BCL-2 as a
563 novel therapeutic strategy in T-cell acute lymphoblastic leukemia. *Blood*. 2014;124(25):3738-
564 3747.
565 41. Chou TC. Drug combination studies and their synergy quantification using the Chou-
566 Talalay method. *Cancer Res*. 2010;70(2):440-446.
567 42. Chonghaile TN, Roderick JE, Glenfield C, et al. Maturation stage of T-cell acute
568 lymphoblastic leukemia determines BCL-2 versus BCL-XL dependence and sensitivity to
569 ABT-199. *Cancer Discov*. 2014;4(9):1074-1087.
570 43. Bicocca VT, Chang BH, Masouleh BK, et al. Crosstalk between ROR1 and the Pre-B
571 cell receptor promotes survival of t(1;19) acute lymphoblastic leukemia. *Cancer Cell*.
572 2012;22(5):656-667.
573 44. Fallah-Tafti A, Foroumadi A, Tiwari R, et al. Thiazolyl N-benzyl-substituted acetamide
574 derivatives: synthesis, Src kinase inhibitory and anticancer activities. *Eur J Med Chem*.
575 2011;46(10):4853-4858.
576 45. Hynes NE, Lane HA. ERBB receptors and cancer: the complexity of targeted inhibitors.
577 *Nat Rev Cancer*. 2005;5(5):341-354.
578 46. Foa R, Vitale A, Vignetti M, et al. Dasatinib as first-line treatment for adult patients
579 with Philadelphia chromosome-positive acute lymphoblastic leukemia. *Blood*.
580 2011;118(25):6521-6528.
581 47. Khaw SL, Suryani S, Evans K, et al. Venetoclax responses of pediatric ALL xenografts
582 reveal MLLr ALL sensitivity, but overall requirement to target both BCL2 and BCLXL. *Blood*.
583 2016.
584 48. Ni Chonghaile T, Sarosiek KA, Vo TT, et al. Pretreatment mitochondrial priming
585 correlates with clinical response to cytotoxic chemotherapy. *Science*. 2011;334(6059):1129-
586 1133.
587 49. Montero J, Sarosiek KA, DeAngelo JD, et al. Drug-induced death signaling strategy
588 rapidly predicts cancer response to chemotherapy. *Cell*. 2015;160(5):977-989.
589 50. Konopleva M, Pollyea DA, Potluri J, et al. Efficacy and Biological Correlates of
590 Response in a Phase II Study of Venetoclax Monotherapy in Patients with Acute Myelogenous
591 Leukemia. *Cancer Discov*. 2016.
592 51. Benito JM, Godfrey L, Kojima K, et al. MLL-Rearranged Acute Lymphoblastic
593 Leukemias Activate BCL-2 through H3K79 Methylation and Are Sensitive to the BCL-2-
594 Specific Antagonist ABT-199. *Cell Reports*. 2015.
595 52. Deenik W, Beverloo HB, van der Poel-van de Luytgaarde SC, et al. Rapid complete
596 cytogenetic remission after upfront dasatinib monotherapy in a patient with a NUP214-ABL1-
597 positive T-cell acute lymphoblastic leukemia. *Leukemia*. 2009;23(3):627-629.
598 53. Zwaan CM, Rizzari C, Mechinaud F, et al. Dasatinib in children and adolescents with
599 relapsed or refractory leukemia: results of the CA180-018 phase I dose-escalation study of the
600 Innovative Therapies for Children with Cancer Consortium. *J Clin Oncol*. 2013;31(19):2460-
601 2468.
602

603

Table 1. Characteristics of the five patients with refractory disease included in this study

FIGURE LEGENDS

Figure 1. Setup of drug response profiling platform.

Patient material, notably from high-risk cases, including relapse cases and cases with translocations linked to poor survival, were prioritized for patient-derived xenograft (PDX) and drug response profiling; PDX stability was evaluated against primary material by comparing targeted deep-sequenced leukemogenesis markers (**A**, top panel). Drug profiling was performed on primary ALL cells in co-culture with mesenchymal bone marrow stroma cells (MSCs). Automated microscopy-based image analysis was used to quantify living ALL and generate dose response curves. Imaging results are analysed with a toolkit that performs dose response normalization, outlier removal, rapid curve fitting, and extraction of response parameters (IC50, AUC, Emax). Selected single compounds and combinations are validated in the xenograft model. This platform enables the identification of drug response phenotypes in individual ALL cases, providing an additional layer of information to facilitate individual treatment approaches (**A**, bottom panel). Our PDX model preserves an average of 74% of the mutations and indels initially detected in patients, making it an ideal source of material for drug response testing in multi-center, co-clinical settings (**B**).

Figure 2. Drug response profiles of BCP-ALL and T-ALL.

Heatmap indicating the response of BCP-ALL (n=44) and T-ALL (n=24) to 60 compounds and represented by IC50 values. Samples (rows) were ordered according to clinical classification and compounds (columns) according to activity. Each compound's IC50 distribution range is shown on the lower panel forming drug clusters:

A: Generally active drugs, mean IC50 values < 10 nM;

B: Drugs more active in BCP-ALLs than T-ALLs;

C: Generally active drugs, IC50 values < 100 nM;

D: Drugs with variable activity

E: Drugs with activity linked to cycling activity;

F: Generally active drugs, high nanomolar range;

G: Generally inactive drugs, with sporadic exceptions.

On the lower part of the graph heatmap of MSC and drug IC50 distribution box plot are demonstrated.

Figure 3. Drug profiling reveals leukemia-intrinsic features.

(**A**) Co-culturing on MSC supports survival of T-ALL (n=22) and BCP-ALL (n=25). Data at day 4 are given, normalized to seeded viable cell numbers at day 0 both in monoculture or in co-culture (left panel). Cell cycle and apoptosis rates of primary T-ALL (n=18) and BCP-ALL (n=14) cells in co-culture is provided on the right. Samples are ranked from highest (top) to lowest (bottom) survival. Ratio of cells in S-phase and apoptosis is given on the far right. ****, *p<0.0001 (Paired t-test)*

(**B**) Engraftment kinetics for ALL cases with >40% of cells in S-phase (dotted lines in red) and with <40% in S-phase (straight blue lines) are given (**i.**). Time to engraftment with 25% ALL blasts in the two groups is indicated in the lower panel (**ii.**). ***, *p<0.001 (Two-sided t-test)*

(**C**) *In vitro* ALL proliferation correlates with drug response to cytarabine (antimetabolite), docetaxel (antimitotic) and other cell cycle targeting drugs (**Figure S4**). ALL cells with >40% of cells in S-phase (red symbols) respond to cytarabine and docetaxel with lower IC50 compared to samples with <40% of cells in S-phase (blue symbols).

(**D**) Cytarabine and docetaxel response profiles predict *in vivo* ALL response (N=8).

Figure 4. Distinct drug activity patterns can be detected for individual samples and patient groups of interest

(**A**) Refractory relapse (RR (PDX), N=12) samples exhibit general resistance to conventional clinical compounds, but remain sensitive to some experimental drugs.

(**C**) Primary refractory relapse patients (RR (primary), N=5) tested before last salvage therapy demonstrate persistent resistance to standard chemotherapy and individual sensitivity to experimental molecules.

All responses are represented as IC50 (log[nM]) and compared to other diagnostic and relapse ALL cases depicted in the background. **, p<0.05; **, p<0.005 (Two-sided t-test)*

Figure 5. *In vitro* sensitivity to the BCL-2 antagonist venetoclax correlates with the response in leukemia xenografts.

(**A**) *In vitro* response to venetoclax for indicated ALL subtypes (black) compared to other ALL (grey). From top to bottom: mature-T-ALL (N=6), cortical-T-ALL (N=13), pre-T-ALL (N=6), *TCF3-HLF* ALL (N=4) and *MLL-AF4* ALL (N=3). Cell viability (7-AAD) was measured by flow cytometry after treatment for 72 hours and normalized against DMSO-treated controls. Arrows indicate samples whose response had been validated *in vivo* for venetoclax (top to bottom: T-VHR-03, T-HR-11 and T-HR-10) or venetoclax in combination with vincristine and dexamethasone (top to bottom: B-HR-24, B-HR-20, B-HR-26 and B-VHR-07). The left panel shows the number of leukemia cells compared to mouse lymphocytes over time. The right panel shows corresponding Kaplan-Meier survival curves (event defined as 25% of $mCD45^-$ $hCD45^+hCD19^+$ or $hCD7^+$ leukemia cells detected by flow cytometry).

(**B**) *In vitro* response to venetoclax correlates with fold increase of survival comparing treatment with venetoclax and vehicle (N=7).

(**C**) BCL2 protein family expression (**i.**) analysed by flow cytometer in T-ALL (N=16) and BCP-ALL (N=20). Correlation of BCL2:BCL-XL and BCL2:MCL1 ratio (**ii.**) with *in vitro* venetoclax response. *****, p<0.0001 (two-tailed t test)*.

Figure 6. Extraordinary *in vitro* sensitivity of T-ALL to dasatinib correlates with anti-leukmeic efficacy in the patient.

(**A**) Subset of T-ALL cases at diagnosis that relapsed (R) and at relapse are highly sensitive to dasatinib *in vitro*.

(**B**) Dasatinib sensitive T-ALL have higher levels of phosphorylated SRC that decreases after treatment with 1μM dasatinib for 2h as measured by flow cytometry. ***, *p<0.001 (Two-sided t-test)*

(**C**) Dasatinib response correlates with sensitivity to the SRC inhibitor KX2-391 (N=16).

(**D**) *In vitro* captured response correlates with *in vivo* response to dasatinib (N=10). Indicated are the % of T-ALL blasts compared to mouse lymphocytes, normalized to vehicle treated controls.

(**E**) Sensitivity of adult and pediatric T-ALL cases to dasatinib reveals 40% of cases with IC50 below 100 nM.

(**F**) Left PET/CT demonstrates significant disease burden throughout the marrow in bilateral upper and lower extremities, the pelvis, vertebrae, and contiguous nodes within the mediastinum. Right PET/CT approximately 15 months after the original presentation, shortly after initiation of dasatanib monotherapy. This image demonstrates complete response with no signs of marrow or nodal involvement.

Table 1. Characteristics of the five patients with refractory disease included in this study

Patient	Sex, age	Clinical Status at time point of drug profiling	Salvage treatment	Current status
Patient 1	F, 2	Relapsed after SCT, early relapse	MLL:MLLT10 positive, blinatumomab	alive, follow up 15 months
Patient 2	M, 7	Relapsed after SCT, second relapse, resistant to anti CD19 therapy	Blinatumomab, second transplant	alive, follow up 9 months
Patient 3	F, 8	Relapsed after SCT, second relapse	Chemotherapy, second transplant	died
Patient 4	F, 5	Very early BM relapse	Resistant to blinatumomab, no response to bortezomib + 4 drugs	died
Patient 5	F, 11	Relapsed after SCT, second (late) relapse	Second transplant, resistant to blinatumomab, partial response to bortezomib + 4 drugs	died

F - female
M - male

Figure 1.

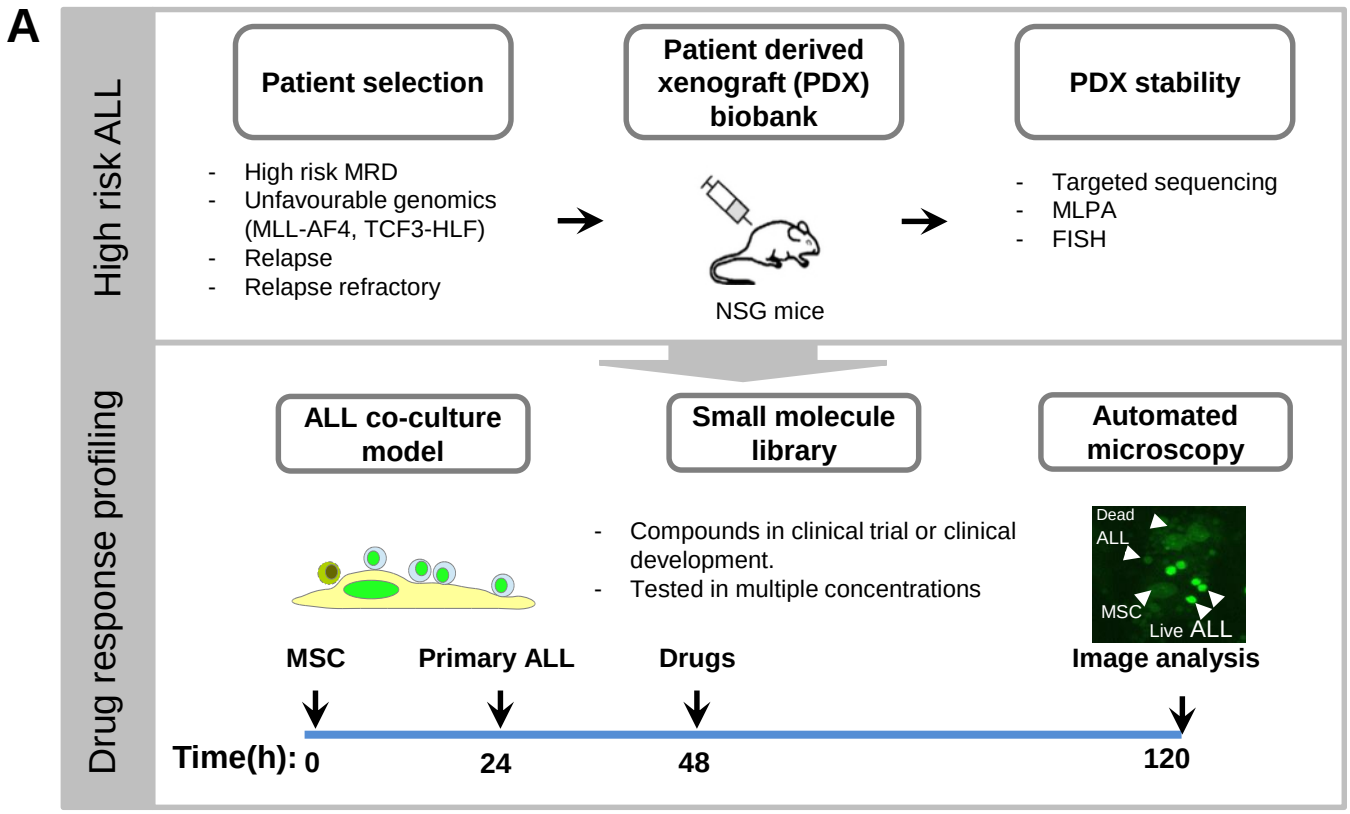
A
High risk ALL
Patient selection
- High risk MRD
- Unfavourable genomics (MLL-AF4, TCF3-HLF)
- Relapse
- Relapse refractory
Patient derived xenograft (PDX) biobank
NSG mice
PDX stability
- Targeted sequencing
- MLPA
- FISH
Drug response profiling
ALL co-culture model
Small molecule library
- Compounds in clinical trial or clinical development.
- Tested in multiple concentrations
Automated microscopy
Dead
ALL
MSC
Live ALL
MSC
Primary ALL
Drugs
Image analysis
Time(h): 0
24
48
120

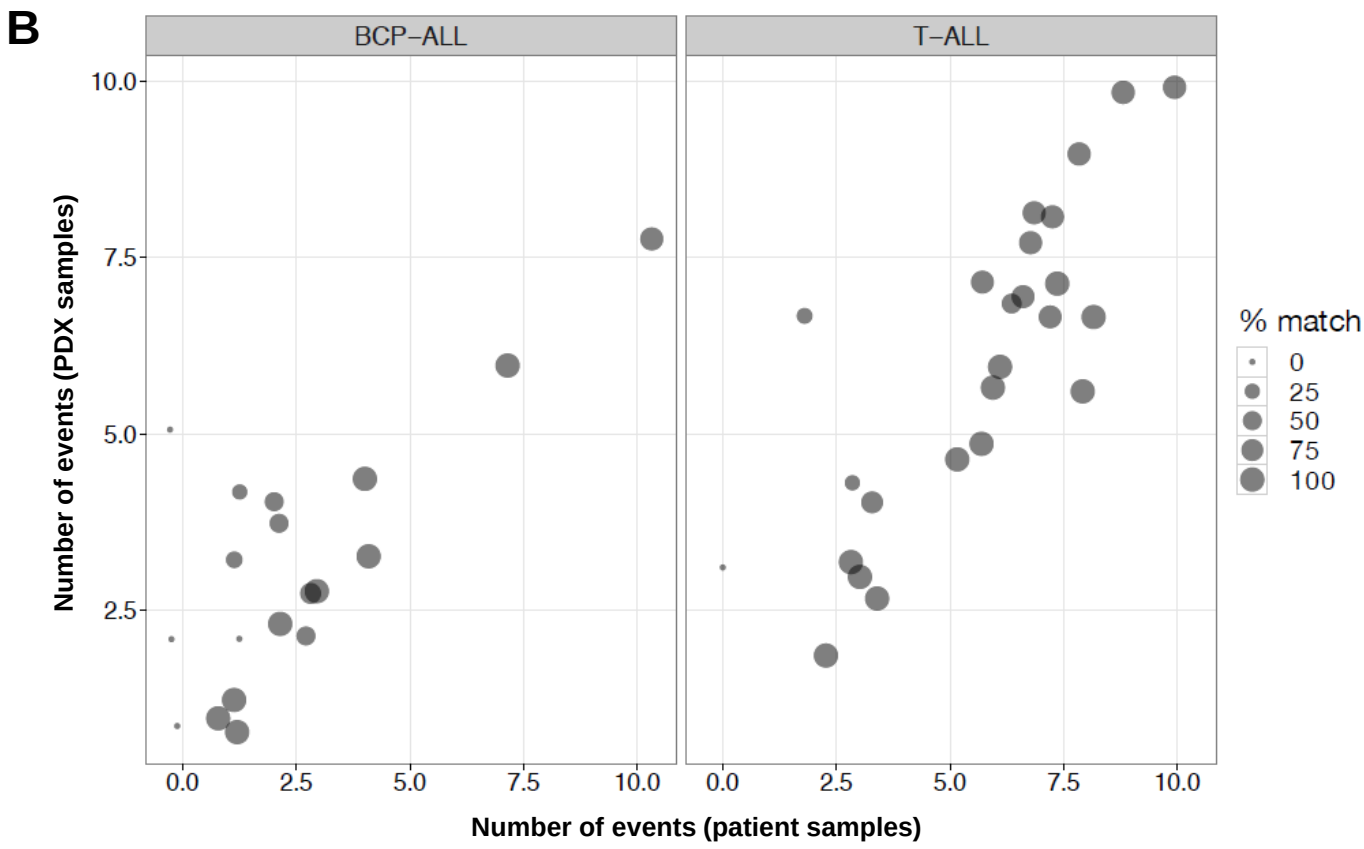
B
BCP–ALL
T–ALL
Number of events (PDX samples)
Number of events (patient samples)
0.0
2.5
5.0
7.5
10.0
% match
0
25
50
75
100

Figure 2.

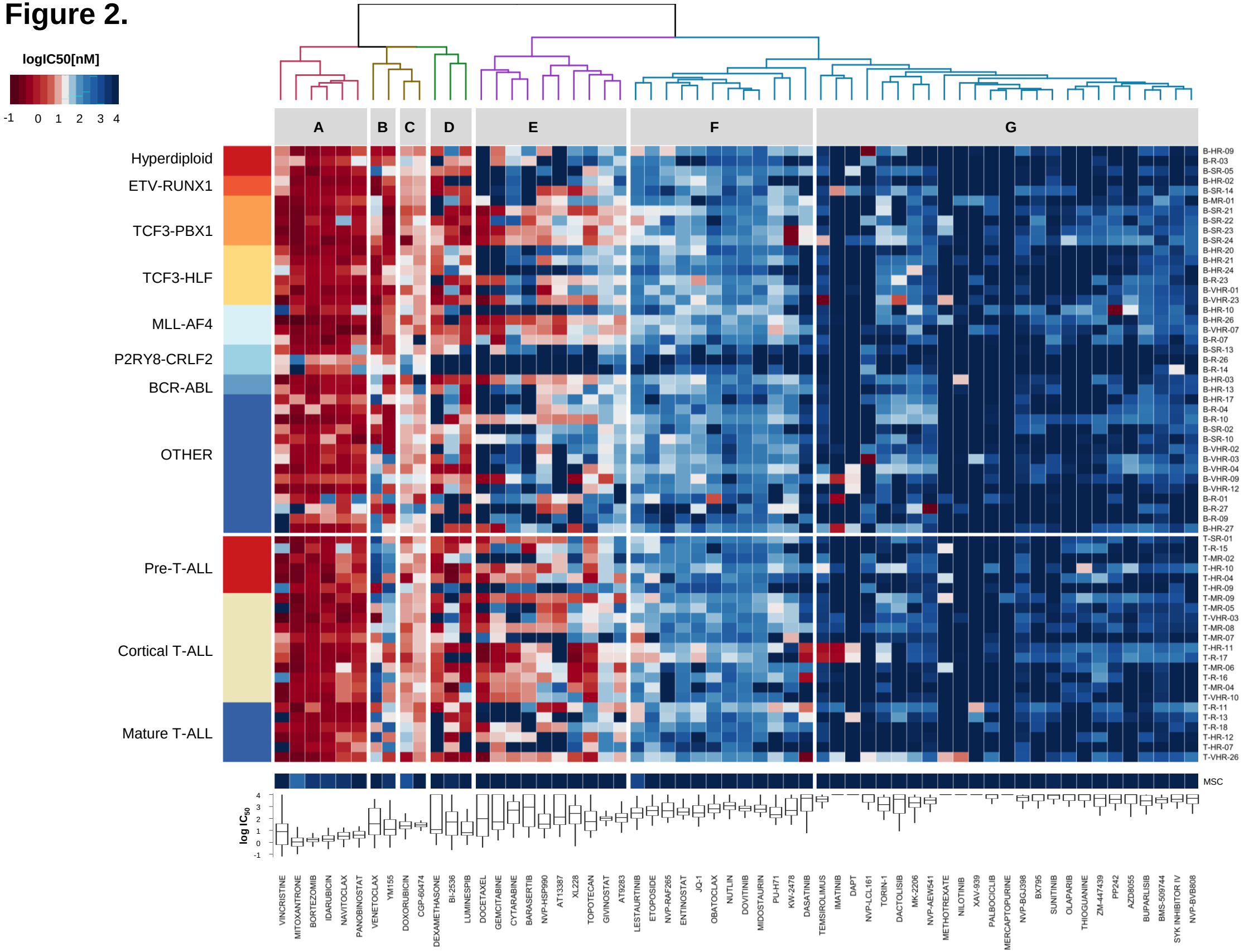
logIC50[nM]
-1 0 1 2 3 4
A
B
C
D
E
F
G
Hyperdiploid
ETV-RUNX1
TCF3-PBX1
TCF3-HLF
MLL-AF4
P2RY8-CRLF2
BCR-ABL
OTHER
Pre-T-ALL
Cortical T-ALL
Mature T-ALL
B-HR-09
B-R-03
B-SR-05
B-HR-02
B-SR-14
B-MR-01
B-SR-21
B-SR-22
B-SR-23
B-SR-24
B-HR-20
B-HR-21
B-HR-24
B-R-23
B-VHR-01
B-VHR-23
B-HR-10
B-HR-26
B-VHR-07
B-R-07
B-SR-13
B-R-26
B-R-14
B-HR-03
B-HR-13
B-HR-17
B-R-04
B-R-10
B-SR-02
B-SR-10
B-VHR-02
B-VHR-03
B-VHR-04
B-VHR-09
B-VHR-12
B-R-01
B-R-27
B-R-09
B-HR-27
T-SR-01
T-R-15
T-MR-02
T-HR-10
T-HR-04
T-HR-09
T-MR-09
T-MR-05
T-VHR-03
T-MR-08
T-MR-07
T-HR-11
T-R-17
T-MR-06
T-R-16
T-MR-04
T-VHR-10
T-R-11
T-R-13
T-R-18
T-HR-12
T-HR-07
T-VHR-26
MSC
log IC50
4
3
2
1
0
-1
VINCRISTINE
MITOXANTRONE
BORTEZOMIB
IDARUBICIN
NAVITOCLAX
PANOBINOSTAT
VENETOCLAX
YM155
DOXORUBICIN
CGP-60474
DEXAMETHASONE
BI-2536
LUMINESPIB
DOCETAXEL
GEMCITABINE
CYTARABINE
BARASERTIB
NVP-HSP990
AT13387
XL228
TOPOTECAN
GIVINOSTAT
AT9283
LESTAURTINIB
ETOPOSIDE
NVP-RAF265
ENTINOSTAT
JQ-1
OBATOCLAX
NUTLIN
DOVITINIB
MIDOSTAURIN
PU-H71
KW-2478
DASATINIB
TEMSIROLIMUS
IMATINIB
DAPT
NVP-LCL161
TORIN-1
DACTOLISIB
MK-2206
NVP-AEW541
METHOTREXATE
NILOTINIB
XAV-939
PALBOCICLIB
MERCAPTOPURINE
NVP-BGJ398
BX795
SUNITINIB
OLAPARIB
THIOGUANINE
ZM-447439
PP242
AZD8055
BUPARLISIB
BMS-509744
SYK INHIBITOR IV
NVP-BVB808

Figure 3.

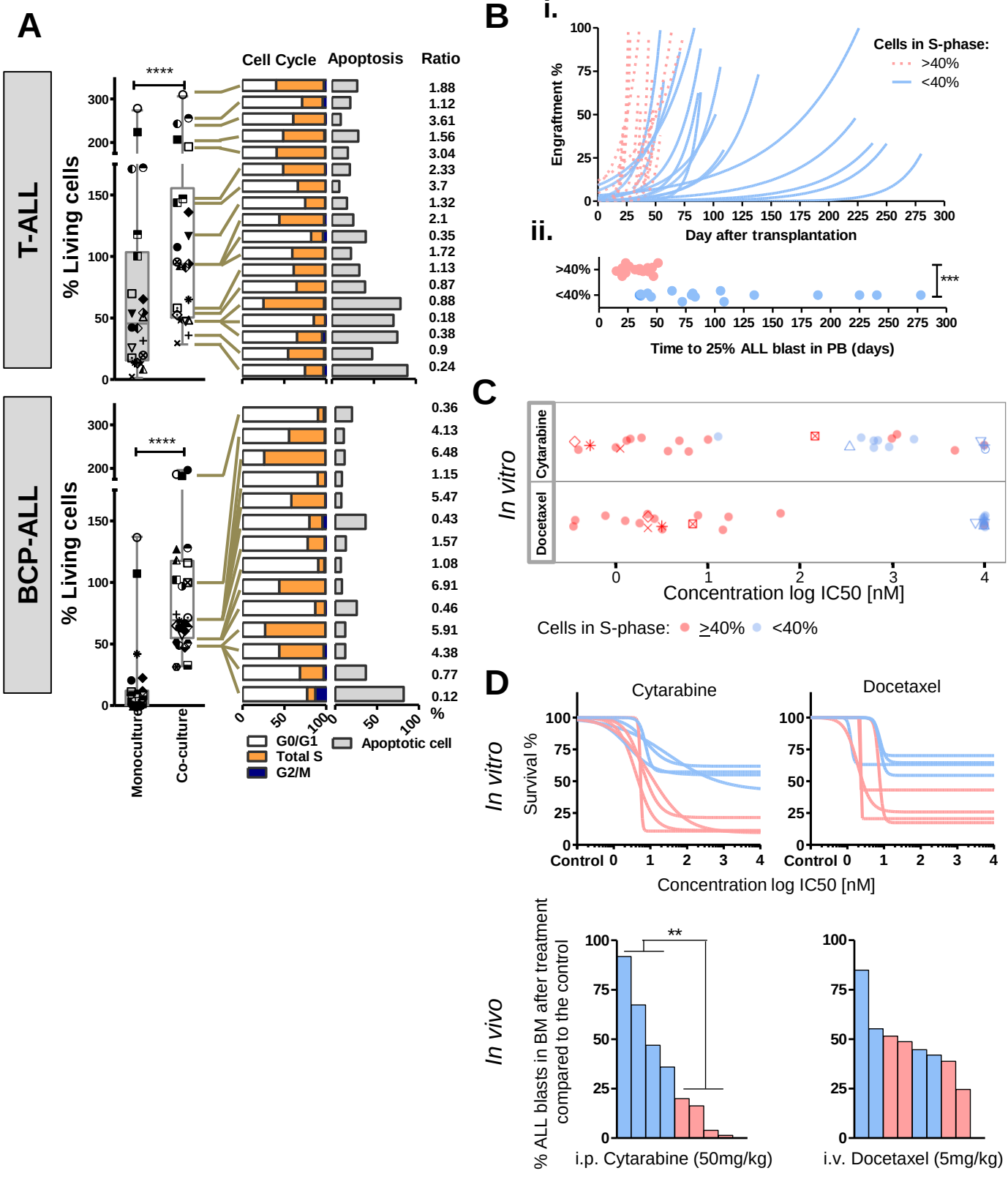
A
T-ALL
BCP-ALL
% Living cells
****
Cell Cycle
Apoptosis
Ratio
1.88
1.12
3.61
1.56
3.04
2.33
3.7
1.32
2.1
0.35
1.72
1.13
0.87
0.88
0.18
0.38
0.9
0.24
0.36
4.13
6.48
1.15
5.47
0.43
1.57
1.08
6.91
0.46
5.91
4.38
0.77
0.12
%
Monoculture
Co-culture
G0/G1
Total S
G2/M
Apoptotic cell
B
i.
Engraftment %
Day after transplantation
Cells in S-phase:
>40%
<40%
ii.
***
Time to 25% ALL blast in PB (days)
C
In vitro
Cytarabine
Docetaxel
Concentration log IC50 [nM]
Cells in S-phase: ≥40% <40%
D
In vitro
Cytarabine
Docetaxel
Survival %
Control
Concentration log IC50 [nM]
In vivo
% ALL blasts in BM after treatment compared to the control
**
i.p. Cytarabine (50mg/kg)
i.v. Docetaxel (5mg/kg)

Figure 4.

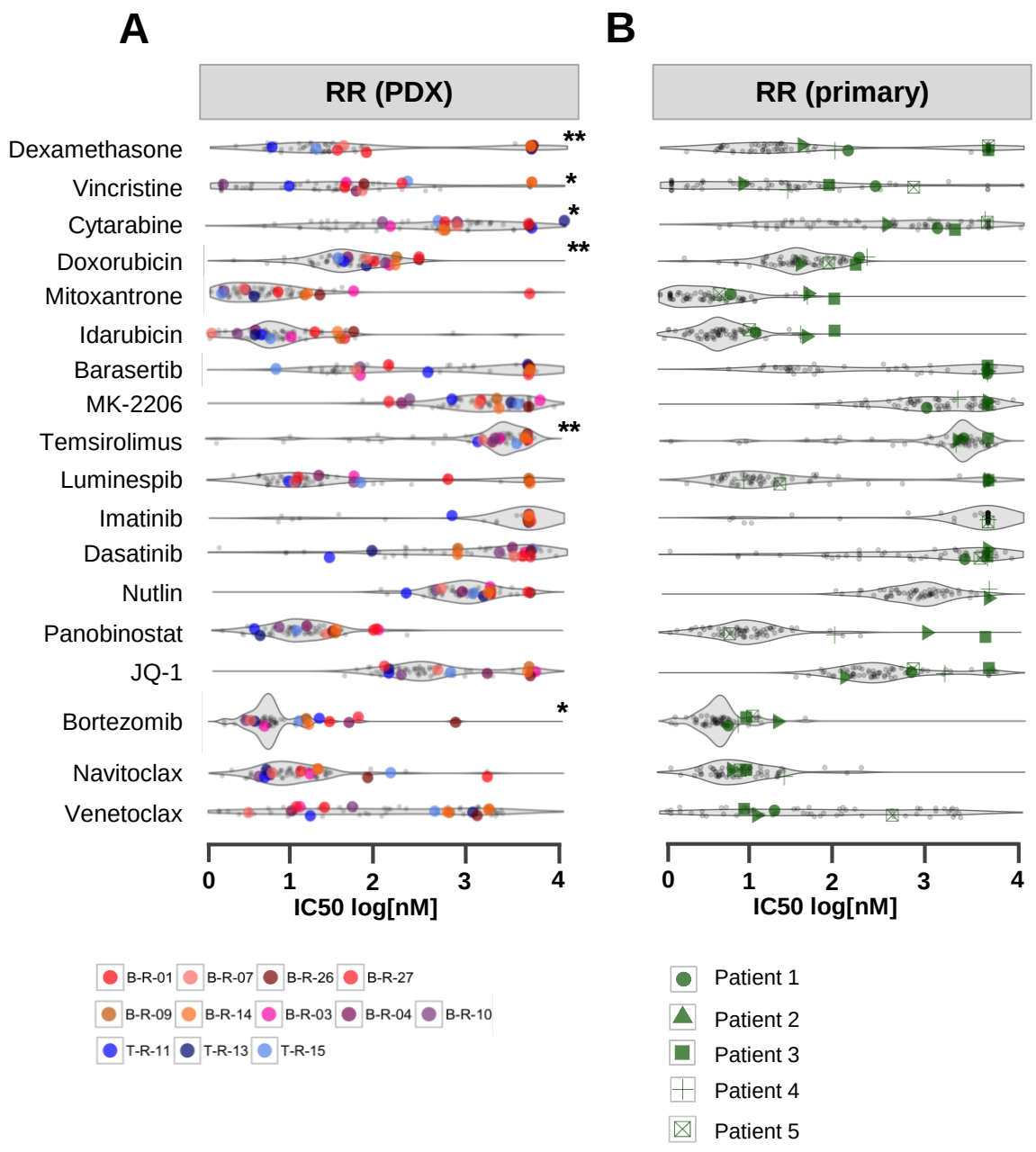
A
B
RR (PDX)
RR (primary)
Dexamethasone
Vincristine
Cytarabine
Doxorubicin
Mitoxantrone
Idarubicin
Barasertib
MK-2206
Temsirolimus
Luminespib
Imatinib
Dasatinib
Nutlin
Panobinostat
JQ-1
Bortezomib
Navitoclax
Venetoclax
**
*
*
**
**
*
0
1
2
3
4
IC50 log[nM]
0
1
2
3
4
IC50 log[nM]
B-R-01
B-R-07
B-R-26
B-R-27
B-R-09
B-R-14
B-R-03
B-R-04
B-R-10
T-R-11
T-R-13
T-R-15
Patient 1
Patient 2
Patient 3
Patient 4
Patient 5

Figure 5.

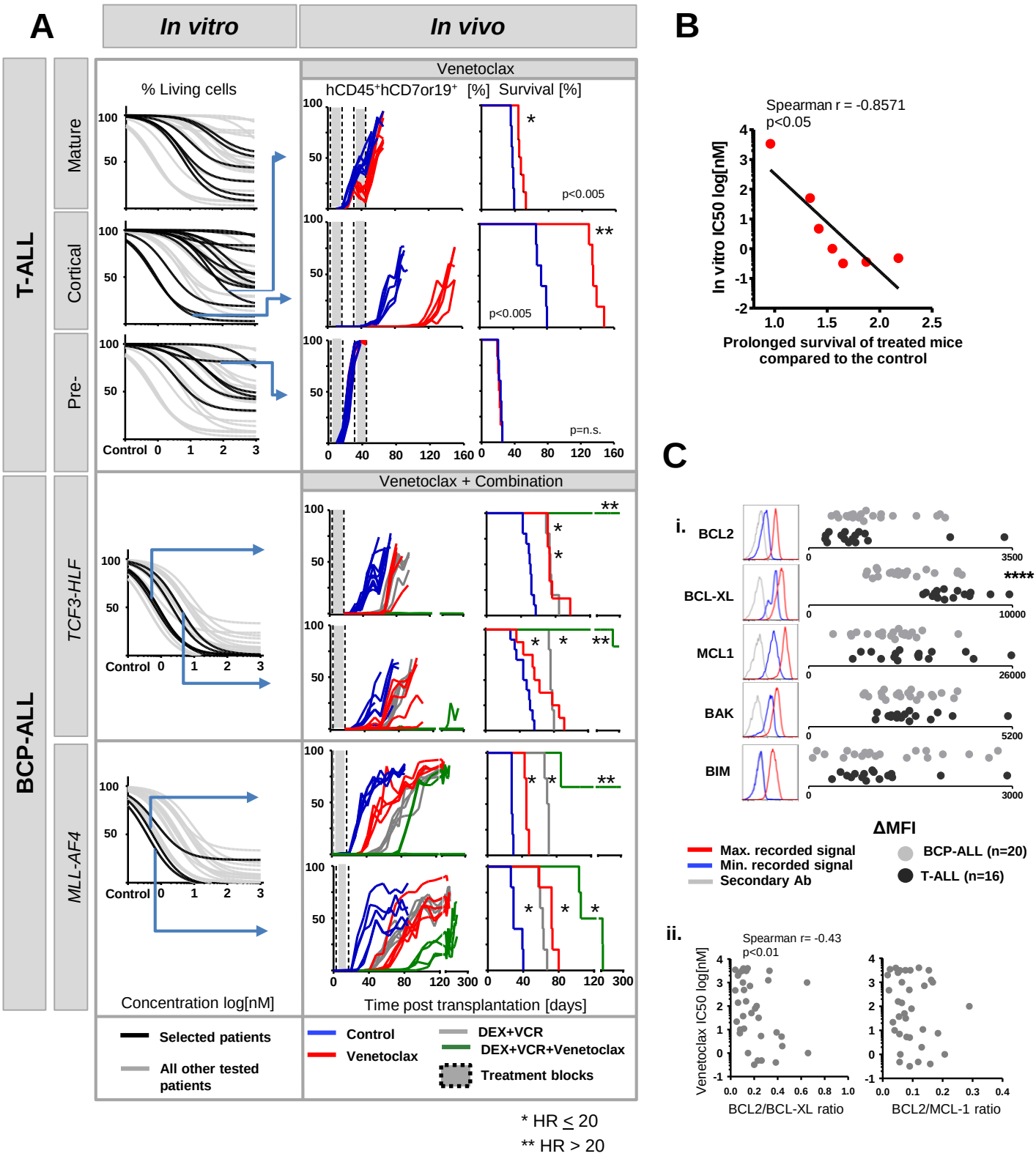
A
In vitro
In vivo
T-ALL
BCP-ALL
Mature
Cortical
Pre-
TCF3-HLF
MLL-AF4
% Living cells
Control
Concentration log[nM]
Venetoclax
hCD45+hCD7or19+ [%]
Survival [%]
p<0.005
p=n.s.
Venetoclax + Combination
Time post transplantation [days]
Selected patients
All other tested patients
Control
Venetoclax
DEX+VCR
DEX+VCR+Venetoclax
Treatment blocks
* HR ≤ 20
** HR > 20
B
Spearman r = -0.8571
p<0.05
ln vitro IC50 log[nM]
Prolonged survival of treated mice compared to the control
C
i.
BCL2
BCL-XL
MCL1
BAK
BIM
ΔMFI
Max. recorded signal
Min. recorded signal
Secondary Ab
BCP-ALL (n=20)
T-ALL (n=16)
ii.
Spearman r= -0.43
p<0.01
Venetoclax IC50 log[nM]
BCL2/BCL-XL ratio
BCL2/MCL-1 ratio

Figure 6.

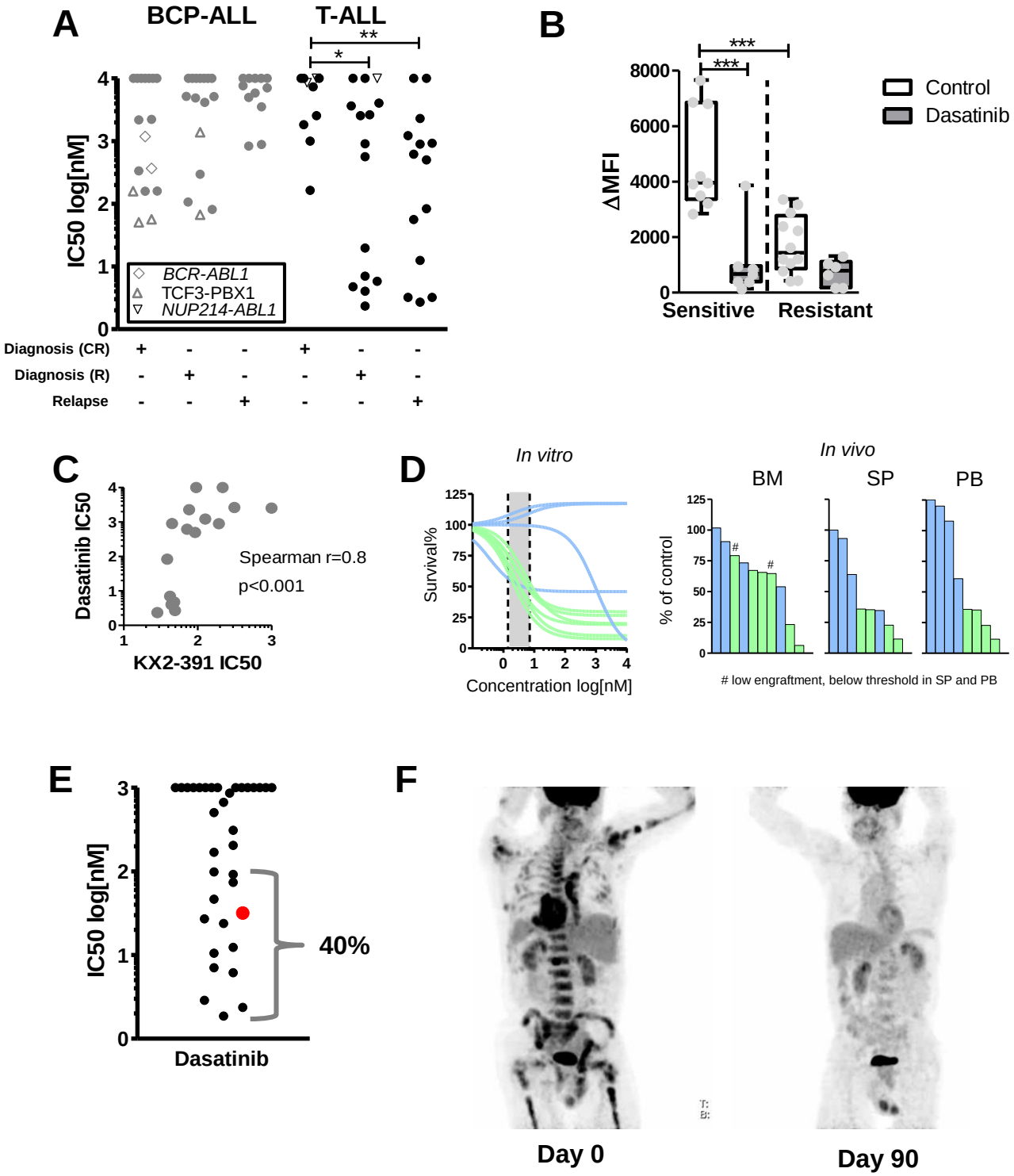
A
BCP-ALL
T-ALL
**
*
IC50 log[nM]
BCR-ABL1
TCF3-PBX1
NUP214-ABL1
Diagnosis (CR)
Diagnosis (R)
Relapse
B
***
***
ΔMFI
Control
Dasatinib
Sensitive
Resistant
C
Dasatinib IC50
KX2-391 IC50
Spearman r=0.8
p<0.001
D
In vitro
Survival%
Concentration log[nM]
In vivo
BM
SP
PB
% of control
# low engraftment, below threshold in SP and PB
E
IC50 log[nM]
40%
Dasatinib
F
Day 0
Day 90

Targeting BET proteins improves the therapeutic efficacy of BCL-2 inhibition in T-cell acute lymphoblastic leukemia

Sofie Peirs[1,2,*], Viktoras Frismantas[3,*], Filip Matthijssens[1,2], Wouter Van Loocke[1,2], Tim Pieters[1,2,4,5], Niels Vandamme[2,4,5], Béatrice Lintermans[1,2], Maria Pamela Dobay[6], Geert Berx[2,4,5], Bruce Poppe[1,2], Beat C Bornhauser[3], Jean-Pierre Bourquin[3,**] and Pieter Van Vlierberghe[1,2,**]

[1]Center for Medical Genetics, Ghent University, Ghent, Belgium

[2]Cancer Research Institute Ghent (CRIG), Ghent, Belgium

[3]Department of Pediatric Oncology, Children's Research Centre, University Children's Hospital Zurich, Zurich, Switzerland

[4]Molecular and Cellular Oncology Lab, VIB Inflammation Research Center, Ghent University, Ghent, Belgium

[5]Department of Biomedical Molecular Biology, Ghent University, Ghent, Belgium

[6]Swiss Institute of Bioinformatics (SIB), Lausanne, Switzerland

[*]SP and VF contributed equally to this work

[**]JPB and PVV contributed equally to this work

Running title Combination of venetoclax and JQ1 in T-ALL

Correspondence Jean-Pierre Bourquin, PhD

University Children's Hospital Zurich

Department of Pediatric Oncology

Children's Research Centre

August-Forelstrasse 1

8032 Zurich, Switzerland

Tel: +41 44 266 7304

Email: Jean-Pierre.Bourquin@kispi.uzh.ch

Conflict of interest The authors declare no conflict of interest.

Abstract

Inhibition of anti-apoptotic BCL-2 has recently emerged as a promising new therapeutic strategy for the treatment of a variety of human cancers, including leukemia. Here, we used T-cell acute lymphoblastic leukemia as a model system to identify novel synergistic drug combinations with the BH3 mimetic venetoclax (ABT-199). *In vitro* drug screening in primary leukemia specimens that were derived from patients with high risk of relapse or relapse and cell lines revealed synergistic activity between venetoclax and the BET bromodomain inhibitor JQ1. Notably, this drug synergism was confirmed *in vivo* using a T-ALL cell line xenograft model. Moreover, the therapeutic benefit of this drug combination might, at least in part, be mediated by an acute induction of the pro-apoptotic factor *BCL2L11* and concomitant loss of BCL-2 upon BET bromodomain inhibition, ultimately resulting in an enhanced binding of BIM (encoded by *BCL2L11*) to BCL-2. Altogether, our work provides a rationale to develop a new type of targeted combination therapy for selected subgroups of high-risk leukemia patients.

Introduction

T-cell acute lymphoblastic leukemia (T-ALL) arises from the malignant transformation of T-cell progenitors and accounts for about 15% of childhood and 25% of adult ALL cases(1). The cure rate for childhood T-ALL has steadily increased over the past decades, with current survival rates reaching approximately 85%(2, 3). Although these numbers are high, the clinical perspective for children that fail induction therapy or suffer from relapsed disease remains extremely poor, with only a 7-23% subset of relapsed T-ALL patients surviving beyond 3 to 5 years after the initial diagnosis(4). Compared to childhood leukemia, the clinical picture for adult T-ALL is even worse, with high relapse rates and long-term disease-free survival of about 40%(5-7). Altogether, these figures suggest that better and less toxic treatment strategies are urgently required to further improve the clinical management of childhood and adult T-ALL patients.

Recently, we and other research groups reported promising therapeutic activity for venetoclax (ABT-199), a highly specific inhibitor of the anti-apoptotic protein BCL-2, in immature subtypes of human T-ALL(8-10). Nevertheless, venetoclax sensitivity is variable between different T-ALL patient samples and the emergence of resistance to venetoclax(11-13) as well as the occurrence of dose-limiting toxicities(14) provides a rationale for the evaluation of venetoclax as part of a combination therapy. Indeed, previous studies have shown that venetoclax can synergize with conventional chemotherapeutic agents in human T-ALL, including doxorubicin, L-asparaginase, dexamethasone and cytarabine(8, 9). Venetoclax has recently also been approved by the FDA for the treatment of chronic lymphocytic leukemia (CLL). Indeed, venetoclax clinical trials demonstrated progress-free survival in more than two thirds of relapsed CLL patients(14), including poor prognostic CLL patients that carry a 17p deletion(15). Nevertheless, complete remission remained uncommon(14), further reinforcing the need for the evaluation of combined therapeutic strategies.

Bromodomains of the bromodomain and extra-terminal (BET) protein family recognize ε-N-acetylation of lysine residues on histone tails. BRD4 is an important BET protein that recruits the positive transcription elongation factor complex (P-TEFb) to acetylated chromatin(16). The transcriptional coactivators BRD4 and Mediator co-occupy enhancers and promoters of active genes and are enriched at large stretches of enhancer sequences, often termed super-enhancers(17-19). Notably, these enhancers regulate the expression of critical oncogenes in a variety of human cancers, providing a rationale for the use of BET bromodomain inhibitors, such as JQ1, as powerful anti-cancer agents(17-19). Also in T-ALL, BET bromodomain inhibitors have shown therapeutic efficacy in a number of *in vitro* and *in vivo* model systems and were shown to inhibit the expression of the T-ALL oncogene *MYC*(20-22). In addition, super-enhancers have been identified in a panel of T-ALL cell lines near putative oncogenes, including *MYB*, *TAL1*, *CDK6* and *NOTCH1*(18).

In this study, we identified synergistic drug combinations with the BH3 mimetic venetoclax in the context of human T-ALL. Most notably, we show that combined targeting of BCL-2 and BET bromodomain proteins synergistically affects leukemic tumor growth in BCL-2 positive T-ALL that were resistant to conventional chemotherapeutic agents.

Materials and methods

Primary patient samples

Primary human ALL cells were recovered from cryopreserved bone marrow aspirates of patients enrolled in the ALL-BFM 2000, 2009 and ALL-REZ-BFM 2002 study. Informed consent was given in accordance with the Declaration of Helsinki and the ethics commission of the Kanton Zurich (approval number 2014-0383). Samples were classified as standard risk (SR), medium risk (MR), high risk (HR), very high risk (VHR) or relapse samples (R) according to the clinical criteria used in ALL-BFM 2000(23).

Drug-screening platform

The *in vitro* drug response of T-ALL primary patient samples was assessed in co-culture with hTERT-immortalized primary bone marrow mesenchymal stromal cells (MSC) as described previously (23). Details are provided in the supplemental data.

Cell lines

Cell lines were purchased from the DSMZ repository (Braunschweig, Germany), except for CUTLL1 (gift Prof. Adolfo Ferrando, Columbia University, New York, USA) and KOPTK1 (gift Prof. Hans-Guido Wendel, Memorial Sloan Kettering Cancer Center, New York, USA). Cells were cultured in RPMI 1640 medium (Life Technologies, Carlsbad, CA, USA; catalog number 52400-025) supplemented with 10% or 20% FBS, 100 U/ml penicillin, 100 µg/ml streptomycin (Life Technologies, 15140-148), 100 µg/ml kanamycin sulfate (Life Technologies, 15160-047) and 2 mM L-glutamine (Life Technologies, 25030024) at 37°C with 5% CO2.

***In vitro* evaluation of synergism between venetoclax and JQ1 in human T-ALL cell lines and primary samples**

The treatment of the cell lines with venetoclax (BioVision, Milpitas, CA; 2253-1) and/or (+)-JQ1 (BPS Bioscience, San Diego, CA, USA; 27401) and viability measurements via the CellTiter Glo Viability assay (Promega, Madison, WI, USA) have previously been described in Peirs et al.(8) CalcuSyn software (Biosoft, Cambridge, United Kingdom) was used to calculate the combination index (CI) with the Chou-Talalay method. The reported CI is the average of the values obtained at the ED50, ED75 and ED90 point. Primary patient samples co-titration experiments were performed for selected drugs. T-ALL cell plates were prepared and handled in the same manner as for drug combination screening described above. Selected drugs in combination with venetoclax were dispensed using Tecan D300 digital dispenser in a concentration matrix. The concentration range tested for venetoclax and JQ-1 were determined for each patient based on initial drug response screening. CI had been calculated using Chou-Talalay method as implemented in R package (https://github.com/xtmgah/DDCV).

Western blot

Western blot analysis was performed as previously described(8). The primary antibodies used were Bcl-2 antibody (C-2) (1:500, Santa Cruz Biotechnology, Dallas, TX, USA; sc-7382), PARP-1 antibody (F-2) (1:1000, Santa Cruz Biotechnology, sc-8007), BIM antibody (1:1000, EMD Millipore, Darmstadt, Germany; AB17003), β-actin antibody (1:10000, Sigma-Aldrich, Saint Louis, MO, USA; Clone AC-75, A2228) and α-tubulin antibody (1:10000, Sigma-Aldrich, T5168). The detection of the blots was done with ChemiDoc-It Imaging System (UVP, Upland, CA, USA). Densitometric analysis of the protein bands was performed using ImageJ (NIH, Bethesda, MD, USA). Images have been cropped for presentation.

AnnexinV/PI staining

FITC Annexin V Apoptosis Detection Kit I (BD Biosciences, San Jose, CA, USA; 556547) was used according to manufacturer's instructions. Samples were measured on the S3 cell sorter (Bio-Rad, Hercules, California, USA).

Mice experiment

Twenty-four female nonobese diabetic/severe combined immunodeficient γ (NSG) mice were injected in the tail vein with 150µl PBS containing $5*10^6$ luciferase-positive LOUCY cells(8). Four weeks after injection (day 0), bioluminescence was measured as previously described(8). Mice were randomly divided into four groups (control, venetoclax, JQ1 and combination) and treatment was started the day after for 13 consecutive days. Mice received daily 50mg venetoclax/kg body weight via oral gavage and/or 50mg JQ1/kg body weight via intraperitoneal injection. Venetoclax (Axon Medchem, Groningen, The Netherlands) was formulated in 60% phosal 50 propylene glycol, 30% polyethylene glycol 400 and 10% ethanol. (+)-JQ1 (MedChem Express, South Brunswick Township, NJ, USA) was formulated in 10% DMSO and 90% of a 10% 2-hydroxypropyl-β-cyclodextrin solution. Bioluminescence was measured at day 6 and the day after the last treatment (day 14). At day 15, blood was taken from the tail vein and mice were sacrificed after which bone marrow and spleens

were collected. The percentage of leukemic cells in the blood and bone marrow was analyzed by staining the cells with an PE-labeled antibody for human CD45 (hCD45) (Miltenyi Biotec, Bergisch Gladbach, Germany; 130-098-141), performing red blood cell lysis and measuring the percentage on a LSRII flow cytometer using FACSDiva software (BD Bioscience). The ethical committee on animal welfare at Ghent University Hospital approved all animal experiments.

Gene expression profiling and GSEA

LOUCY cells were seeded at 0.7 x 10^6 cells/ml and treated with DMSO or (+)-JQ1. Three biological replicates of this treatment were performed and RNA was isolated using the miRNeasy mini kit (Qiagen, Venlo, The Netherlands) with on-column DNase digestion. The RNA quality was evaluated by the Experion RNA StdSens analysis kit (Bio-Rad). RNA was amplified and labeled using the Low Input Quick Amp Labeling Kit, One Color (Agilent Technologies, Santa Clara, CA, USA; 5190-2305) and hybridized with the Gene Expression Hybridization Kit (Agilent Technologies, 5188-5242) to the SurePrint G3 Human Gene Expression Microarray G4851A (design ID 028004, Agilent Technologies). Normalization of microarray intensities was done using the variance stabilization and calibration (VSN, version 3.30.0) package in R (version 3.0.2). Only probes with a signal 10% higher than the negative control probes were considered for analysis. Differential expression analysis was performed using the limma package (version 3.18.13) with p-value adjustment using the Benjamini and Hochberg method. The design matrix took into account the pairing information of the data. Enrichment analysis was performed on theMSigDB gene sets collection c2.all.v5.0.symbols.gmt using the GSEA desktop application (Broad Institute, version v2.2.0) run with the default parameters and with gene set permutations. The data have been deposited in NCBI's Gene Expression Omnibus(24) and are accessible through GEO Series accession number GSE81918.

Real-time quantitative PCR (RT-qPCR)

The miRNeasy mini kit (Qiagen) and the RNAse-Free Dnase set (Qiagen) were used to isolate RNA. cDNA synthesis was performed with the iScript Advanced cDNA synthesis kit (Bio-Rad). The

SsoAdvanced Universal SYBR Green Supermix (Bio-Rad) was used for the PCR reactions while amplification and detection was done with the LightCycler 480 instrument (Roche, Vilvoorde, Belgium). Every sample was analyzed in duplicate and the gene expression was normalized against 3 housekeeping genes. qBasePLUS software (Biogazelle, Zwijnaarde, Belgium) was used for analysis. Primer sequences are listed in Supplemental Table 4.

Co-immunoprecipitation

Protein lysates were incubated with 2 µg of antibody. After 4h rotation at 4°C, 20 µl of Protein A UltraLink Resin (Thermo Scientific, Waltham, MA, USA; 53139) was added for overnight incubation at 4°C. Beads were collected by centrifugation (1000 rpm, 1 min., 4°C), washed 3 times with RIPA buffer and immunoprecipitates were eluted by heating the beads at 95 °C in 2× SDS loading buffer (62 mM Tris–HCl (pH 6.8), 4% SDS, 20% glycerol, 0.01% BFB (bromophenol blue), 2.5% beta-mercaptoethanol) for 10 min. A part of the original lysates were similarly denaturated by heating at 95 °C for 10 min after adding 5× SDS loading buffer (155 mM Tris–HCl (pH 6.8), 5% SDS, 32% glycerol, 0.025% BFB, 2,5% beta mercapto-ethanol).

Modulation of BIM expression

The pENTR223-BCL2L11 (LMBP ORF81079-A09) plasmid was available from the BCCM/LMBP Plasmid Collection(25) and was used to clone *BCL2L11* in the pInducer21 plasmid(26). Virus production was performed in HEK293TN cells using JetPEI polyplus with pMD2.G (envelope plasmid), psPAX2 (packaging plasmid) and pInducer21-BCL2L11 (target plasmid) in 0.1/0.9/1 ratios. Transduced KARPAS-45 cells expressing GFP were selected by cell sorting using a S3 cell sorter (Bio-Rad). Cells were cultured in medium with tetracycline-free FCS and *BCL2L11* expression was induced by adding doxycyclin (1µg/ml). Sensitivity to venetoclax was evaluated by adding venetoclax together with or without doxycycline for 48h to the cells. Viability was evaluated with CellTiter Glo as described above.

Statistics

GraphPad Prism 5.04 (La Jolla, CA, USA) was used for statistical analyses.

Results

Identification of synergistic drug combinations with venetoclax in primary human T-ALL

Previous studies have shown promising anti-tumor activity for venetoclax in the context of human T-ALL(8-10). However, drug responses have been variable across patients both *in vitro* as well as in xenografts, suggesting the need for predictive biomarkers and further investigation towards synergistic drug combinations with venetoclax. Given this, we took advantage of a drug-profiling platform(27) (**Figure 1A**) to test 21 clinically relevant compounds (**Supplemental Table 1**) for their ability to synergize with venetoclax in six primary human T-ALLs, including five diagnostic and one relapse specimen. Notably, the selected patient samples represented different molecular genetic subtypes of human T-ALL and displayed a variety of tumor immunophenotypes. In addition, most of these high-risk T-ALL patient samples experienced significant levels of minimal residual disease upon first line therapy (**Supplemental Table 2**).

First, we generated venetoclax response curves for each T-ALL sample and selected a sub-lethal dose of venetoclax for screening purposes (**Figure 1A**). Two T-ALL samples were sensitive at concentrations below 100nM, whereas the remaining cases were more resistant to venetoclax (**Supplemental Figure 1**). This variability in venetoclax sensitivity amongst T-ALL patient samples corresponded to large differences in the area under the curve (AUC), a parameter that captures both IC_{50} and E_{max} as relevant endpoints of drug activity (**Figure 1B**). Next, we generated dose response curves (1nM, 10 nM, 100nM, 1µM and 10µM) for the 21 compounds in the presence or absence of a sublethal dose of venetoclax (**Figure 1A**). The results of this initial screening are visualised by scatterplots of AUC values, in which decreased AUC upon addition of venetoclax is indicative of increased antileukemic activity (**Figure 1B**; **Supplemental Figure 2**). In line with previous studies, combination of venetoclax with conventional chemotherapeutic agents including vincristine, dexamethasone, etoposide, doxorubicin or topotecan increased therapeutic efficacy in some of the T-ALL cases analysed (**Figure 1B, Supplemental Figure 2**). The strongest effects, however, were

observed for the combination of venetoclax with the BET bromodomain inhibitor JQ1, which resulted in reduced leukemic tumor growth in 5 out of 6 primary T-ALL patient samples (**Figure 1B**). As a confirmation, we validated responsive (**Figure 1C**) as well as non-responsive (**Supplemental Figure 3**) drug interactions identified in this initial screen. Altogether, this screening effort identified clinically relevant drugs that could increase the therapeutic efficacy of venetoclax in the context of human T-ALL.

Combined targeting of BCL-2 and BET bromodomain proteins in human T-ALL

Given that our initial screen pointed towards increased efficacy of venetoclax upon BET bromodomain inhibition in a significant proportion of T-ALLs, we subsequently analysed the synergistic potential of this drug combination in more detail by performing co-titration experiments with individually-optimized concentration ranges in primary leukemias and a panel of human T-ALL cell lines.

First, we determined the combination indexes (CI) for the 6 primary T-ALLs that were also used for the initial screening and identified synergistic activities (CI<1) between venetoclax and JQ1 in five out of six cases analysed (**Figure 2A**). Notably, similar results were obtained using OTX015 (MK-8628), another BET bromodomain inhibitor currently being tested in clinical trials for various tumor entities(28, 29) (**Supplemental Figure 4**).

Next, we determined dose response curves in a panel of 13 human T-ALL cell lines with different BCL-2 levels and varying sensitivities towards venetoclax (**Figure 2B** and **Supplemental Figure 5**). Notably, T-ALL cell lines displayed variable levels of synergism with the lowest CI values (strongest synergism) detected for tumor lines with high BCL-2 expression (**Figure 2B**). Indeed, the combination index showed a negative correlation with BCL-2 protein levels in T-ALL cell lines (**Figure 2C**). Moreover, synergistic activity of this drug combination corresponded to increased cell death induction in T-ALL cell lines with low CI values (**Supplemental Figure 6**).

Evaluation of the venetoclax and JQ1 combination therapy in a LOUCY-derived xenograft model

To evaluate the therapeutic potential of combined BCL-2 and BET bromodomain inhibition in human T-ALL, we subsequently performed *in vivo* drug treatment experiments using a xenograft model of luciferase-positive LOUCY cells(8). Four weeks after injection in immunodeficient mice, successful engraftment was confirmed by bioluminescence imaging and daily drug treatment was initiated (day 0). Leukemia still progressed under JQ1 monotherapy (n=5), albeit to a lesser extent as compared to vehicle-treated control mice (n=8) (**Figure 3A** and **Supplemental Figure 7**). Mice treated for 13 days with venetoclax alone (n=5) initially showed disease regression, but this therapeutic response was not durable (**Figure 3A** and **Supplemental Figure 7**). In contrast, combination of venetoclax with JQ1 (n=5) resulted in durable disease regression (**Figure 3A-B**). In line with these results, analysis of the percentage of human leukemic cells in peripheral blood and bone marrow as well as examination of the spleen size confirmed the superior therapeutic effect of this combination treatment (**Figure 3C-D** and **Supplemental Figure 8**). Of note, mice receiving JQ1 alone or in combination with venetoclax displayed significant weight loss (**Supplemental Figure 8**), a putative side effect of BET bromodomain inhibition.

Mechanistic insights into the synergistic activities of venetoclax and JQ1 in human T-ALL

To understand how BET bromodomain inhibition might synergize with the BCL-2 inhibitor venetoclax, we subsequently analyzed the transcriptional consequences of JQ1 treatment in the T-ALL cell line LOUCY by microarray analysis. Short-term exposure to a low dose of JQ1 (4h, 250nM) provided insights in the genes whose expression was immediately affected by BET bromodomain inhibition (**Figure 4A**, left). In contrast, sustained exposure at a higher concentration (48h, 1µM) revealed broader transcriptional effects with more than half of the expressed probesets showing significant up- or downregulation (adj. p-value<0.05; **Figure 4A**, right). Significantly downregulated genes upon short-term drug treatment included stem-cell associated genes and putative oncogenes such as

BAALC, *WT1*, *MN1*, *MEF2C*, *LMO1* and *LMO2*, whereas other oncogenic factors, including *BCL2*, *IGFBP7*, *ZEB2*, *GFI1B*, *MYB* and *LYL1*, only changed significantly after 48h.

In line with previous reports(17-19), these JQ1 responsive genes were regulated by strong and active enhancer elements characterized by broad binding of the H3K27ac histone mark in LOUCY cells(30) (**Figure 4B**). Indeed, genes associated with the 500 highest ranked enhancer regions in LOUCY were significantly enriched in genes downregulated after JQ1 treatment (**Figure 4C**). Moreover, enrichment analysis using gene sets from the Molecular Signatures database (MSigDB) revealed that genes upregulated after JQ1 in LOUCY cells significantly overlapped with genes activated upon HDAC inhibition or UV treatment (**Figure 4D**). In line with this notion, the Library of Integrated Cellular Signatures (LINCS) revealed a strong connection between the JQ1-induced expression signature in LOUCY and gene signatures induced by HDAC inhibitors (**Supplemental Table 3**).

Given that binding of the pro-apoptotic BIM (encoded by *BCL2L11*) to the BH3 domain of BCL-2 is an important mediator of venetoclax activity(31-34), we subsequently focused on the transcriptional effects of JQ1 on the expression of both factors. Notably, in LOUCY cells, *BCL2L11* expression was induced after short-term JQ1 exposure (**Figure 4A**, left), whereas loss of *BCL2* expression was only detected at later time points (**Figure 4A**, right). Upregulation of pro-apoptotic *BCL2L11* and concomitant loss of anti-apoptotic *BCL-2* could be confirmed in all T-ALL cell lines that displayed strong synergy (CI<0.5) for the ABT199/JQ1 drug combination. As a result, BET bromodomain inhibition triggered an increased BIM to BCL-2 ratio (**Figure 5A and 5B**), providing a putative explanation for the improved therapeutic efficacy of venetoclax upon JQ1 treatment. Indeed, co-immunoprecipitation experiments demonstrated an increased BIM to BCL-2 binding (**Figure 5C**) upon JQ1 treatment. Finally, doxycycline inducible overexpression of BIM in the KARPAS-45 cell line mimicked the effect of JQ1 and resulted in an increased sensitivity towards venetoclax (**Figure 5D**).

Discussion

Venetoclax is a promising new molecular therapy that is currently being evaluated in clinical trials for different hematological malignancies(14, 15, 35). However, the limited number of complete remissions(14) and the emergence of resistance with venetoclax as single agent prompts for a systematic evaluation of combinations with rationally-designed small molecules to assess its true therapeutic potential. Indeed, synergistic cytotoxic effects have been described for the combination of venetoclax with BTK(36-38), galectin(39), Aurora Kinase A(40), CDK(41, 42) and PI3K/AKT/mTOR inhibition(13, 43).

Given the promising single agent activity of venetoclax in human T-ALL subsets(8-10), we systematically evaluated clinically relevant drugs in order to identify synergistic combinations with venetoclax. The strongest and most consistent effect was detected for the combination with the bromodomain inhibitors JQ1 and OTX015, both targeting critical mechanisms that are deregulated in cancer cells. This effect could be validated *in vivo* using a leukemia xenograft model. Notably, this concept has recently been suggested as an experimental therapy for double hit lymphoma, triple hit lymphoma and mantle cell lymphoma in which both *MYC* and *BCL2* are deregulated(44-46). Interestingly, our preclinical data indicate that relevant activity can be obtained with this combination of agents irrespectively from their activity as single agent, which may possibly broaden the cohort of eligible cancer types (or subsets) for clinical translation. However, the challenge will be to identify useful biomarkers to better define patients that may benefit from such experimental combinations. Interestingly, an increase of BCL-2 protein levels in human T-ALL cell lines correlated with synergism between venetoclax and JQ1. Nevertheless, the value of additional methodologies such as BH3-profiling(47) should also be taken into consideration in future studies of this therapeutic rationale.

The importance of BRD4 in processes that lead to abnormal activation of cancer driving genetic programs is increasingly being understood(17-19). The proof of concept in T-ALL was provided by

studies of BET bromodomain inhibitors with a focus on *MYC* inhibition(20-22). Given the central importance of super-enhancer deregulation in cancer (18, 19), a similar principle may apply to many different transcriptional programs in leukemia cells. However, the broad transcriptional effects of these inhibitors on T-ALL cells remain largely unexplored. Gene expression profiling of LOUCY cells treated with JQ1 confirmed that BET bromodomain inhibition results in reduced expression of super-enhancer-associated oncogenes as previously described by Lovén et al. (17). However, we also observed acute gene re-activation within 4 hours of JQ1 treatment, suggesting that BET bromodomain inhibition could also trigger direct induction of gene transcription. Indeed, Bhadury et al.(48) previously described a model in which JQ1 treatment can release the transcription elongation factor p-TEFb from its inhibitory HEXIM-7SK small nuclear ribonucleoprotein (7SK snRNP) complex. Subsequently, free p-TEFb can phosphorylate RNA polymerase II and drive transcription at specific target genes, including stress-induced transcripts as well as *HEXIM1* itself. Notably, a similar release of p-TEFb has been observed upon UV light exposure or after HDAC inhibitor treatment (48, 49), providing a putative explanation for the enrichment of UV or HDAC inhibitor associated gene sets in the gene signature that was reactivated upon JQ1 treatment in LOUCY cells. Moreover, repositioning of p-TEFb and RNA pol II upon BET bromodomain inhibition resulting in direct induction of gene transcription has also been described in non-cancer settings such as HIV(49).

BCL2L11 (encoding BIM) is one of the genes that showed such an acute induction of gene expression upon JQ1 treatment in the context of T-ALL. BIM is an activator BH3-only pro-apoptotic protein that can directly interact with BAX and/or BAK to induce apoptosis. BCL-2 can prevent apoptosis by sequestering pro-apoptotic proteins such as BIM(50). Studies demonstrated the requirement for BCL-2 complexed to the pro-apoptotic activator BIM in order to sensitize lymphoid cells to BCL-2 inhibition by venetoclax or ABT-737(31-34). In our study, BET bromodomain inhibition increased BIM to BCL-2 binding, and could provide a putative explanation for the observed synergism between venetoclax and JQ1/OTX015 in the context of human T-ALL. Importantly, upregulation of pro-apoptotic BIM upon JQ1 treatment has also been described in a variety of other tumor entities(51-

54), suggesting that the synergistic activity between these molecules might not be restricted to human T-ALL.

In summary, our study provides a rationale to select patients with treatment resistant T-ALL for an innovative combination treatment based on mechanisms that are not exploited by conventional chemotherapy regimens. Interference with the balance between pro- and anti-apoptotic proteins in BCL2-dependent T-ALL using the combination BET bromodomain inhibition and the BCL2-inhibitor venetoclax should be considered in future clinical trials for this indication.

Acknowledgments

The authors would like to thank following funding agencies: Fund for Scientific Research Flanders ('FWO Vlaanderen' research projects GA00113N, 3G065614, G.0C47.13N and 31500615W to PVV; research projects G.0529.12N and G.0817.13N to GB; doctoral grant to SP; BP is a senior clinical investigator), Children Cancer Fund Ghent, Belgian Foundation Against Cancer (grant 365W3415W and B/13590) and the Belgian Stand Up To Cancer Foundation (research grant 365Y9115W; postdoctoral grants to TP and FM), agency for Innovation by Science and Technology ('IWT', SB Grant 111528 to NV), Geconcerteerde Onderzoeksacties Ghent University (GOA-01GB1013W to GB), Cancer League of the Canton of Zurich, Empiris Foundation, Kinderkrebsforschung Schweiz, Sassella Foundation, Stiftung für Krebsbekämpfung, Swiss National Science Foundation (310030-133108), Fondation Panacée and the clinical research focus program "Human Hemato-Lymphatic Diseases" of the University of Zurich.

The authors also thank Lindy Reunes for excellent technical assistance and the Innovative Flemish in vivo imaging technology (INFINITY) laboratory at Ghent University Hospital. Finally, the computational resources (Stevin Supercomputer Infrastructure) and services used in this work were provided by the VSC (Flemish Supercomputer Center), funded by Ghent University, the Hercules Foundation and the Flemish Government – department EWI.

Conflict of Interest

The authors declare no conflict of interest.

Supplementary information is available at Leukemia's website.

References

1. Pui C-H, Relling MV, Downing JR. Acute Lymphoblastic Leukemia. New England Journal of Medicine. 2004;350(15):1535-48.
2. Pui CH, Pei D, Campana D, Cheng C, Sandlund JT, Bowman WP, et al. A revised definition for cure of childhood acute lymphoblastic leukemia. Leukemia. 2014;28(12):2336-43.
3. Pui CH, Mullighan CG, Evans WE, Relling MV. Pediatric acute lymphoblastic leukemia: where are we going and how do we get there? Blood. 2012;120(6):1165-74.
4. Bhojwani D, Pui CH. Relapsed childhood acute lymphoblastic leukaemia. The Lancet Oncology. 2013;14(6):e205-17.
5. Bassan R, Hoelzer D. Modern therapy of acute lymphoblastic leukemia. Journal of clinical oncology : official journal of the American Society of Clinical Oncology. 2011;29(5):532-43.
6. Oriol A, Vives S, Hernandez-Rivas JM, Tormo M, Heras I, Rivas C, et al. Outcome after relapse of acute lymphoblastic leukemia in adult patients included in four consecutive risk-adapted trials by the PETHEMA Study Group. Haematologica. 2010;95(4):589-96.
7. Faderl S, O'Brien S, Pui CH, Stock W, Wetzler M, Hoelzer D, et al. Adult acute lymphoblastic leukemia: concepts and strategies. Cancer. 2010;116(5):1165-76.
8. Peirs S, Matthijssens F, Goossens S, Van de Walle I, Ruggero K, de Bock CE, et al. ABT-199 mediated inhibition of BCL-2 as a novel therapeutic strategy in T-cell acute lymphoblastic leukemia. Blood. 2014;124(25):3738-47.
9. Anderson NM, Harrold I, Mansour MR, Sanda T, McKeown M, Nagykary N, et al. BCL2-specific inhibitor ABT-199 synergizes strongly with cytarabine against the early immature LOUCY cell line but not more-differentiated T-ALL cell lines. Leukemia. 2014;28(5):1145-8.

399 10. Chonghaile TN, Roderick JE, Glenfield C, Ryan J, Sallan SE, Silverman LB, et al. Maturation
400 Stage of T-cell Acute Lymphoblastic Leukemia Determines BCL-2 versus BCL-XL
401 Dependence and Sensitivity to ABT-199. Cancer discovery. 2014.
402 11. Fresquet V, Rieger M, Carolis C, Garcia-Barchino MJ, Martinez-Climent JA. Acquired
403 mutations in BCL2 family proteins conferring resistance to the BH3 mimetic ABT-199 in
404 lymphoma. Blood. 2014;123(26):4111-9.
405 12. Tahir SK, Smith ML, Hessler P, Roberts-Rapp L, Leverson JD, Lam LT. Abstract B30:
406 Mechanisms of resistance to ABT-199 in leukemia and lymphoma cell lines. Clinical
407 Cancer Research. 2015;21(4 Supplement):B30.
408 13. Choudhary GS, Al-Harbi S, Mazumder S, Hill BT, Smith MR, Bodo J, et al. MCL-1 and BCL-
409 xL-dependent resistance to the BCL-2 inhibitor ABT-199 can be overcome by preventing
410 PI3K/AKT/mTOR activation in lymphoid malignancies. Cell death & disease.
411 2015;6:e1593.
412 14. Roberts AW, Davids MS, Pagel JM, Kahl BS, Puvvada SD, Gerecitano JF, et al. Targeting
413 BCL2 with Venetoclax in Relapsed Chronic Lymphocytic Leukemia. N Engl J Med.
414 2016;374(4):311-22.
415 15. Stilgenbauer S, Eichhorst B, Schetelig J, Coutre S, Seymour JF, Munir T, et al. Venetoclax in
416 relapsed or refractory chronic lymphocytic leukaemia with 17p deletion: a multicentre,
417 open-label, phase 2 study. The Lancet Oncology. 2016.
418 16. Filippakopoulos P, Qi J, Picaud S, Shen Y, Smith WB, Fedorov O, et al. Selective inhibition
419 of BET bromodomains. Nature. 2010;468(7327):1067-73.
420 17. Loven J, Hoke HA, Lin CY, Lau A, Orlando DA, Vakoc CR, et al. Selective inhibition of tumor
421 oncogenes by disruption of super-enhancers. Cell. 2013;153(2):320-34.
422 18. Hnisz D, Abraham BJ, Lee TI, Lau A, Saint-Andre V, Sigova AA, et al. Super-enhancers in
423 the control of cell identity and disease. Cell. 2013;155(4):934-47.
424 19. Filippakopoulos P, Knapp S. Targeting bromodomains: epigenetic readers of lysine
425 acetylation. Nature reviews Drug discovery. 2014;13(5):337-56.

20. Loosveld M, Castellano R, Gon S, Goubard A, Crouzet T, Pouyet L, et al. Therapeutic targeting of c-Myc in T-cell acute lymphoblastic leukemia, T-ALL. Oncotarget. 2014;5(10):3168-72.

21. Roderick JE, Tesell J, Shultz LD, Brehm MA, Greiner DL, Harris MH, et al. c-Myc inhibition prevents leukemia initiation in mice and impairs the growth of relapsed and induction failure pediatric T-ALL cells. Blood. 2014;123(7):1040-50.

22. King B, Trimarchi T, Reavie L, Xu L, Mullenders J, Ntziachristos P, et al. The ubiquitin ligase FBXW7 modulates leukemia-initiating cell activity by regulating MYC stability. Cell. 2013;153(7):1552-66.

23. Bonapace L, Bornhauser BC, Schmitz M, Cario G, Ziegler U, Niggli FK, et al. Induction of autophagy-dependent necroptosis is required for childhood acute lymphoblastic leukemia cells to overcome glucocorticoid resistance. J Clin Invest. 2010;120(4):1310-23.

24. Edgar R, Domrachev M, Lash AE. Gene Expression Omnibus: NCBI gene expression and hybridization array data repository. Nucleic Acids Res. 2002;30(1):207-10.

25. Yang X, Boehm JS, Yang X, Salehi-Ashtiani K, Hao T, Shen Y, et al. A public genome-scale lentiviral expression library of human ORFs. Nat Methods. 2011;8(8):659-61.

26. Meerbrey KL, Hu G, Kessler JD, Roarty K, Li MZ, Fang JE, et al. The pINDUCER lentiviral toolkit for inducible RNA interference in vitro and in vivo. Proc Natl Acad Sci U S A. 2011;108(9):3665-70.

27. Fischer U, Forster M, Rinaldi A, Risch T, Sungalee S, Warnatz HJ, et al. Genomics and drug profiling of fatal TCF3-HLF-positive acute lymphoblastic leukemia identifies recurrent mutation patterns and therapeutic options. Nat Genet. 2015;47(9):1020-9.

28. Berthon C, Raffoux E, Thomas X, Vey N, Gomez-Roca C, Yee K, et al. Bromodomain inhibitor OTX015 in patients with acute leukaemia: a dose-escalation, phase 1 study. Lancet Haematol. 2016;3(4):e186-95.

29. Amorim S, Stathis A, Gleeson M, Iyengar S, Magarotto V, Leleu X, et al. Bromodomain inhibitor OTX015 in patients with lymphoma or multiple myeloma: a dose-escalation, open-label, pharmacokinetic, phase 1 study. Lancet Haematol. 2016;3(4):e196-204.
30. Wallaert A, Durinck K, Van Loocke W, Van de Walle I, Matthijssens F, Volders PJ, et al. Long noncoding RNA signatures define oncogenic subtypes in T-cell acute lymphoblastic leukemia. Leukemia. 2016.
31. Souers AJ, Leverson JD, Boghaert ER, Ackler SL, Catron ND, Chen J, et al. ABT-199, a potent and selective BCL-2 inhibitor, achieves antitumor activity while sparing platelets. Nature medicine. 2013;19(2):202-8.
32. Del Gaizo Moore V, Brown JR, Certo M, Love TM, Novina CD, Letai A. Chronic lymphocytic leukemia requires BCL2 to sequester prodeath BIM, explaining sensitivity to BCL2 antagonist ABT-737. J Clin Invest. 2007;117(1):112-21.
33. Merino D, Khaw SL, Glaser SP, Anderson DJ, Belmont LD, Wong C, et al. Bcl-2, Bcl-x(L), and Bcl-w are not equivalent targets of ABT-737 and navitoclax (ABT-263) in lymphoid and leukemic cells. Blood. 2012;119(24):5807-16.
34. Khaw SL, Merino D, Anderson MA, Glaser SP, Bouillet P, Roberts AW, et al. Both leukaemic and normal peripheral B lymphoid cells are highly sensitive to the selective pharmacological inhibition of prosurvival Bcl-2 with ABT-199. Leukemia. 2014;28(6):1207-15.
35. Cang S, Iragavarapu C, Savooji J, Song Y, Liu D. ABT-199 (venetoclax) and BCL-2 inhibitors in clinical development. J Hematol Oncol. 2015;8:129.
36. Cervantes-Gomez F, Lamothe B, Woyach JA, Wierda WG, Keating MJ, Balakrishnan K, et al. Pharmacological and Protein Profiling Suggests Venetoclax (ABT-199) as Optimal Partner with Ibrutinib in Chronic Lymphocytic Leukemia. Clin Cancer Res. 2015;21(16):3705-15.
37. Chiron D, Dousset C, Brosseau C, Touzeau C, Maiga S, Moreau P, et al. Biological rational for sequential targeting of Bruton tyrosine kinase and Bcl-2 to overcome CD40-induced ABT-199 resistance in mantle cell lymphoma. Oncotarget. 2015;6(11):8750-9.

38. Zhao X, Bodo J, Sun D, Durkin L, Lin J, Smith MR, et al. Combination of ibrutinib with ABT-199: synergistic effects on proliferation inhibition and apoptosis in mantle cell lymphoma cells through perturbation of BTK, AKT and BCL2 pathways. Br J Haematol. 2015;168(5):765-8.

39. Ruvolo PP, Ruvolo VR, Benton CB, AlRawi A, Burks JK, Schober W, et al. Combination of galectin inhibitor GCS-100 and BH3 mimetics eliminates both p53 wild type and p53 null AML cells. Biochim Biophys Acta. 2016;1863(4):562-71.

40. Ham J, Costa C, Sano R, Lochmann TL, Sennott EM, Patel NU, et al. Exploitation of the Apoptosis-Primed State of MYCN-Amplified Neuroblastoma to Develop a Potent and Specific Targeted Therapy Combination. Cancer Cell. 2016;29(2):159-72.

41. Phillips DC, Xiao Y, Lam LT, Litvinovich E, Roberts-Rapp L, Souers AJ, et al. Loss in MCL-1 function sensitizes non-Hodgkin's lymphoma cell lines to the BCL-2-selective inhibitor venetoclax (ABT-199). Blood Cancer J. 2015;5:e368.

42. Choudhary GS, Tat TT, Misra S, Hill BT, Smith MR, Almasan A, et al. Cyclin E/Cdk2-dependent phosphorylation of Mcl-1 determines its stability and cellular sensitivity to BH3 mimetics. Oncotarget. 2015;6(19):16912-25.

43. Lee JS, Tang SS, Ortiz V, Vo TT, Fruman DA. MCL-1-independent mechanisms of synergy between dual PI3K/mTOR and BCL-2 inhibition in diffuse large B cell lymphoma. Oncotarget. 2015;6(34):35202-17.

44. Sun B, Shah B, Fiskus W, Qi J, Rajapakshe K, Coarfa C, et al. Synergistic activity of BET protein antagonist-based combinations in mantle cell lymphoma cells sensitive or resistant to ibrutinib. Blood. 2015;126(13):1565-74.

45. Cinar M, Rosenfelt F, Rokhsar S, Lopategui J, Pillai R, Cervania M, et al. Concurrent inhibition of MYC and BCL2 is a potentially effective treatment strategy for double hit and triple hit B-cell lymphomas. Leuk Res. 2015;39(7):730-8.

503 46. Johnson-Farley N, Veliz J, Bhagavathi S, Bertino JR. ABT-199, a BH3 mimetic that
504 specifically targets Bcl-2, enhances the antitumor activity of chemotherapy, bortezomib
505 and JQ1 in "double hit" lymphoma cells. Leuk Lymphoma. 2015;56(7):2146-52.
506 47. Certo M, Del Gaizo Moore V, Nishino M, Wei G, Korsmeyer S, Armstrong SA, et al.
507 Mitochondria primed by death signals determine cellular addiction to antiapoptotic BCL-
508 2 family members. Cancer Cell. 2006;9(5):351-65.
509 48. Bhadury J, Nilsson LM, Muralidharan SV, Green LC, Li Z, Gesner EM, et al. BET and HDAC
510 inhibitors induce similar genes and biological effects and synergize to kill in Myc-induced
511 murine lymphoma. Proc Natl Acad Sci U S A. 2014;111(26):E2721-30.
512 49. Bartholomeeusen K, Xiang Y, Fujinaga K, Peterlin BM. Bromodomain and extra-terminal
513 (BET) bromodomain inhibition activate transcription via transient release of positive
514 transcription elongation factor b (P-TEFb) from 7SK small nuclear ribonucleoprotein. J
515 Biol Chem. 2012;287(43):36609-16.
516 50. Hata AN, Engelman JA, Faber AC. The BCL2 Family: Key Mediators of the Apoptotic
517 Response to Targeted Anticancer Therapeutics. Cancer discovery. 2015;5(5):475-87.
518 51. Sun B, Shah B, Fiskus W, Qi J, Rajapakshe K, Coarfa C, et al. Synergistic activity of BET
519 protein antagonist-based combinations in mantle cell lymphoma cells sensitive or
520 resistant to ibrutinib. Blood. 2015.
521 52. Tinsley S, Meja K, Shepherd C, Khwaja A. Synergistic induction of cell death in
522 haematological malignancies by combined phosphoinositide-3-kinase and BET
523 bromodomain inhibition. Br J Haematol. 2015;170(2):275-8.
524 53. Patel AJ, Liao CP, Chen Z, Liu C, Wang Y, Le LQ. BET bromodomain inhibition triggers
525 apoptosis of NF1-associated malignant peripheral nerve sheath tumors through Bim
526 induction. Cell reports. 2014;6(1):81-92.
527 54. Li GQ, Guo WZ, Zhang Y, Seng JJ, Zhang HP, Ma XX, et al. Suppression of BRD4 inhibits
528 human hepatocellular carcinoma by repressing MYC and enhancing BIM expression.
529 Oncotarget. 2016;7(3):2462-74.
530

Figure Legends

Figure 1 Drug-screening platform to identify novel synergistic combinations of venetoclax and other drugs

(A) In a panel of primary T-ALL samples the effect of venetoclax treatment on cell viability was measured by flow cytometry using 7-AAD 72 hours after venetoclax treatment. Six representative samples (blue curves: sensitive to venetoclax; red curves: more resistant to venetoclax) were selected. For each sample, an optimal sub-lethal dose of venetoclax was calculated based on area under the curve (AUC) calculations of venetoclax as single agent. A single venetoclax dose was combined with selected clinically relevant compounds and the response change was compared to the control plate. Promising single compound combinations were validated in co-titration experiments.

(B) (i.) Scatterplots representing response of T-ALL samples (N=6) to venetoclax alone, shown as area under the curve (AUC). (ii.) Responses of T-ALL patient samples to combination of a sub-lethal venetoclax dose and indicated chemotherapeutic agents. AUC values of dose response curves from individual drug treatments (circles) or combined with venetoclax (triangles) are shown.

(C) Representative examples of co-titration assays for compounds found to synergize with venetoclax in preselected T-ALL samples from initial combination screening. (i) topoisomerase I inhibitor topotecan, (ii) dual PI3K and mTOR inhibitor dactolosib and (iii) BRD4 inhibitor JQ1.

Figure 2 *In vitro* synergism between venetoclax and JQ1 in primary patient samples and T-ALL cell lines

(A) Dose response curves are given for co-titration assays in primary T-ALL samples with increasing concentrations of both venetoclax and the BRD4 inhibitor JQ1. Combination

indices (CIs) indicate synergism for five of the six cases, and additive activity for the remaining sample.

(B) Overview of CIs between venetoclax and JQ1 in a panel of human T-ALL cell lines with indication of the degree of synergism. Mean and standard deviation of at least three independent experiments per cell line are represented. Western blot (bottom panel) indicates the BCL-2 protein levels in this cell line panel with β-actin as loading control.

(C) Scatterplot demonstrating the correlation between BCL-2 protein level and CI in the T-ALL cell lines.

Figure 3 Combination treatment of mice xenografted with luciferase-positive human LOUCY cells

(A) Leukemic burden was followed during the experiment on the basis of the luminescence of the leukemia cells. For each treatment group, one mouse is represented from day 0 (i.e. the day before the treatment started) till day 14 (i.e. the end of the experiment). The graph shows the average and standard deviation of the total flux of luminescence for all the mice in the group relative to the signal on day 0.

(B) Total flux of each mouse within a treatment group on day 14 relative to day 0.

(C) Percentage of hCD45+ leukemic cells in the peripheral blood for each mouse. All viable cells after red blood cell lysis were selected based on the forward and side scatter parameters. One sample from the control group could not be analyzed correctly.

(D) Percentage of hCD45+ leukemic cells in the bone marrow for each mouse. All the viable cells after red blood cell lysis were selected based on the forward and side scatter parameters.

The two-tailed Mann-Whitney test was used to compare the treatment groups statistically. ns not significant, * $P<0.05$, ** $P<0.01$, *** $P<0.001$. Horizontal lines on the graph indicate the median for each group.

Figure 4 Transcriptional effects of JQ1 on LOUCY

(A) Volcano plots displaying the differentially expressed genes in LOUCY after 4h of treatment with 250nM JQ1 (left) and 48h of treatment with 1µM JQ1 (right). In case multiple probes for one gene were present on the array, the differentially expressed probe with largest fold change was plotted.

(B) Hockey-stick plot showing the ranked H3K27Ac-seq signal of all enhancers in LOUCY. Super-enhancers are indicated with blue dots. The red dots are examples of enhancers associated with interesting downregulated genes upon JQ1 treatment.

(C) GSEA showing a significant enrichment of the genes associated with the top 500 super-enhancers in LOUCY among the downregulated genes after treatment with 250nM JQ1 for 4h (top) or 1µM JQ1 for 48h (bottom). The nearest TSS to each super-enhancer was determined via Peak Analyzer (OriginLab). This list of super-enhancer-associated genes was then used as a gene set for GSEA.

(D) GSEA showing a significant enrichment of gene sets containing upregulated genes after HDACi or UV treatment are among the upregulated genes after treatment of LOUCY with 250nM JQ1 for 4h. Left: DACOSTA_UV_RESPONSE_VIA_ERCC3_COMMON_UP, i.e. common up-regulated transcripts in fibroblasts expressing either XP/CS or TDD mutant forms of ERCC3 after UVC irradiation. Middle: DALESSIO_TSA_RESPONSE, i.e. top genes up-regulated in HEK293 cells in response to trichostatin A (TSA). Right: PEART_HDAC_PROLIFERATION_CLUSTER_UP, i.e. cell proliferation genes up-regulated by histone deacetylase (HDAC) inhibitors SAHA and depsipeptide.

Figure 5 Molecular insights in the mechanism of synergism

(A) The *BCL2L11* (coding for BIM)/*BCL2* mRNA ratio increases in synergistic T-ALL cell lines upon treatment with 1µM JQ1 for 48h. The average and standard deviation of the ratio of calibrated normalized relative quantities (CNRQ) from three independent experiments is

plotted. The two-tailed t test was used to compare the DMSO and JQ1 treatment. * P<0.05, ** P<0.01, *** P<0.001.

(B) Western blot showing the increase of the BIM/BCL-2 protein ratio in synergistic T-ALL cell lines upon treatment with 1µM JQ1 for 48h. Only the upper band of BIM was quantified.

(C) Immunoprecipitation with anti-BIM antibody illustrates the increased binding of BIM to BCL-2 after JQ1 treatment.

(D) Induction of BIM expression in KARPAS-45 pInducer21-BCL2L11 cells increases the sensitivity to venetoclax. The average and stdev from 3 independent experiments is plotted. Western blot shows BIM induction for 3 independent replicates. The doublet seen for BIM_{EL} (largest isoform) may represent phosphorylation.

Figure 1

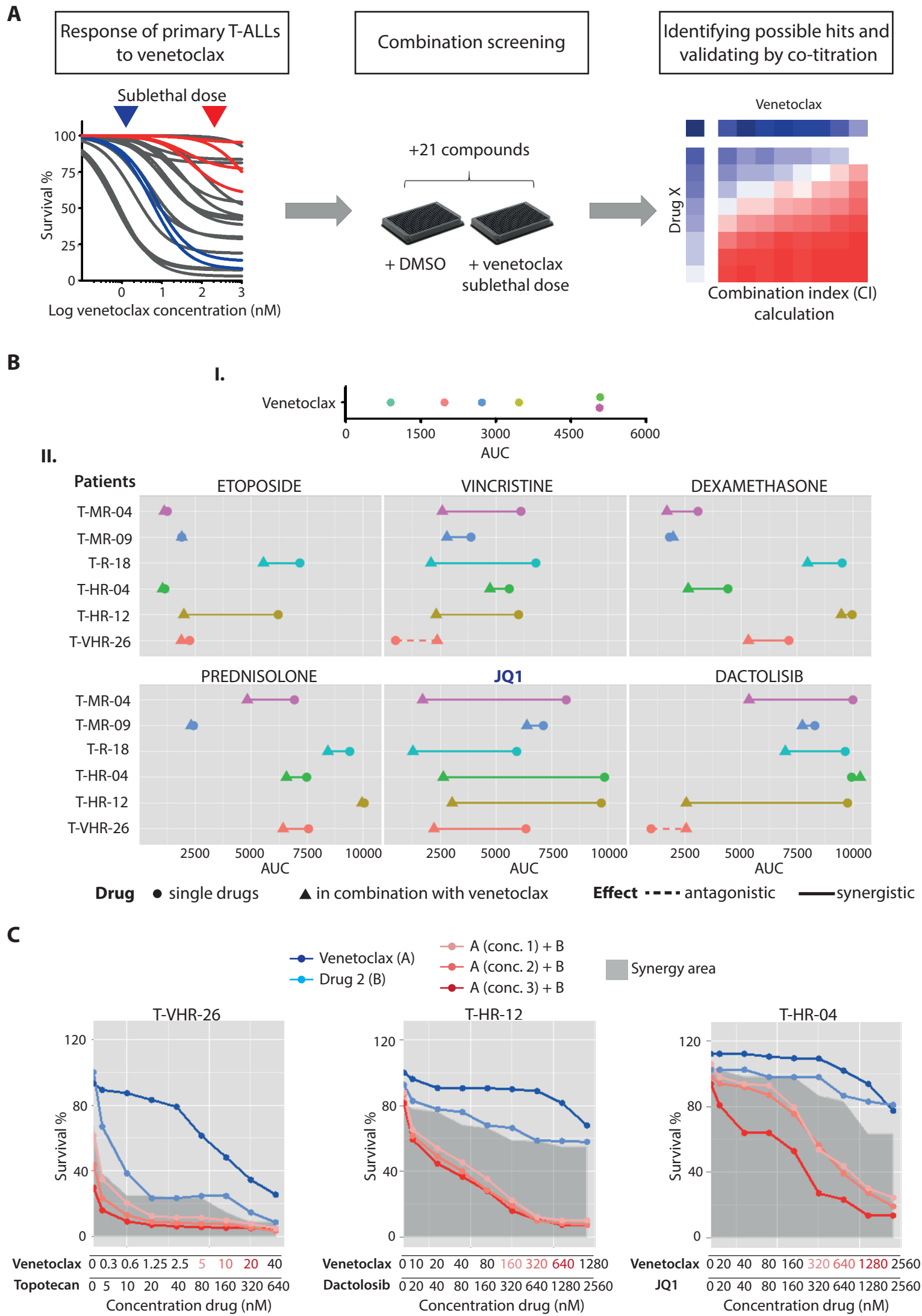
A
Response of primary T-ALLs to venetoclax
Combination screening
Identifying possible hits and validating by co-titration
Sublethal dose
Survival %
Log venetoclax concentration (nM)
+21 compounds
+ DMSO
+ venetoclax sublethal dose
Venetoclax
Drug X
Combination index (CI) calculation
B
I.
Venetoclax
AUC
II.
Patients
ETOPOSIDE
VINCRISTINE
DEXAMETHASONE
PREDNISOLONE
JQ1
DACTOLISIB
T-MR-04
T-MR-09
T-R-18
T-HR-04
T-HR-12
T-VHR-26
AUC
Drug ● single drugs ▲ in combination with venetoclax
Effect antagonistic synergistic
C
Venetoclax (A)
Drug 2 (B)
A (conc. 1) + B
A (conc. 2) + B
A (conc. 3) + B
Synergy area
T-VHR-26
T-HR-12
T-HR-04
Survival %
Venetoclax 0 0.3 0.6 1.25 2.5 5 10 20 40
Topotecan 0 5 10 20 40 80 160 320 640
Venetoclax 0 10 20 40 80 160 320 640 1280
Dactolosib 0 20 40 80 160 320 640 1280 2560
Venetoclax 0 20 40 80 160 320 640 1280 2560
JQ1 0 20 40 80 160 320 640 1280 2560
Concentration drug (nM)

Figure 2

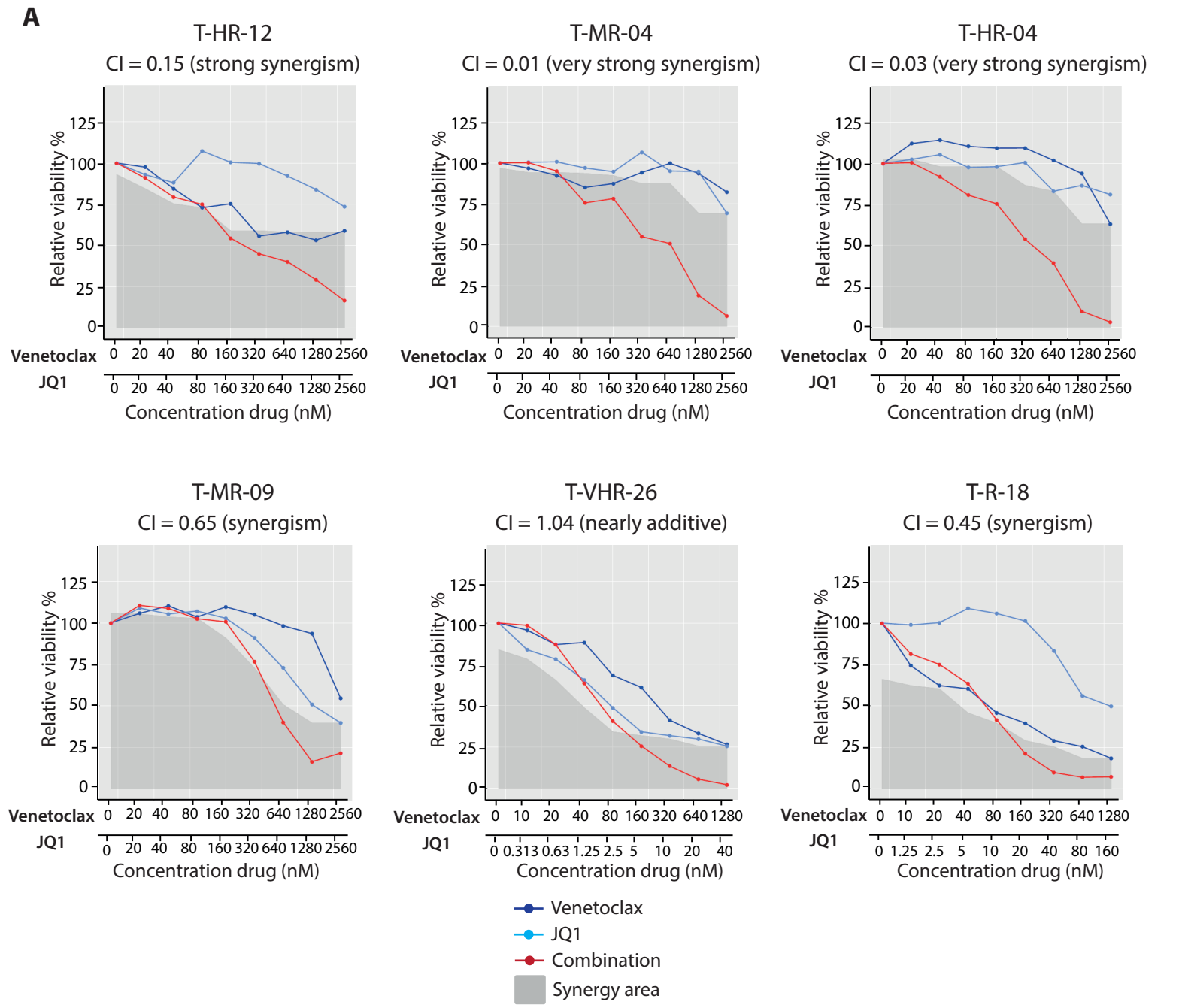
A
T-HR-12
CI = 0.15 (strong synergism)
T-MR-04
CI = 0.01 (very strong synergism)
T-HR-04
CI = 0.03 (very strong synergism)
T-MR-09
CI = 0.65 (synergism)
T-VHR-26
CI = 1.04 (nearly additive)
T-R-18
CI = 0.45 (synergism)
Relative viability %
Venetoclax
JQ1
Concentration drug (nM)
Venetoclax
JQ1
Combination
Synergy area

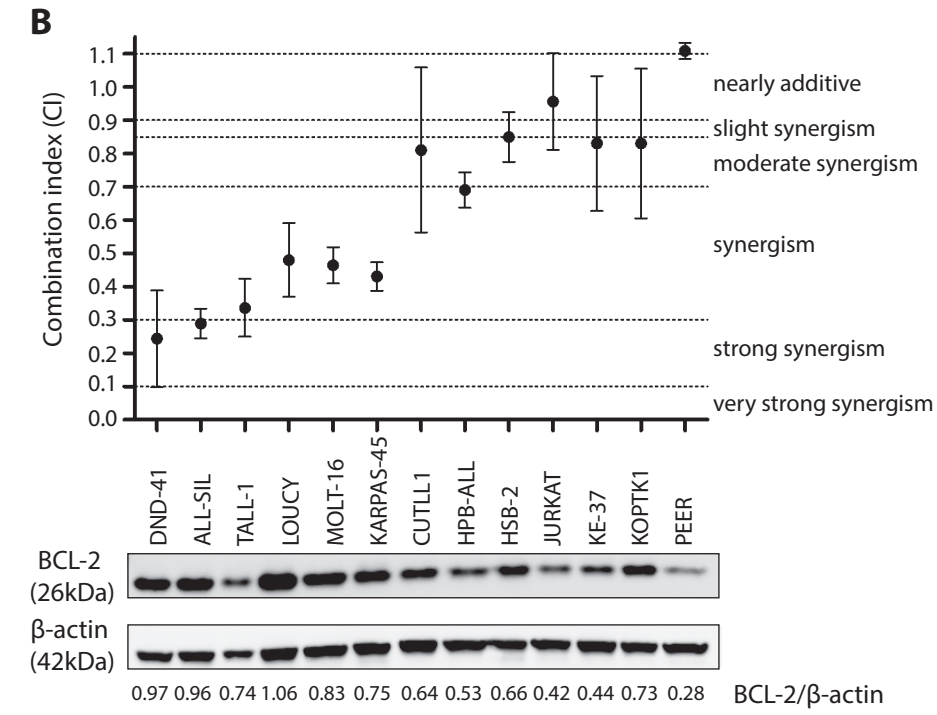
B
Combination index (CI)
nearly additive
slight synergism
moderate synergism
synergism
strong synergism
very strong synergism
DND-41
ALL-SIL
TALL-1
LOUCY
MOLT-16
KARPAS-45
CUTLL1
HPB-ALL
HSB-2
JURKAT
KE-37
KOPTK1
PEER
BCL-2 (26kDa)
β-actin (42kDa)
0.97 0.96 0.74 1.06 0.83 0.75 0.64 0.53 0.66 0.42 0.44 0.73 0.28
BCL-2/β-actin

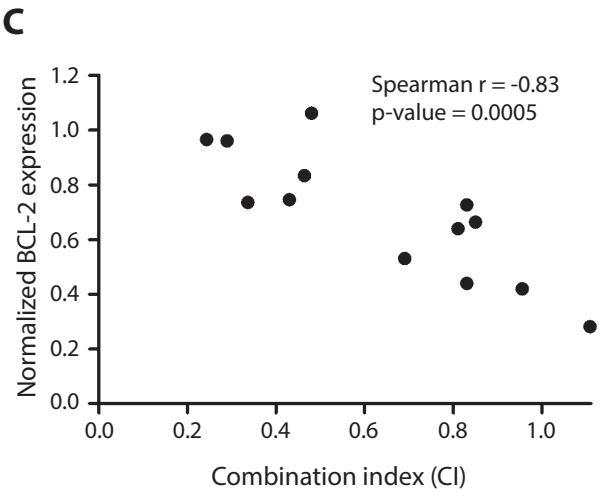
C
Normalized BCL-2 expression
Spearman r = -0.83
p-value = 0.0005
Combination index (CI)

Figure 3

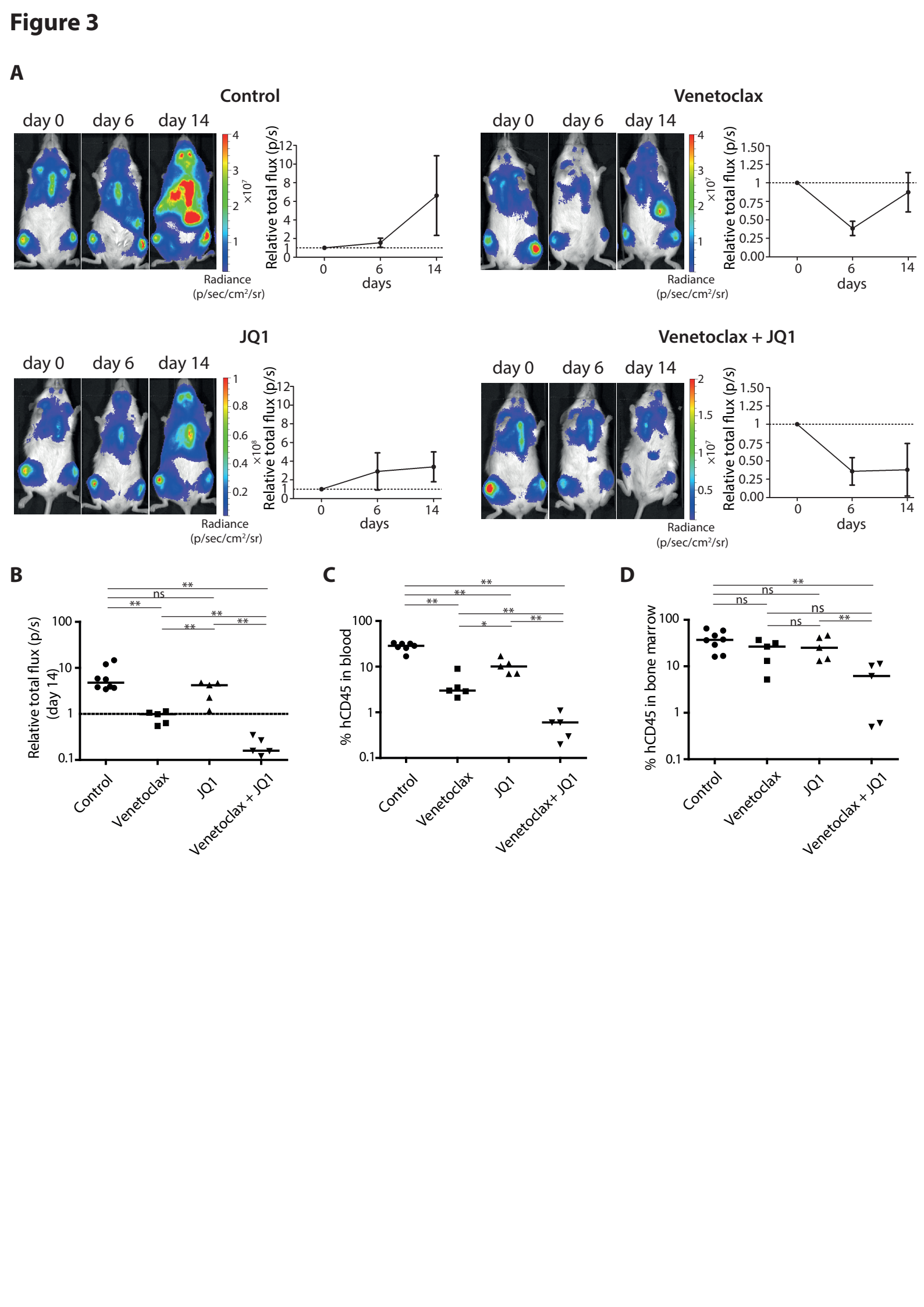
A
Control
day 0
day 6
day 14
Radiance (p/sec/cm²/sr)
Relative total flux (p/s)
days
Venetoclax
JQ1
Venetoclax + JQ1
B
Relative total flux (p/s) (day 14)
Control
Venetoclax
JQ1
Venetoclax + JQ1
C
% hCD45 in blood
Venetoclax+ JQ1
D
% hCD45 in bone marrow
ns

Figure 4

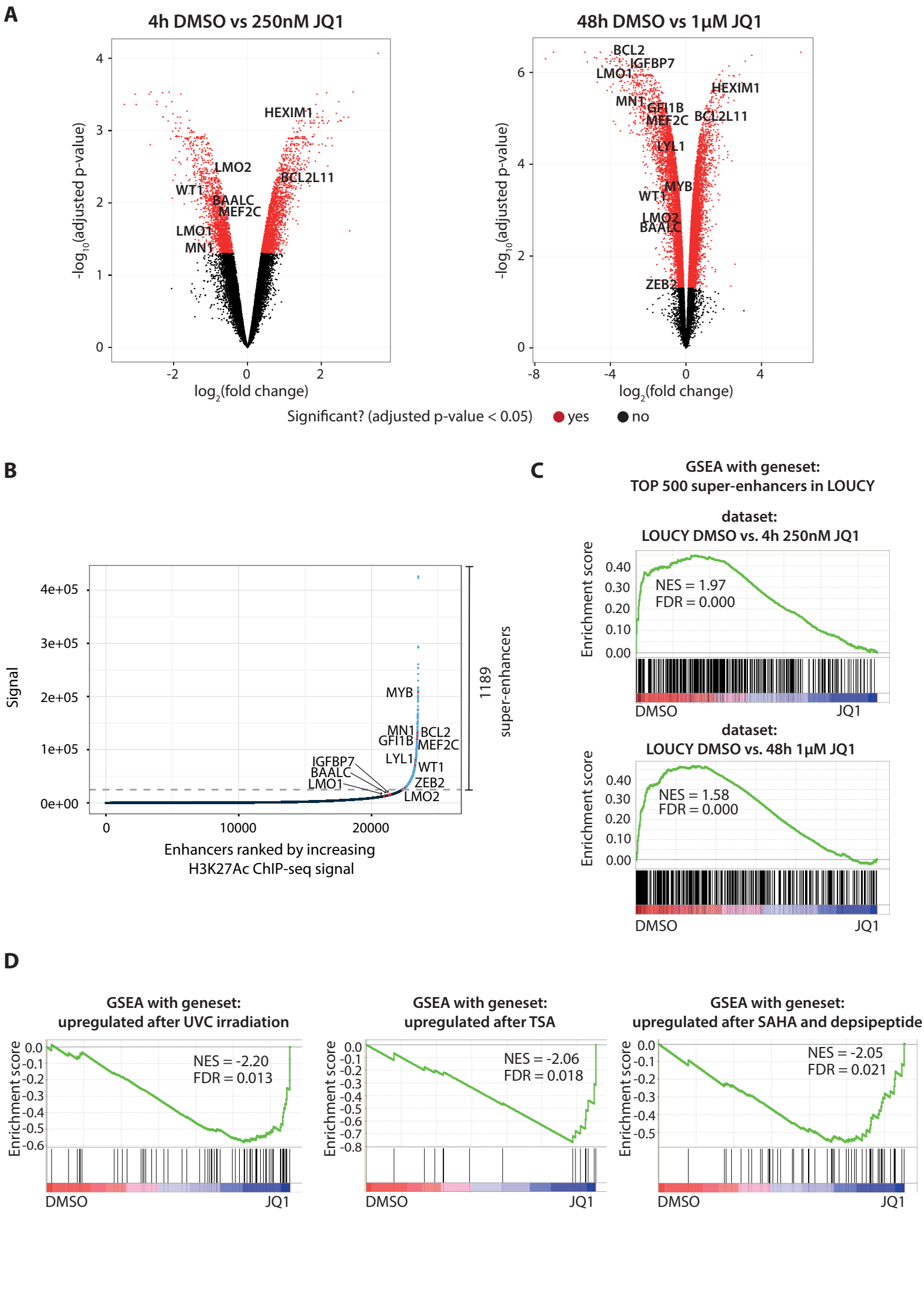
A
4h DMSO vs 250nM JQ1
48h DMSO vs 1µM JQ1
-log10(adjusted p-value)
log2(fold change)
HEXIM1
LMO2
BCL2L11
WT1
BAALC
MEF2C
LMO1
MN1
BCL2
IGFBP7
GFI1B
LYL1
MYB
ZEB2
Significant? (adjusted p-value < 0.05)
yes
no
B
Signal
Enhancers ranked by increasing
H3K27Ac ChIP-seq signal
1189
super-enhancers
C
GSEA with geneset:
TOP 500 super-enhancers in LOUCY
dataset:
LOUCY DMSO vs. 4h 250nM JQ1
Enrichment score
NES = 1.97
FDR = 0.000
DMSO
JQ1
dataset:
LOUCY DMSO vs. 48h 1µM JQ1
NES = 1.58
FDR = 0.000
D
GSEA with geneset:
upregulated after UVC irradiation
NES = -2.20
FDR = 0.013
GSEA with geneset:
upregulated after TSA
NES = -2.06
FDR = 0.018
GSEA with geneset:
upregulated after SAHA and depsipeptide
NES = -2.05
FDR = 0.021

Figure 5

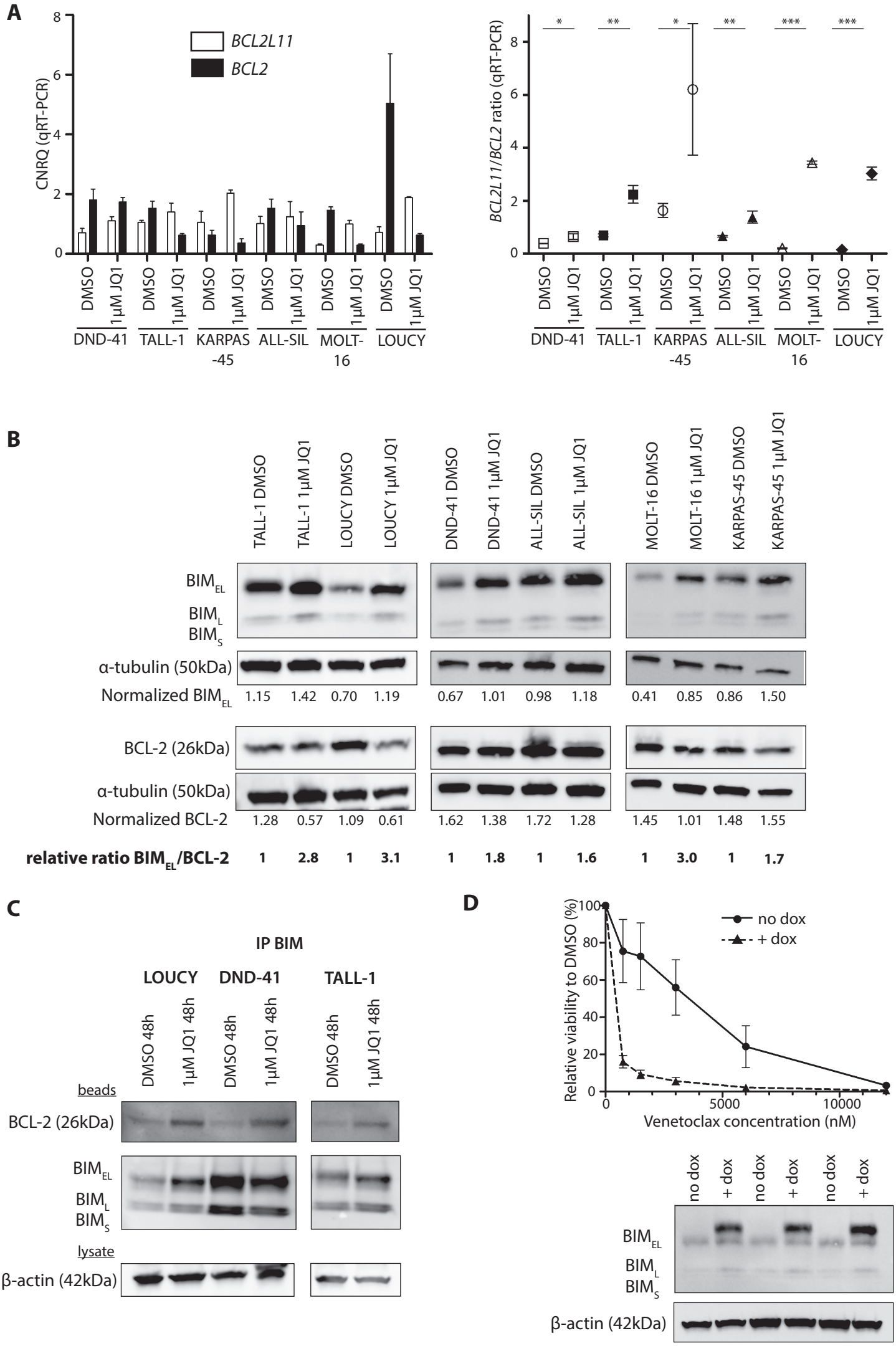
A
BCL2L11
BCL2
CNRQ (qRT-PCR)
BCL2L11/BCL2 ratio (qRT-PCR)
DMSO
1μM JQ1
DND-41
TALL-1
KARPAS -45
ALL-SIL
MOLT-16
LOUCY
B
TALL-1 DMSO
TALL-1 1μM JQ1
LOUCY DMSO
LOUCY 1μM JQ1
DND-41 DMSO
DND-41 1μM JQ1
ALL-SIL DMSO
ALL-SIL 1μM JQ1
MOLT-16 DMSO
MOLT-16 1μM JQ1
KARPAS-45 DMSO
KARPAS-45 1μM JQ1
BIM_EL
BIM_L
BIM_S
α-tubulin (50kDa)
Normalized BIM_EL
1.15 1.42 0.70 1.19
0.67 1.01 0.98 1.18
0.41 0.85 0.86 1.50
BCL-2 (26kDa)
α-tubulin (50kDa)
Normalized BCL-2
1.28 0.57 1.09 0.61
1.62 1.38 1.72 1.28
1.45 1.01 1.48 1.55
relative ratio BIM_EL/BCL-2
1 2.8 1 3.1
1 1.8 1 1.6
1 3.0 1 1.7
C
IP BIM
LOUCY
DND-41
TALL-1
DMSO 48h
1μM JQ1 48h
beads
BCL-2 (26kDa)
BIM_EL
BIM_L
BIM_S
lysate
β-actin (42kDa)
D
no dox
+ dox
Relative viability to DMSO (%)
Venetoclax concentration (nM)
β-actin (42kDa)

Personalized Medicine and Imaging

Clinical Cancer Research

Cell and Molecular Determinants of *In Vivo* Efficacy of the BH3 Mimetic ABT-263 against Pediatric Acute Lymphoblastic Leukemia Xenografts

Santi Suryani[1], Hernan Carol[1], Triona Ni Chonghaile[2], Viktoras Frismantas[3], Chintanu Sarmah[1], Laura High[1], Beat Bornhauser[3], Mark J. Cowley[4], Barbara Szymanska[1], Kathryn Evans[1], Ingrid Boehm[1], Elise Tonna[1], Luke Jones[1], Donya Moradi Manesh[1], Raushan T. Kurmasheva[5], Catherine Billups[6], Warren Kaplan[4], Anthony Letai[2], Jean-Pierre Bourquin[3], Peter J. Houghton[5], Malcolm A. Smith[7], and Richard B. Lock[1]

Abstract

Purpose: Predictive biomarkers are required to identify patients who may benefit from the use of BH3 mimetics such as ABT-263. This study investigated the efficacy of ABT-263 against a panel of patient-derived pediatric acute lymphoblastic leukemia (ALL) xenografts and utilized cell and molecular approaches to identify biomarkers that predict *in vivo* ABT-263 sensitivity.

Experimental Design: The *in vivo* efficacy of ABT-263 was tested against a panel of 31 patient-derived ALL xenografts composed of MLL-, BCP-, and T-ALL subtypes. Basal gene expression profiles of ALL xenografts were analyzed and confirmed by quantitative RT-PCR, protein expression and BH3 profiling. An *in vitro* coculture assay with immortalized human mesenchymal cells was utilized to build a predictive model of *in vivo* ABT-263 sensitivity.

Results: ABT-263 demonstrated impressive activity against pediatric ALL xenografts, with 19 of 31 achieving objective responses. Among *BCL2* family members, *in vivo* ABT-263 sensitivity correlated best with low *MCL1* mRNA expression levels. BH3 profiling revealed that resistance to ABT-263 correlated with mitochondrial priming by NOXA peptide, suggesting a functional role for MCL1 protein. Using an *in vitro* coculture assay, a predictive model of *in vivo* ABT-263 sensitivity was built. Testing this model against 11 xenografts predicted *in vivo* ABT-263 responses with high sensitivity (50%) and specificity (100%).

Conclusion: These results highlight the *in vivo* efficacy of ABT-263 against a broad range of pediatric ALL subtypes and shows that a combination of *in vitro* functional assays can be used to predict its *in vivo* efficacy. *Clin Cancer Res; 20(17); 4520–31. ©2014 AACR.*

Introduction

Despite significant improvements in the treatment of childhood acute lymphoblastic leukemia (ALL) over the past 5 decades, curing those patients who relapse with this most common pediatric malignancy remains a significant challenge (1). These relapse cases are often associated with broad-range drug resistance (2), which remains a significant problem, thus highlighting the need to develop new therapies. Because evasion of apoptosis is recognized as one of the hallmarks of cancer (3), recent drug development has focused on targeting key components of the apoptosis signaling pathway (4). The BCL2 family of proteins includes key regulators of the intrinsic apoptosis pathway, with cell fate being determined by the balance of prosurvival (e.g., BCL2 and MCL1) and proapoptotic (e.g., PUMA, NOXA) members (5, 6).

BH3-mimetic drugs, such as ABT-737 and its orally available analog ABT-263, were specifically designed to inhibit prosurvival BCL2 family proteins (7). Although these drugs bind with high affinity to BCL2, BCLW, and BCLXL, they exhibit lower affinity for MCL1 and A1 (7, 8). ABT-737 and ABT-263 have shown significant *in vivo* efficacy in preclinical xenograft models of hematolymphoid and solid malignancies (9, 10). Although clinical trials of ABT-263 in adults

[1]Children's Cancer Institute Australia for Medical Research, Lowy Cancer Research Centre, UNSW, Sydney, Australia. [2]Department of Medical Oncology, Dana-Farber Cancer Institute, Boston, Massachusetts. [3]Division of Pediatric Oncology, University Children's Hospital, Zurich, Switzerland. [4]Peter Wills Bioinformatics Centre, Garvan Institute of Medical Research, Darlinghurst, Australia. [5]Center for Childhood Cancer, Nationwide Children's Hospital, Columbus, Ohio. [6]Department of Biostatistics, St. Jude Children's Research Hospital, Memphis, Tennessee. [7]Cancer Therapy Evaluation Program, NCI, Bethesda, Maryland.

Note: Supplementary data for this article are available at Clinical Cancer Research Online (http://clincancerres.aacrjournals.org/).

S. Suryani and H. Carol contributed equally to this article.

Corresponding Author: Richard B. Lock, Children's Cancer Institute Australia for Medical Research, Lowy Cancer Research Centre, UNSW, P.O. Box 81, Randwick NSW 2031, Australia. Phone: 1800-685-686; Fax: 61-2-9662-6583; E-mail: rlock@ccia.unsw.edu.au

doi: 10.1158/1078-0432.CCR-14-0259

Translational Relevance

Manipulation of the apoptosis pathway is an appealing strategy for cancer treatment using BH3 mimetics such as ABT-263, although predictive biomarkers are required to identify patients who may benefit from their use. This study showed that ABT-263 exhibited broad *in vivo* efficacy against preclinical xenograft models of pediatric acute lymphoblastic leukemia (ALL). High *MCL1* expression, at the mRNA and protein level, correlated with *in vivo* ABT-263 resistance, which was confirmed functionally by BH3 profiling. In addition, *in vitro* coculture assays predicted *in vivo* ABT-263 responses with high sensitivity and specificity. Therefore, a combination of functional assays could be used to predict ABT-263 activity *in vivo*. Given the strong efficacy of ABT-263 against a significant proportion of xenografts tested, these in-principle approaches could be included in the design of prospective clinical trials to determine if they can identify patients who may respond to treatment with this class of therapeutic agents.

have shown promising results (11–13), the main dose-limiting toxicity of thrombocytopenia has hindered its progression into pediatric patients.

Consistent with the low affinity of ABT-737 and ABT-263 for MCL1, several reports have shown an inverse correlation of MCL1 expression with sensitivity to these drugs (14–16). Other proteins in the BCL2 family have also been implicated in determining sensitivity or resistance. For example, high BCL2 expression was associated with increased ABT-737 sensitivity in Non-Hodgkin's lymphoma (NHL) cell lines and in murine fetal liver cells (15). However, recent studies provided evidence that MCL1 or prosurvival protein expression levels contribute to, but are not sufficient determinants of, resistance (17–20). Disruption of the interaction between MCL1 and BAK increased drug sensitivity (17, 18), suggesting that protein–protein interactions, rather than absolute levels, play a critical role in determining the sensitivity to BH3 mimetics. This interpretation was reinforced by "mitochondrial BH3 profiling," which utilizes a panel of peptides derived from BH3-domains and their binding to antiapoptotic proteins, to predict a cell's susceptibility to apoptosis induction (19, 20). Mitochondrial sensitivity to the BAD BH3 peptide, which has a pattern of interaction with antiapoptotic proteins similar to ABT-737 and ABT-263, was shown to predict *in vitro* ABT-737 sensitivity in small cell lung cancer, lymphoma, ALL, and acute myelogenous leukemia cell lines (19). Clinical responses to conventional chemotherapy in acute leukemia, multiple myeloma, and ovarian cancer instead were found to correlate with mitochondrial sensitivity with promiscuous interacting BH3 peptides such as Puma BH3 (20).

The Pediatric Preclinical Testing Program previously reported that ABT-263 was effective as a single agent against *in vivo* models of childhood cancer, and in particular pediatric ALL xenografts (10). The results suggested preferential efficacy against 2 T-cell ALL (T-ALL) in comparison to B-cell precursor (BCP)-ALL xenografts, albeit testing against a small panel of xenografts. In this study, we tested the *in vivo* efficacy of ABT-263 against a diverse panel of 31 molecularly characterized xenografts derived from T-ALL, BCP-ALL, and infant ALL with translocations of the mixed lineage leukemia (*MLL*) gene (infant MLL-ALL), as well as the efficacy of ABT-263 in combination with established drugs. To identify determinants of *in vivo* ABT-263 response, we then correlated gene expression profiles, mitochondrial BH3 profiling and *in vitro* ABT-263 sensitivity with single-agent ABT-263 efficacy. This powerful approach can be used as proof-of-principle to identify determinants of *in vivo* responses to other novel antileukemic drugs.

Materials and Methods

Xenografts and *in vivo* drug treatments

All experimental studies were conducted with approval from the Animal Care and Ethics Committee of the University of New South Wales (Sydney, Australia). Procedures by which we established continuous xenografts from childhood ALL biopsies in immune-deficient NOD/SCID (NOD.CB17-Prkdc^{scid}/SzJ) or NOD/SCID, IL2 receptor γ negative (NOD.Cg-Prkdc^{scid} Il2rg^{tm1Wjl}/SzJ, NSG) mice, and tested their *in vivo* ABT-263 responses, have been described in detail previously (10, 21, 22). ALL subtypes were categorized at biopsy by their immunophenotype. Xenografts are available from the corresponding author upon request. ABT-263 (obtained from AbbVie under a standard Material Transfer Agreement) was administered orally at a dose of 100 mg/kg, daily for 21 days, as previously described (10). ABT-263 was also administered in combination with the conventional chemotherapeutic drugs vincristine (Baxter Healthcare; 1 mg/kg, days 0 and 7), dexamethasone (Sigma-Aldrich; 15 mg/kg, Mon–Fri × 2 weeks) or L-asparaginase (Aventis; 1,500 U/kg, Mon-Fri × 2 weeks) on a Mon to Fri × 2-week schedule at least 1 hour after administration of the established drug. It was necessary to attenuate the dose of ABT-263 to 25 mg/kg when combined with vincristine, and to 50 mg/kg when combined with dexamethasone and L-asparaginase in order to achieve a tolerable dose.

Leukemia engraftment and progression were assessed in groups of 6 to 10 female mice each of 20 to 25 g by weekly enumeration of the proportion of human CD45$^+$ cells in the peripheral blood (%huCD45$^+$; ref. 22). Individual mouse event-free survival (EFS) was calculated as the days from treatment initiation until the %huCD45$^+$ reached 25%. EFS was represented graphically by Kaplan–Meier analysis. The efficacy of drug treatment was evaluated by leukemia growth delay (LGD), calculated as the difference between the median EFS of vehicle control and drug-treated cohorts, as well as an objective response measure (ORM), modeled after stringent clinical criteria as described previously (21). Detailed methodology is presented in the Supplementary Methods and Table S1. Responses were also

expressed in a "COMPARE-like" format, which combines EFS and ORMs around the midpoint (0) representative of SD. Bars to the right or left of the midpoint represent objective responses or nonobjective responses, respectively. Significant and nonsignificant differences in EFS distribution between control and treated cohorts are represented by solid or dotted bars, respectively. Xenografts were excluded from analysis if >25% of mice within a cohort experienced nonleukemia-related toxicity or morbidity. Mice were excluded from the study if they developed spontaneous murine lymphomas.

To evaluate interactions between drugs *in vivo*, therapeutic enhancement was considered if the EFS of mice treated with the drug combination was significantly greater than those induced by both single agents used at their maximum tolerated doses (23, 24).

Protein expression

Preparation of extracts from xenograft cells previously harvested from the spleens of engrafted mice, determination of protein concentrations, and analysis of cellular proteins by immunoblotting have been described in detail elsewhere (25). Membranes were probed with anti-MCL1 (Genesearch) and anti-actin antibodies (Sigma-Aldrich) followed by horseradish peroxidase (HRP)—conjugated secondary antibody (GE Healthcare). Signal was detected by Immobilon Western Chemiluminescent HRP Substrate (Merck Millipore) and visualized using a VersaDoc 5000 Imaging System (Bio-Rad). Data were analyzed with QuantityOne software (Version 4.00; Bio-Rad).

RNA extraction, real-time quantitative reverse transcription PCR and gene expression analysis

Total RNA was extracted from xenograft cells, previously harvested from the spleens of engrafted mice and cryopreserved, using a combination of TRizol (Invitrogen) and Qiagen RNeasy Kit. RNA was purified with QIAGEN RNeasy spin columns, according to the manufacturer's protocol. RNA purity was considered acceptable if the ratio of $OD_{260/280}$ was between 1.8 and 2.0. For use in microarrays, the RNA integrity number was determined using an Agilent Bioanalyzer and considered acceptable if >7.

Real-time quantitative reverse transcription PCR (RT-qPCR) was carried out using standard techniques. First-strand cDNA was synthesized using 2 μg of total RNA, random primers (Roche), and M-MLV Reverse Transcriptase (Invitrogen). Primers and probes for *MCL1* were purchased from Life Technologies (Hs03043899_m1). Quantitative real-time PCR analysis was carried out in triplicate under the following cycling conditions: 50°C for 2 minutes and 95°C for 10 minutes, followed by 40 cycles of 95°C for 15 seconds and 60°C for 1 minute. Elongation factor-1α (*EF1α*) was used as an internal normalization standard in each reaction (primers EF1αF, 5′-CTGAACCATCCAGGCCAAAT-3′; EF1αR, 5′-GCCGTGTGGCAATCCAAT-3′; probe, 5′-VIC-AGCGCCGGCTATGCCCCTG-TAMRA-3′).

RNA samples were used to prepare cRNA with Illumina TotalPrep RNA Amplification Kit (Life Technologies). cRNA was then hybridized to Illumina Human Beadchip HT12 Arrays. Gene expression datasets were analyzed using GenePattern v3.2.3 as we have previously described (26). Gene expression datasets can be accessed at www.ncbi.nlm.nih.gov/geo (Accession No. GSE52991; reviewer's access: http://www.ncbi.nlm.nih.gov/geo/query/acc.cgi?token=glwjgwusrnadfsr&acc=GSE52991). Benjamini and Hochberg false discovery rate (FDR; ref. 27) measurement and Smyth unadjusted *P* value (28) were used for evaluation of differential gene expression. Gene expression heatmaps were generated using GenePattern, whereby the range of color coding extends from minimum to maximum values per gene (per row). In each case, red indicates high, and blue low, level of expression. Unsupervised hierarchical clustering was performed using the Hierarchical Clustering module in GenePattern using the entire 47,323 probes representative of 34,694 genes present in the Illumina Human Beadchip HT-12 Arrays.

Assessment of mitochondrial priming by BH3 profiling

Xenograft cells permeabilized by digitonin were exposed to BH3 peptides derived from BAD, NOXA, and PUMA proteins, and mitochondrial depolarization measured using the fluorescent dye JC-1, as we have previously described (20). Comparison of mitochondrial depolarization of nonresponders versus responders was performed using a *t* test (unpaired, 2-tailed).

***In vitro* cytotoxicity assays**

The *in vitro* sensitivity of xenograft cells to ABT-263 was assessed by coculture using *hTERT*-immortalized primary bone marrow mesenchymal stromal cells (hTERT-MSC), as described previously (29) and detailed in the Supplementary Methods. Briefly, hTERT-MSCs were seeded at 2,000 cells/well in a 384-well plate (Greiner) in serum-free medium (AIM-V; Life Technologies). After 24 hours, 20,000 viable leukemia cells and ABT-263 were added to final concentrations of 1, 2.5, 5, 10, 25, 50, 100 and 1,000 nmol/L in duplicate. After 72 hours of incubation live-cell numbers were determined using 7-AAD analyses by flow cytometry (BD FACSCantoII). Data were normalized using SPHERO AccuCount Particles. Examples of flow cytometry analysis are included in Supplementary Fig. S1. To build a predictive model of *in vivo* ABT-263 sensitivity, we used upper and lower limits of the 95% confidence intervals of the proportion of live cells after exposure to 10 nmol/L of ABT-263 *in vitro*.

Statistical analysis

EFS curves were compared by the log-rank test. Differences in responses to single-agent ABT-263 *in vivo* between MLL-ALL, BCP-ALL, and T-ALL xenografts were evaluated using one-way ANOVA and a Tukey multiple comparison analysis as well as χ^2 test. A Pearson correlation test was utilized for all datasets with normal distribution, which included gene expression analysis versus LGD, and *MCL1* Illumina mRNA versus *MCL1* RT-qPCR mRNA levels. A Spearman correlation test was used to compare *MCL1*

RT-qPCR mRNA versus protein expression. Comparison of *MCL1* RT-qPCR mRNA and protein levels between non-responders and responders was performed using a Mann–Whitney test. Significance was inferred from tests with *P* values lower than 0.05.

Results

Gene expression profiles of ALL xenografts reflect the primary disease

To identify cell and molecular determinants of *in vivo* ABT-263 responses in pediatric ALL, panels of a total of 31 xenografts were established from direct patient explants representative of MLL-ALL (8 infant MLL-ALLs and 1 pediatric MLL-ALL, ALL-3), BCP-ALL ($n = 7$), and T-ALL ($n = 15$) and were characterized by gene expression profiling. The patient demographics focused on high-risk or poor outcome cases: infant MLL-ALL is a known high-risk ALL subtype; the T-ALL panel included 3 xenografts derived from patients with early T-cell precursor (ETP) ALL (ETP-1, ETP-2, and ETP-3), a very high-risk subgroup (30); the BCP-ALL and non-ETP T-ALL panels included 4 of 7 and 9 of 12 patients, respectively, who had relapsed and/or died from their disease (22, 30, 31). More detailed descriptions of the infant MLL-ALL and expanded T-ALL xenograft panels will be reported elsewhere. Chromosomal translocations in the original biopsy sample, where known, are summarized in Supplementary Table S2.

Unsupervised hierarchical clustering of xenograft basal gene expression profiles revealed 3 distinct branches reflecting each leukemia subtype (Fig. 1A). The MLL-ALL and BCP-ALL panels seemed more closely related and distinct from the T-ALL xenografts. Xenograft ALL-3 was originally classified by immunophenotype as a BCP-ALL but clustered with the MLL-ALLs. Upon further investigation it was confirmed that ALL-3 harbors an *MLL* gene rearrangement (Supplementary Table S2). The 4 MLL-ALLs with translocations involving chromosome 19 (MLL-6, MLL-8, MLL-14, and ALL-3) clustered separately from 2 MLL-ALLs with chromosome 4 translocations (MLL-2 and MLL-7; Fig. 1A and Supplementary Table S2). The 3 ETP-ALLs, while not clustering as a separate branch, did cluster within the T-ALL panel (Fig. 1A).

We next identified subtype-specific differentially expressed genes using the LimmaGP (Cowley and colleagues, manuscript in preparation) module in GenePattern, whereby each subtype was compared with the remaining 2 ALL subtypes (1 vs. rest comparison). Subtype-specific genes were determined with a cut-off value of FDR < 0.05. At this level of stringency, there were 2,141 MLL-ALL specific genes, 643 BCP-ALL specific genes, and 18,692 T-ALL specific genes (Supplementary Table S3). The top 25 differentially expressed probesets between each xenograft panel included previously identified subtype-specific genes, such as *MEIS1*, *ZNF827*, and *CCNA1* in MLL-ALL (32), *MME* (CD10) in BCP-ALL, and components of the CD3 receptor (*CD3D*, *CD3E*, *CD3G*, and *CD247*), *CD2* and *SH2D1A* in T-ALL (ref. 33; Fig. 1B). ALL subtype-specific genesets were identified using GSEA preranked module in GenePattern with FDR < 0.05 (Supplementary Table S4). For MLL-ALL, the top 4 genesets reflected MLL-specific genesets, for BCP-ALL, 9 B-cell–specific genesets were identified within the top 30 genesets and for T-ALL, 6 T-cell–specific genesets were identified within the top 10 genesets. Therefore, these analyses confirmed the xenograft subtype classification according to the primary disease.

ABT-263 exhibits single-agent *in vivo* efficacy against a broad range of pediatric ALL subtypes

We previously reported the results of *in vivo* ABT-263 testing against a panel of 6 ALL xenografts, with higher sensitivity observed in 2 T-ALL compared with 4 BCP-ALL xenografts (10). To further investigate this possible subtype-specific *in vivo* efficacy of ABT-263 against pediatric ALL, we expanded the analysis to the 31 xenografts described above. ABT-263 significantly delayed the progression of 29 of 31 xenografts tested (Table 1, Fig. 2A–C, and Supplementary Figs. S2–S4). LGDs ranged from 0.5 (ALL-2; $P = 0.46$) to 78 (ALL-31; $P = 0.0008$) days. When stratified according to ALL subtype the median LGDs were 17.9 days for MLL (range 3.1–53.7), 25.8 days for BCP-ALL (range 0.5–37.9), and 29.6 days for T-ALL (range 4.0–78; Fig. 2D and Table 1). There was no significant differential efficacy of ABT-263 against any of the 3 ALL subtypes.

ABT-263 elicited objective responses in 19 of 31 xenografts, with 3 MCRs, 11 CRs, and 5 PRs (Table 1 and Fig. 2). Figure 2E represents the *in vivo* ABT-263 responses of each xenograft panel in a "COMPARE-like" format. In agreement with the LGD data, no significant differences were observed between the ALL subtypes.

We previously showed that the *in vivo* sensitivity of a subset of these xenografts to an induction-type regiment of vincristine, dexamethasone, and L-asparaginase (VXL) correlated with the clinical outcome of the patients from whom the xenografts were derived (34). However, the *in vivo* ABT-263 sensitivity of the same subset of xenografts did not correlate with their VXL responses ($R = 0.46$, $P = 0.18$; Supplementary Fig. S5), indicating that ABT-263 can exert significant *in vivo* efficacy against ALL xenografts that are resistant to established drugs.

A complete summary of results is provided in Supplementary Figs. S2 to S4 and Table S5, including total numbers of mice, number of mice that died (or were otherwise excluded), numbers of mice with events and average times to events, LGD values, as well as numbers in each of the ORM categories and "treated over controls" (*T*/*C*) values.

MCL1 gene expression correlates with *in vivo* ABT-263 sensitivity in ALL xenografts

We next analyzed basal *BCL2* family gene expression levels in relation to *in vivo* ABT-263 sensitivity across the 31 xenografts using 2 approaches. Both approaches were applied to the entire xenograft cohort as well as all 3 subtypes separately. The first approach assessed the correlation between gene expression and progression delay (LGD; Pearson product moment correlation coefficient), with a positive correlation denoting genes whose higher

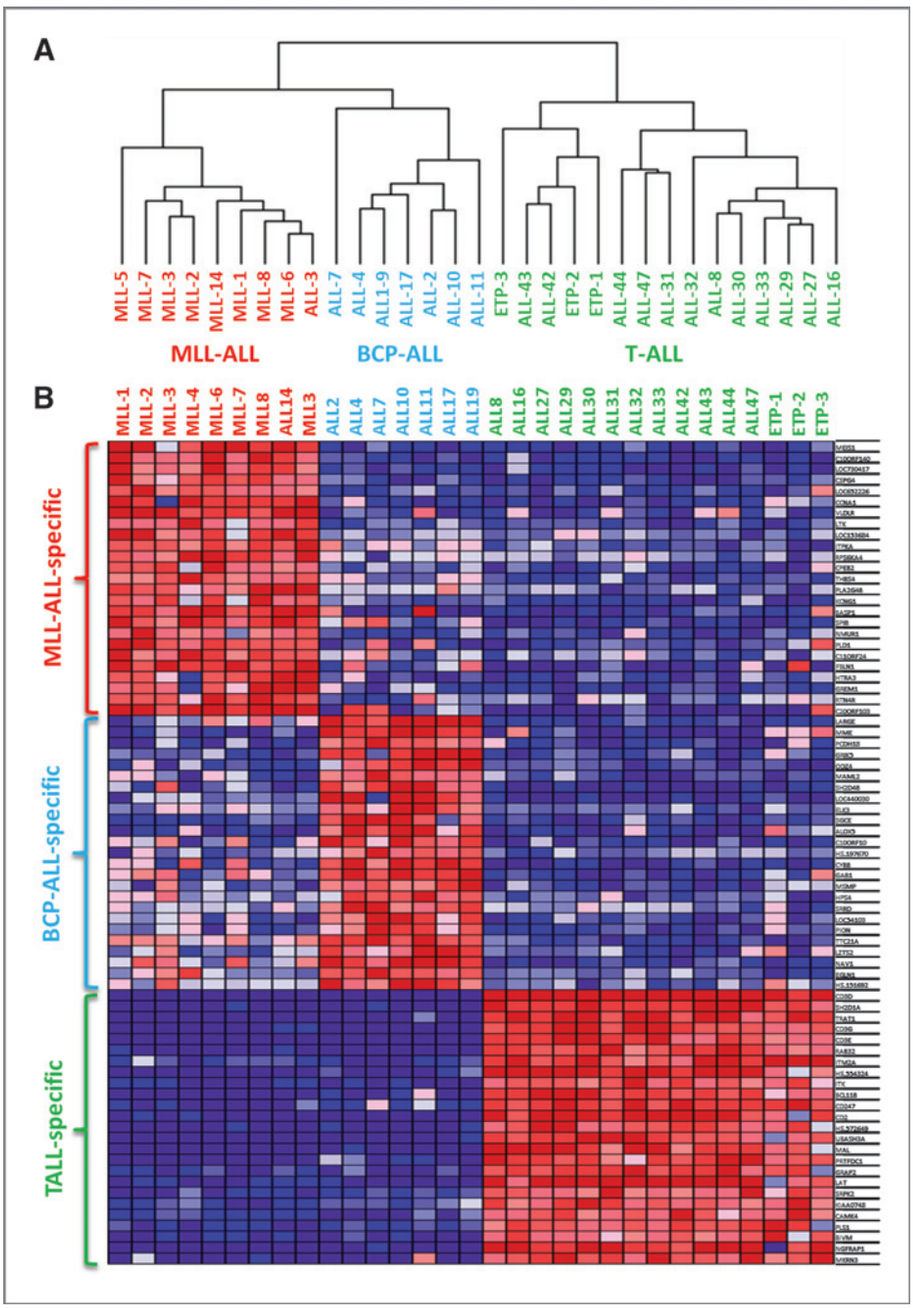

Figure 1. Comparison of MLL-ALL, BCP-ALL, and T-ALL xenografts by gene expression profiling. A total of 31 ALL xenografts (MLL-ALL, $n = 9$; BCP-ALL, $n = 7$; T-ALL, $n = 15$) were profiled on Illumina Human HT-12 Beadchip arrays. A, nonsupervised hierarchical clustering of all xenografts. B, heatmap of the top 25 upregulated genes that were specific to MLL-ALL, BCP-ALL, and T-ALL subtypes ordered according to their *P* value. The colors in the heatmaps represent the relative expression per gene across all samples. Red indicates relative high expression and blue indicates relative low expression.

expression was associated with ABT-263 sensitivity, and *vice versa*. Using this approach, *MCL1* expression correlated significantly with *in vivo* ABT-263 sensitivity across the entire xenograft panel ($R = -0.43$, $P = 0.015$; Fig. 3A), indicating that high *MCL1* expression was associated with *in vivo* resistance. *BCLXL/XS* ($R = 0.79$, $P = 0.01$) and *BCLW* ($R = 0.69$, $P = 0.039$) showed significant positive correlations between expression and drug sensitivity in the MLL-ALL panel (Supplementary Fig. S6 and Table S6). In contrast, no significant correlations were observed in the BCP-ALL panel (Supplementary Fig. S7 and Table S6) whereas *BID* levels were negatively correlated with sensitivity in the T-ALL xenografts ($R = -0.52$, $P = 0.046$; Supplementary Fig. S8 and Table S6).

In the second approach, xenografts were stratified according to their ORM into responders (PRs, CRs, and MCRs) and nonresponders (PDs and SDs) and differentially expressed genes were identified using an unadjusted *P* value of ≤ 0.05 from an empirical Bayes moderated *t* test (28). *MCL1* was the *BCL2* family member with the strongest differential expression among the entire xenograft panel between responders and nonresponders (Fig. 3B and Supplementary Table S6). This was also the case for the MLL-ALL ($P = 0.027$) and BCP-ALL ($P = 0.008$) subtypes (Supplementary

Table 1. *In vivo* responses of pediatric ALL xenografts to ABT-263

		EFS (days)					
ALL lineage	**Xenograft ID**	**Vehicle control**	**ABT-263**	**LGD (days)**	***P* value (log-rank)**	**Median ORM**	**ORM heatmap**
MLL-ALL	MLL-1	19.2	39.7	20.5	0.0003	6	PR
	MLL-2	14.8	26.8	12.0	0.002	6	PR
	MLL-3	8.3	34.1	25.8	0.0002	8	CR
	MLL-5	8.7	14.6	5.9	0.0006	2	PD2
	MLL-6	6.3	29.1	22.8	0.0002	2	PD2
	MLL-7	12.7	30.6	17.9	0.0002	6	PR
	MLL-8	13.7	16.8	3.1	0.0002	0	PD1
	MLL-14	8.7	24.9	16.2	0.0006	2	PD2
	ALL-3	9.6	63.3	53.7	0.008	8	CR
BCP-ALL	ALL-2[a]	4.7	5.2	0.5	0.46	0	PD1
	ALL-4[a]	1.5	28.6	27.1	0.029	2	PD2
	ALL-7	6.8	31.4	24.6	0.0003	8	CR
	ALL-10	7.5	33.3	25.8	0.008	8	CR
	ALL-11	20.2	56.3	36.1	0.008	8	CR
	ALL-17[a]	2.5	24.2	21.7	0.0001	2	PD2
	ALL-19[a]	5.0	>43	>37.9	0.002	8	CR
T-ALL	ALL-8[a]	11.8	62.8	51.0	0.004	10	MCR
	ALL-16[a]	18.2	85.5	67.3	0.0002	10	MCR
	ALL-27	3.3	19.6	16.3	0.30	2	PD2
	ALL-29	4.4	48.8	44.0	0.0002	8	CR
	ALL-30	5.3	16.2	10.9	0.004	2	PD2
	ALL-31	13.9	91.9	78.0	0.0008	10	MCR
	ALL-32[b]	6.7	18.9	12.2	0.0002	2	PD2
	ALL-33[b]	6.0	37.8	31.8	0.0003	8	CR
	ALL-42	1.9	5.9	4.0	0.0002	2	PD2
	ALL-43	14.0	43.9	29.9	0.0002	8	CR
	ALL-44	11.4	27.2	15.8	0.0005	2	PD2
	ALL-47	11.9	41.5	29.6	<0.0001	8	CR
ETP-ALL	ETP-1	7.8	23.8	16.0	0.0002	6	PR
	ETP-2	14.2	44.7	30.5	0.0002	8	CR
	ETP-3	20.0	32.5	12.5	0.0002	6	PR

[a]*In vivo* ABT-263 sensitivity data previously reported (10).

[b]Dose of ABT-263 reduced to 75 mg/kg on day 9 (ALL-32) or day 13 (ALL-33) because of toxicity.

Figs. S6 and S7 and Table S6). Among the MLL-ALL xenografts, differential expression of *BIM* ($P = 0.044$); also reached statistical significance, being paradoxically lower in the responders compared with nonresponders (Supplementary Fig. S6 and Table S6). Similarly, *HRK* ($P = 0.005$) was significantly increased in the BCP-ALL responders (Supplementary Fig. S7 and Table S6), whereas *BAK* ($P = 0.03$) and *NOXA* ($P = 0.049$) were significantly increased in the T-ALL nonresponders and responders, respectively (Supplementary Fig. S8 and Table S6).

Both of the above analysis approaches had also been applied to the entire 34,694 genes represented on the Illumina Beadchip HT-12 arrays, although no genes satisfied the significance or FDR cutoff criteria (data not shown).

Because *MCL1* expression was the strongest overall predictor of *in vivo* ABT-263 response across the entire panel of 31 xenografts, we next assessed *MCL1* expression at the mRNA and protein levels. Although RT-qPCR analysis showed a significantly higher *MCL1* expression in the nonresponders (Fig. 3C), this difference was not confirmed by increased MCL1 protein levels (Fig. 3D and Supplementary Fig. S9). Despite no significant difference in MCL1 protein levels between non-responders and responders, *MCL1* mRNA levels correlated between qRT-PCR and microarray (Fig. 3E), and MCL1 protein levels significantly correlated with *MCL1* mRNA expression measured by qRT-PCR (Fig. 3F). MCL1 protein expression was also investigated after exposure of 2 non-responders and 2 responders to ABT-263 *in vitro*, however no consistent differences were observed (data not shown). Because of these discrepancies in MCL1 protein expression, we next assessed BCL2 family protein

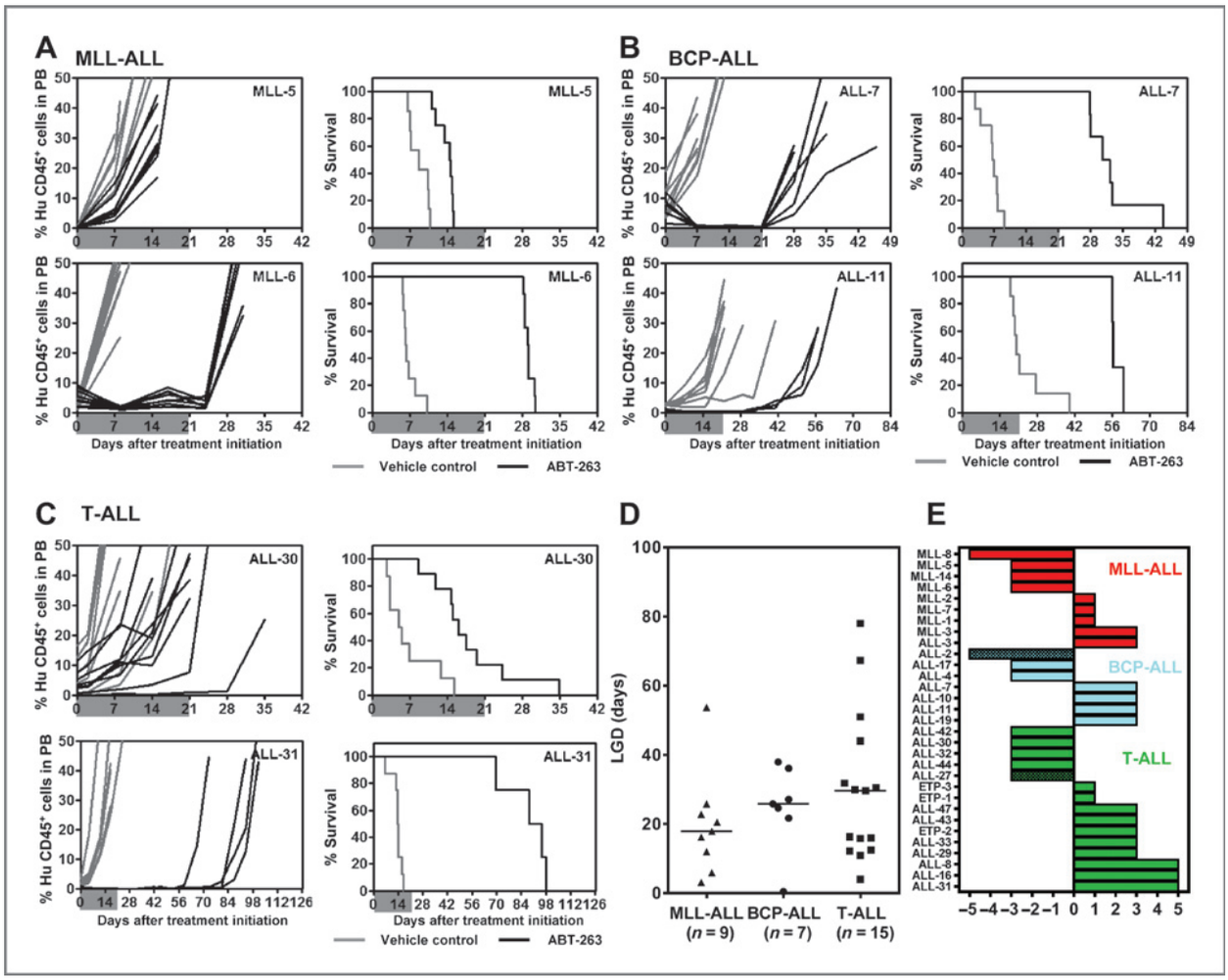

Figure 2. *In vivo* single-agent ABT-263 responses of pediatric ALL xenografts. Responses of representative xenografts from the MLL-ALL (A), BCP-ALL (B), and T-ALL (C) subpanels treated with ABT-263 (100 mg/kg for 21 days, black lines) or vehicle control (gray lines). In each case, the left panels represent the %huCD45$^+$ of individual mice over time, whereas the right panels represent the proportion of mice remaining event free. Shaded areas indicate the treatment period. D, comparison of the LGD of ALL xenograft subtypes in response to ABT-263 treatment. Each data point represents a single xenograft; the horizontal bar represents the median. E, "COMPARE-like" plot of the midpoint difference representing the median ORM of xenografts shown in Table 1.

function with respect to *in vivo* ABT-263 sensitivity using BH3 profiling of the entire xenograft panel.

BH3 profiling identifies MCL1 function as a determinant of *in vivo* ABT-263 sensitivity

The mitochondrial priming assay measures mitochondrial sensitivity to peptides derived from the BH3 domains of proapoptotic BCL2 family proteins. The *in vivo* ABT-263 responses of the xenografts were then compared with the status of mitochondrial priming by the ability of BH3 peptides derived from PUMA, BAD, and NOXA to cause mitochondrial depolarization in xenograft cells. PUMA BH3 interacts promiscuously with all 5 antiapoptotic proteins, BAD BH3 interacts with BCL2, BCLXL, and BCLW (like ABT-263), whereas NOXA BH3 interacts only with MCL1. Out of the 3 peptides, only NOXA-induced mitochondrial depolarization significantly discriminated between non-responder and responder groups (Fig. 3G–I), implicating MCL1 protein function as a major determinant of *in vivo* ABT-263 response. The extent of mitochondrial depolarization did not correlate with leukemia progression (LGD) for any of the peptides tested (data not shown).

In vitro ABT-263 sensitivity of ALL xenografts predicts their *in vivo* responses

We next tested whether the *in vitro* ABT-263 responses of ALL xenografts predicted their *in vivo* sensitivity. Using a coculture method (29), a predictive model was built using a training subset of 17 xenografts (Fig. 4A). Exposure of xenograft cells to a range of ABT-263 concentrations (1 μmol/L–1 nmol/L) revealed that 10 nmol/L gave the best discrimination between *in vivo* non-responders and responders (Fig. 4B and Supplementary Fig. S10). Using the 95%

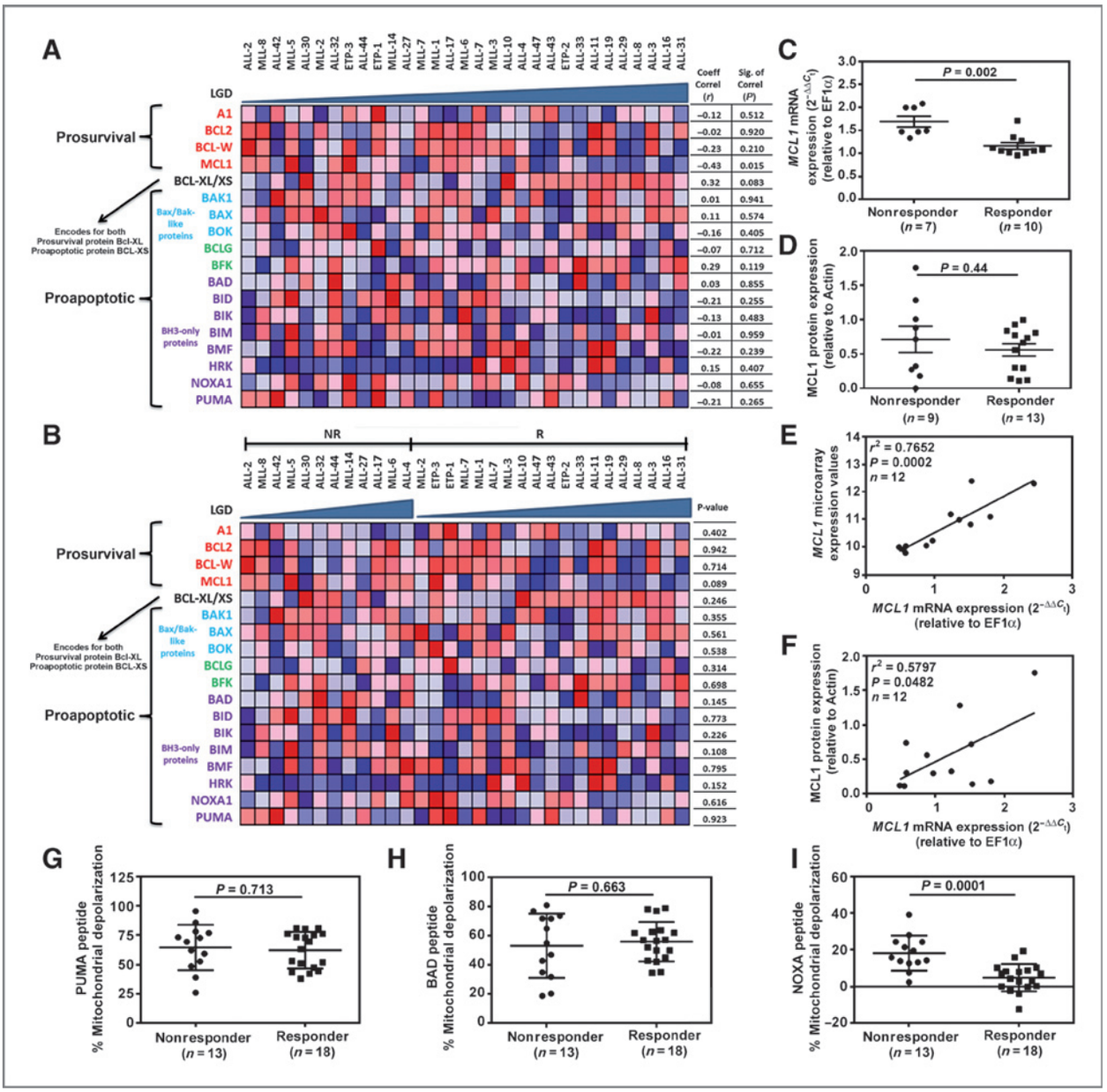

Figure 3. Cell and molecular determinants of the *in vivo* sensitivity of pediatric ALL xenografts to ABT-263. A, xenografts (columns) were ordered by increasing LGD from left to right, with each row representing a *BCL2* family member. B, xenografts were stratified into nonresponders (NR) and responders (R) then ordered by increasing LGD from left to right within each category. The colors in the heatmaps represent the relative expression per gene across all samples. Red indicates relative high expression and blue indicates relative low expression. C, comparison of *MCL1* mRNA expression between NR and R by RT-qPCR. D, comparison of MCL1 protein expression between NR and R by immunoblot. E, correlation between *MCL1* mRNA expression by microarray and RT-qPCR. F, correlation between MCL1 protein expression by immunoblot and *MCL1* mRNA expression by RT-qPCR. In C–F, each data point represents a single xenograft. G–I, the percentage of mitochondrial depolarization induced by BH3 peptides derived from (G) PUMA, (H) BAD, and (I) NOXA peptides in xenograft cells was plotted for individual xenografts stratified as NR or R according to Table 1.

confidence intervals of both responder and nonresponder groups, a three-tier classification was created. It was established that >14.9% live cells after drug treatment (lower limit of confidence interval of nonresponders) stratified xenografts as nonresponders, <8.0% (upper limit of confidence interval of responders) as responders, and those in between were considered as unclassified. Three xenografts (MLL-1, MLL-7, and ETP-3) were excluded from the analysis because their survival was not supported by the coculture assay.

The *in vivo* ABT-263 responses of the remaining 11 xenografts, constituting the test set, were initially blinded. When the test set was classified using the predictive model 7 xenografts were correctly classified according to their *in vivo*

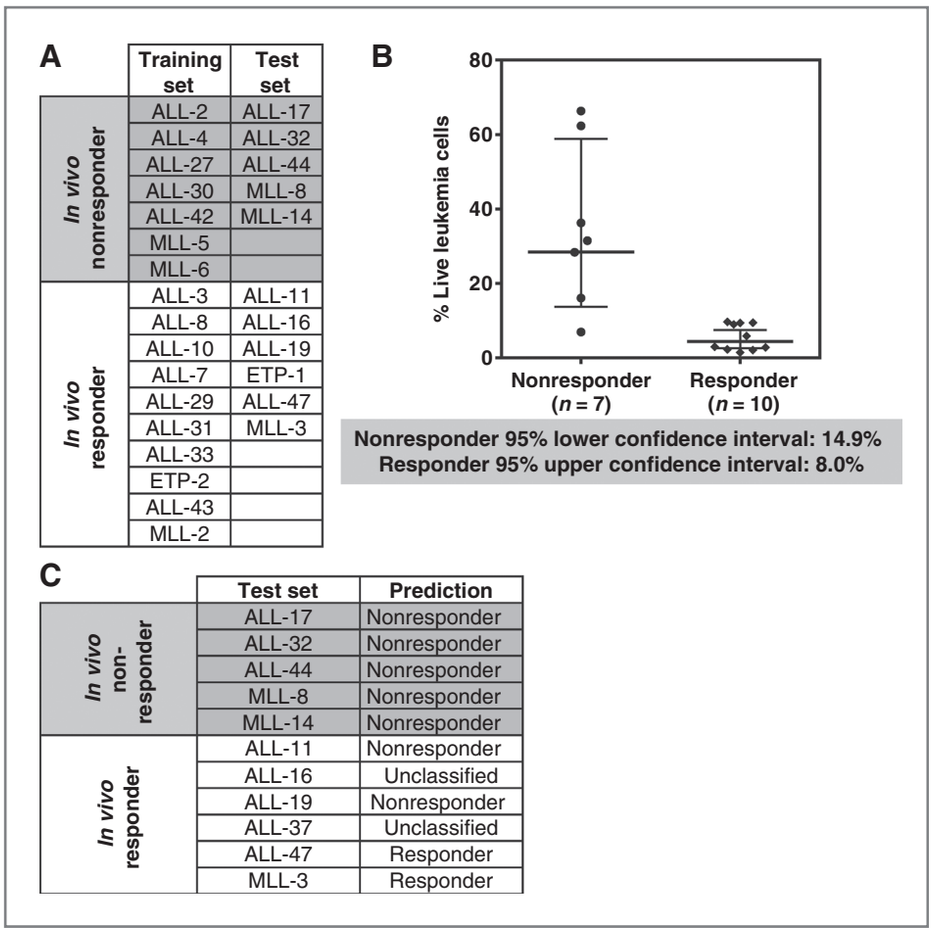

Figure 4. *In vitro* sensitivity of pediatric ALL xenograft cells to ABT-263 predicts their *in vivo* responses. A, xenografts were subgrouped into a training set to build a predictive model, and a test set to test the model. B, percentages of live leukemia cells after exposure to ABT-263 (10 nmol/L, 72 hours). Each data point represents an individual xenograft. Lines indicate the geometric mean with 95% confidence interval indicated by the bars. C, actual and predicted *in vivo* ABT-263 responses of the test xenografts.

ABT-263 responses (Fig. 4C), 2 were incorrectly classified and 2 were unclassified. The sensitivity and specificity of the predictive method (Supplementary Fig. S11) were 50% and 100%, respectively (leaving out of this assessment the 2 unclassified xenografts).

Live and dead cell analysis at 72 hours for each xenograft is shown in Supplementary Fig. S12, which includes the % live/dead cells, the absolute numbers of live/dead cells, and the number of live cells seeded and harvested. In addition, a comparison of the coculture system versus single cell suspension was performed with 5 xenograft samples, and revealed the importance of the coculture assay to assess ALL xenograft cell sensitivity to ABT-263 *in vitro* (Supplementary Fig. S13).

In vivo efficacy of ABT-263 in combination with established chemotherapeutic drugs

We next sought to test the efficacy of ABT-263 in paired combinations with established drugs against xenografts representative of the 2 most common pediatric ALL subtypes, BCP-ALL and T-ALL. Three xenografts were selected based on their range of single-agent ABT-263 responses (ALL-2, resistant; ALL-19, intermediate; ALL-31, sensitive; Table 1). Preliminary tolerability experiments showed that it was necessary to attenuate the dose of ABT-263 to 25 mg/kg when combined with vincristine, and to 50 mg/kg when combined with dexamethasone and L-asparaginase. Of the 3 xenografts tested, the combination of ABT-263 with vincristine caused therapeutic enhancement only in ALL-31 and although for ALL-19 it induced an LGD of >73.7 days, because variation among individual mice it did not reach statistical significance versus ABT-263 alone (Supplementary Tables S7 and S8 and Fig. S14). The dexamethasone/ABT-263 combination did not exert therapeutic enhancement for any xenografts, whereas ABT-263 in combination with L-asparaginase exerted therapeutic enhancement in ALL-31, and the *P* value approached significance for ALL-19. Thus, the expectation that ABT-263 would broadly enhance the *in vivo* efficacy of established chemotherapeutic drugs was not met.

Discussion

We report the utilization of a large panel of ALL xenografts to define the cell and molecular determinants of *in vivo* ABT-263 responses using gene expression profiling, BH3 profiling, and *in vitro* coculture cytotoxicity assays. The principal findings of this study are: (i) ABT-263 is effective *in vivo* as a single agent against pediatric ALL xenografts; (ii) *MCL1*

gene expression and MCL1 protein function correlate with *in vivo* ABT-263 sensitivity; and (iii) an *in vitro* coculture cytotoxicity assay is able to predict *in vivo* ABT-263 responses of ALL xenografts with a high level of sensitivity and specificity.

Xenograft models of pediatric ALL are recognized to accurately recapitulate several cellular and molecular features of the original disease, including blast morphology, immunophenotype, clonal selection, gene expression profiles, and genetic lesions (22, 31, 35–37). Our results describe the subtype classification of a large panel of xenografts, which were appropriately clustered into MLL-ALL, BCP-, and T-ALL subtypes by gene expression profiling. Differentially expressed genes and GSEA analysis within each subtype were consistent with the primary disease state, and a BCP-ALL xenograft previously established from a teenage female (31) was reclassified as an MLL-ALL based in this analysis. Subclusters within each xenograft subtype were also consistent with specific chromosomal translocations. For example, all 4 of the MLL-ALL xenografts harboring a translocation involving chromosome 19 coclustered in 1 subbranch of MLL-ALL, whereas the 3 ETP-ALLs appeared under 1 subbranch of T-ALL.

Despite our previous report of ABT-263 efficacy testing against 6 ALL xenografts indicating a preferential effect against 2 T-ALL xenografts (10), in this study ABT-263 exhibited a broad spectrum of *in vivo* efficacy with no apparent subtype specificity, and induced regressions in 19 of 31 xenografts. However, all 3 xenografts that achieved MCRs were T-ALL, suggesting that ABT-263 may be particularly useful for the treatment of aggressive T-ALL cases. ABT-263 also induced regressions (2 PRs and 1 CR) in the 3 ETP-ALL xenografts. ETP-ALL arises from a subset of thymocytes that are recent emigrants from the bone marrow to the thymus, retaining stem cell–like features and multilineage differential potential, and is a particularly aggressive and refractory T-ALL subtype (30).

In this study, we also attempted to identify cell and molecular signatures that could be used to predict *in vivo* responsiveness to single-agent ABT-263. Studies primarily carried out using cultured cell lines have consistently identified elevated *MCL1* expression to be associated with resistance to ABT-737 and ABT-263 (14–16, 38). Although our study is no exception, we believe this to be the first report to strongly implicate *MCL1* in resistance to ABT-263 *in vivo* using a large panel of direct-patient explants established as continuous xenografts. This relationship only became apparent when we restricted the gene expression analysis to the *BCL2* gene family, a finding that we attribute to the heterogeneity in gene expression profiles between and within each xenograft subtype. Nevertheless, the molecular determinants of *in vivo* ABT-263 sensitivity in pediatric ALL are complex since additional, and occasionally paradoxically, *BCL2* family genes were significantly associated with ABT-263 responses within individual xenograft subtypes.

A confounding factor in our analysis was that, although *MCL1* mRNA expression determined by RT-qPCR correlated with MCL1 protein expression and microarray data, MCL1 protein expression did not reach statistical significance between the ABT-263 responders and non-responders despite a higher trend in the nonresponders (Fig. 3D). Technical issues associated with the harvesting, purifying, and cryopreservation of spleen-derived cells and the very short half-life of MCL1 (<1 hour; refs. 39 and 40) may have contributed to this lack of correlation because of MCL1 protein degradation (Supplementary Fig. S15). Moreover, Gao and Koide reported that there are 2 MCL1 splice variants regulated by *SF3B1*, one with proapoptotic and another with antiapoptotic functions (41). However, we found no correlation between *SF3B1* levels and drug sensitivity (data not shown). Similarly, Boiani and colleagues showed that the HSP70 protein BAG3 stabilizes MCL1, thereby extending its half-life (42). Similarly, we found no correlation between *BAG3* expression and *in vivo* ABT-263 efficacy (data not shown). Because of the aforementioned complexity associated with correlating gene expression profiles and MCL1 protein expression with *in vivo* ABT-263 sensitivity, we next tested the established functional readouts of mitochondrial priming status by BH3 profiling and *in vitro* chemosensitivity testing. Mitochondrial depolarization induced by NOXA peptide correlated with *in vivo* ABT-263 sensitivity (Fig. 3I), thereby strongly implicating MCL1 function. However, this finding differs from a previous report that identified a correlation between BIM, but not NOXA, peptide-induced mitochondrial depolarization and clinical complete response to conventional therapy using pediatric ALL biopsy samples (20).

Murine or human bone marrow–derived stromal cells improve the *ex vivo* survival of pediatric ALL cells (29, 43) whereas both coculture and tetrazolium dye-based assays have been used for chemosensitivity testing in this disease (44–46). In our study, ABT-263 sensitivity of pediatric ALL xenograft cells cocultured with MSC-hTERT cells provided a sensitive (50%) and highly specific (100%) prediction of *in vivo* response. This model accurately predicted resistance, because all 5 of the *in vivo* nonresponders were correctly identified. However, although both of the xenografts predicted to be responders were correct, the model incorrectly predicted no response in 2 of the *in vivo* responders. Therefore, this model could be further refined, because although it might accurately predict which patients are unlikely to respond, it can potentially fail to identify a subset of patients who may benefit from such treatment. Nevertheless, we believe this to be the first report of a functional assay that is able to accurately predict *in vivo* single-agent ABT-263 responses.

Despite substantial evidence, primarily using cultured cell lines, that ABT-737 and ABT-263 can potentiate the effects of standard chemotherapeutic drugs both *in vitro* and *in vivo* (9, 16, 47, 48), using stringent criteria we only observed Therapeutic Enhancement in 2 instances in which ABT-263 was combined with 3 established drugs against 3 xenografts. Although our results are not sufficient to make broad conclusions for combining ABT-263 with these established drugs for patient management, we reason that this divergence from previous reports is because of the necessity

to attenuate the ABT-263 dose in all of the combinations (down to 25 mg/kg in the case of vincristine), while maintaining the maximal ABT-263 dose (100 mg/kg) in the single-agent arms. Future investigations in which small-molecule BCL2 inhibitors with reduced thrombocytopenic effects, such as ABT-199 (49, 50), are combined with established drugs in pediatric ALL may prove more beneficial.

In summary, BCL2-targeted agents appear as a promising class of anticancer drugs for the treatment of pediatric ALL, with no apparent specificity across MLL-ALL, BCP-ALL, or T-ALL subtypes. *MCL1* expression and function seem to be important determinants of *in vivo* ABT-263 sensitivity, although an *in vitro* coculture assay predicted *in vivo* ABT-263 responses with high sensitivity and specificity. This combined cell and molecular analysis provides a proof-of-concept approach for prioritizing other novel drugs for pediatric ALL clinical trials, and for the identification of biomarkers predictive of *in vivo* response.

Disclosure of Potential Conflicts of Interest

Anthony Letai is a consultant/advisory board member for AbbVie. No potential conflicts of interest were disclosed by the other authors.

Authors' Contributions

Conception and design: H. Carol, C. Sarmah, P.J. Houghton, M.A. Smith, R.B. Lock

Development of methodology: H. Carol, T.N. Chonghaile, V. Frismantas, B. Bornhauser, A. Letai, J.-P. Bourquin, P.J. Houghton, M.A. Smith, R.B. Lock

Acquisition of data (provided animals, acquired and managed patients, provided facilities, etc.): S. Suryani, H. Carol, T.N. Chonghaile, V. Frismantas, L. High, B. Szymanska, K. Evans, I. Boehm, E. Tonna, L. Jones, D.M. Manesh, A. Letai, J.-P. Bourquin

Analysis and interpretation of data (e.g., statistical analysis, biostatistics, computational analysis): S. Suryani, H. Carol, T.N. Chonghaile, V. Frismantas, C. Sarmah, L. High, B. Bornhauser, M.J. Cowley, B. Szymanska, K. Evans, I. Boehm, E. Tonna, L. Jones, R.T. Kurmasheva, C. Billups, W. Kaplan, A. Letai, J.-P. Bourquin, P.J. Houghton, M.A. Smith, R.B. Lock

Writing, review, and/or revision of the manuscript: S. Suryani, H. Carol, C. Sarmah, B. Bornhauser, M.J. Cowley, B. Szymanska, K. Evans, E. Tonna, L. Jones, P.J. Houghton, M.A. Smith, R.B. Lock

Administrative, technical, or material support (i.e., reporting or organizing data, constructing databases): S. Suryani, K. Evans, E. Tonna, R.T. Kurmasheva

Study supervision: S. Suryani, H. Carol, R.B. Lock

Acknowledgments

The authors thank AbbVie Inc. for providing ABT-263, the Tissue Resources Core Facility of St Jude Children's Research Hospital (Memphis, TN) for the provision of primary ETP-ALL samples, and Dr Dario Campana (St Jude Children's Research Hospital, Memphis, TN) for providing *hTERT*-immortalized MSCs. Children's Cancer Institute Australia for Medical Research is affiliated with the University of New South Wales and The Sydney Children's Hospitals Network.

Grant Support

This research was funded by grants from the National Cancer Institute (NOI-CM-42216 and NOI-CM-91001-03); the Leukaemia Foundation of Australia the Cancer Council New South Wales; the Krebsliga Zurich to B. Bornhauser, and the Foundation Kind und Krebs, the Hanne Liebermann Stiftung, and the Swiss National Research Foundation to J.-P. Bourquin. S. Suryani is supported by Postdoctoral Fellowships from the Leukaemia Foundation of Australia and the Cure Cancer Australia Foundation, and an Early Career Fellowship from the Cancer Institute NSW. R.B. Lock is supported by a Fellowship from the National Health and Medical Research Council.

The costs of publication of this article were defrayed in part by the payment of page charges. This article must therefore be hereby marked *advertisement* in accordance with 18 U.S.C. Section 1734 solely to indicate this fact.

Received January 31, 2014; revised June 10, 2014; accepted June 29, 2014; published OnlineFirst July 10, 2014.

References

1. Hunger SP, Lu X, Devidas M, Camitta BM, Gaynon PS, Winick NJ, et al. Improved survival for children and adolescents with acute lymphoblastic leukemia between 1990 and 2005: a report from the children's oncology group. J Clin Oncol 2012;30:1663–9.
2. Ko RH, Ji L, Barnette P, Bostrom B, Hutchinson R, Raetz E, et al. Outcome of patients treated for relapsed or refractory acute lymphoblastic leukemia: a therapeutic advances in childhood leukemia consortium study. J Clin Oncol 2010;28:648–54.
3. Hanahan D, Weinberg RA. Hallmarks of cancer: the next generation. Cell 2011;144:646–74.
4. Cragg MS, Harris C, Strasser A, Scott CL. Unleashing the power of inhibitors of oncogenic kinases through BH3 mimetics. Nat Rev Cancer 2009;9:321–6.
5. Chen L, Willis SN, Wei A, Smith BJ, Fletcher JI, Hinds MG, et al. Differential targeting of prosurvival Bcl-2 proteins by their BH3-only ligands allows complementary apoptotic function. Mol Cell 2005;17:393–403.
6. Kelly PN, Strasser A. The role of Bcl-2 and its pro-survival relatives in tumourigenesis and cancer therapy. Cell Death Differ 2011;18:1414–24.
7. Oltersdorf T, Elmore SW, Shoemaker AR, Armstrong RC, Augeri DJ, Belli BA, et al. An inhibitor of Bcl-2 family proteins induces regression of solid tumours. Nature 2005;435:677–81.
8. Tse C, Shoemaker AR, Adickes J, Anderson MG, Chen J, Jin S, et al. ABT-263: a potent and orally bioavailable Bcl-2 family inhibitor. Cancer Res 2008;68:3421–8.
9. High LM, Szymanska B, Wilczynska-Kalak U, Barber N, O'Brien R, Khaw SL, et al. The Bcl-2 homology domain 3 mimetic ABT-737 targets the apoptotic machinery in acute lymphoblastic leukemia resulting in synergistic in vitro and in vivo interactions with established drugs. Mol Pharmacol 2010;77:483–94.
10. Lock R, Carol H, Houghton PJ, Morton CL, Kolb EA, Gorlick R, et al. Initial testing (stage 1) of the BH3 mimetic ABT-263 by the pediatric preclinical testing program. Pediatr Blood Cancer 2008;50:1181–9.
11. Gandhi L, Camidge DR, Ribeiro de Oliveira M, Bonomi P, Gandara D, Khaira D, et al. Phase I study of Navitoclax (ABT-263), a novel Bcl-2 family inhibitor, in patients with small-cell lung cancer and other solid tumors. J Clin Oncol 2011;29:909–16.
12. Wilson WH, O'Connor OA, Czuczman MS, LaCasce AS, Gerecitano JF, Leonard JP, et al. Navitoclax, a targeted high-affinity inhibitor of BCL-2, in lymphoid malignancies: a phase 1 dose-escalation study of safety, pharmacokinetics, pharmacodynamics, and antitumour activity. Lancet Oncol 2010;11:1149–59.
13. Rudin CM, Hann CL, Garon EB, Ribeiro de Oliveira M, Bonomi PD, Camidge DR, et al. Phase II study of single-agent navitoclax (ABT-263) and biomarker correlates in patients with relapsed small cell lung cancer. Clin Cancer Res 2012;18:3163–9.
14. Doi K, Li R, Sung SS, Wu H, Liu Y, Manieri W, et al. Discovery of marinopyrrole A (maritoclax) as a selective Mcl-1 antagonist that overcomes ABT-737 resistance by binding to and targeting Mcl-1 for proteasomal degradation. J Biol Chem 2012;287:10224–35.
15. Merino D, Khaw SL, Glaser SP, Anderson DJ, Belmont LD, Wong C, et al. Bcl-2, Bcl-x(L), and Bcl-w are not equivalent targets of ABT-737 and navitoclax (ABT-263) in lymphoid and leukemic cells. Blood 2012;119:5807–16.
16. van Delft MF, Wei AH, Mason KD, Vandenberg CJ, Chen L, Czabotar PE, et al. The BH3 mimetic ABT-737 targets selective Bcl-2 proteins

and efficiently induces apoptosis via Bak/Bax if Mcl-1 is neutralized. Cancer Cell 2006;10:389–99.
17. Yamaguchi R, Janssen E, Perkins G, Ellisman M, Kitada S, Reed JC. Efficient elimination of cancer cells by deoxyglucose-ABT-263/737 combination therapy. PLoS ONE 2011;6:e24102.
18. Yamaguchi R, Perkins G. Mcl-1 levels need not be lowered for cells to be sensitized for ABT-263/737-induced apoptosis. Cell Death Diff 2011;2:e227.
19. Certo M, Del Gaizo Moore V, Nishino M, Wei G, Korsmeyer S, Armstrong SA, et al. Mitochondria primed by death signals determine cellular addiction to antiapoptotic BCL-2 family members. Cancer Cell 2006;9:351–65.
20. Ni Chonghaile T, Sarosiek KA, Vo TT, Ryan JA, Tammareddi A, Moore Vdel G, et al. Pretreatment mitochondrial priming correlates with clinical response to cytotoxic chemotherapy. Science 2011;334: 1129–33.
21. Houghton PJ, Morton CL, Tucker C, Payne D, Favours E, Cole C, et al. The pediatric preclinical testing program: description of models and early testing results. Pediatr Blood Cancer 2007;49:928–40.
22. Liem NL, Papa RA, Milross CG, Schmid MA, Tajbakhsh M, Choi S, et al. Characterization of childhood acute lymphoblastic leukemia xenograft models for the preclinical evaluation of new therapies. Blood 2004; 103:3905–14.
23. Houghton PJ, Morton CL, Gorlick R, Lock RB, Carol H, Reynolds CP, et al. Stage 2 combination testing of rapamycin with cytotoxic agents by the Pediatric Preclinical Testing Program. Mol Cancer Ther 2010;9:101–12.
24. Rose WC, Wild R. Therapeutic synergy of oral taxane BMS-275183 and cetuximab versus human tumor xenografts. Clin Cancer Res 2004;10:7413–7.
25. Bachmann PS, Gorman R, Papa RA, Bardell JE, Ford J, Kees UR, et al. Divergent mechanisms of glucocorticoid resistance in experimental models of pediatric acute lymphoblastic leukemia. Cancer Res 2007;67:4482–90.
26. Bhadri VA, Cowley MJ, Kaplan W, Trahair TN, Lock RB. Evaluation of the NOD/SCID xenograft model for glucocorticoid-regulated gene expression in childhood B-cell precursor acute lymphoblastic leukemia. BMC Genomics 2011;12:565.
27. Benjamini Y, Hochberg Y. Controlling the false discovery rate: a practical and powerful approach to multiple testing. J R Statist Soc 1995;57:289–300.
28. Smyth GK. Linear models and empirical bayes methods for assessing differential expression in microarray experiments. Stat Appl Genet Mol Biol 2004;3:Article3.
29. Bonapace L, Bornhauser BC, Schmitz M, Cario G, Ziegler U, Niggli FK, et al. Induction of autophagy-dependent necroptosis is required for childhood acute lymphoblastic leukemia cells to overcome glucocorticoid resistance. J Clin Invest 2010;120:1310–23.
30. Coustan-Smith E, Mullighan CG, Onciu M, Behm FG, Raimondi SC, Pei D, et al. Early T-cell precursor leukaemia: a subtype of very high-risk acute lymphoblastic leukaemia. Lancet Oncol 2009;10:147–56.
31. Lock RB, Liem N, Farnsworth ML, Milross CG, Xue C, Tajbakhsh M, et al. The nonobese diabetic/severe combined immunodeficient (NOD/SCID) mouse model of childhood acute lymphoblastic leukemia reveals intrinsic differences in biologic characteristics at diagnosis and relapse. Blood 2002;99:4100–8.
32. Armstrong SA, Staunton JE, Silverman LB, Pieters R, den Boer ML, Minden MD, et al. MLL translocations specify a distinct gene expression profile that distinguishes a unique leukemia. Nat Genet 2002;30:41–7.
33. Nordlund J, Kiialainen A, Karlberg O, Berglund EC, Goransson-Kultima H, Sonderkaer M, et al. Digital gene expression profiling of primary acute lymphoblastic leukemia cells. Leukemia 2012;26:1218–27.
34. Szymanska B, Wilczynska-Kalak U, Kang MH, Liem NL, Carol H, Boehm I, et al. Pharmacokinetic modeling of an induction regimen for *in vivo* combined testing of novel drugs against pediatric acute lymphoblastic leukemia xenografts. PLoS ONE 2012;7:e33894.
35. Anderson K, Lutz C, van Delft FW, Bateman CM, Guo Y, Colman SM, et al. Genetic variegation of clonal architecture and propagating cells in leukaemia. Nature 2011;469:356–61.
36. Clappier E, Gerby B, Sigaux F, Delord M, Touzri F, Hernandez L, et al. Clonal selection in xenografted human T cell acute lymphoblastic leukemia recapitulates gain of malignancy at relapse. J Exp Med 2011;208:653–61.
37. Schmitz M, Breithaupt P, Scheidegger N, Cario G, Bonapace L, Meissner B, et al. Xenografts of highly resistant leukemia recapitulate the clonal composition of the leukemogenic compartment. Blood 2011;118:1854–64.
38. Tahir SK, Wass J, Joseph MK, Devanarayan V, Hessler P, Zhang H, et al. Identification of expression signatures predictive of sensitivity to the Bcl-2 family member inhibitor ABT-263 in small cell lung carcinoma and leukemia/lymphoma cell lines. Mol Cancer Ther 2010;9:545–57.
39. Maurer U, Charvet C, Wagman AS, Dejardin E, Green DR. Glycogen synthase kinase-3 regulates mitochondrial outer membrane permeabilization and apoptosis by destabilization of MCL-1. Mol Cell 2006;21:749–60.
40. Nijhawan D, Fang M, Traer E, Zhong Q, Gao W, Du F, et al. Elimination of Mcl-1 is required for the initiation of apoptosis following ultraviolet irradiation. Genes Dev 2003;17:1475–86.
41. Gao Y, Koide K. Chemical perturbation of Mcl-1 pre-mRNA splicing to induce apoptosis in cancer cells. ACS Chem Biol 2013;8: 895–900.
42. Boiani M, Daniel C, Liu X, Hogarty MD, Marnett LJ. The stress protein BAG3 stabilizes Mcl-1 protein and promotes survival of cancer cells and resistance to antagonist ABT-737. J Biol Chem 2013;288:6980–90.
43. Manabe A, Coustan-Smith E, Behm FG, Raimondi SC, Campana D. Bone marrow-derived stromal cells prevent apoptotic cell death in B-lineage acute lymphoblastic leukemia. Blood 1992;79:2370–7.
44. Klumper E, Pieters R, Veerman AJP, Huismans DR, Loonen AH, Hahlen K, et al. In vitro cellular drug resistance in children with relapsed/refractory acute lymphoblastic leukemia. Blood 1995;86:3861–8.
45. Kumagai M, Manabe A, Pui C-H, Behm FG, Raimondi SC, Hancock ML, et al. Stroma-supported culture of childhood B-lineage acute lymphoblastic leukaemia cells predicts treatment outcome. J Clin Invest 1996;97:755–60.
46. Pieters R, Loonen AH, Huismans DR, Broekema GJ, Dirven MWJ, Heyenbrok MW, et al. *In vitro* drug sensitivity of cells from children with leukemia using the MTT assay with improved culture conditions. Blood 1990;76:2327–36.
47. Ackler S, Mitten MJ, Foster K, Oleksijew A, Refici M, Tahir SK, et al. The Bcl-2 inhibitor ABT-263 enhances the response of multiple chemotherapeutic regimens in hematologic tumors *in vivo*. Cancer Chemother Pharmacol 2010;66:869–80.
48. Kang MH, Kang YH, Szymanska B, Wilczynska-Kalak U, Sheard MA, Harned TM, et al. Activity of vincristine, L-ASP, and dexamethasone against acute lymphoblastic leukemia is enhanced by the BH3-mimetic ABT-737 in vitro and in vivo. Blood 2007;110:2057–66.
49. Souers AJ, Leverson JD, Boghaert ER, Ackler SL, Catron ND, Chen J, et al. ABT-199, a potent and selective BCL-2 inhibitor, achieves antitumor activity while sparing platelets. Nat Med 2013; 19:202–8.
50. Vandenberg CJ, Cory S. ABT-199, a new Bcl-2-specific BH3 mimetic, has *in vivo* efficacy against aggressive Myc-driven mouse lymphomas without provoking thrombocytopenia. Blood 2013;121:2285–8.

Genomics and drug profiling of fatal *TCF3-HLF*–positive acute lymphoblastic leukemia identifies recurrent mutation patterns and therapeutic options

***TCF3-HLF*–positive acute lymphoblastic leukemia (ALL) is currently incurable. Using an integrated approach, we uncovered distinct mutation, gene expression and drug response profiles in *TCF3-HLF*–positive and treatment-responsive *TCF3-PBX1*–positive ALL. We identified recurrent intragenic deletions of *PAX5* or *VPREB1* in constellation with the fusion of *TCF3* and *HLF*. Moreover somatic mutations in the non-translocated allele of *TCF3* and a reduction of *PAX5* gene dosage in *TCF3-HLF* ALL suggest cooperation within a restricted genetic context. The enrichment for stem cell and myeloid features in the *TCF3-HLF* signature may reflect reprogramming by *TCF3-HLF* of a lymphoid-committed cell of origin toward a hybrid, drug-resistant hematopoietic state. Drug response profiling of matched patient-derived xenografts revealed a distinct profile for *TCF3-HLF* ALL with resistance to conventional chemotherapeutics but sensitivity to glucocorticoids, anthracyclines and agents in clinical development. Striking on-target sensitivity was achieved with the BCL2-specific inhibitor venetoclax (ABT-199). This integrated approach thus provides alternative treatment options for this deadly disease.**

One of the hallmarks of pediatric ALL is the presence of subtype-defining chromosomal translocations that cause gene fusions involving master regulators of hematopoietic development. These initiating lesions often cooperate with specific somatic aberrations, including monoallelic deletions of B cell developmental genes, such as *PAX5, IKZF1* and *EBF1* (ref. 1). Other cooperative liaisons are represented by trisomy 21q22 with *CRLF2* activation[2–4] or near-haploid ALL with activation of receptor tyrosine kinase or RAS signaling[5]. RAS pathway mutations appear in high-risk ALL but are often lost with disease progression, which suggests involvement of additional tumorigenic factors[6,7]. The patterns of recurrent genomic alterations need to be better understood, because apart from tyrosine kinase inhibitor–supplemented treatment of *BCR-ABL1*–positive ALL, the only proven successful first-line treatment strategies for high-risk ALL are chemotherapy intensification and early allogeneic hematopoietic stem cell transplantation[8].

The translocation t(1;19)[9] that results in a fusion of the transcriptional activation domain of the B cell developmental transcription factor TCF3 to the DNA-binding domain of PBX1 occurs in about 5–10% of precursor B cell (pre-B cell) ALL patients and is associated with a median five-year event-free survival probability of 78–85%[10]. In contrast, the translocation t(17;19)(q22;p13), resulting in the fusion gene *TCF3-HLF*, defines a rare subtype of ALL (<1% of pediatric ALL) that is typically associated with relapse and death within two years from diagnosis[11,12]. Both translocations disrupt one allele of *TCF3,* which drives the B cell differentiation program upstream of the transcription factor *PAX5* (ref. 13). As an initiating event, expression of *TCF3-HLF* leads to transcriptional reprogramming in pre-leukemic cells. Possible direct targets of TCF3-HLF include the transcription factor gene *LMO2*, which is implicated in initiation of T cell ALL[14,15], and the transcriptional repressor *SNAI1* (*SLUG*), which regulates embryonic development and apoptosis[16,17]. Further targets have been proposed, including *BCL2* (ref. 14). The *TCF3-HLF* fusion likely requires additional events to cause leukemia, because *TCF3-HLF* transgenic and knock-in mice did not recapitulate the human phenotype[18,19].

Here we report that the genomic and transcriptomic landscape of *TCF3-HLF*–positive ALL differs markedly from *TCF3-PBX1*–positive ALL. The *TCF3-HLF* fusion likely occurs in B lymphoid progenitors in the context of *PAX5* haploinsufficiency and is associated with transcriptional reprogramming toward an immature, hybrid hematopoietic state. Drug response profiling in patient-derived xenografts, which maintained the genomic and global transcriptome landscapes of the corresponding primary leukemic samples, identified resistance patterns to drugs commonly used for the treatment of *TCF3-HLF*–positive patients. A general trait of *TCF3-HLF*–positive ALL in our study is extreme sensitivity toward the BCL2-specific inhibitor ABT-199 (venetoclax), indicating new therapeutic options for this fatal ALL subtype.

RESULTS

The *TCF3-HLF* ALL patient cohort

We applied high-throughput sequencing analysis integrating short and large insert size paired-end whole-genome, whole-exome and transcriptome sequencing to a discovery cohort consisting of five diagnostic pre-treatment samples of *TCF3-PBX1*–positive ALL (samples 1a–5a) and *TCF3-HLF*–positive ALL (samples 6a–9a and 11a). As nontumor controls we used matched bone marrow samples collected after induction treatment for minimal residual disease (MRD) evaluation (maximum leukemic cell load $\leq 10^{-3}$; samples

A full list of authors and affiliations appears at the end of the paper.

Received 2 December 2014; accepted 29 June 2015; published online 27 July 2015; doi:10.1038/ng.3362

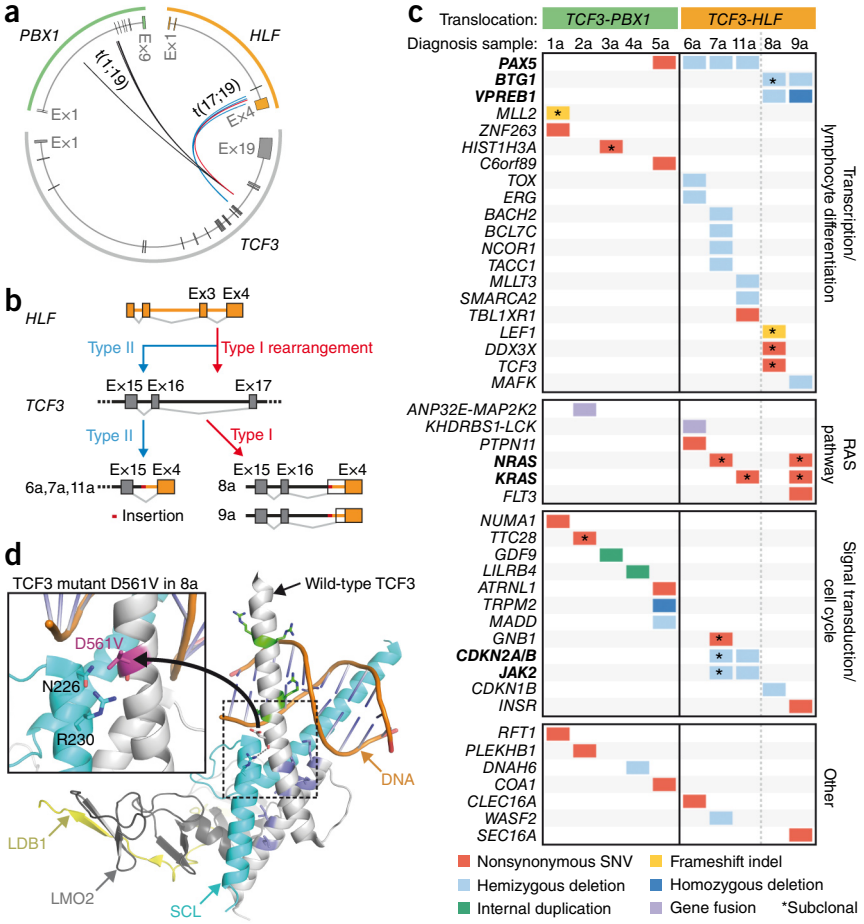

Figure 1 Genetic lesions identified in pediatric *TCF3-HLF*– and *TCF3-PBX1*–positive ALL. (**a**) Breakpoints in *TCF3*, *PBX1* and *HLF* cluster in genomic hotspot regions. Boxes correspond to exonic regions; arcs represent fusions in patient samples. (**b**) *TCF3* breakpoints cluster in two *TCF3* intronic regions: between exons 16 and 17 (type I) and between exons 15 and 16 (type II). On the transcript level, type I translocations join *TCF3* exon 16 to *HLF* exon 4, including inserted nontemplate and intronic sequences and new splice acceptor sites (patients 8 and 9). Type II translocations occur downstream of exon 15 and exclude *TCF3* exon 16 from the fusion transcript (patients 6, 7 and 11). (**c**) Schematic of somatic structural and nucleotide variations in samples. *TCF3-HLF*–positive ALL is characterized by mutually exclusive *PAX5, BTG1* and *VPREB1* deletions and nonsynonymous nucleotide variations in *TCF3* (p.Asp561Val, 'D561V' in patient 8). Indel, insertion-deletion. Recurrently affected genes are indicated by bold symbols. (**d**) Models of wild-type and mutant TCF3 based on the crystal structure of TCF3 in complex with the transcription factors SCL, LMO2 and LDB1 bound to DNA[58]. Upon LMO2 binding, bonds are formed between TCF3 and SCL, including a hydrogen bond (dashed line) between D561 and R230, reducing the DNA binding capacity of the complex. Inset, D561V introduces a hydrophobic valine residue close to polar residues that may interfere with hydrogen bonding, thus altering the DNA-binding properties of the complex.

1b–9b and 11b; **Supplementary Table 1**).

For validation, we used additional DNA samples from seven *TCF3-HLF*–positive cases (diagnostic samples 10a, 12a, 13a, 14a, 15a, 16a, 17a, remission samples 10b, 12b, 13b) and 24 *TCF3-PBX1*–positive cases (**Supplementary Tables 2** and **3**). In most cases *TCF3-HLF*–positive ALL responded to induction chemotherapy but remained MRD-positive. Nine children included in this study died owing to disease progression and treatment-related toxicities within 2 years on average, and only one patient is in remission after a short follow-up time, reflecting the dismal prognosis of *TCF3-HLF*–positive ALL.

TCF3 breakpoints suggest a committed lymphoid cell of origin

Consistent with previous reports[20,21], all *TCF3* translocation breakpoints were restricted to three hotspot regions (**Fig. 1a**,**b** and **Supplementary Fig. 1**). Those were associated with small non-template nucleotide insertions indicative of terminal deoxynucleotide transferase (TdT) activity characteristic of an early B cell stage (**Supplementary Table 4**). In *TCF3*, the breakpoints clustered in close proximity to CpG elements in the absence of classical RAG consensus sequence sites (**Supplementary Fig. 1**), which is a characteristic feature of translocations that occur in lymphoid progenitors at the pro-/pre-B stage. This may represent illegitimate RAG-mediated recombination at cryptic sites, possibly in the context of deaminated CpG nucleotides as proposed for *TCF3-PBX1* translocations[22]. Consistent with the idea that *TCF3-HLF* fusion may occur at a lymphoid-committed rather than a pluripotent progenitor stage, we detected this translocation only in sorted pre-B cell populations containing leukemic cells but neither in stem cells nor in myeloid progenitor cells (**Supplementary Fig. 2**).

TCF3-HLF ALL and impaired pro– to pre–B cell transition

Pre–B cell ALL is frequently associated with somatic copy number alterations affecting B cell developmental genes. *PAX5* deletions are generally observed in 13% of ALL cases and in up to 28% of high-risk ALL[23]. We observed enrichment for monoallelic *PAX5* deletions in *TCF3-HLF*–positive ALL, identifying such events in 67% of the cases (**Fig. 1c** and **Supplementary Table 2**). Illegitimate RAG-mediated recombination appears to be implicated in the generation of such events in *TCF3-HLF*–positive ALL, given the close proximity to RSS motifs (**Supplementary Table 5**). In most samples without *PAX5* deletion, we identified hemi- and homozygous deletions of *VPREB1,* which encodes a component of the surrogate light chain of the pre–B cell receptor (**Fig. 1c** and **Supplementary Table 6**), independent of the lambda light chain locus. *VPREB1* deletions in pediatric ALL result in failure to form a viable surrogate light chain in the pre-B cell receptor, an event associated with lower overall survival[24]. In addition, we detected *BTG1* gene deletions in three of eight *TCF3-HLF*–positive cases without *PAX5* deletions (**Supplementary Fig. 3a**,**b**). *BTG1* deletions occur frequently in ALL positive for *ETV6-RUNX1* (19%) or *BCR-ABL1* (26%) and may confer a proliferative advantage[25]. In contrast, we detected no deletion, but only a single *PAX5* nonsense mutation in 29 *TCF3-PBX1*–positive cases (**Fig. 1** and **Supplementary Table 3**). Our results indicate that cooperative genetic events affecting genes regulating the pro- to pre-B cell transition, in particular *PAX5, BTG1* and *VPREB1,* but not *IKZF1,* are selected in *TCF3-HLF*–translocated cells. Other deleted genes associated with pre-B cell ALL[26] were *JAK2* and *CDKN2A/B* (patient 7a and 11a) and transcriptional regulators such as *ERG, NCOR1, TOX, BACH2, BCL7C, MLLT3, SMARCA2* and *MAFK* (**Fig. 1c**).

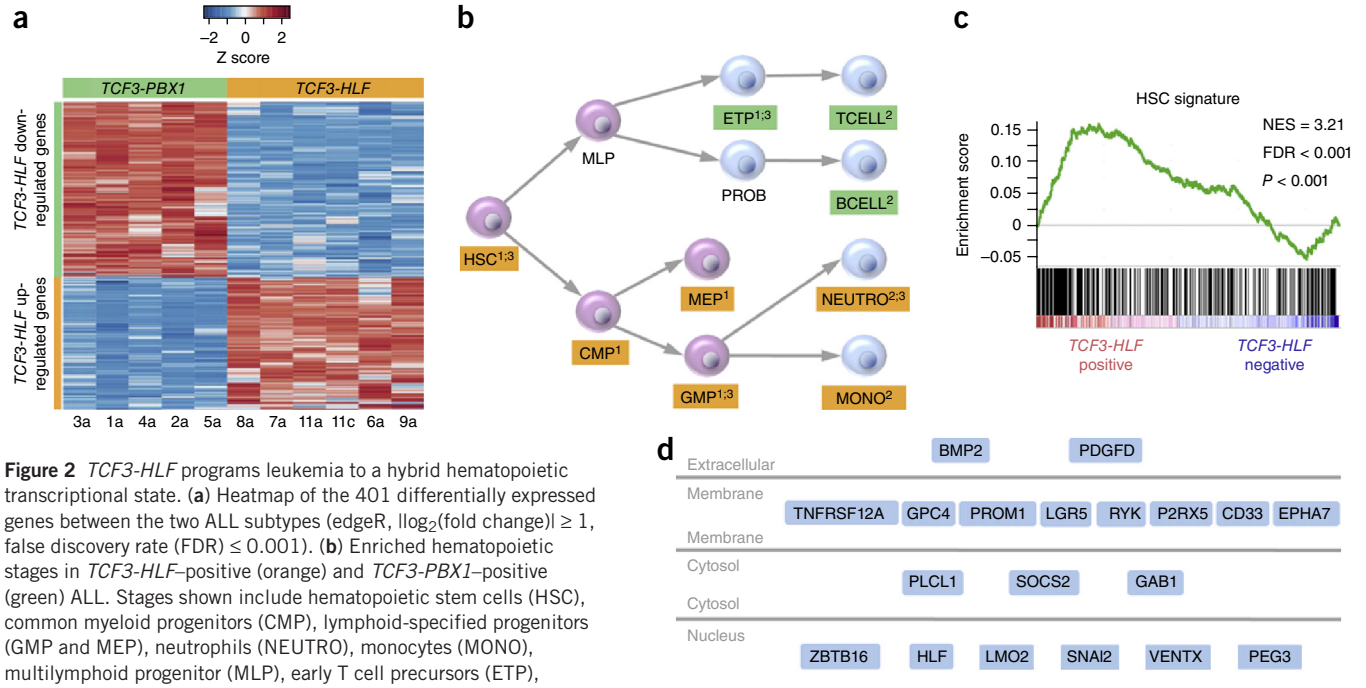

Figure 2 *TCF3-HLF* programs leukemia to a hybrid hematopoietic transcriptional state. (**a**) Heatmap of the 401 differentially expressed genes between the two ALL subtypes (edgeR, $|\log_2(\text{fold change})| \geq 1$, false discovery rate (FDR) ≤ 0.001). (**b**) Enriched hematopoietic stages in *TCF3-HLF*–positive (orange) and *TCF3-PBX1*–positive (green) ALL. Stages shown include hematopoietic stem cells (HSC), common myeloid progenitors (CMP), lymphoid-specified progenitors (GMP and MEP), neutrophils (NEUTRO), monocytes (MONO), multilymphoid progenitor (MLP), early T cell precursors (ETP), pro-B cells (PROB), T cells (TCELL) and B cells (BCELL). Gene set enrichment analysis was carried out using a Genomatix genome analyzer and gene set enrichment analysis (GSEA)[77] (GSEA: FDR ≤ 0.02; Genomatix genome analyzer: adjusted $P \leq 0.02$). The source of the significantly enriched gene sets is noted by the superscript: 1, curated gene sets of hematopoietic precursors[31]; 2, human immunologic gene signatures (MSigDB v4.0)[32]; 3, text mining–based tissue-specific gene sets[78]. (**c**) Enrichment plot for the HSC signature[31]. FDR, false discovery rate. NES, normalized enrichment score. (**d**) Components of the *TCF3-HLF*–positive ALL signature reveal functional annotation related to stem cells and their cellular location (Genomatix genome analyzer: $P = 4.65 \times 10^{-4}$, adjusted $P < 0.001$).

Recurrent RAS pathway mutations in *TCF3-HLF* ALL

We identified only a few additional somatic alterations affecting protein-coding sequences in both *TCF3-PBX1*- and *TCF3-HLF*–positive ALL (**Fig. 1c**, and **Supplementary Tables 6** and **7**), involving among others, genes associated with pre-B cell ALL[26] (*TCF3*, *PAX5* and *LEF1*) and transcriptional and chromatin regulation (*ZNF263*, *MLL2*, *HIST1H3A* and *C6orf89*). We observed a prominent association of *TCF3-HLF*–positive ALL with activating mutations in RAS signaling pathway genes (*NRAS*, *KRAS* and *PTPN11*), detectable in four of five discovery cases (**Fig. 1c**) and in three of five additional *TCF3-HLF*–positive validation samples (*PTPN11* and *SPHK1)* (**Supplementary Table 2**). We identified no RAS pathway mutations in the *TCF3-PBX1*–positive discovery cohort and only one oncogenic *NRAS* mutation in the 24 *TCF3-PBX1*–positive validation cases (**Supplementary Table 3**). *NRAS* and *KRAS* mutations were generally detected in subclones (**Supplementary Table 7**). We discovered a new fusion gene, *KHDRBS1-LCK*, due to an interstitial chromosomal deletion in one *TCF3-HLF*–positive sample (6a), triggering the overexpression of the *LCK* tyrosine kinase (**Supplementary Fig. 4**). This was also present in three of 74 randomly selected ALL samples, demonstrating that *KHDRBS1-LCK* fusion is recurrent in ALL (**Supplementary Fig. 5**). LCK is a drug target in RAS-dependent cancer cells that have higher *LCK* expression[27], suggesting a possible interplay with RAS-related signaling networks in *TCF3-HLF*–positive ALL. Oncogenic activation of LCK associated with t(1;7)(p34;q34) translocation had been reported in the T cell leukemia cell line HSB2 (ref. 28). Our data indicate a frequent association of proliferation-driving mutations in *TCF3-HLF*–positive ALL in the context of stalled B cell differentiation.

Mutations affecting the second *TCF3* allele in *TCF3-HLF* ALL

We identified a mutation in the basic helix-loop-helix region of *TCF3* (p.Asp561Val, D561V, **Fig. 1c**,**d**) affecting the non-translocated chromosome in one *TCF3-HLF*–positive case (8a). Mutations at this position have been reported in sporadic Burkitt lymphoma[29] and may reduce binding to its negative regulator ID3 (ref. 29). Based on available crystal structure data, p.Asp561Glu may affect the interaction of TCF3 with the transcription factor SCL (also known as TAL1; **Fig. 1d**), possibly altering TCF3 protein complexes. We detected a second *TCF3* mutation (p.Ser467Gly) in another *TCF3-HLF*–positive case (13a, **Supplementary Table 2**). The functional consequences of this mutation are currently unclear. We could not detect any somatic mutations in *TCF3* by targeted sequencing of 1,033 unselected ALL patients from the European multicenter trial AIEOP-BFM ALL 2000, suggesting a specific association with *TCF3-HLF*–positive ALL (**Supplementary Table 8**). Thus, deregulation of normal TCF3 function may also contribute to *TCF3-HLF*–positive ALL. Corroborating our findings, a recent study included a single *TCF3-HLF* case, as part of a cohort comparing diagnostic and relapse ALL samples, which showed a *PAX5* deletion and two mutations in *TCF3* (p.His460Tyr and p.Gly470fs), all of which were conserved at relapse[30]. The relapse sample featured a *VPREB1* deletion as well as a shift in subclonal mutations in *NRAS* (p.Gly12Asp and p.Gly12Val), reinforcing the idea of cooperative effects between *TCF3-HLF*, and alteration of *PAX5* and *VPREB1* gene dosage. Taken together, seven of 11 *TCF3-HLF* cases were hemizygous for *PAX5*, whereas five samples featured *VPREB1* deletions (**Supplementary Fig. 6**).

Reprogramming toward a more immature state in *TCF3-HLF* ALL

Consistent with the occurrence of *TCF3-HLF* and *TCF3-PBX1* translocations in lymphoid precursors, both leukemia subtypes had in common a gene expression signature of B lymphoid cells (including *PAX5, BLK, CD19, CD22, CD79B, TCF3, EBF1, VPREB1, RAG1, ROR1, BLNK* and *DNTT*; **Supplementary Tables 9** and **10**), but differential expression of 401 genes (false discovery rate ≤ 0.001) strongly distinguished

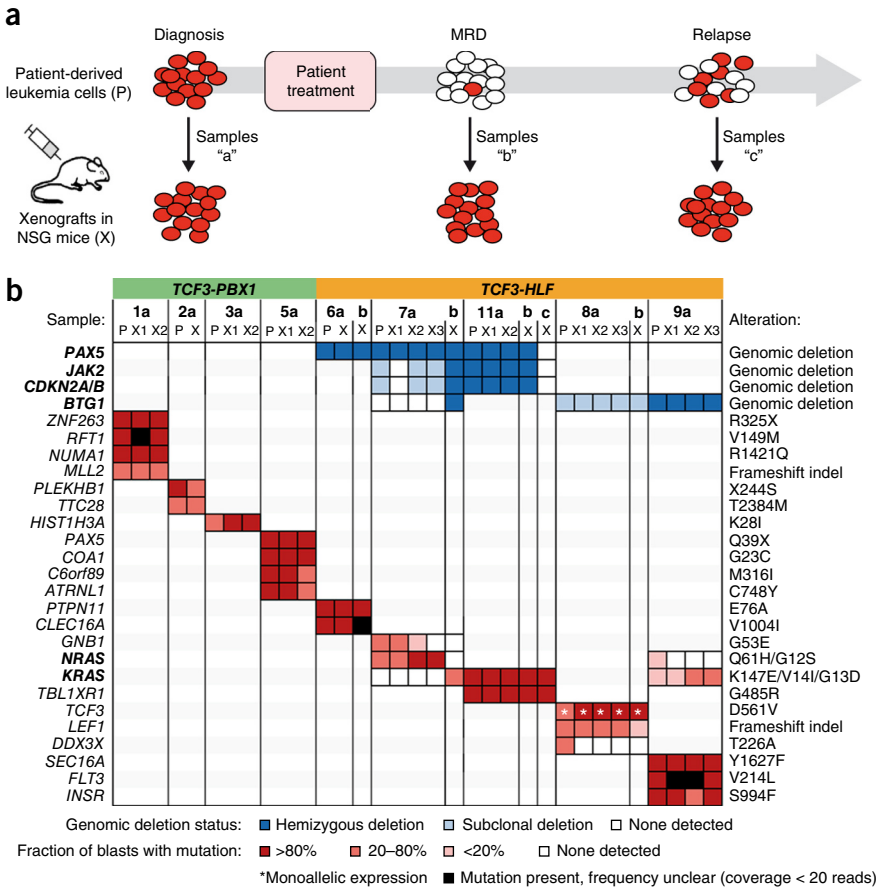

Figure 3 The genomic landscape of *TCF3-HLF*– and *TCF3-PBX1*–positive ALL is preserved in patient-derived leukemia xenografts. (**a**) Xenografts were established from cryopreserved patient samples at diagnosis (samples "a"), at follow-up with minimal residual disease (MRD, <1 leukemic cell in 10,000 cells, samples "b") or from disease progression (samples "c") and subjected to whole exome and transcriptome sequencing as well as multiplex ligation-dependent probe amplification (MLPA). All available MRD samples from *TCF3-HLF*–positive cases were successfully engrafted. (**b**) Comparison of all transcriptionally expressed nucleotide variations and of selected recurrent deletions frequently found in pediatric ALL in corresponding patient (P) and xenograft (X) samples. Deletions and nucleotide variations are colored according to their frequency in the analyzed leukemic cell population. Deletion frequencies were calculated by integrating whole genome and whole exome sequencing data with MLPA data. Nucleotide variation frequencies were calculated by integrating whole genome, whole exome and transcriptome sequencing data. Recurrently affected genes are indicated by bold symbols.

the two *TCF3*-translocated subtypes (**Fig. 2a**, and **Supplementary Tables 11** and **12**). *In silico* prediction of transcription factor binding sites in the corresponding promoter regions revealed enrichment for PBX (*Z* score = 3.72) and HLF (*Z* score = 2.99) binding motifs associated with *TCF3-PBX1* and *TCF3-HLF* gene signatures, respectively (**Supplementary Tables 13** and **14**). Further, *PBX1* and *HLF* were the only transcription factors among those with enriched binding motifs that were significantly differentially expressed between the two ALL subtypes, and between leukemia and remission samples. The chimeric *HLF* transcript was strongly induced in *TCF3-HLF*, but we detected no wild-type *HLF* expression. We predicted 39 potential HLF targets, including the known target *SNAI2* (*SLUG*)[16], *GPC4* and *BMP3* involved in stem cell proliferation, which showed induced expression in *TCF3-HLF* samples (**Supplementary Table 15**). Other potential TCF3-HLF targets that regulate developmental programs and cell survival, such as *LMO2* (ref. 14) and *BCL2* (ref. 14), were not predicted. However, their expression was increased in *TCF3-HLF*–positive ALL.

Gene set enrichment analysis using gene sets from sorted human hematopoietic stem cells and early progenitor populations[31] as well as curated oncogenic (C6) and human immunologic (C7) signatures from MsigDB[32] revealed an enrichment for stem cell and myeloid signatures in *TCF3-HLF*–positive ALL. In contrast, lymphoid features were more prominent in *TCF3-PBX1*–positive ALL (**Fig. 2b** and **Supplementary Table 16**). The hematopoietic stem cell signature[31] ranked among the top gene sets enriched in *TCF3-HLF*–positive ALL (**Fig. 2c** and **Supplementary Table 17**). We obtained similar results using an independent method based on text mining annotations (**Fig. 2d**, and **Supplementary Tables 18** and **19**). We also consistently detected high expression of the stem cell marker *LGR5* (ref. 33) in *TCF3-HLF*–positive ALL, suggesting a reactivation of immature features shared with other stem cell populations. Consistent with previous reports, the myeloid marker CD33 was expressed in *TCF3-HLF*–positive blasts, which provides a target for antibody-directed therapy[12,34]. Other differentially expressed genes, such as *BMP2* (ref. 35), could present additional therapeutic targets.

Our results are consistent with a model in which *TCF3-HLF* arises in lymphoid cells and promotes transcriptional reprogramming toward a hybrid hematopoietic state. We also detected features of mesenchyme-derived tissues in *TCF3-HLF*–positive ALL, which may indicate a profound cellular reprogramming toward a drug-resistant state.

Mutation profiles of *TCF3-HLF* ALL are conserved in xenografts

We generated leukemia xenografts in nonobese diabetic severe combined immunodeficiency (NOD/SCID)/IL2rγ^{null} (NSG) mice for all cases included in this study (**Supplementary Table 20**)[36,37]. We also established for the first time to our knowledge leukemia xenografts from follow-up samples with MRD, some with less than 0.1% ALL cells after induction chemotherapy (**Fig. 3a**, and **Supplementary Tables 1** and **20**). Leukemia and MRD engraftment was rapid with conserved and predictable kinetics for xenografts derived from the same patient (**Supplementary Fig. 7**), suggesting that no major adaptation to the mouse microenvironment was needed for proliferation. Most SNVs and intra-chromosomal deletions that had been present at diagnosis were conserved in the corresponding xenografts (**Fig. 3b** and **Supplementary Table 7**). Only deletions detected in the relapse sample 11c were not conserved in the corresponding xenografts, and a deletion in *BTG1* emerged in one MRD-derived sample (7b, **Supplementary Fig. 3c**,**d**). A few mutations were lost in MRD or relapse xenograft samples, including *GNB1* and *DDX3X*, indicating that these are probably dispensable or may cause drug sensitivity. Mutations in the RAS pathway were largely maintained in xenografts. However, the *NRAS* mutation p.Gln61His identified in the primary

MRD sample 7b was not detected in the corresponding xenograft. Instead, we identified a heterozygous damaging mutation in *KRAS* (p.Lys147Glu) associated with Noonan syndrome[38]. In patient 9a, we identified two subclones displaying either a *KRAS* (p.Gly13Asp) or an *NRAS* (p.Gly12Ser) mutation. The corresponding xenograft retained only the *KRAS* mutated subclone. Thus, maintenance and acquisition of RAS pathway mutations in xenografts support the notion that they occur later during selection at a multiclonal level and confer a selective advantage in *TCF3-HLF*–positive ALL. No other SNVs emerged *de novo* in the xenografts. In summary, the molecular characteristics of both leukemia subtypes were largely conserved in the xenografts, confirming the validity of this model.

TCF3-HLF–associated gene expression is maintained in xenografts

Hierarchical clustering based on the gene signature specifying the two leukemia subtypes showed that the expression profile and the subtype specificity of the primary leukemia were maintained in the xenografts (**Fig. 4**). The genes most significantly upregulated in matched patient and xenograft samples from *TCF3-HLF*–positive leukemia specified stem cell features (**Supplementary Tables 21** and **22**). Similar to the case in patient samples, we detected features of mesenchyme-derived tissues in xenografts derived from *TCF3-HLF*–positive ALL. *TCF3-HLF*–positive leukemias and xenografts displayed systematic downregulation of *PAX5* expression to halved levels. Though monoallelic deletions of *PAX5* were a prominent feature of *TCF3-HLF*–positive ALL, we also saw reduced expression in diploid cases, hinting at alternative molecular mechanisms. The recapitulation of this pattern in the xenograft samples enforces the notion that *TCF3-HLF*–positive leukemia emerges in a specific cellular context with reduced *PAX5* expression (**Supplementary Fig. 8**). The essential molecular features of *TCF3-HLF*–positive samples were maintained in xenografts, providing a useful model of this disease.

Drug activity profiling of *TCF3-HLF* and *TCF3-PBX1* ALL

To determine drug sensitivity and resistance profiles, we established ALL cocultures on human mesenchymal stromal cells under serum-free conditions[39]. Both subtypes depend on stroma for survival (**Supplementary Fig. 9**). *TCF3-PBX1*–positive ALL had a higher proportion of cells in S phase than *TCF3-HLF*–positive ALL on such cultures, reflecting consistent biological differences. By screening 98 bioactive agents, including many agents in clinical development (**Supplementary Table 23**), on an automated microscopy–based platform, we unambiguously discriminated the two translocations based on their drug sensitivity profiles, using either single (log half maximal inhibitory concentration (IC_{50}), **Fig. 5a** and **Supplementary Fig. 10**) or multiple response parameters ($logIC_{50}$, log 90% effective concentration (EC_{90}), $logEC_{50}$ and area under the curve (AUC), **Fig. 5b** and **Supplementary Table 24**). To capture informative differences, we compared the responses of xenografts derived from *TCF3-HLF*–positive ALL to xenografts derived from other high-risk pre-B and T ALL patients on the same platform (**Fig. 5c** and **Supplementary Table 25**). This provided information about the activity range of each drug on the respective ALL subtype. *TCF3-HLF*–positive cases were consistently more resistant to various drugs from the same class, including nucleotide analogs (for example, cytarabine), mitotic spindle inhibitors (for example, vincristine), polo-like and aurora kinase inhibitors. Given the importance of cytarabine and vincristine in standard ALL therapy, the implications of these observations need to be further explored. *TCF3-HLF*–positive ALL was very resistant to dasatinib in this assay, whereas *TCF3-PBX1*–positive ALL responded well. This partly challenges a recent report[40], which had proposed dasatinib as an alternative for the treatment of these leukemias based on strong *in vitro* activity in one *TCF3-HLF*– and ten *TCF3-PBX1*–positive primary ALL samples. However, *in vivo* studies will be required to verify these differences in drug response, as differences in cell-cycle activity may influence the pattern of response *in vitro*.

TCF3-HLF–positive ALL were sensitive to glucocorticoids (prednisone and dexamethasone) and to other drugs that could be relevant for the treatment of resistant ALL, including mTOR inhibitors, anthracyclines, bortezomib, the HSP90 inhibitor AUY922 and panobinostat. However, in spite of the good response of patients with *TCF3-HLF*–positive leukemia to prednisone therapy and the observed responsiveness of *TCF3-HLF*–positive ALL cells to glucocorticoids and anthracyclines that are commonly used in ALL treatment, patients who undergo this treatment relapse. Our transcriptome data suggested that resistance to apoptosis due to high expression of the anti-apoptotic oncoprotein BCL2 might promote cancer cell survival and constitute a druggable target (**Supplementary Fig. 11**). *BCL2* is a putative transcriptional target of TCF3-HLF[14]. Of note, PAX5, commonly deleted in our cohort, normally represses *BCL2* transcription[41].

TCF3-HLF ALL is extremely sensitive to the BCL2 antagonist venetoclax

To assess the role of *BCL2* overexpression in *TCF3-HLF*–positive ALL and to provide preclinical evidence for therapeutic activity,

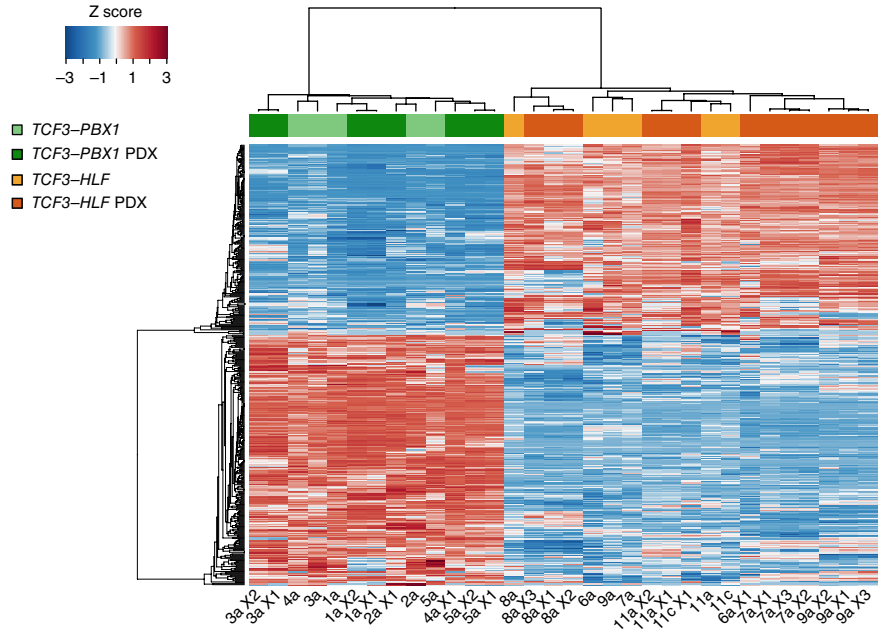

Figure 4 Major components of the gene expression signature of *TCF3-HLF*– and *TCF3-PBX1*–positive ALL are conserved in patient-derived xenografts. Hierarchical clustering of primary and patient derived xenograft (PDX) ALL samples based on the expression of the 401 genes of the signature defined with primary samples (**Fig. 2**) shows that xenografts clearly group with their corresponding primary samples.

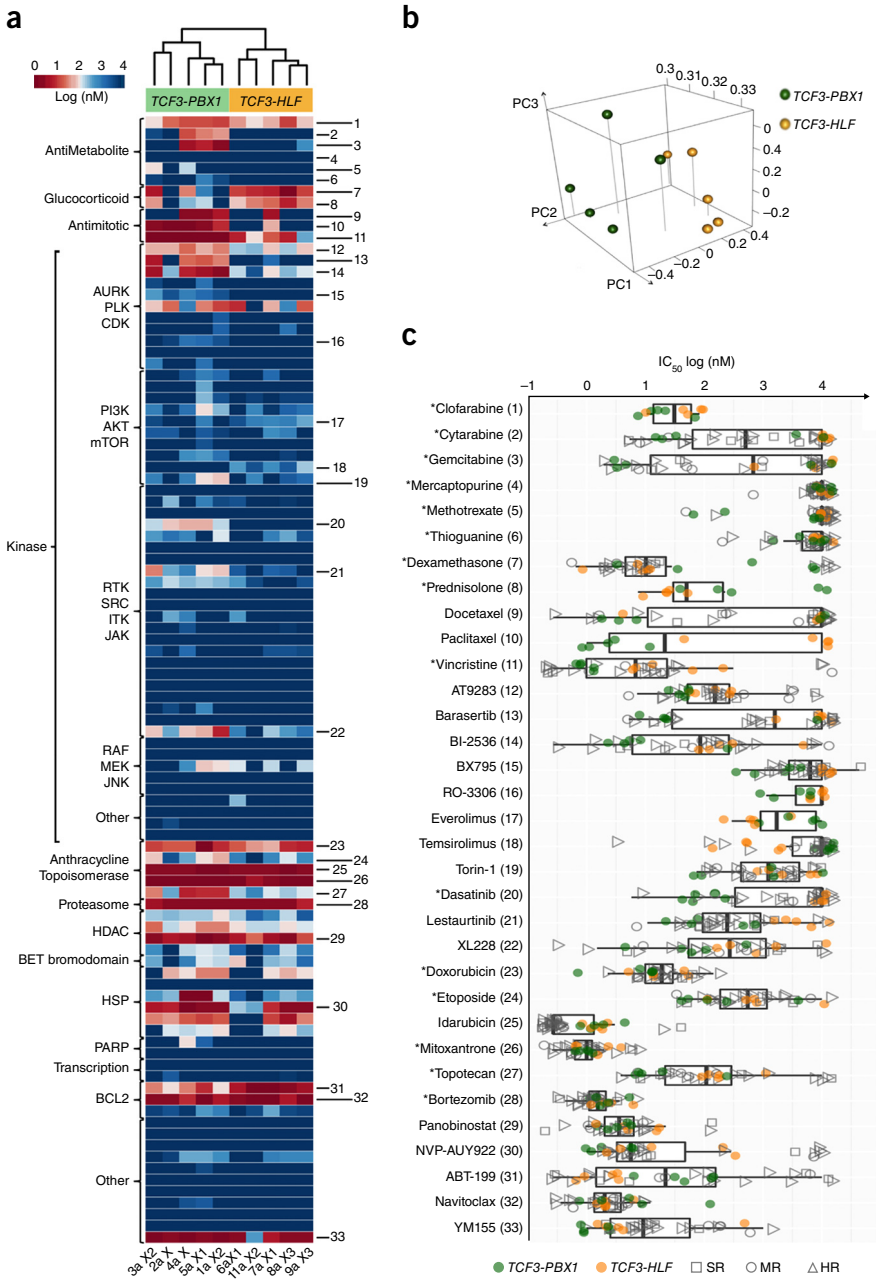

Figure 5 Drug activity profiling of *TCF3*-translocated leukemia reveals relevant differences in drug sensitivity. (**a**) Unsupervised clustering based on the drug activity profile of 98 compounds (log IC_{50}). Fitted values are provided in **Supplementary Table 24** (absolute IC_{50}). Numbers identify the compounds shown in **c**. (**b**) Principal component analysis of the response variables IC_{50}, EC_{50}, EC_{90} and AUC (**Supplementary Table 24**) show *TCF3-PBX1*–positive and *TCF3-HLF*–positive ALL in two distinct clusters. The separation of *TCF3-PBX1*–positive and *TCF3-HLF*–positive ALL is determined by responses to topoisomerases, BCL2 inhibitors, glucocorticoids and antimitotic agents, which correlate with the first three principal components. (**c**) Selection of drugs based on differences in sensitivity or resistance in *TCF3-PBX1*–positives and *TCF3-HLF*–positives. For comparison, the corresponding drug activity is indicated for 25 additional ALL samples tested on the same platform, including standard risk (SR, $n = 5$), medium risk (MR, $n = 4$) and high risk (HR, $n = 16$) cases (**Supplementary Table 25**). Boxplots extend from the first to the third quartiles (hinges) of the response range for each compound. Whiskers correspond to values from the hinge to the lowest or highest values within 1.5× of the distance between the first and third quartiles, respectively. Drugs with differential activity include docetaxel, paclitaxel, vincristine, AT9283, barasertib, BI2536, torin-1, dasatinib, lestaurtinib and XL228 ($P \leq 0.05$). Drugs which are active across the patients include doxorubicin, idarubicin, mitoxantrone, bortezomib, panobinostat, NVP-AUY922, ABT-199 (venetoclax) and navitoclax. Asterisks indicate drugs currently in clinical use.

we tested the BCL2-targeting drug venetoclax (ABT-199) in our xenograft model (**Fig. 5c**). This BH3-mimetic compound is a highly specific small molecule inhibitor that competes with pro-apoptotic BCL2 family proteins for binding to BCL2, and shifts the balance of pro-death and pro-survival signals inside the cell in favor of cell death[42]. Venetoclax is in clinical development (phase II and III trials) for chronic lymphocytic leukemia and lymphoma, and holds promise for ALL and acute myeloid leukemia.

TCF3-HLF–positive ALL samples were more sensitive to venetoclax than *TCF3-PBX1*–positive samples (**Fig. 6a**), which correlated with higher *BCL2* transcript and protein expression (**Fig. 6b**). A two-week treatment course of daily venetoclax administration delayed leukemia progression significantly in ALL xenografts from three different *TCF3-HLF*–positive cases (**Fig. 6c**,**d**). Treatment of mice in the control arm that reached maximal leukemia burden resulted in very rapid reduction of the leukemic load (**Fig. 6e**). Xenografts from MRD or relapse remained sensitive to venetoclax (**Supplementary Fig. 11**). Profiling of primary cells from two additional cases with refractory ALL confirmed exquisite sensitivity to venetoclax (**Supplementary Fig. 12**). Combined treatment of patient-derived xenografts from patients 6–11 with venetoclax and either vincristine or dexamethasone indicated a potentially synergistic effect in some of those patients (**Supplementary Fig. 13** and **Supplementary Table 26**). Our data identified BCL2 dependency in *TCF3-HLF* ALL as a druggable target, and illustrate how integration of drug response profiling and molecular genetic analyses can inform the development of innovative treatment strategies in patients with unmet therapeutic needs.

DISCUSSION

To our knowledge, a long-term cure has never been achieved for patients with *TCF3-HLF*–positive ALL. Our study revealed a recurrent pattern of *TCF3-HLF* accompanied by abnormalities that affect transcriptional regulation of lymphoid development. We found frequent deletions of *PAX5* and *VPREB1* in association with *TCF3-HLF*, but did not detect deletions of Ikaros family members, which are commonly affected in ALL[1,23]. We also uncovered recurrent mutations of the transcription factor TCF3, which acts upstream of PAX5 in

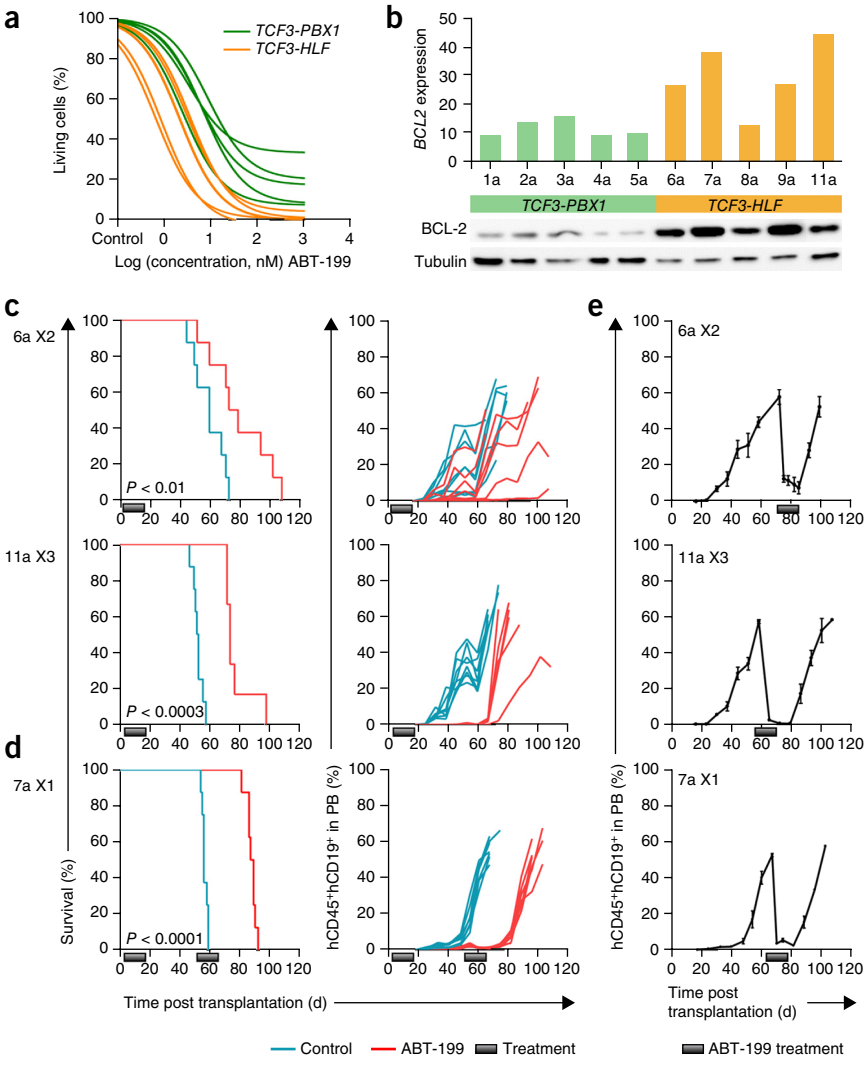

Figure 6 The BCL2 antagonist ABT-199 (venetoclax) shows promising anti-leukemic activity in *TCF3-HLF*–positive xenografts. (**a**) *In vitro* dose response curves normalized against DMSO-treated controls. (**b**) Merged absolute reads per kilobase of exon model per million mapped reads (RPKM) values of xenografts derived from the same primary leukemia sample (top) and immunoblot for BCL2 (bottom) in patient-derived xenografts as indicated. Tubulin was used as a loading control. (**c**,**d**) *In vivo* response to ABT-199 on *TCF3-HLF*–positive xenografts. Treatment (gray bars) with 100 mg kg^{-1} qd ABT-199 (red) or with vehicle control (turquoise) were administered orally for 14 d (6–8 mice per treatment arm). Two treatment courses were administrated to xenograft 7a. For survival analysis an event was defined when at least 25% of leukemic cells were detected by FACS ($mCD45^{-}hCD19^{+}hCD45^{+}$) in the peripheral blood. Differences in the survival of mice receiving ABT-199 or vehicle control were determined by the Mantel-Cox test and verified by the Gehan-Breslow-Wilcoxon test. (**e**) Mice from the control arm of **c**,**d** were treated with ABT-199 when more than 50% of ALL cells were detected in the blood. Mean and s.d. are shown ($n = 4$).

lymphoid development, potentially impairing structural interactions with other transcription cofactors[29]. *PAX5* expression was reduced by twofold in all *TCF3-HLF*–positive cases, underscoring the possibility of an interaction between TCF3-HLF, TCF3 and PAX5. *PAX5* is required for B lymphoid lineage commitment and maturation[43], and is frequently deleted in high-risk ALL with complex patterns of copy number abnormalities[23]. Similarly, deletions in *IKFZ1*, which is required for the development of B and T lymphoid lineages and has additional stem cell–like functions[44], are detected both in high-risk *BCR-ABL1*–positive and –negative ALL, and in the more favorable *ERG*-altered ALL subtype[45], but never in *TCF3-HLF*–positive ALL. We also detected focal deletions of *VPREB1* in *TCF3-HLF* ALL, which may lead to a developmental arrest associated with lack of pre–B cell receptor formation and the resulting loss of negative feedback on RAG-mediated recombination[46]. *VPREB1* deletions were present at a similar frequency compared to other high-risk ALLs, such as *BCR-ABL1*–like and *BCR-ABL1*–positive ALL (~30–40% of cases)[47] or hypodiploid ALL (~30%)[24], associated with poorer overall survival in high-risk pre–B cell ALL patients[24]. However, specific ALL subtypes associated with good prognosis (for example, *ETV6-RUNX1*–positive ALL) also present high frequencies of *VPREB1* deletions[24], suggesting an important impact of the genomic context[24]. Thus, distinct patterns of association emerge that are likely to reflect important underlying biological mechanisms. Based on our results, we propose that a reduction of *PAX5* gene dosage constitutes a favorable context for the oncogenic activity of *TCF3-HLF*.

As observed for hypodiploid ALL[5] and in subsets of *MLL*-rearranged ALL[48], we identified mutations in *NRAS*, *KRAS* and *PTPN11* in *TCF3-HLF*–positive ALL. In our xenograft models we detected variable persistence of *NRAS* and a switch to *KRAS* mutations, indicating that RAS mutations are multiclonal and might not be strictly required for disease progression in *TC3-HLF*–positive ALL. Indeed, mutations in the RAS pathway are enriched at relapse in ALL[7,30,48] but mostly in a subclonal pattern with losses or switches in *NRAS* and *KRAS* from diagnosis to relapse. These represent secondary events, possibly compensating functional effects of the initiating events. Mutations in the RAS pathway might not represent optimal therapeutic targets, given their volatility and the potential to select for slower-proliferating, more resistant subclones. The *TCF3-HLF* gene expression signature, enriched for components of stem cell and myelomonocytic stages, was very similar among leukemias and maintained in xenografts, specifying additional, novel markers associated with stem cell function, such as *LGR5*, which marks epithelial stem cells[49] and embryonic and fetal hematopoietic progenitor cells in mice[50]. Thus, in analogy to experimental induction of pluripotent stem cells[51,52], *TCF3-HLF* likely induces a whole set of factors that carry out reprogramming and leukemic transformation in the context of low *PAX5* expression. Deletion of *PAX5* in early B cell progenitors induced dedifferentiation to a state with myeloid and T cell potential[43,53]. Moreover, rescue with low-level expression of PAX5 in knockout mice generates a stalled biphenotypic B-lymphoid/myeloid state[54]. Together with an activating mutation in *STAT5*, *PAX5* haploinsufficiency initiates ALL in mice[41]. Based on these data, we propose that the initiating *TCF3-HLF* fusion results in severe transcriptional reprogramming with dedifferentiation. The favorable context for transformation is secured through

secondary cooperating lesions in early B cell differentiation genes including *TCF3* and *PAX5*.

A central question remains pertaining to the cell of origin in different ALL subtypes. Our study provides important clues that should be further addressed using disease models. The molecular analysis of the *TCF3-HLF* and *TCF3-PBX1* fusion gene breakpoints indicated that the *TCF3-HLF*, like the *TCF-PBX1* translocation, originates in cells already committed to lymphoid differentiation. Furthermore, we found the associated somatic structural variants to be RAG-mediated, which is comparable to patterns identified recently in *ETV6-RUNX1*–positive ALL, the most frequent pre-B cell ALL subtype, which is consistent with expression of RAG in *TCF3-HLF*–positive ALL[55]. We favor the hypothesis that the *TCF3-HLF* translocation occurs in a B cell progenitor and that the specific lineage context is constrained further in a restricted developmental stage by additional mutations. The detection of *TCF3-HLF* being restricted to leukemic cells supports this idea, although initiation in a more immature compartment cannot be formally excluded.

The molecular landscapes of *TCF3-HLF*–positive ALL were largely conserved in xenografts, providing a valuable, well characterized, model for preclinical testing. Drug activity profiling revealed that *TCF3-HLF*–positive cases were more resistant to several standard ALL drugs, such as nucleotide analogs (for example, cytarabin) and mitotic spindle inhibitors (for example, vincristine). We detected activity for other relevant drug classes, such as mTOR inhibitors, the proteasome inhibitor bortezomib, the HSP90 inhibitor AUY922 and the HDAC inhibitor panobinostat. The BCL2 inhibitor venetoclax (ABT-199)[42] was highly active in all *TCF3-HLF*–positive cases analyzed, which we confirmed using primary ALL cells from two additional cases with refractory disease. These results refine data obtained using the broader spectrum BH3 mimetic ABT-737 in *TCF3-HLF*–positive cell lines[14]. Given the activity of venetoclax also in other ALL subsets including immature T cell ALL (refs. 56,57 and our own unpublished data) and the lack of on-target thrombocytopenia caused by ABT-737, venetoclax should be explored for experimental therapy in refractory ALL in selected cases based on such functional data. Thus integrated genomic and functional analyses of *TCF3-HLF*–positive ALL provide insight into the molecular context and associated components and offer unprecedented possibilities to investigate new agents for the treatment of these children who currently lack effective therapeutic options.

URLs. Information on the two image processing programs used for *in vitro* drug screening and automated microscopy can be found at http://acc.ethz.ch/.

METHODS

Methods and any associated references are available in the online version of the paper.

Accession codes. Sequencing data are available from the public POPGEN repository (2015-UFO-NG-1; Christian Albrechts University, Kiel) upon written request accompanied by a positive internal review board vote for research addressing leukemia-related questions. Sequencing data transfer can proceed upon positive review and signing of a material transfer agreement.

ACKNOWLEDGMENTS

We thank all participants and personnel involved in the clinical trials in Austria, France, Germany, United Kingdom and Switzerland. We thank T. Radimerski and Novartis for providing essential compounds. We thank the Leukaemia & Lymphoma Research (LLR) Childhood Leukaemia Cell Bank in the UK for providing primary patient samples. This work was supported by the German Federal Office for Radiation Protection (grant St.Sch. 3611S70014), by the Swiss National Research Foundation SNF 310030-133108, the foundation 'Kinderkrebsforschung Schweiz', the 'Krebsliga Zurich', the Sassella Foundation, the Fondation Panacée, the clinical research focus program 'Human Hemato-Lymphatic Diseases' of the University of Zurich, the Deutsche Forschungsgemeinschaft (DFG), Clusters of Excellence 'Inflammation at Interfaces', the EU Seventh Framework Program (FP7/2007-2013, grant 262055, ESGI; FP7-HEALTH-F2-2011 grant 261474, ENCCA; ERA-Net Transcan, Validation of biomarkers for personalized cancer medicine, TRANSCALL; Health-F2-2010 grant 260791, EUROCANPLATFORM), the 'Katharina Hardt Stiftung', the 'Deutsche José Carreras Leukämie-Stiftung', the 'Madeleine Schickedanz-Kinderkrebs-Stiftung', the 'Deutsche Krebshilfe – Dr. Mildred Scheel Stiftung' (grants 108613, 102588 and 108588), the Foundation of Experimental Biomedicine in Zurich, the Max Planck Society, and the 'Verein für krebskranke Kinder Hannover e.V.'. We thank A. Dehos, B. Grosche, T. Jung, W. Weiss and G. Ziegelberger, German Federal Office for Radiation Protection, as well as B. Heinzow, State Office for Social Services of Schleswig-Holstein, and A. Böttger, German Federal Ministry for the Environment, Nature Conservation, Building and Nuclear Safety for their support and critical discussions. We are grateful for the excellent technical assistance offered by the sequencing team of the Department of Vertebrate Genomics of the Max Planck Institute for Molecular Genetics (Berlin) and by the team of the Genomics Core facility of the European Molecular Biology Laboratory. We thank K. Alemazkour for excellent technical assistance regarding whole exome sequencing at the Department of Pediatric Oncology, Hematology and Clinical Immunology (Düsseldorf, Germany). We thank N. Forgo, Institute for Legal Informatics, Leibniz University Hannover, and H.-D. Tröger, Hannover Medical School, for legal and ethical counselling.

AUTHOR CONTRIBUTIONS

A. Borkhardt, A.F., J.O.K., J.-P.B., M.-L.Y. and M. Stanulla jointly designed the project. A. Baruchel, A.V., A.V.M., C.C., C.P.K., F.N., G.B., G.C., G.t.K., H.C., M. Schrappe, M. Stanulla, N.v.d.W., O.A.H., C.E. and R.P.-G. provided samples or clinical data. A. Borkhardt, A.C.M., A.F., A.V., C.E., G.H.-S., H.L., J.-P.B., J.O.K., J.T., M.D., M.F., M.-L.Y., M.P.D., M. Schrappe, M. Stanulla, M. Zimmermann, O.A.H., P.R. and T.Z. contributed reagents, materials or analysis tools. A.M.S., B.B., B.M., C.E., C.L.W., H.-J.W., J.I.H., J.-P.B., M.F., M.G., S. Sungalee and U.F. designed experiments. A.M.S., A.R., B.B., B.R., B.S., B.S.P., C.E., C.K., C.L.W., D.D., D.S., H.-J.W., J.T., K.H., L.Z., M.G., M.R., M. Zaliova, M. Sultan, P.K., S.E., S. Sungalee, T.B., U.F. and V.F. performed experiments. A.R., B.S., B.S.P., C.E., C.K., C.L.W., D.S., E.E., J.I.H., H.-J.W., M.G., M.P.D., M.F., N.B., S.G., G.H.-S., P.H., P.K., M.-L.Y., M.R., M. Stanulla, M. Schütte, M. Zaliova, S. Sungalee, T.R., U.F. and V.A. analyzed data. A. Borkhardt, A.C.M., A.F., B.B., H.L., J.-P.B., J.O.K., M.D., M.F., M.-L.Y., M. Stanulla, O.H., R.T. and S. Schreiber, U.F. supervised research. A.R., C.L.W., D.S., H.-J.W., M.F., M.P.D., M. Stanulla, P.K., S. Sungalee, T.R. and U.F. prepared tables and figures. J.-P.B., M. Stanulla and M.-L.Y. wrote the manuscript. A. Borkhardt, A.F., A.R., A.V.M., H.-J.W., J.O.K., M.F., M.P.D., O.H., S.H., S. Sungalee, T.R. and U.F. contributed to the writing of the manuscript. All authors critically reviewed the manuscript for its content.

COMPETING FINANCIAL INTERESTS

The authors declare no competing financial interests.

1. Mullighan, C.G. *et al.* Genome-wide analysis of genetic alterations in acute lymphoblastic leukaemia. *Nature* **446**, 758–764 (2007).
2. Russell, L.J. *et al.* Deregulated expression of cytokine receptor gene, CRLF2, is involved in lymphoid transformation in B-cell precursor acute lymphoblastic leukemia. *Blood* **114**, 2688–2698 (2009).
3. Mullighan, C.G. *et al.* Rearrangement of CRLF2 in B-progenitor- and Down syndrome-associated acute lymphoblastic leukemia. *Nat. Genet.* **41**, 1243–1246 (2009).
4. Hertzberg, L. *et al.* Down syndrome acute lymphoblastic leukemia, a highly heterogeneous disease in which aberrant expression of CRLF2 is associated with mutated JAK2: a report from the International BFM Study Group. *Blood* **115**, 1006–1017 (2010).
5. Holmfeldt, L. *et al.* The genomic landscape of hypodiploid acute lymphoblastic leukemia. *Nat. Genet.* **45**, 242–252 (2013).
6. Zhang, J. *et al.* Key pathways are frequently mutated in high-risk childhood acute lymphoblastic leukemia: a report from the Children's Oncology Group. *Blood* **118**, 3080–3087 (2011).
7. Irving, J. *et al.* Ras pathway mutations are highly prevalent in relapsed childhood acute lymphoblastic leukaemia, may act as relapse-drivers and confer sensitivity to MEK inhibition. *Blood* **124**, 3420–3430 (2014).

8. Inaba, H., Greaves, M. & Mullighan, C.G. Acute lymphoblastic leukaemia. *Lancet* **381**, 1943–1955 (2013).
9. Kwon, K. *et al.* Instructive role of the transcription factor E2A in early B lymphopoiesis and germinal center B cell development. *Immunity* **28**, 751–762 (2008).
10. Felice, M.S. *et al.* Prognostic impact of t(1;19)/ TCF3–PBX1 in childhood acute lymphoblastic leukemia in the context of Berlin-Frankfurt-Munster-based protocols. *Leuk. Lymphoma* **52**, 1215–1221 (2011).
11. Hunger, S.P., Ohyashiki, K., Toyama, K. & Cleary, M.L. Hlf, a novel hepatic bZIP protein, shows altered DNA-binding properties following fusion to E2A in t(17;19) acute lymphoblastic leukemia. *Genes Dev.* **6**, 1608–1620 (1992).
12. Inukai, T. *et al.* Hypercalcemia in childhood acute lymphoblastic leukemia: frequent implication of parathyroid hormone-related peptide and E2A-HLF from translocation 17;19. *Leukemia* **21**, 288–296 (2007).
13. Boller, S. & Grosschedl, R. The regulatory network of B-cell differentiation: a focused view of early B-cell factor 1 function. *Immunol. Rev.* **261**, 102–115 (2014).
14. de Boer, J. *et al.* The E2A-HLF oncogenic fusion protein acts through Lmo2 and Bcl-2 to immortalize hematopoietic progenitors. *Leukemia* **25**, 321–330 (2011).
15. Hirose, K. *et al.* Aberrant induction of LMO2 by the E2A-HLF chimeric transcription factor and its implication in leukemogenesis of B-precursor ALL with t(17;19). *Blood* **116**, 962–970 (2010).
16. Inukai, T. *et al.* SLUG, a ces-1-related zinc finger transcription factor gene with antiapoptotic activity, is a downstream target of the E2A-HLF oncoprotein. *Mol. Cell* **4**, 343–352 (1999).
17. Inoue, A. *et al.* Slug, a highly conserved zinc finger transcriptional repressor, protects hematopoietic progenitor cells from radiation-induced apoptosis in vivo. *Cancer Cell* **2**, 279–288 (2002).
18. Honda, H. *et al.* Expression of E2A-HLF chimeric protein induced T-cell apoptosis, B-cell maturation arrest, and development of acute lymphoblastic leukemia. *Blood* **93**, 2780–2790 (1999).
19. Smith, K.S., Rhee, J.W., Naumovski, L. & Cleary, M.L. Disrupted differentiation and oncogenic transformation of lymphoid progenitors in E2A-HLF transgenic mice. *Mol. Cell. Biol.* **19**, 4443–4451 (1999).
20. Hunger, S.P. Chromosomal translocations involving the E2A gene in acute lymphoblastic leukemia: clinical features and molecular pathogenesis. *Blood* **87**, 1211–1224 (1996).
21. Wiemels, J.L. *et al.* Site-specific translocation and evidence of postnatal origin of the t(1;19) E2A–PBX1 fusion in childhood acute lymphoblastic leukemia. *Proc. Natl. Acad. Sci. USA* **99**, 15101–15106 (2002).
22. Tsai, A.G. *et al.* Human chromosomal translocations at CpG sites and a theoretical basis for their lineage and stage specificity. *Cell* **135**, 1130–1142 (2008).
23. Moorman, A.V. *et al.* A novel integrated cytogenetic and genomic classification refines risk stratification in pediatric acute lymphoblastic leukemia. *Blood* **124**, 1434–1444 (2014).
24. Mangum, D.S. *et al.* VPREB1 deletions occur independent of lambda light chain rearrangement in childhood acute lymphoblastic leukemia. *Leukemia* **28**, 216–220 (2014).
25. Waanders, E. *et al.* The origin and nature of tightly clustered BTG1 deletions in precursor B-cell acute lymphoblastic leukemia support a model of multiclonal evolution. *PLoS Genet.* **8**, e1002533 (2012).
26. Tijchon, E., Havinga, J., van Leeuwen, F.N. & Scheijen, B. B-lineage transcription factors and cooperating gene lesions required for leukemia development. *Leukemia* **27**, 541–552 (2013).
27. Balbin, O.A. *et al.* Reconstructing targetable pathways in lung cancer by integrating diverse omics data. *Nat. Commun.* **4**, 2617 (2013).
28. Wright, D.D., Sefton, B.M. & Kamps, M.P. Oncogenic activation of the Lck protein accompanies translocation of the LCK gene in the human HSB2 T-cell leukemia. *Mol. Cell. Biol.* **14**, 2429–2437 (1994).
29. Schmitz, R. *et al.* Burkitt lymphoma pathogenesis and therapeutic targets from structural and functional genomics. *Nature* **490**, 116–120 (2012).
30. Ma, X. *et al.* Rise and fall of subclones from diagnosis to relapse in pediatric B-acute lymphoblastic leukaemia. *Nat. Commun.* **6**, 6604 (2015).
31. Laurenti, E. *et al.* The transcriptional architecture of early human hematopoiesis identifies multilevel control of lymphoid commitment. *Nat. Immunol.* **14**, 756–763 (2013).
32. Subramanian, A., Kuehn, H., Gould, J., Tamayo, P. & Mesirov, J.P. GSEA-P: a desktop application for Gene Set Enrichment Analysis. *Bioinformatics* **23**, 3251–3253 (2007).
33. Schepers, A.G. *et al.* Lineage tracing reveals Lgr5$^+$ stem cell activity in mouse intestinal adenomas. *Science* **337**, 730–735 (2012).
34. Akahane, K. *et al.* Specific induction of CD33 expression by E2A-HLF: the first evidence for aberrant myeloid antigen expression in ALL by a fusion transcription factor. *Leukemia* **24**, 865–869 (2010).
35. Nissim, S. *et al.* Prostaglandin E2 regulates liver versus pancreas cell-fate decisions and endodermal outgrowth. *Dev. Cell* **28**, 423–437 (2014).
36. Schmitz, M. *et al.* Xenografts of highly resistant leukemia recapitulate the clonal composition of the leukemogenic compartment. *Blood* **118**, 1854–1864 (2011).
37. Bonapace, L. *et al.* Induction of autophagy-dependent necroptosis is required for childhood acute lymphoblastic leukemia cells to overcome glucocorticoid resistance. *J. Clin. Invest.* **120**, 1310–1323 (2010).
38. Stark, Z. *et al.* Two novel germline KRAS mutations: expanding the molecular and clinical phenotype. *Clin. Genet.* **81**, 590–594 (2012).
39. Boutter, J. *et al.* Image-based RNA interference screening reveals an individual dependence of acute lymphoblastic leukemia on stromal cysteine support. *Oncotarget* **5**, 11501–11512 (2014).
40. Bicocca, V.T. *et al.* Crosstalk between ROR1 and the Pre-B cell receptor promotes survival of t(1;19) acute lymphoblastic leukemia. *Cancer Cell* **22**, 656–667 (2012).
41. Heltemes-Harris, L.M. *et al.* Ebf1 or Pax5 haploinsufficiency synergizes with STAT5 activation to initiate acute lymphoblastic leukemia. *J. Exp. Med.* **208**, 1135–1149 (2011).
42. Souers, A.J. *et al.* ABT-199, a potent and selective BCL-2 inhibitor, achieves antitumor activity while sparing platelets. *Nat. Med.* **19**, 202–208 (2013).
43. Rolink, A.G., Nutt, S.L., Melchers, F. & Busslinger, M. Long-term in vivo reconstitution of T-cell development by Pax5-deficient B-cell progenitors. *Nature* **401**, 603–606 (1999).
44. Joshi, I. *et al.* Loss of Ikaros DNA-binding function confers integrin-dependent survival on pre-B cells and progression to acute lymphoblastic leukemia. *Nat. Immunol.* **15**, 294–304 (2014).
45. Clappier, E. *et al.* An intragenic ERG deletion is a marker of an oncogenic subtype of B-cell precursor acute lymphoblastic leukemia with a favorable outcome despite frequent IKZF1 deletions. *Leukemia* **28**, 70–77 (2014).
46. Grawunder, U. *et al.* Down-regulation of RAG1 and RAG2 gene expression in preB cells after functional immunoglobulin heavy chain rearrangement. *Immunity* **3**, 601–608 (1995).
47. Den Boer, M.L. *et al.* A subtype of childhood acute lymphoblastic leukaemia with poor treatment outcome: a genome-wide classification study. *Lancet Oncol.* **10**, 125–134 (2009).
48. Andersson, A.K. *et al.* The landscape of somatic mutations in infant MLL-rearranged acute lymphoblastic leukemias. *Nat. Genet.* **47**, 330–337 (2015).
49. Barker, N. *et al.* Identification of stem cells in small intestine and colon by marker gene Lgr5. *Nature* **449**, 1003–1007 (2007).
50. Liu, D. *et al.* Leucine-rich repeat-containing G-protein-coupled Receptor 5 marks short-term hematopoietic stem and progenitor cells during mouse embryonic development. *J. Biol. Chem.* **289**, 23809–23816 (2014).
51. Riddell, J. *et al.* Reprogramming committed murine blood cells to induced hematopoietic stem cells with defined factors. *Cell* **157**, 549–564 (2014).
52. Sandler, V.M. *et al.* Reprogramming human endothelial cells to haematopoietic cells requires vascular induction. *Nature* **511**, 312–318 (2014).
53. Urbánek, P., Wang, Z.Q., Fetka, I., Wagner, E.F. & Busslinger, M. Complete block of early B cell differentiation and altered patterning of the posterior midbrain in mice lacking Pax5/BSAP. *Cell* **79**, 901–912 (1994).
54. Simmons, S. *et al.* Biphenotypic B-lymphoid/myeloid cells expressing low levels of Pax5: potential targets of BAL development. *Blood* **120**, 3688–3698 (2012).
55. Papaemmanuil, E. *et al.* RAG-mediated recombination is the predominant driver of oncogenic rearrangement in ETV6-RUNX1 acute lymphoblastic leukemia. *Nat. Genet.* **46**, 116–125 (2014).
56. Peirs, S. *et al.* ABT-199 mediated inhibition of BCL-2 as a novel therapeutic strategy in T-cell acute lymphoblastic leukemia. *Blood* **124**, 3738–3747 (2014).
57. Chonghaile, T.N. *et al.* Maturation stage of T-cell acute lymphoblastic leukemia determines BCL-2 versus BCL-XL dependence and sensitivity to ABT-199. *Cancer Discov.* **4**, 1074–1087 (2014).
58. El Omari, K. *et al.* Structural basis for LMO2-driven recruitment of the SCL: E47bHLH heterodimer to hematopoietic-specific transcriptional targets. *Cell Rep.* **4**, 135–147 (2013).

Ute Fischer[1,26], Michael Forster[2,26], Anna Rinaldi[3,26], Thomas Risch[4,26], Stéphanie Sungalee[5,26], Hans-Jörg Warnatz[4,26], Beat Bornhauser[3], Michael Gombert[1], Christina Kratsch[6], Adrian M Stütz[5], Marc Sultan[4], Joelle Tchinda[3], Catherine L Worth[4], Vyacheslav Amstislavskiy[4], Nandini Badarinarayan[2], André Baruchel[7], Thies Bartram[8], Giuseppe Basso[9], Cengiz Canpolat[10], Gunnar Cario[8], Hélène Cavé[11], Dardane Dakaj[3], Mauro Delorenzi[12,13], Maria Pamela Dobay[13], Cornelia Eckert[14], Eva Ellinghaus[2], Sabrina Eugster[3], Viktoras Frismantas[3], Sebastian Ginzel[1,15], Oskar A Haas[16], Olaf Heidenreich[17], Georg Hemmrich-Stanisak[2], Kebria Hezaveh[1], Jessica I Höll[1], Sabine Hornhardt[18], Peter Husemann[1],

Priyadarshini Kachroo[2], Christian P Kratz[19], Geertruy te Kronnie[9], Blerim Marovca[3], Felix Niggli[3], Alice C McHardy[6], Anthony V Moorman[17], Renate Panzer-Grümayer[16], Britt S Petersen[2], Benjamin Raeder[5], Meryem Ralser[4], Philip Rosenstiel[2], Daniel Schäfer[1], Martin Schrappe[8], Stefan Schreiber[2], Moritz Schütte[20], Björn Stade[2], Ralf Thiele[15], Nicolas von der Weid[21], Ajay Vora[22], Marketa Zaliova[19,23], Langhui Zhang[1,24], Thomas Zichner[5], Martin Zimmermann[19], Hans Lehrach[4,20,25], Arndt Borkhardt[1,27], Jean-Pierre Bourquin[3,27], Andre Franke[2,27], Jan O Korbel[5,27], Martin Stanulla[19,27] & Marie-Laure Yaspo[4,27]

[1]Clinic for Pediatric Oncology, Hematology and Clinical Immunology, Medical Faculty, Heinrich Heine University, Düsseldorf, Germany. [2]Institute of Clinical Molecular Biology, Christian Albrechts University of Kiel, Kiel, Germany. [3]Pediatric Oncology, Children's Research Centre, University Children's Hospital Zurich, Zurich, Switzerland. [4]Department of Vertebrate Genomics, Max Planck Institute for Molecular Genetics, Berlin, Germany. [5]European Molecular Biology Laboratory (EMBL), Genome Biology Unit, Heidelberg, Germany. [6]Department of Algorithmic Bioinformatics, Heinrich Heine University, Düsseldorf, Germany. [7]Department of Pediatric Hemato-Immunology, Hôpital Robert Debré and Paris Diderot University, Paris, France. [8]Department of Pediatrics, Christian Albrechts University of Kiel and University Medical Center Schleswig-Holstein, Kiel, Germany. [9]Department of Pediatrics, Laboratory of Pediatric Hematology/Oncology, University of Padova, Padova, Italy. [10]Department of Pediatrics, Acıbadem University Medical School, Ataşehir, Istanbul, Turkey. [11]Department of Genetics, Hôpital Robert Debré and Paris Diderot University, Paris, France. [12]Ludwig Center for Cancer Research, University of Lausanne, Lausanne, Switzerland. [13]Swiss Institute for Bioinformatics (SIB), Lausanne, Switzerland. [14]Pediatric Hematology and Oncology, Charité University Hospital, Berlin, Germany. [15]Department of Computer Science, Bonn Rhine Sieg University of Applied Sciences, Sankt Augustin, Germany. [16]Children's Cancer Research Institute, Vienna, Austria. [17]Northern Institute of Cancer Research, Newcastle University, Newcastle upon Tyne, United Kingdom. [18]Federal Office for Radiation Protection, Oberschleissheim, Germany. [19]Pediatric Hematology and Oncology, Hannover Medical School, Hannover, Germany. [20]Alacris Theranostics GmbH, Berlin, Germany. [21]Universitäts-Kinderspital beider Basel (UKBB), Basel, Switzerland. [22]Sheffield Children's Hospital, Sheffield, United Kingdom. [23]Childhood Leukaemia Investigation Prague (CLIP), Department of Pediatric Hematology/Oncology, Second Faculty of Medicine, Charles University Prague, Prague, Czech Republic. [24]Department of Hematology, Union Hospital, Fujian Medical University, Fuzhou, China. [25]Dahlem Centre for Genome Research and Medical Systems Biology, Berlin, Germany. [26]These authors contributed equally to this work. [27]These authors jointly supervised this work. Correspondence should be addressed to M.S. (stanulla.martin@mh-hannover.de) or J.-P.B. (jean-pierre.bourquin@kispi.uzh.ch).

ONLINE METHODS

Study individuals and sample selection. Samples and associated clinical information from patients included in sequencing and validation analyses were collected from different countries within the International BFM Study Group (I-BFM-SG). All patients were enrolled in multicenter trials on treatment of pediatric ALL conducted by individual member groups of the I-BFM-SG: the AIEOP-BFM study group (Austria, Germany, Italy and Switzerland), the FRALLE study group (France) and the United Kingdom (UK) National Cancer Research Institute (NCRI) Childhood Cancer and Leukemia Group[59,60]. All treatment trials were approved by the respective national institutional review boards, and informed consent for the use of spare specimens for research was obtained from study individuals, parents or legal guardians. The specific research project reported here was approved by the Ethics Committee of the Medical Faculty of the Christian Albrechts University, Kiel, Germany (vote D508/13). Depending on consent and availability of samples, all enrolled patients positive for the rare *TCF3-HLF* gene fusion were included. These patients were matched with *TCF3-PBX1*–positive patients.

Cell isolation and nucleic acid purification. Mononuclear cells were isolated by Ficoll-Paque gradient centrifugation (Pharmacia) from bone marrow or peripheral blood samples followed by extraction of nucleic acids according to standardized protocols using Qiagen DNA Blood Kits (Qiagen) for DNA and Qiagen RNeasy columns (Qiagen) for RNA. The quantity of nucleic acids was determined by spectrophotometry. DNA quality was assessed visually by inspection of agarose gel electrophoresis while RNA integrity was evaluated by using the Bioanalyzer 2100 (Agilent). Nucleic acids isolated from bone marrow aspirates collected in morphological remission served as individual germ-line surrogates/references.

Sequencing. *Whole genome sequencing.* For structural variants, Illumina v2 mate-pair libraries with 5 kbp insert size and 2 × 101 bp reads were prepared from 10 µg of DNA and sequenced on the Illumina HiSeq 2000 platform (Illumina) to obtain a physical coverage of 30×. For copy number alterations, breakpoints and short variants (SNVs, short indels), Illumina TruSeq paired-end libraries with 2 × 101 bp reads were prepared from 1 µg of DNA and sequenced on HiSeq 2000/2500 instruments to a coverage of 40× for reference samples and 80× for tumor samples.

Whole exome sequencing. To increase the sensitivity of detecting short variants in coding regions, 1 µg of DNA each from the diagnostic leukemic and a corresponding remission sample of patients was used for whole exome sequencing. Whole exome capture employed a TruSeq enrichment kit (Illumina) and paired-end libraries with 2 × 101 bp reads on a HiSeq 2500 according to the manufacturer's protocol.

Whole transcriptome sequencing. Illumina TruSeq custom stranded paired-end libraries with 2 × 51 bp reads were prepared from 1 µg RNA using the Ribo-Zero Gold Kit (Epicentre) and sequenced on a HiSeq 2000 with a loading of one library per lane.

Sanger sequencing validation. Structural variant breakpoints from whole-genome sequencing approaches and SNVs from exome sequencing were validated by Sanger sequencing.

Targeted sequencing of TCF3 and RAS pathway candidate genes. TCF3 binding domain (E47 isoform, exon 18) mutations were screened for in 1,033 ALL patients using Sanger sequencing. Primer sequences are listed in **Supplementary Table 27**. Sanger sequencing was also applied for validation of relative absence of RAS pathway mutations in 24 *TCF3-PBX1*–positive ALL samples. The latter analysis included *KRAS* exon 1, *NRAS* exons 1 and 2, *FLT3* exons 14 and 20, *PTPN11* exons 3 and 13, and was conducted as described[61].

Multiplex ligation-dependent probe amplification. Detection of genomic aberrations in B cell differentiation–associated and other genes frequently deleted in ALL (*PAX5*, *IKZF1*, *ETV6*, *RB1*, *BTG1*, *EBF1*, *CDKN2A, CDKN2B* and *P2RY8-CRLF2*) were investigated by the Multiplex Ligation-dependent Probe Amplification (MLPA) assay SALSA p335 kit (MRC-Holland) using 125 ng of genomic DNA. The assays were performed according to the manufacturer's protocol as described[62]. An intensity ratio between 0.75 and 1.3 was considered to represent normal copy number, a ratio between 0.25 and 0.75 was considered a monoallelic deletion and a ratio <0.25, a biallelic deletion.

Bioinformatics analysis. *DNA data processing.* DNA reads were aligned to the human reference genome hg19 (downloaded from the UCSC Genome browser) using Elandv2 (ref. 63; mate pairs) and BWA[64] (paired ends). For xenograft samples, the human DNA reads were deconvoluted after mapping to a combined reference consisting of human hg19 and mouse mm9.

Structural variant detection. Structural variants were detected using DELLY[65] and BIC-seq[66] (DNA data) and TopHat2 (ref. 67) /deFuse[68] (RNA data).

SNV detection. Somatic protein-changing SNVs were detected using established pipelines incorporating GATK[69], MuTect[70], pibase[71], Picard, SAMtools[72] and VarScan2 (ref. 73).

Indel detection. Somatic indels in coding regions were detected using SAMtools followed by Dindel[74].

Transcriptome data analysis. RNA reads were aligned to hg19 using BWA and SAMtools and used for integrated data analysis. For xenograft samples, the human RNA reads were deconvoluted after mapping to a combined reference consisting of human hg19 and mouse mm9. Mapped reads were annotated using Ensembl v.70. Gene expression levels were quantified in reads per kilobase of exon model per million mapped reads (RPKM)[75]. RPKM calculation and differential gene expression (DGE) analysis was performed using the R package edgeR[76]. To identify DGE between ALL subtypes, and between leukemia and remission the following set-up was performed: *TCF3-PBX1* vs. *TCF3-HLF* (comparison 1), *TCF3-PBX1* vs. remission (comparison 2), *TCF3-HLF* vs. remission (comparison 3). The results were filtered by fold change (FC, $|\log_2(FC)| \geq 1$) and false discovery rate (FDR, FDR ≤ 0.001). The final list of 401 genes was created by combining the intersection between comparison 1 and comparison 2 as well as between comparison 1 and comparison 3. The functional analyses of gene lists were done using gene set enrichment analysis (GSEA)[77] and the Genomatix genome analyzer (v. 3.00801; Genomatix Software GmbH). The GeneRanker tool in Genomatix was used to test for enriched gene sets, which were based on gene-tissue annotations obtained by text mining[78]. For GSEA, protein-coding genes were filtered by a minimum expression of 1 RPKM in at least four samples among the primary pre–B cell ALLs. The remaining 11,315 genes were tested for DGE between the ALL subtypes using edgeR. The provided FDR and fold-change values were used to obtain a ranking score to measure the degree of differential expression between the ALL subtype. A pre-ranked classic GSEA was performed using the ranking score, a gene set permutation and a FDR ≤ 0.02. The analysis included gene sets for hematopoietic stages[31] and signatures from MsigDB[77] pathways (C2): KEGG, BIOCARTA, REACTOME; curated oncogenic signatures (C6); human immunologic signatures (C7).

In silico transcription factor binding site (TFBS) analysis. TFBSs in promoter regions of genes (2 kbp upstream region) corresponding to the specific transcriptome signatures of *TCF3-PBX1*- and *TCF3-HLF*–positive ALL, respectively, were analyzed using the Genomatix Genome Analyzer (v3.10124). Based on a matrix of known TFBS motifs, the software tool predicted TFBSs in the investigated promoters and compared their frequency against (i) the background of TFBSs in the promoter regions of all known protein-coding genes in the Ensembl database (v.70, 22864 genes) and (ii) the background of TFBSs in the whole genome. A *Z* score was calculated based on the TFBS frequency in the investigated promoters and the expected frequency and s.d. were estimated from the background[79]. The resulting lists were filtered by the *Z* scores based on the two backgrounds (|genomic $Z| \geq 2$, promoter $Z \geq 2$). TFBSs overrepresented in genes upregulated in both *TCF3-PBX1*- and *TCF3-HLF*–positive ALL were filtered out, to retain only TFBS specifically enriched in the respective subtypes.

Integrated data analysis. SNVs and indels were orthogonally validated by integrating genome, exome and transcriptome data of patients and xenografts, and further confirmed by Sanger sequencing. Structural variants were validated by integrating whole genome paired-end and mate-pair data and whole-transcriptome data, and finally by Sanger sequencing. Ensembl v.70 and ANNOVAR[80] were used to annotate the variants. Silent variants and known germline variants in the 1000 Genomes Project[81] population data, in 136 North German healthy controls (publicly available through GrabBlur[82]), or in the International Cancer Genome Consortium's internal healthy controls were eliminated. All final somatic non synonymous variants were inspected using IGV[83].

doi:10.1038/ng.3362

Preclinical characterization. *Xenograft model.* Animal experiments were approved by the veterinary office of the Canton of Zurich, Switzerland. Approval for experiments with human samples in the mouse xenograft model was obtained from the ethics commission of the Canton Zurich (approval number 2014-0383). In brief, primary ALL cells were recovered from cryopreserved samples and transplanted intrafemorally to NSG mice as previously described[36]. Mice were 5–10 weeks old; both males and females were randomly used. Leukemia progression was monitored by flow cytometry with rat anti-mouse CD45 (eFluor450, clone 30-F11, REF 48-451-82, eBioscience), mouse anti-human CD45 (Alexa Flour 647, clone HI30, REF 304018, BioLegend), and mouse anti-human CD19 (PE, clone HIB19, REF 302208, BioLegend). ALL cells recovered from spleens of NSG mice were used for molecular characterization in *in vitro* and *in vivo* experiments.

Immunophenotyping. Immunophenotyping of patient and xenograft-amplified human ALL cells after recovery from the spleen was performed as described before[84]. All included xenograft samples consisted of at least 95% human leukemic cells.

Cell culture. Human hTERT immortalized primary bone marrow mesenchymal stromal cells (MSC; provided by D. Campana, St. Jude Children's Research Hospital, Memphis, USA) were cultured in RPMI 1640 medium supplemented with 10% heat-inactivated FBS; L-glutamine (2 mM), penicillin/streptomycin (P/S; 100 IU/ml) and hydrocortisone (1 μM). Xenograft-amplified human ALL cells were co-cultured on MSC in AIM V medium (Gibco by Life Technologies) at a ratio of 10:1. All cultured cells were kept in the incubator at 37 °C, 5% CO_2. For cryopreservation, cells were frozen in heat-inactivated FBS with 10% dimethylsulfoxide and subsequently stored in liquid nitrogen.

Cell viability assay. MSCs were seeded in 24-well plates at a number of 50,000 cells per well in RPMI 1640 medium (10% heat-inactivated FBS). After 24 h primary ALL cells were thawed and seeded as suspension culture alone or in co-culture with MSCs at a number of 400,000 cells per well in AIM-V medium. Three days later, ALL cells were collected from monoculture or co-culture by scraping and stained with 7-AAD (BD Pharmingen). Cell viability (7-AAD negative population) was measured by FACS using counting beads (SPHERO Accu Count Blanc Particles, Spherotech Inc.) for cell counts normalization. Viabilities shown are average viabilities of duplicate wells (normalized to input) and s.d.

Cell cycle assay. MSCs were seeded in 96-well tissue culture plates at a concentration of 10,000 cells per well in 100 μl AIM-V medium. After 24 h ALL cells were added at a concentration of 100,000 cells per well in 90 μl AIM-V. The Click-iTEdU Alexa Fluor 488 Flow Cytometry Assay Kit (Life Technologies) in combination with propidium iodide was used to measure proliferation and to identify the different phases of the cell cycle on days 1 and 3. Co-cultured cells were incubated with EdU (10 μM) for 20 h before cell cycle read-out with flow cytometry. The cell cycle assay was performed in triplicate, and at least two independent experiments were performed for each sample. Similar variances were obtained between the groups that were statistically compared.

In vitro drug screening and automated microscopy. MSCs were seeded in 384-well plates at a concentration of 2,500 cells per well in 30 μl AIM-V medium. After 24 h, ALL cells were added at a concentration of 25,000–30,000 cells per well in 27.5 μl AIM-V. Drugs were added as single agents after an additional 24 h using the pipetting robot epMotion 5070 (Eppendorf). Drug response was normalized to ALL cells treated with the drug vehicle alone. Experiments were performed in duplicate in five different dilutions (1, 10, 100, 1,000 and 10,000 nM). For two samples comparable results were obtained in two independent drug screening experiments. After 72 h or 96 h of drug incubation, cells were stained using the CyQUANT direct cell proliferation assay (Life technologies). 20 μl staining mix (AIM V medium, CyQUANT (1:300), repressor (1:20)) was added into each well followed by an incubation time of 1 h at 37 °C, 5% CO_2. Subsequently, automated imaging was performed using the ImageXpress Micro microscope (Molecular Devices) equipped with a CoolSNAP HQ camera (Photometrics) and a 10× plan fluor objective with 0.3 NA (Nikon). Nine images were taken per well, covering 50% of each well and captured employing the MetaXpress software (Molecular Devices). Images were processed using CellProfiler software (Broad Institute). Cells were classified and counted using the Advanced Cell Classifier software. This software uses random forest classification to assign ALL cells properly.

Immunoblot. Whole cell extracts were prepared from 1×10^6 cells using radioimmunoprecipitation assay (RIPA) buffer (20 mM Tris-Cl pH 7.5, 150 mM NaCl, 1% NP-40, 1 mM EDTA pH 8.0, 0.1% SDS) supplemented with Complete mini protease inhibitor cocktail (Roche Life Science) for 20 min on ice, sonicated as necessary, and diluted with SDS loading buffer (250 mM Tris pH 6.8, 4% SDS, 0.02% bromophenol blue, 40% glycerol, 4% (vol/vol) β-mercaptoethanol). After SDS-PAGE, proteins were blotted onto nitrocellulose membranes. Membranes were blocked in 5% non-fat dry milk and incubated with primary Bcl-2 (clone 124; Dako) and tubulin antibodies diluted 1:1,000 in milk. Horseradish peroxidase–labeled anti-mouse antibodies were used for signal detection with chemiluminescence substrate and direct scanning.

In vivo experiments. ALL cells were recovered from cryopreserved xenograft samples, and per thawed sample 12 to 16 mice were transplanted with 1,000,000 cells per mouse. After three days, randomized cohorts were treated with 100 mg/kg of ABT-199 (ABBVIE) or vehicle control with 6 to 8 mice per treatment arm[85]. ABT-199 or vehicle control were administered orally daily for two weeks. Mice of the ABT-199 group transplanted with sample 7a were additionally treated with a second block (100 mg/kg of ABT-199 for 14 d) starting at day 66, when the frequency of circulating leukemia cells started to increase again. Follow-up of circulating leukemia cells was performed every 7 d by flow cytometry with rat anti-mouse CD45, mouse anti-human CD45, and mouse anti-human CD19; frequency of leukemia cells as ratio of $mCD45^-$ $hCD45^+$ $hCD19^+$ count to total lymphocytes. The investigator was blinded to the group allocation during the assessment of outcome. To evaluate the ability of ABT-199 to decrease tumor burden, four mice in the control group were treated when the frequency of leukemia cells in the peripheral blood was equal or higher than 50%. Follow-up of circulating leukemia cells was performed every 4–7 d. *In vivo* experiments were terminated when the frequency of circulating leukemia cells reached 50% or earlier if the mice showed abnormal behavior. One *in vivo* experiment was performed per each sample.

Statistical analysis. Differences in the distribution of categorical variables among patient subsets were analyzed using Fisher's exact or chi-squared test. Comparisons of continuous variables between groups were performed by *t*-test or Mann-Whitney *U* test.

Drug responses were evaluated by fitting DMSO-normalized response data with the four-parameter log-logistic function of the form:

$$f(x) = \text{base} + \frac{E_{max} - \text{base}}{1 + (x_{1/2}/x)\,\text{Coeff}}$$

as implemented in the drc package of R (version 2.3-96). Outliers were detected and removed before curve fitting using Bayesian change point analysis[25] (R package bcp, version 3.0.1). Non-convergent cases (for example, drugs with no activity) were identified based on linear fit parameters. Hierarchical clustering was performed to group patients according to their drug-response profiles (R package gplots version 2.14.2). Drugs with differential activity in patients with *TCF3-PBX1*– compared to *TCF3-HLF*–positive ALL were identified using a *t*-test ($P \leq 0.05$). In *in vivo* experiments, 25% of circulating leukemia cells or termination of the experiment if 25% of leukemia was not reached were considered as an event in the Kaplan-Meier analysis. For sample 9a, 50% was used because of the rapid engraftment. Differences in the survival of mice receiving ABT-199 or vehicle control were determined by the Mantel-Cox test and verified by the Gehan-Breslow-Wilcoxon test.

59. Conter, V. *et al.* Molecular response to treatment redefines all prognostic factors in children and adolescents with B-cell precursor acute lymphoblastic leukemia: results in 3184 patients of the AIEOP-BFM ALL 2000 study. *Blood* **115**, 3206–3214 (2010).

60. Harrison, C.J. *et al.* Detection of prognostically relevant genetic abnormalities in childhood B-cell precursor acute lymphoblastic leukaemia: recommendations from the Biology and Diagnosis Committee of the International Berlin-Frankfurt-Munster study group. *Br. J. Haematol.* **151**, 132–142 (2010).
61. Case, M. *et al.* Mutation of genes affecting the RAS pathway is common in childhood acute lymphoblastic leukemia. *Cancer Res.* **68**, 6803–6809 (2008).
62. Dörge, P. *et al.* IKZF1 deletion is an independent predictor of outcome in pediatric acute lymphoblastic leukemia treated according to the ALL-BFM 2000 protocol. *Haematologica* **98**, 428–432 (2013).
63. Bauer, M.J., Cox, A.J. & Evers, D.J. Fast gapped read mapping for Illumina reads. *In ISMB, ISBC* (2010).
64. Li, H. & Durbin, R. Fast and accurate short read alignment with Burrows-Wheeler transform. *Bioinformatics* **25**, 1754–1760 (2009).
65. Rausch, T. *et al.* DELLY: structural variant discovery by integrated paired-end and split-read analysis. *Bioinformatics* **28**, i333–i339 (2012).
66. Xi, R. *et al.* Copy number variation detection in whole-genome sequencing data using the Bayesian information criterion. *Proc. Natl. Acad. Sci. USA* **108**, E1128–E1136 (2011).
67. Kim, D. *et al.* TopHat2: accurate alignment of transcriptomes in the presence of insertions, deletions and gene fusions. *Genome Biol.* **14**, R36 (2013).
68. McPherson, A. *et al.* deFuse: an algorithm for gene fusion discovery in tumor RNA-Seq data. *PLOS Comput. Biol.* **7**, e1001138 (2011).
69. McKenna, A. *et al.* The Genome Analysis Toolkit: a MapReduce framework for analyzing next-generation DNA sequencing data. *Genome Res.* **20**, 1297–1303 (2010).
70. Cibulskis, K. *et al.* Sensitive detection of somatic point mutations in impure and heterogeneous cancer samples. *Nat. Biotechnol.* **31**, 213–219 (2013).
71. Forster, M. *et al.* From next-generation sequencing alignments to accurate comparison and validation of single-nucleotide variants: the pibase software. *Nucleic Acids Res.* **41**, e16 (2013).
72. Li, H. *et al.* The Sequence Alignment/Map format and SAMtools. *Bioinformatics* **25**, 2078–2079 (2009).
73. Koboldt, D.C. *et al.* VarScan 2: somatic mutation and copy number alteration discovery in cancer by exome sequencing. *Genome Res.* **22**, 568–576 (2012).
74. Albers, C.A. *et al.* Dindel: accurate indel calls from short-read data. *Genome Res.* **21**, 961–973 (2011).
75. Mortazavi, A., Williams, B.A., McCue, K., Schaeffer, L. & Wold, B. Mapping and quantifying mammalian transcriptomes by RNA-Seq. *Nat. Methods* **5**, 621–628 (2008).
76. Robinson, M.D., McCarthy, D.J. & Smyth, G.K. edgeR: a Bioconductor package for differential expression analysis of digital gene expression data. *Bioinformatics* **26**, 139–140 (2010).
77. Subramanian, A. *et al.* Gene set enrichment analysis: a knowledge-based approach for interpreting genome-wide expression profiles. *Proc. Natl. Acad. Sci. USA* **102**, 15545–15550 (2005).
78. Frisch, M., Klocke, B., Haltmeier, M. & Frech, K. LitInspector: literature and signal transduction pathway mining in PubMed abstracts. *Nucleic Acids Res.* **37**, W135–W140 (2009).
79. Ho Sui, S.J. *et al.* oPOSSUM: identification of over-represented transcription factor binding sites in co-expressed genes. *Nucleic Acids Res.* **33**, 3154–3164 (2005).
80. Wang, K., Li, M. & Hakonarson, H. ANNOVAR: functional annotation of genetic variants from high-throughput sequencing data. *Nucleic Acids Res.* **38**, e164 (2010).
81. 1000 Genomes Project Consortium. A map of human genome variation from population-scale sequencing. *Nature* **467**, 1061–1073 (2010).
82. Stade, B., Seelow, D., Thomsen, I., Krawczak, M. & Franke, A. GrabBlur–a framework to facilitate the secure exchange of whole-exome and -genome SNV data using VCF files. *BMC Genomics* **15** (suppl. 4), S8 (2014).
83. Robinson, J.T. *et al.* Integrative genomics viewer. *Nat. Biotechnol.* **29**, 24–26 (2011).
84. Ratei, R. *et al.* Lineage classification of childhood acute lymphoblastic leukemia according to the EGIL recommendations: results of the ALL-BFM 2000 trial. *Klin. Padiatr.* **225** (suppl. 1), S34–S39 (2013).
85. Festing, M.F. & Altman, D.G. Guidelines for the design and statistical analysis of experiments using laboratory animals. *ILAR J.* **43**, 244–258 (2002).